IEEE STANDARDS ASSOCIATION

IEEE Guide for Safety in AC Substation Grounding

IEEE Power and Energy Society

Sponsored by the
Substations Committee

IEEE
3 Park Avenue
New York, NY 10016-5997
USA

IEEE Std 80™-2013
(Revision of
IEEE Std 80-2000/
Incorporates
IEEE Std 80-2013/Cor 1-2015)

--`,,,,,,`,```,,`,`,,`,-`-`,,`,,`,`,,`---

Copyright The Institute of Electrical and Electronics Engineers, Inc.
Provided by IHS under license with IEEE
No reproduction or networking permitted without license from IHS

Order Number: 02120914
Sold to:EGAT [700166108393] - VARRIS.Y@EGAT.CO.TH,
Not for Resale,2016-09-15 03:57:51 UTC

Copyright The Institute of Electrical and Electronics Engineers, Inc.
Provided by IHS under license with IEEE
No reproduction or networking permitted without license from IHS

Order Number: 02120914
Sold to:EGAT [700166108393] - VARRIS.Y@EGAT.CO.TH,
Not for Resale,2016-09-15 03:57:51 UTC

IEEE Std 80™-2013
(Revision of
IEEE Std 80-2000/
Incorporates
IEEE Std 80-2013/Cor 1-2015)

IEEE Guide for Safety in AC Substation Grounding

Sponsor

Substations Committee
of the
IEEE Power and Energy Society

Approved 11 December 2013

IEEE-SA Standards Board

Copyright The Institute of Electrical and Electronics Engineers, Inc.
Provided by IHS under license with IEEE
No reproduction or networking permitted without license from IHS

Order Number: 02120914
Sold to:EGAT [700166108393] - VARRIS.Y@EGAT.CO.TH,
Not for Resale,2016-09-15 03:57:51 UTC

Copyrights and permissions: Annex E translated by T. W. Stringfield from Koch, W., "Erdungsmassnahmen fur Hochstspannungsanlagen mit Geerdetem Sternpunkt," *Electrotechnische Zeitschrift,* vol. 71, no. 4, pp. 8–91, Feb. 1950.

Annex F is taken from Dawalibi, F., and Mukhedkar, D., "Parametric analysis of grounding systems," *IEEE Transactions on Power Apparatus and Systems,* vol. PAS-98, no. 5, pp. 1659–1668, Sept./Oct. 1979; and Dawalibi, F., and Mukhedkar, D., "Influence of ground rods on grounding systems," *IEEE Transactions on Power Apparatus and Systems,* vol. PAS-98, no. 6, pp. 2089–2098, Nov./Dec. 1979.

Annex G translated by T. W. Stringfield from Koch, W., "Erdungsmassnahmen fur Hochstspannungsanlagen mit Geerdetem Sternpunkt," *Electrotechnische Zeitschrift,* vol. 71, no. 4, pp. 8–91, Feb. 1950.

Abstract: This guide is primarily concerned with outdoor ac substations, either conventional or gas-insulated. These include distribution, transmission, and generating plant substations. With proper caution, the methods described herein are also applicable to indoor portions of such substations, or to substations that are wholly indoors. No attempt is made to cover the grounding problems peculiar to dc substations. A quantitative analysis of the effects of lightning surges is also beyond the scope of this guide.

Keywords: ground grids, grounding, IEEE 80™, substation design, substation grounding

The Institute of Electrical and Electronics Engineers, Inc.
3 Park Avenue, New York, NY 10016-5997, USA

Copyright © 2015 by The Institute of Electrical and Electronics Engineers, Inc.
All rights reserved. Published 15 May 2015. Printed in the United States of America.

IEEE is a registered trademark in the U.S. Patent & Trademark Office, owned by The Institute of Electrical and Electronics Engineers, Incorporated.

National Electrical Safety Code and NESC are registered trademarks in the U.S. Patent & Trademark Office, owned by The Institute of Electrical and Electronics Engineers, Incorporated.

PDF: ISBN 978-0-7381-8850-8 STD98495
Print: ISBN 978-0-7381-8851-5 STDPD98495

IEEE prohibits discrimination, harassment, and bullying.
For more information, visit http://www.ieee.org/web/aboutus/whatis/policies/p9-26.html.
No part of this publication may be reproduced in any form, in an electronic retrieval system or otherwise, without the prior written permission of the publisher.

--`,,,,,,`,```,,`,`,,`,-`-`,,`,,,`---

Copyright The Institute of Electrical and Electronics Engineers, Inc.
Provided by IHS under license with IEEE
No reproduction or networking permitted without license from IHS

Order Number: 02120914
Sold to:EGAT [700166108393] - VARRIS.Y@EGAT.CO.TH,
Not for Resale,2016-09-15 03:57:51 UTC

Important Notices and Disclaimers Concerning IEEE Standards Documents

IEEE documents are made available for use subject to important notices and legal disclaimers. These notices and disclaimers, or a reference to this page, appear in all standards and may be found under the heading "Important Notice" or "Important Notices and Disclaimers Concerning IEEE Standards Documents."

Notice and Disclaimer of Liability Concerning the Use of IEEE Standards Documents

IEEE Standards documents (standards, recommended practices, and guides), both full-use and trial-use, are developed within IEEE Societies and the Standards Coordinating Committees of the IEEE Standards Association ("IEEE-SA") Standards Board. IEEE ("the Institute") develops its standards through a consensus development process, approved by the American National Standards Institute ("ANSI"), which brings together volunteers representing varied viewpoints and interests to achieve the final product. Volunteers are not necessarily members of the Institute and participate without compensation from IEEE. While IEEE administers the process and establishes rules to promote fairness in the consensus development process, IEEE does not independently evaluate, test, or verify the accuracy of any of the information or the soundness of any judgments contained in its standards.

IEEE does not warrant or represent the accuracy or content of the material contained in its standards, and expressly disclaims all warranties (express, implied and statutory) not included in this or any other document relating to the standard, including, but not limited to, the warranties of: merchantability; fitness for a particular purpose; non-infringement; and quality, accuracy, effectiveness, currency, or completeness of material. In addition, IEEE disclaims any and all conditions relating to: results; and workmanlike effort. IEEE standards documents are supplied "AS IS" and "WITH ALL FAULTS."

Use of an IEEE standard is wholly voluntary. The existence of an IEEE standard does not imply that there are no other ways to produce, test, measure, purchase, market, or provide other goods and services related to the scope of the IEEE standard. Furthermore, the viewpoint expressed at the time a standard is approved and issued is subject to change brought about through developments in the state of the art and comments received from users of the standard.

In publishing and making its standards available, IEEE is not suggesting or rendering professional or other services for, or on behalf of, any person or entity nor is IEEE undertaking to perform any duty owed by any other person or entity to another. Any person utilizing any IEEE Standards document, should rely upon his or her own independent judgment in the exercise of reasonable care in any given circumstances or, as appropriate, seek the advice of a competent professional in determining the appropriateness of a given IEEE standard.

IN NO EVENT SHALL IEEE BE LIABLE FOR ANY DIRECT, INDIRECT, INCIDENTAL, SPECIAL, EXEMPLARY, OR CONSEQUENTIAL DAMAGES (INCLUDING, BUT NOT LIMITED TO: PROCUREMENT OF SUBSTITUTE GOODS OR SERVICES; LOSS OF USE, DATA, OR PROFITS; OR BUSINESS INTERRUPTION) HOWEVER CAUSED AND ON ANY THEORY OF LIABILITY, WHETHER IN CONTRACT, STRICT LIABILITY, OR TORT (INCLUDING NEGLIGENCE OR OTHERWISE) ARISING IN ANY WAY OUT OF THE PUBLICATION, USE OF, OR RELIANCE UPON ANY STANDARD, EVEN IF ADVISED OF THE POSSIBILITY OF SUCH DAMAGE AND REGARDLESS OF WHETHER SUCH DAMAGE WAS FORESEEABLE.

Translations

The IEEE consensus development process involves the review of documents in English only. In the event that an IEEE standard is translated, only the English version published by IEEE should be considered the approved IEEE standard.

Copyright The Institute of Electrical and Electronics Engineers, Inc.
Provided by IHS under license with IEEE
No reproduction or networking permitted without license from IHS

Order Number: 02120914
Sold to:EGAT [700166108393] - VARRIS.Y@EGAT.CO.TH,
Not for Resale,2016-09-15 03:57:51 UTC

Official statements

A statement, written or oral, that is not processed in accordance with the IEEE-SA Standards Board Operations Manual shall not be considered or inferred to be the official position of IEEE or any of its committees and shall not be considered to be, or be relied upon as, a formal position of IEEE. At lectures, symposia, seminars, or educational courses, an individual presenting information on IEEE standards shall make it clear that his or her views should be considered the personal views of that individual rather than the formal position of IEEE.

Comments on standards

Comments for revision of IEEE Standards documents are welcome from any interested party, regardless of membership affiliation with IEEE. However, IEEE does not provide consulting information or advice pertaining to IEEE Standards documents. Suggestions for changes in documents should be in the form of a proposed change of text, together with appropriate supporting comments. Since IEEE standards represent a consensus of concerned interests, it is important that any responses to comments and questions also receive the concurrence of a balance of interests. For this reason, IEEE and the members of its societies and Standards Coordinating Committees are not able to provide an instant response to comments or questions except in those cases where the matter has previously been addressed. For the same reason, IEEE does not respond to interpretation requests. Any person who would like to participate in revisions to an IEEE standard is welcome to join the relevant IEEE working group.

Comments on standards should be submitted to the following address:

Secretary, IEEE-SA Standards Board
445 Hoes Lane
Piscataway, NJ 08854 USA

Laws and regulations

Users of IEEE Standards documents should consult all applicable laws and regulations. Compliance with the provisions of any IEEE Standards document does not imply compliance to any applicable regulatory requirements. Implementers of the standard are responsible for observing or referring to the applicable regulatory requirements. IEEE does not, by the publication of its standards, intend to urge action that is not in compliance with applicable laws, and these documents may not be construed as doing so.

Copyrights

IEEE draft and approved standards are copyrighted by IEEE under U.S. and international copyright laws. They are made available by IEEE and are adopted for a wide variety of both public and private uses. These include both use, by reference, in laws and regulations, and use in private self-regulation, standardization, and the promotion of engineering practices and methods. By making these documents available for use and adoption by public authorities and private users, IEEE does not waive any rights in copyright to the documents.

Photocopies

Subject to payment of the appropriate fee, IEEE will grant users a limited, non-exclusive license to photocopy portions of any individual standard for company or organizational internal use or individual, non-commercial use only. To arrange for payment of licensing fees, please contact Copyright Clearance Center, Customer Service, 222 Rosewood Drive, Danvers, MA 01923 USA; +1 978 750 8400. Permission to photocopy portions of any individual standard for educational classroom use can also be obtained through the Copyright Clearance Center.

Copyright The Institute of Electrical and Electronics Engineers, Inc.
Provided by IHS under license with IEEE
No reproduction or networking permitted without license from IHS

Order Number: 02120914
Sold to:EGAT [700166108393] - VARRIS.Y@EGAT.CO.TH,
Not for Resale,2016-09-15 03:57:51 UTC

Updating of IEEE Standards documents

Users of IEEE Standards documents should be aware that these documents may be superseded at any time by the issuance of new editions or may be amended from time to time through the issuance of amendments, corrigenda, or errata. An official IEEE document at any point in time consists of the current edition of the document together with any amendments, corrigenda, or errata then in effect.

Every IEEE standard is subjected to review at least every ten years. When a document is more than ten years old and has not undergone a revision process, it is reasonable to conclude that its contents, although still of some value, do not wholly reflect the present state of the art. Users are cautioned to check to determine that they have the latest edition of any IEEE standard.

In order to determine whether a given document is the current edition and whether it has been amended through the issuance of amendments, corrigenda, or errata, visit the IEEE-SA Website at http://ieeexplore.ieee.org/xpl/standards.jsp or contact IEEE at the address listed previously. For more information about the IEEE-SA or IEEE's standards development process, visit the IEEE-SA Website at http://standards.ieee.org.

Errata

Errata, if any, for all IEEE standards can be accessed on the IEEE-SA Website at the following URL: http://standards.ieee.org/findstds/errata/index.html. Users are encouraged to check this URL for errata periodically.

Patents

Attention is called to the possibility that implementation of this standard may require use of subject matter covered by patent rights. By publication of this standard, no position is taken by the IEEE with respect to the existence or validity of any patent rights in connection therewith. If a patent holder or patent applicant has filed a statement of assurance via an Accepted Letter of Assurance, then the statement is listed on the IEEE-SA Website at http://standards.ieee.org/about/sasb/patcom/patents.html. Letters of Assurance may indicate whether the Submitter is willing or unwilling to grant licenses under patent rights without compensation or under reasonable rates, with reasonable terms and conditions that are demonstrably free of any unfair discrimination to applicants desiring to obtain such licenses.

Essential Patent Claims may exist for which a Letter of Assurance has not been received. The IEEE is not responsible for identifying Essential Patent Claims for which a license may be required, for conducting inquiries into the legal validity or scope of Patents Claims, or determining whether any licensing terms or conditions provided in connection with submission of a Letter of Assurance, if any, or in any licensing agreements are reasonable or non-discriminatory. Users of this standard are expressly advised that determination of the validity of any patent rights, and the risk of infringement of such rights, is entirely their own responsibility. Further information may be obtained from the IEEE Standards Association.

--`,,,,,,`,```,,`,`,,`,-`-`,,```,,,`---

Copyright The Institute of Electrical and Electronics Engineers, Inc.
Provided by IHS under license with IEEE
No reproduction or networking permitted without license from IHS

Order Number: 02120914
Sold to:EGAT [700166108393] - VARRIS.Y@EGAT.CO.TH,
Not for Resale,2016-09-15 03:57:51 UTC

Participants

IEEE Std 80-2013

At the time this IEEE guide was completed, the Grounding (PE/SUB/WGD7) Working Group had the following membership:

Richard P. Keil, *Chair*
Curtis R. Stidham, *Secretary*

Hanna Abdallah
Stan J. Arnot
Thomas Barnes
Bryan Beske
Dale Boling
Steven Brown
James Cain
Bill Carman
K. S. Chan
Koushik Chanda
Carson Day
Dennis DeCosta
E. Peter Dick
William K. Dick
Marcia Eblen
D. Lane Garrett
Joseph Gravelle
Steven Greenfield
Charles Haahr
Thomas Harger
Martin Havelka
Dave Kelley
Donald N. Laird
Henri Lemeilleur
Cary Mans
Sakis Meliopoulos
Mike Noori
Shashi G. Patel
Christian Robles
Jesse Rorabaugh
Hamid Sharifnia
William Sheh
Douglas Smith
David Stamm
Greg J. Steinman
Brian Story
Yance Syarif
Keith Wallace
Alexander Wong

The following members of the individual balloting committee voted on this guide. Balloters may have voted for approval, disapproval, or abstention.

William Ackerman
Michael Adams
Ali Al Awazi
Ficheux Arnaud
Stan J. Arnot
Adam Bagby
Thomas Barnes
George Bartok
George Becker
W. J. (Bill) Bergman
Bryan Beske
Steven Bezner
Wallace Binder
Michael Bio
Derek Brown
Steven Brown
William Bush
William Byrd
James Cain
Thomas Callsen
K. S. Chan
Koushik Chanda
Robert Christman
Randy Clelland
Chuanyou Dai
Ray Davis
Dennis DeCosta
Charles DeNardo
Gary Donner
Michael Dood
Douglas Dorr
Randall Dotson
Gearoid O'hEidhin
C. Erven
Dan Evans
Keith Flowers
Rabiz Foda
Doaa Galal
D. Lane Garrett
Frank Gerleve
David Giegel
David Gilmer
Jalal Gohari
Edwin Goodwin
James Graham
Lance Grainger
Joseph Gravelle
Steven Greenfield
Randall Groves
Ajit Gwal
Charles Haahr
Thomas Harger
Martin Havelka
Lee Herron
Scott Hietpas
Robert Hoerauf
Gary Hoffman
Richard P. Keil
Gael Kennedy
Mohamed Abdel Khalek
Yuri Khersonsky
James Kinney
Joseph L. Koepfinger*
David Krause
Jim Kulchisky
Saumen Kundu
Donald N. Laird
Chung-Yiu Lam
Benjamin Lanz
Michael Lauxman
Duane Leschert
Hua Liu
Debra Longtin
Greg Luri
Bruce Mackie
John Mcalhaney, Jr.
John Merando
T. David Mills
Georges Montillet
Kimberly Mosley
Adi Mulawarman
Jerry Murphy
Arun Narang
Dennis Neitzel
Arthur Neubauer
Michael Newman
Matthew Norwalk
Robert Nowell
Ted Olsen
Lorraine Padden
Shashi G. Patel
Donald Platts
Percy Pool

Copyright © 2015 IEEE. All rights reserved.

Copyright The Institute of Electrical and Electronics Engineers, Inc.
Provided by IHS under license with IEEE
No reproduction or networking permitted without license from IHS

Order Number: 02120914
Sold to:EGAT [700166108393] - VARRIS.Y@EGAT.CO.TH,
Not for Resale,2016-09-15 03:57:51 UTC

Moises Ramos
Reynaldo Ramos
Michael Roberts
Charles Rogers
Jesse Rorabaugh
Thomas Rozek
Steven Sano
Bartien Sayogo
Dennis Schlender
Robert Schuerger
Hamid Sharifnia
Devki Sharma
William Sheh
Suresh Shrimavle
Gil Shultz
Hyeong Sim
Garry Simms
David Singleton
Douglas Smith
Jerry Smith
David Solhtalab
Curtis R. Stidham
Gary Stoedter
Brian Story
Raymond Strittmatter
Peter Sutherland
Michael Swearingen
William Taylor
David Tepen
Wayne Timm
John Toth
Joe Uchiyama
Eric Udren
Marcelo Valdes
John Vergis
Jane Verner
Keith Wallace
S. Frank Waterer
Donald Wengerter
Kenneth White
James Wilson
Alexander Wong
Jonathan Woodworth
Larry Young
Roland Youngberg
Jian Yu
Luis Zambrano

When the IEEE-SA Standards Board approved this guide on 11 December 2013, it had the following membership:

John Kulick, *Chair*
David J. Law, *Vice Chair*
Richard H. Hulett, *Past Chair*
Konstantinos Karachalios, *Secretary*

Masayuki Ariyoshi
Peter Balma
Farooq Bari
Ted Burse
Stephen Dukes
Jean-Philippe Faure
Alexander Gelman
Mark Halpin
Gary Hoffman
Paul Houzé
Jim Hughes
Michael Janezic
Joseph L. Koepfinger*
Oleg Logvinov
Ron Petersen
Gary Robinson
Jon Walter Rosdahl
Adrian Stephens
Peter Sutherland
Yatin Trivedi
Phil Winston
Yu Yuan

*Member Emeritus

Also included are the following non-voting IEEE-SA Standards Board liaisons:

Richard DeBlasio, *DOE Representative*
Michael Janezic, *NIST Representative*

Don Messina
IEEE-SA Content Production and Management

Erin Spiewak
IEEE-SA Technical Program Operations

Copyright © 2015 IEEE. All rights reserved.

Copyright The Institute of Electrical and Electronics Engineers, Inc.
Provided by IHS under license with IEEE
No reproduction or networking permitted without license from IHS

Order Number: 02120914
Sold to:EGAT [700166108393] - VARRIS.Y@EGAT.CO.TH,
Not for Resale,2016-09-15 03:57:51 UTC

Participants

At the time this IEEE corrigendum was completed, the Grounding (PE/SUB/WGD7) Working Group had the following membership:

Richard P. Keil, *Chair*
Curtis R. Stidham, *Secretary*

Hanna Abdallah
Stan J. Arnot
Thomas Barnes
Bryan Beske
Dale Boling
Steven Brown
James Cain
Bill Carman
K. S. Chan
Koushik Chanda
Carson Day
Dennis DeCosta
E. Peter Dick
William K. Dick
Marcia Eblen
D. Lane Garrett
Joseph Gravelle
Steven Greenfield
Charles Haahr
Thomas Harger
Martin Havelka
Dave Kelley
Donald N. Laird
Henri Lemeilleur
Cary Mans
Sakis Meliopoulos
Mike Noori
Shashi G. Patel
Christian Robles
Jesse Rorabaugh
Hamid Sharifnia
William Sheh
Douglas Smith
David Stamm
Greg J. Steinman
Brian Story
Yance Syarif
Keith Wallace
Alexander Wong

The following members of the individual balloting committee voted on this corrigendum. Balloters may have voted for approval, disapproval, or abstention.

William Ackerman
Michael Adams
Ali Al Awazi
Ficheux Arnaud
Stan J. Arnot
Adam Bagby
Thomas Barnes
George Bartok
George Becker
W. J. (Bill) Bergman
Bryan Beske
Steven Bezner
Wallace Binder
Michael Bio
Derek Brown
Steven Brown
William Bush
William Byrd
James Cain
Thomas Callsen
K. S. Chan
Koushik Chanda
Robert Christman
Randy Clelland
Chuanyou Dai
Ray Davis
Dennis DeCosta
Charles DeNardo
Gary Donner
Michael Dood
Douglas Dorr
Randall Dotson
Gearoid O'hEidhin
C. Erven
Dan Evans
Keith Flowers
Rabiz Foda
Doaa Galal
D. Lane Garrett
Frank Gerleve
David Giegel
David Gilmer
Jalal Gohari
Edwin Goodwin
James Graham
Lance Grainger
Joseph Gravelle
Steven Greenfield
Randall Groves
Ajit Gwal
Charles Haahr
Thomas Harger
Martin Havelka
Lee Herron
Scott Hietpas
Robert Hoerauf
Gary Hoffman
Richard P. Keil
Gael Kennedy
Mohamed Abdel Khalek
Yuri Khersonsky
James Kinney
Joseph L. Koepfinger*
David Krause
Jim Kulchisky
Saumen Kundu
Donald N. Laird
Chung-Yiu Lam
Benjamin Lanz
Michael Lauxman
Duane Leschert
Hua Liu
Debra Longtin
Greg Luri
Bruce Mackie
John Mcalhaney, Jr.
John Merando
T. David Mills
Georges Montillet
Kimberly Mosley
Adi Mulawarman
Jerry Murphy
Arun Narang
Dennis Neitzel
Arthur Neubauer
Michael Newman
Matthew Norwalk
Robert Nowell
Ted Olsen
Lorraine Padden
Shashi G. Patel
Donald Platts
Percy Pool

Copyright © 2015 IEEE. All rights reserved.

Copyright The Institute of Electrical and Electronics Engineers, Inc.
Provided by IHS under license with IEEE
No reproduction or networking permitted without license from IHS

Order Number: 02120914
Sold to:EGAT [700166108393] - VARRIS.Y@EGAT.CO.TH,
Not for Resale,2016-09-15 03:57:51 UTC

Moises Ramos
Reynaldo Ramos
Michael Roberts
Charles Rogers
Jesse Rorabaugh
Thomas Rozek
Steven Sano
Bartien Sayogo
Dennis Schlender
Robert Schuerger
Hamid Sharifnia
Devki Sharma
William Sheh
Suresh Shrimavle
Gil Shultz
Hyeong Sim
Garry Simms
David Singleton
Douglas Smith
Jerry Smith
David Solhtalab
Curtis R. Stidham
Gary Stoedter
Brian Story
Raymond Strittmatter
Peter Sutherland
Michael Swearingen
William Taylor
David Tepen
Wayne Timm
John Toth
Joe Uchiyama
Eric Udren
Marcelo Valdes
John Vergis
Jane Verner
Keith Wallace
S. Frank Waterer
Donald Wengerter
Kenneth White
James Wilson
Alexander Wong
Jonathan Woodworth
Larry Young
Roland Youngberg
Jian Yu
Luis Zambrano

When the IEEE-SA Standards Board approved this corrigendum on March 26, 2015, it had the following membership:

John D. Kulick, *Chair*
Jon Walter Rosdah, *Vice Chair*
Richard H. Hulett, *Past Chair*
Konstantinos Karachalios, *Secretary*

Masayuki Ariyoshi
Ted Burse
Stephen Dukes
Jean-Philippe Faure
J. Travis Griffith
Gary Hoffman
Michael Janezic
Joseph L. Koepfinger*
David J. Law
Hung Ling
Andrew Myles
T. W. Olsen
Glenn Parsons
Ronald C. Petersen
Annette D. Reilly
Stephen J. Shellhammer
Adrian P. Stephens
Yatin Trivedi
Phillip Winston
Don Wright
Yu Yuan
Daidi Zhong

*Member Emeritus

Don Messina
IEEE-SA Content Production and Management

Erin Spiewak
IEEE-SA Operational Program Management

Copyright © 2015 IEEE. All rights reserved.

Copyright The Institute of Electrical and Electronics Engineers, Inc.
Provided by IHS under license with IEEE
No reproduction or networking permitted without license from IHS

Order Number: 02120914
Sold to:EGAT [700166108393] - VARRIS.Y@EGAT.CO.TH,
Not for Resale,2016-09-15 03:57:51 UTC

Introduction

This introduction is not part of IEEE Std 80™-2013, IEEE Guide for Safety in AC Substation Grounding.

This fifth edition represents the third major revision of this guide since its first issue in 1961. Previous editions extended the equations for calculating touch and step voltages to include L-shaped and T-shaped grids; they introduced curves to help determine current division, changed the criteria for selection of conductors and connections, and provided more information on resistivity measurement interpretation; and added the discussion of multilayer soils.

This edition introduces the calculations to determine *TCAP* for materials not listed in Table 1. This information can be used to calculate *TCAP* for different combinations of bi-metallic electrodes used in grounding systems. This edition also introduces benchmarks. The benchmarks have two purposes. First, the benchmarks compare the equations in IEEE Std 80 to commercially available ground grid design software. The benchmarks show where IEEE Std 80 equations work well and their limitations. Second, the benchmarks provide software users a way to verify their understanding of the software.

The fifth edition continues to build on over 50 years of work by dedicated members of working groups: AIEE Working Group 56.1 and IEEE Working Groups 69.1, 78.1, and D7.

As required by IEEE Std 80-2013/Cor 1-2015, corrections were made to Clause 11, Clause 17, Annex C, Annex H as well as to Table 1 and Table 2; two equations following Figure 45; Table H.5 was replaced by a new Table H.5, and Table H.6 through Table H.10 were added.

Copyright © 2015 IEEE. All rights reserved.

Copyright The Institute of Electrical and Electronics Engineers, Inc.
Provided by IHS under license with IEEE
No reproduction or networking permitted without license from IHS

Order Number: 02120914
Sold to:EGAT [700166108393] - VARRIS.Y@EGAT.CO.TH,
Not for Resale,2016-09-15 03:57:51 UTC

Contents

1. Overview 1
1.1 Scope 1
1.2 Purpose 1

2. Normative references 2

3. Definitions 3

4. Safety in grounding 8
4.1 Basic problem 8
4.2 Conditions of danger 10

5. Range of tolerable current 11
5.1 Effect of frequency 11
5.2 Effect of magnitude and duration 12
5.3 Importance of high-speed fault clearing 12

6. Tolerable body current limit 13
6.1 Duration formula 13
6.2 Alternative assumptions 14
6.3 Comparison of Dalziel's equations and Biegelmeier's curve 15
6.4 Note on reclosing 16

7. Accidental ground circuit 16
7.1 Resistance of the human body 16
7.2 Current paths through the body 17
7.3 Accidental circuit equivalents 17
7.4 Effect of a thin layer of surface material 21

8. Criteria of tolerable voltage 24
8.1 Criteria of tolerable voltage definitions 24
8.2 Typical shock situations for air-insulated substations 27
8.3 Typical shock situations for gas-insulated substations 28
8.4 Step and touch voltage criteria 28
8.5 Effect of sustained ground currents 30

9. Principal design considerations 30
9.1 Definitions 30
9.2 General concept 30
9.3 Primary and auxiliary ground electrodes 31
9.4 Basic aspects of grid design 31
9.5 Design in difficult conditions 32
9.6 Connections to grid 33

10. Special considerations for gas-insulated substations (GIS) 33
10.1 Special considerations for GIS definitions 33
10.2 GIS characteristics 34
10.3 Enclosures and circulating currents 35
10.4 Grounding of enclosures 35
10.5 Cooperation between GIS manufacturer and user 36
10.6 Other special aspects of GIS grounding 37

Copyright © 2015 IEEE. All rights reserved.

Copyright The Institute of Electrical and Electronics Engineers, Inc.
Provided by IHS under license with IEEE
No reproduction or networking permitted without license from IHS

Order Number: 02120914
Sold to:EGAT [700166108393] - VARRIS.Y@EGAT.CO.TH,
Not for Resale,2016-09-15 03:57:51 UTC

10.7 Notes on grounding of GIS foundations 37
10.8 Touch voltage criteria for GIS 38
10.9 Recommendations 40

11. Selection of conductors and connections 40
11.1 Basic requirements 40
11.2 Choice of material for conductors and related corrosion problems 40
11.3 Conductor sizing factors 42
11.4 Selection of connections 52

12. Soil characteristics 52
12.1 Soil as a grounding medium 52
12.2 Effect of voltage gradient 53
12.3 Effect of current magnitude 53
12.4 Effect of moisture, temperature, and chemical content 53
12.5 Use of surface material layer 54

13. Soil structure and selection of soil model 55
13.1 Investigation of soil structure 55
13.2 Classification of soils and range of resistivity 55
13.3 Resistivity measurements 56
13.4 Interpretation of soil resistivity measurements 59

14. Evaluation of ground resistance 66
14.1 Usual requirements 66
14.2 Simplified calculations 66
14.3 Schwarz's equations 67
14.4 Note on ground resistance of primary electrodes 70
14.5 Soil treatment to lower resistivity 70
14.6 Concrete-encased electrodes 70

15. Determination of maximum grid current 74
15.1 Determination of maximum grid current definitions 74
15.2 Procedure 75
15.3 Types of ground faults 75
15.4 Effect of substation ground resistance 78
15.5 Effect of fault resistance 78
15.6 Effect of overhead ground wires and neutral conductors 79
15.7 Effect of direct buried pipes and cables 79
15.8 Worst fault type and location 79
15.9 Computation of current division 80
15.10 Effect of asymmetry 85
15.11 Effect of future changes 87

16. Design of grounding system 88
16.1 Design criteria 88
16.2 Critical parameters 89
16.3 Index of design parameters 90
16.4 Design procedure 90
16.5 Calculation of maximum step and mesh voltages 94
16.6 Refinement of preliminary design 96
16.7 Application of equations for E_m and E_s 97
16.8 Use of computer analysis in grid design 97

17. Special areas of concern 98

Copyright © 2015 IEEE. All rights reserved.

Copyright The Institute of Electrical and Electronics Engineers, Inc.
Provided by IHS under license with IEEE
No reproduction or networking permitted without license from IHS

Order Number: 02120914
Sold to:EGAT [700166108393] - VARRIS.Y@EGAT.CO.TH,
Not for Resale,2016-09-15 03:57:51 UTC

17.1 Service areas 98
17.2 Switch shaft and operating handle grounding 98
17.3 Grounding of substation fence 101
17.4 Results of voltage profiles for fence grounding 104
17.5 Control cable sheath grounding 110
17.6 GIS bus extensions 111
17.7 Surge arrester grounding 111
17.8 Separate grounds 111
17.9 Transferred potentials 111

18. Construction of a grounding system 114
18.1 Ground grid construction—trench method 114
18.2 Ground grid construction—conductor plowing method 115
18.3 Installation of connections, pigtails, and ground rods 115
18.4 Construction sequence consideration for ground grid installation 116
18.5 Safety considerations during subsequent excavations 116

19. Field measurements of a constructed grounding system 116
19.1 Measurements of grounding system impedance 116
19.2 Field survey of potential contours and touch and step voltages 118
19.3 Assessment of field measurements for safe design 119
19.4 Ground grid integrity test 119
19.5 Periodic checks of installed grounding system 120

20. Physical scale models 120

Annex A (informative) Bibliography 121

Annex B (informative) Sample calculations 129
B.1 Square grid without ground rods—Example 1 130
B.2 Square grid with ground rods—Example 2 135
B.3 Rectangular grid with ground rods—Example 3 137
B.4 L-shaped grid with ground rods—Example 4 140
B.5 Equally spaced grid with ground rods in two-layer soil—Exhibit 1 143
B.6 Unequally spaced grid with ground rods in uniform soil—Exhibit 2 143

Annex C (informative) Graphical and approximate analysis of current division 146
C.1 Introduction 146
C.2 How to use the graphs and equivalent impedance table 147
C.3 Examples 148
C.4 Equations for computing line impedances 149

Annex D (informative) Simplified step and mesh equations 165

Annex E (informative) Equivalent uniform soil model for non-uniform soils 169

Annex F (informative) Parametric analysis of grounding systems 172
F.1 Uniform soil 172
F.2 Two-layer soil 183
F.3 Summary 185

Annex G (informative) Grounding methods for high-voltage stations with grounded neutrals 187
G.1 Summary 190

--`,,,,,,`,,`,,`

Annex H (informative) Benchmark 195
H.1 Overview 195
H.2 Soil analysis 195
H.3 Grounding system analysis 199
H.4 Grid current analysis (current division) 206

Copyright © 2015 IEEE. All rights reserved.

Copyright The Institute of Electrical and Electronics Engineers, Inc.
Provided by IHS under license with IEEE
No reproduction or networking permitted without license from IHS

Order Number: 02120914
Sold to:EGAT [700166108393] - VARRIS.Y@EGAT.CO.TH,
Not for Resale,2016-09-15 03:57:51 UTC

IEEE Guide for Safety in AC Substation Grounding

IMPORTANT NOTICE: IEEE Standards documents are not intended to ensure safety, security, health, or environmental protection, or ensure against interference with or from other devices or networks. Implementers of IEEE Standards documents are responsible for determining and complying with all appropriate safety, security, environmental, health, and interference protection practices and all applicable laws and regulations.

This IEEE document is made available for use subject to important notices and legal disclaimers. These notices and disclaimers appear in all publications containing this document and may be found under the heading "Important Notice" or "Important Notices and Disclaimers Concerning IEEE Documents." They can also be obtained on request from IEEE or viewed at http://standards.ieee.org/IPR/disclaimers.html.

1. Overview

1.1 Scope

This guide is primarily concerned with outdoor ac substations, either conventional or gas-insulated. Distribution, transmission, and generating plant substations are included. With proper caution, the methods described herein are also applicable to indoor portions of such substations, or to substations that are wholly indoors.

No attempt is made to cover the grounding problems peculiar to dc substations. A quantitative analysis of the effects of lightning surges is also beyond the scope of this guide.

1.2 Purpose

The intent of this guide is to provide guidance and information pertinent to safe grounding practices in ac substation design.

Copyright © 2015 IEEE. All rights reserved.

Copyright The Institute of Electrical and Electronics Engineers, Inc.
Provided by IHS under license with IEEE
No reproduction or networking permitted without license from IHS

Order Number: 02120914
Sold to:EGAT [700166108393] - VARRIS.Y@EGAT.CO.TH,
Not for Resale,2016-09-15 03:57:51 UTC

The specific purposes of this guide are to:

a) Establish, as a basis for design, safety limits of potential differences that can exist in a substation under fault conditions between points that can be contacted by the human body.

b) Review substation grounding practices with special reference to safety, and develop safety criteria for design.

c) Provide a procedure for the design of practical grounding systems, based on these criteria.

d) Develop analytical methods as an aid in the understanding and solution of typical voltage gradient problems.

e) Provide benchmarks cases to compare the results of IEEE Std 80™ equations to commercially available software programs.

The concept and use of safety criteria are described in Clause 1 through Clause 8, practical aspects of designing a grounding system are covered in Clause 9 through Clause 13, and procedures and evaluation techniques for the grounding system assessment (in terms of safety criteria) are described in Clause 14 through Clause 20. Supporting material is organized in Annex A through Annex H.

This guide is primarily concerned with safe grounding practices for power frequencies in the range of 50 Hz to 60 Hz. The problems peculiar to dc substations and the effects of lightning surges are beyond the scope of this guide. A grounding system designed as described herein will, nonetheless, provide some degree of protection against steep wave front surges entering the substation and passing to earth through its ground.

2. Normative references

The following referenced documents are indispensable for the application of this document (i.e., they must be understood and used, so each referenced document is cited in text and its relationship to this document is explained). For dated references, only the edition cited applies. For undated references, the latest edition of the referenced document (including any amendments or corrigenda) applies.

This guide should be used in conjunction with the following publications. When the following standards are superseded by an approved revision, the revision shall apply.

IEEE Std 81™, IEEE Guide for Measuring Earth Resistivity, Ground Impedance, and Earth Surface Potentials of a Grounding System.[1]

[1] IEEE publications are available from The Institute of Electrical and Electronics Engineers (http://standards.ieee.org/).

Copyright © 2015 IEEE. All rights reserved.

Copyright The Institute of Electrical and Electronics Engineers, Inc.
Provided by IHS under license with IEEE
No reproduction or networking permitted without license from IHS

Order Number: 02120914
Sold to:EGAT [700166108393] - VARRIS.Y@EGAT.CO.TH,
Not for Resale,2016-09-15 03:57:51 UTC

3. Definitions

For the purposes of this document, the following terms and definitions apply. The *IEEE Standards Dictionary Online* should be consulted for terms not defined in this clause.[2]

auxiliary ground electrode: A ground electrode with certain design or operating constraints. Its primary function may be other than conducting the ground fault current into earth.

continuous enclosure: A bus enclosure in which the consecutive sections of the housing along the same phase conductor are bonded together to provide an electrically continuous current path throughout the entire enclosure length. Cross-bondings, connecting the other phase enclosures, are made only at the extremities of the installation and at a few selected intermediate points.

dc offset: Difference between the symmetrical current wave and the actual current wave during a power system transient condition. Mathematically, the actual fault current can be broken into two parts, a symmetrical alternating component and a unidirectional (dc) component. The unidirectional component can be of either polarity, but will not change polarity, and will decrease at some predetermined rate.

decrement factor: An adjustment factor used in conjunction with the symmetrical ground fault current parameter in safety-oriented grounding calculations. It determines the rms equivalent of the asymmetrical current wave for a given fault duration, t_f, accounting for the effect of initial dc offset and its attenuation during the fault.

effective asymmetrical fault current: The rms value of asymmetrical current wave, integrated over the interval of fault duration (see Figure 1).

$$I_F = D_f \times I_f \tag{1}$$

where

I_F is the effective asymmetrical fault current in A
I_f is the rms symmetrical ground fault current in A
D_f is the decrement factor

[2] *IEEE Standards Dictionary Online* subscription is available at: http://www.ieee.org/portal/innovate/products/standard/standards_dictionary.html.

Copyright © 2015 IEEE. All rights reserved.

Copyright The Institute of Electrical and Electronics Engineers, Inc.
Provided by IHS under license with IEEE
No reproduction or networking permitted without license from IHS

Order Number: 02120914
Sold to:EGAT [700166108393] - VARRIS.Y@EGAT.CO.TH,
Not for Resale,2016-09-15 03:57:51 UTC

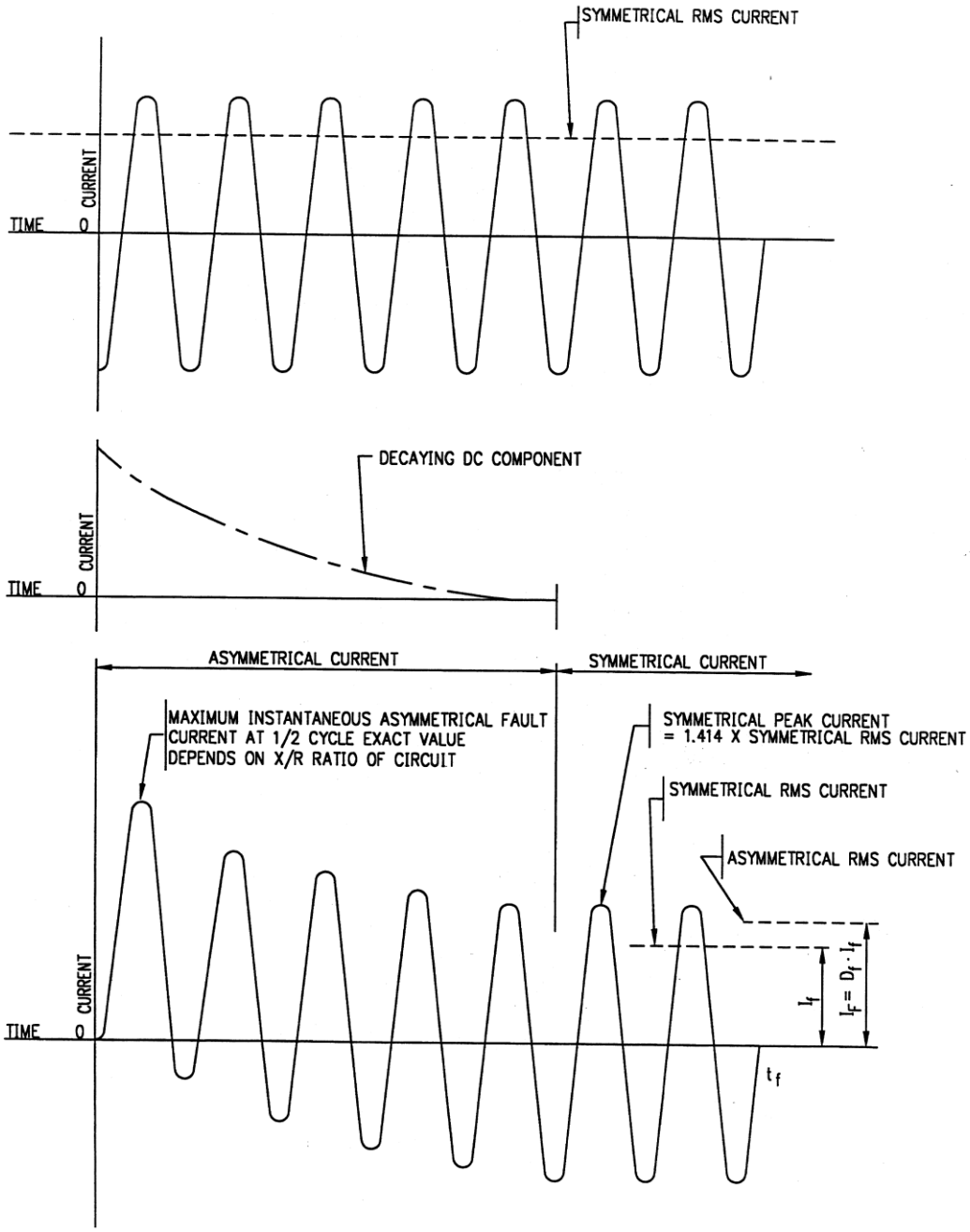

Figure 1—Relationship between actual values of fault current and values of I_F, I_f, and D_f for fault duration t_f

enclosure currents: Currents that result from the voltages induced in the metallic enclosure by the current(s) flowing in the enclosed conductor(s).

fault current division factor: A factor representing the inverse of a ratio of the symmetrical fault current to that portion of the current that flows between the ground grid and surrounding earth.

Copyright © 2015 IEEE. All rights reserved.

Copyright The Institute of Electrical and Electronics Engineers, Inc.
Provided by IHS under license with IEEE
No reproduction or networking permitted without license from IHS

Order Number: 02120914
Sold to:EGAT [700166108393] - VARRIS.Y@EGAT.CO.TH,
Not for Resale,2016-09-15 03:57:51 UTC

$$S_f = \frac{I_g}{3I_0} \tag{2}$$

where

S_f is the fault current division factor
I_g is the rms symmetrical grid current in A
I_0 is the zero-sequence fault current in A

NOTE—In reality, the current division factor would change during the fault duration, based on the varying decay rates of the fault contributions and the sequence of interrupting device operations. However, for the purposes of calculating the design value of maximum grid current and symmetrical grid current per definitions of symmetrical grid current and maximum grid current, the ratio is assumed constant during the entire duration of a given fault.[3]

gas-insulated substation (GIS): A compact, multi-component assembly, enclosed in a grounded metallic housing in which the primary insulating medium is a gas, and that normally consists of buses, switchgear, and associated equipment (subassemblies).

ground: A conducting connection, whether intentional or accidental, by which an electric circuit or equipment is connected to the earth or to some conducting body of relatively large extent that serves in place of the earth.

grounded: A system, circuit, or apparatus provided with a ground(s) for the purposes of establishing a ground return circuit and for maintaining its potential at approximately the potential of earth.

ground current: A current flowing into or out of the earth or its equivalent serving as a ground.

ground electrode: A conductor imbedded in the earth and used for collecting ground current from, or dissipating ground current into, the earth.

ground grid: A system of interconnected ground electrodes arranged in a pattern over a specified area and buried below the surface of the earth.

NOTE—Grids buried horizontally near the earth's surface are also effective in controlling the surface potential gradients. A typical grid usually is supplemented by a number of ground rods and may be further connected to auxiliary ground electrodes to lower its resistance with respect to remote earth.

ground mat: A solid metallic plate or a system of closely spaced bare conductors that are connected to and often placed in shallow depths above a ground grid or elsewhere at the earth's surface, in order to obtain an extra protective measure minimizing the danger of the exposure to high step or touch voltages in a critical operating area or places that are frequently used by people. Grounded metal gratings, placed on or above the soil surface, or wire mesh placed directly under the surface material, are common forms of a ground mat.

ground potential rise (GPR): The maximum electrical potential that a ground electrode may attain relative to a distant grounding point assumed to be at the potential of remote earth. This voltage, GPR, is equal to the maximum grid current multiplied by the grid resistance.

NOTE—Under normal conditions, the grounded electrical equipment operates at near zero ground potential. That is, the potential of a grounded neutral conductor is nearly identical to the potential of remote earth. During a ground fault the portion of fault current that is conducted by a substation ground grid into the earth causes the rise of the grid potential with respect to remote earth.

[3] Notes in text, tables, and figures of a standard are given for information only and do not contain requirements needed to implement this standard.

Copyright © 2015 IEEE. All rights reserved.

Copyright The Institute of Electrical and Electronics Engineers, Inc.
Provided by IHS under license with IEEE
No reproduction or networking permitted without license from IHS

Order Number: 02120914
Sold to:EGAT [700166108393] - VARRIS.Y@EGAT.CO.TH,
Not for Resale,2016-09-15 03:57:51 UTC

ground return circuit: A circuit in which the earth or an equivalent conducting body is utilized to complete the circuit and allow current circulation from or to its current source.

grounding system: Comprises all interconnected grounding facilities in a specific area.

main ground bus: A conductor or system of conductors provided for connecting all designated metallic components of the gas-insulated substation (GIS) to a substation grounding system.

maximum grid current: A design value of the maximum grid current, defined as follows:

$$I_G = D_f \times I_g \tag{3}$$

where

I_G is the maximum grid current in A
D_f is the decrement factor for the entire duration of fault t_f, given in s
I_g is the rms symmetrical grid current in A

mesh voltage: The maximum touch voltage within a mesh of a ground grid.

metal-to-metal touch voltage: The difference in potential between metallic objects or structures within the substation site that may be bridged by direct hand-to-hand or hand-to-feet contact.

NOTE—The metal-to-metal touch voltage between metallic objects or structures bonded to the ground grid is assumed to be negligible in conventional substations. However, the metal-to-metal touch voltage between metallic objects or structures bonded to the ground grid and metallic objects internal to the substation site, such as an isolated fence, but not bonded to the ground grid may be substantial. In the case of a gas-insulated substation (GIS), the metal-to-metal touch voltage between metallic objects or structures bonded to the ground grid may be substantial because of internal faults or induced currents in the enclosures.

In a conventional substation, the worst touch voltage is usually found to be the potential difference between a hand and the feet at a point of maximum reach distance. However, in the case of a metal-to-metal contact from hand-to-hand or from hand-to-feet, both situations should be investigated for the possible worst reach conditions. Figure 12 and Figure 13 illustrate these situations for air-insulated substations, and Figure 14 illustrates these situations in GIS.

non-continuous enclosure: A bus enclosure with the consecutive sections of the housing of the same phase conductor electrically isolated (or insulated from each other), so that no current can flow beyond each enclosure section.

primary ground electrode: A ground electrode specifically designed or adapted for discharging the ground fault current into the ground, often in a specific discharge pattern, as required (or implicitly called for) by the grounding system design.

step voltage: The difference in surface potential that could be experienced by a person bridging a distance of 1 m with the feet without contacting any grounded object.

subtransient reactance: Reactance of a generator at the initiation of a fault. This reactance is used in calculations of the initial symmetrical fault current. The current continuously decreases, but it is assumed to be steady at this value as a first step, lasting approximately 0.05 s after an applied fault.

surface material: A material installed over the soil consisting of, but not limited to, rock or crushed stone, asphalt, or man-made materials. The surfacing material, depending on the resistivity of the material, may significantly impact the body current for touch and step voltages involving the person's feet.

Copyright © 2015 IEEE. All rights reserved.

Copyright The Institute of Electrical and Electronics Engineers, Inc.
Provided by IHS under license with IEEE
No reproduction or networking permitted without license from IHS

Order Number: 02120914
Sold to:EGAT [700166108393] - VARRIS.Y@EGAT.CO.TH,
Not for Resale,2016-09-15 03:57:51 UTC

symmetrical grid current: That portion of the symmetrical ground fault current that flows between the ground grid and surrounding earth. It may be expressed as

$$I_g = S_f \times I_f \tag{4}$$

where

I_g is the rms symmetrical grid current in A

I_f is the rms symmetrical ground fault current in A

S_f is the fault current division factor

symmetrical ground fault current: The maximum rms value of symmetrical fault current after the instant of a ground fault initiation. As such, it represents the rms value of the symmetrical component in the first half-cycle of a current wave that develops after the instant of fault at time zero. For phase-to-ground faults

$$I_{f(0+)} = 3I_0'' \tag{5}$$

where

$I_{f(0+)}$ is initial rms symmetrical ground fault current

I_0'' is the rms value of zero-sequence symmetrical current that develops immediately after the instant of fault initiation, reflecting the subtransient reactance of rotating machines contributing to the fault

This rms symmetrical fault current is shown in an abbreviated notation as I_f, or is referred to only as $3I_0$. The underlying reason for the latter notation is that, for purposes of this guide, the initial symmetrical fault current is assumed to remain constant for the entire duration of the fault.

touch voltage: The potential difference between the ground potential rise (GPR) of a ground grid or system and the surface potential at the point where a person could be standing while at the same time having a hand in contact with a grounded structure. Touch voltage measurements can be “open circuit” (without the equivalent body resistance included in the measurement circuit) or “closed circuit” (with the equivalent body resistance included in the measurement circuit).

transferred voltage: A special case of the touch voltage where a voltage is transferred into or out of the substation from or to a remote point external to the substation site.

transient enclosure voltage (TEV): Very fast transient phenomena, which are found on the grounded enclosure of gas-insulated substation (GIS) systems. Typically, ground leads are too long (inductive) at the frequencies of interest to effectively prevent the occurrence of TEV. The phenomenon is also known as transient ground rise (TGR) or transient ground potential rise (TGPR).

very fast transient (VFT): A class of transients generated internally within a gas-insulated substation (GIS) characterized by short duration and very high frequency. VFT is generated by the rapid collapse of voltage during breakdown of the insulating gas, either across the contacts of a switching device or line-to-ground during a fault. These transients can have rise times in the order of nanoseconds, implying a frequency content extending to about 100 MHz. However, dominant oscillation frequencies, which are related to physical lengths of GIS bus, are usually in the 20 MHz to 40 MHz range.

Copyright © 2015 IEEE. All rights reserved.

Copyright The Institute of Electrical and Electronics Engineers, Inc.
Provided by IHS under license with IEEE
No reproduction or networking permitted without license from IHS

Order Number: 02120914
Sold to:EGAT [700166108393] - VARRIS.Y@EGAT.CO.TH,
Not for Resale,2016-09-15 03:57:51 UTC

very fast transients overvoltage (VFTO): System overvoltages that result from generation of VFT. While VFT is one of the main constituents of VFTO, some lower frequency (≅ 1 MHz) component may be present as a result of the discharge of lumped capacitance (voltage transformers). Typically, VFTO will not exceed 2.0 per unit, though higher magnitudes are possible in specific instances.

***X/R* ratio**: Ratio of the system reactance to resistance. It is indicative of the rate of decay of any dc offset. A large *X/R* ratio corresponds to a large time constant and a slow rate of decay.

4. Safety in grounding

4.1 Basic problem

In principle, a safe grounding design has the following two objectives:

— To provide means to carry electric currents into the earth under normal and fault conditions without exceeding any operating and equipment limits or adversely affecting continuity of service.

— To reduce the risk of a person in the vicinity of grounded facilities being exposed to the danger of critical electric shock.

A practical approach to safe grounding thus concerns and strives for controlling the interaction of two grounding systems, as follows:

— The intentional ground, consisting of ground electrodes buried at some depth below the earth's surface.

— The accidental ground, temporarily established by a person exposed to a potential gradient in the vicinity of a grounded facility.

People often assume that any grounded object can be safely touched. A low substation ground resistance is not, in itself, a guarantee of safety. There is no simple relation between the resistance of the ground system as a whole and the maximum shock current to which a person might be exposed. Therefore, a substation of relatively low ground resistance may be dangerous, while another substation with very high resistance may be less dangerous or can be made less dangerous by careful design. For instance, if a substation is supplied from an overhead line with no shield or neutral wire, a low grid resistance is important. Most, or all, of the total ground fault current enters the earth causing an often steep rise of the local ground potential [see Figure 2(a)]. If a shield wire, neutral wire, gas-insulated bus, or underground cable feeder, etc., is used, a part of the fault current returns through this metallic path directly to the source. Since this metallic link provides a low impedance parallel path to the return circuit, the rise of local ground potential is ultimately of lesser magnitude [see Figure 2(b)]. In either case, the effect of that portion of fault current that enters the earth within the substation area should be further analyzed. If the geometry, location of ground electrodes, local soil characteristics, and other factors contribute to an excessive potential gradient at the earth's surface, the grounding system may be inadequate despite its capacity to carry the fault current in magnitudes and durations permitted by protective relays.

Clause 5 through Clause 8 detail those principal assumptions and criteria that enable the evaluation of important factors for reducing the risk to human life.

Copyright © 2015 IEEE. All rights reserved.

Copyright The Institute of Electrical and Electronics Engineers, Inc.
Provided by IHS under license with IEEE
No reproduction or networking permitted without license from IHS

Order Number: 02120914
Sold to:EGAT [700166108393] - VARRIS.Y@EGAT.CO.TH,
Not for Resale,2016-09-15 03:57:51 UTC

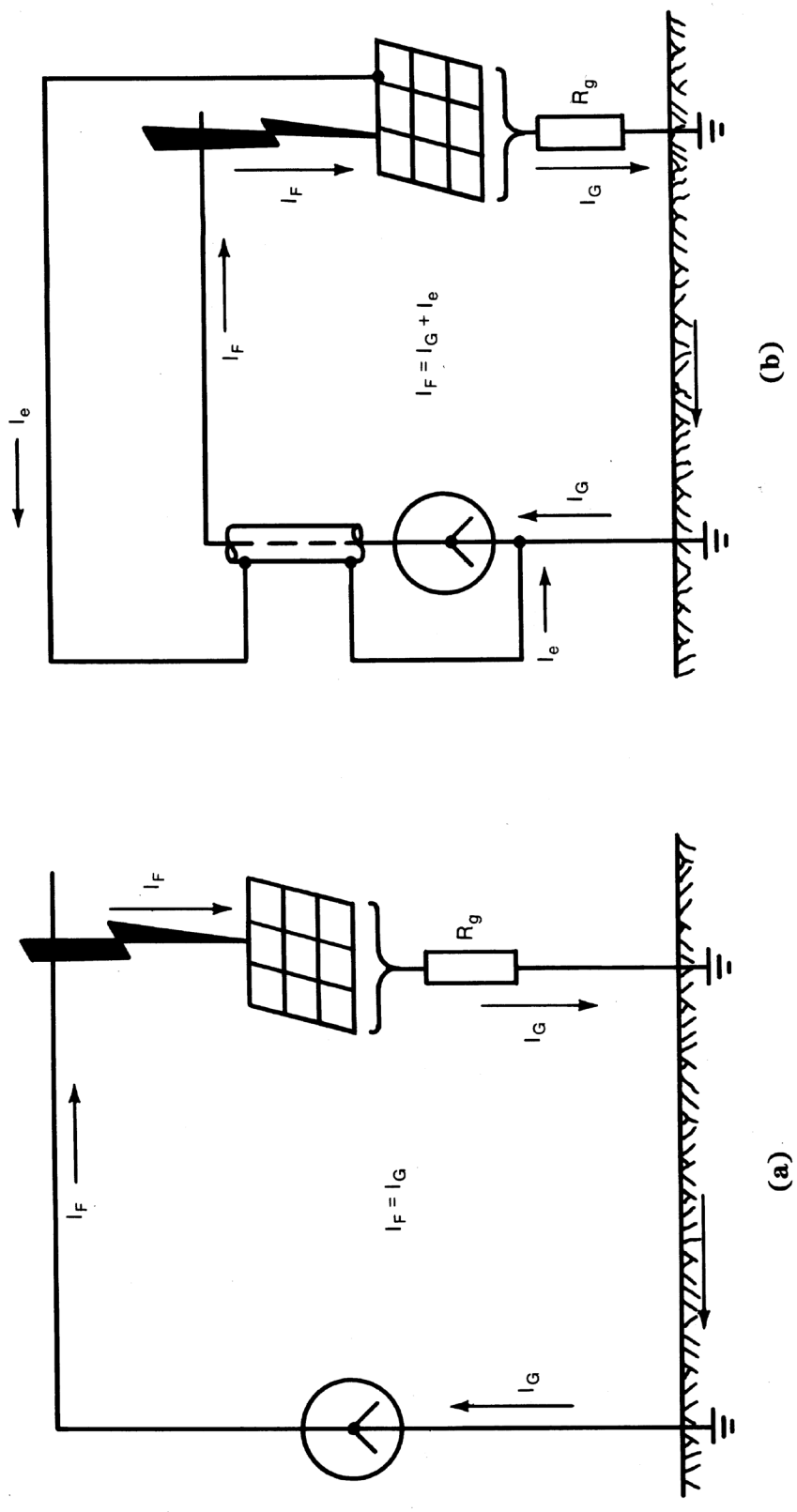

Figure 2—Faulted substation with and without multiple grounds

Copyright © 2015 IEEE. All rights reserved.

Copyright The Institute of Electrical and Electronics Engineers, Inc.
Provided by IHS under license with IEEE
No reproduction or networking permitted without license from IHS

Order Number: 02120914
Sold to:EGAT [700166108393] - VARRIS.Y@EGAT.CO.TH,
Not for Resale,2016-09-15 03:57:51 UTC

4.2 Conditions of danger

During typical ground fault conditions, the flow of current to earth will produce potential gradients within and around a substation. Figure 3 shows this effect for a substation with a simple rectangular ground grid in homogeneous soil.

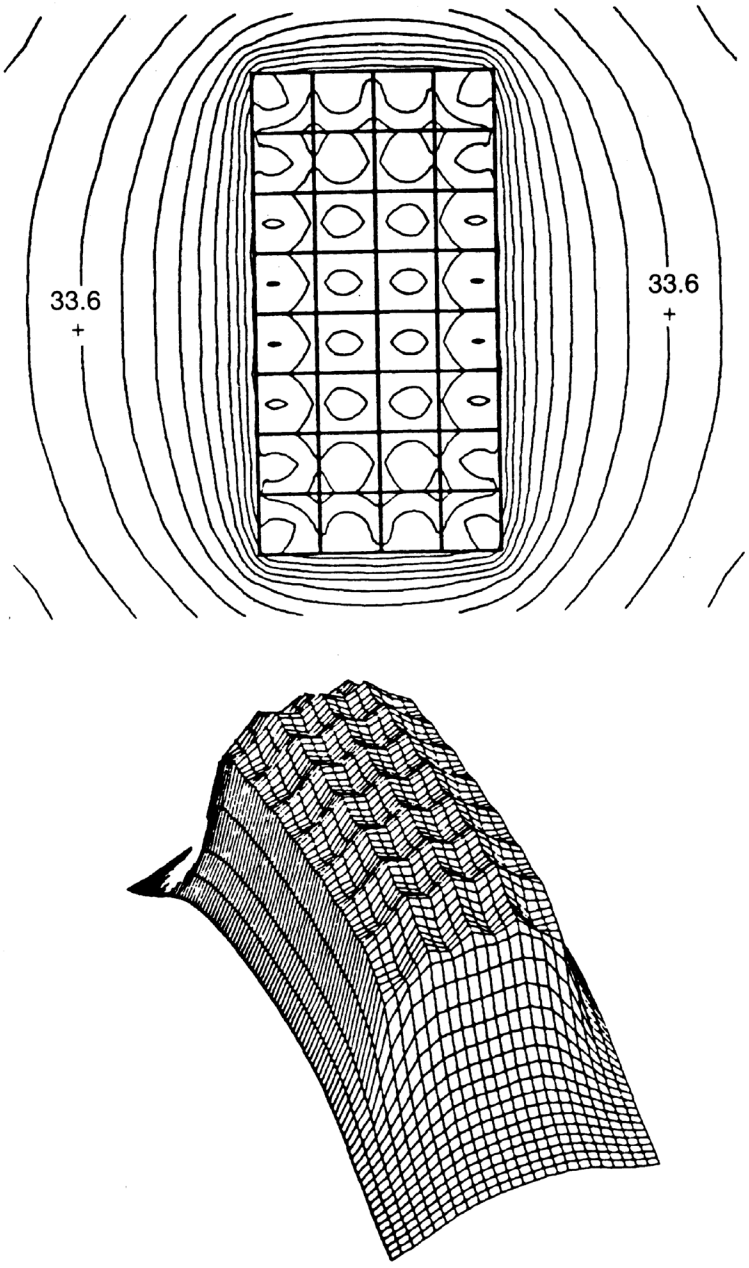

Figure 3—Equipotential contours of a typical ground grid

Copyright © 2015 IEEE. All rights reserved.

Copyright The Institute of Electrical and Electronics Engineers, Inc.
Provided by IHS under license with IEEE
No reproduction or networking permitted without license from IHS

Order Number: 02120914
Sold to:EGAT [700166108393] - VARRIS.Y@EGAT.CO.TH,
Not for Resale,2016-09-15 03:57:51 UTC

Unless proper precautions are taken in design, the maximum potential gradients along the earth's surface may be of sufficient magnitude during ground fault conditions to endanger a person in the area. Moreover, dangerous voltages may develop between grounded structures or equipment frames and the nearby earth.

The circumstances that make electric shock accidents possible can include the following:

a) Relatively high fault current to ground in relation to the area of ground system and its resistance to remote earth.

b) Soil resistivity and distribution of ground currents such that high potential gradients may occur at points at the earth's surface.

c) Presence of an individual at such a point, time, and position that the body is bridging two points of high potential difference.

d) Absence of sufficient contact resistance or other series resistance to limit current through the body to a safe value under circumstances a) through c).

e) Duration of the fault and body contact, and hence, of the flow of current through a human body for a sufficient time to cause harm at the given current intensity.

The relative low frequency of accidents is due largely to the low probability of coincidence of all the unfavorable conditions listed above.

5. Range of tolerable current

Effects of an electric current passing through the vital parts of a human body depend on the duration, magnitude, and frequency of this current. The most dangerous consequence of such an exposure is a heart condition known as ventricular fibrillation, resulting in immediate arrest of blood circulation.

5.1 Effect of frequency

Humans are very vulnerable to the effects of electric current at frequencies of 50 Hz or 60 Hz. Currents of approximately 0.1 A can be lethal. Research indicates that the human body can tolerate a slightly higher 25 Hz current and approximately five times higher direct current. At frequencies of 3000 Hz to 10 000 Hz, even higher currents can be tolerated (Dalziel and Mansfield [B34][4]; Dalziel, Ogden, and Abbott [B37]). In some cases the human body is able to tolerate very high currents due to lightning surges. The International Electrotechnical Commission provides curves for the tolerable body current as a function of frequency and for capacitive discharge currents (IEC 60479-2 (1987-03) [B84]). Other studies of the effects of both direct and oscillatory impulse currents are reported in Dalziel [B26][B28].

Information regarding special problems of dc grounding is contained in the 1957 report of the AIEE Substations Committee [B22]. The hazards of an electric shock produced by the electrostatic effects of overhead transmission lines are reviewed in Part 1 of the 1972 report of the General Systems Subcommittee [B91]. Additional information on the electrostatic effects of overhead transmission lines can be found in Chapter 8 of the EPRI Transmission Line Reference Book 345 kV and Above [B59].

[4] The numbers in brackets correspond to those of the bibliography in Annex A.

Copyright © 2015 IEEE. All rights reserved.

Copyright The Institute of Electrical and Electronics Engineers, Inc.
Provided by IHS under license with IEEE
No reproduction or networking permitted without license from IHS

Order Number: 02120914
Sold to:EGAT [700166108393] - VARRIS.Y@EGAT.CO.TH,
Not for Resale,2016-09-15 03:57:51 UTC

5.2 Effect of magnitude and duration

The most common physiological effects of electric current on the body, stated in order of increasing current magnitude, are threshold perception, muscular contraction, unconsciousness, fibrillation of the heart, respiratory nerve blockage, and burning (Geddes and Baker [B75]; IEC 60479-1 (1994-09) [B83]).

Current of 1 mA is generally recognized as the threshold of perception; that is, the current magnitude at which a person is just able to detect a slight tingling sensation in his hands or fingertips caused by the passing current (Dalziel [B27]).

Currents of 1 mA to 6 mA, often termed let-go currents, though unpleasant to sustain, generally do not impair the ability of a person holding an energized object to control his muscles and release it. Dalziel's classic experiment with 28 women and 134 men provides data indicating an average let-go current of 10.5 mA for women and 16 mA for men, and 6 mA and 9 mA as the respective threshold values (Dalziel and Massogilia [B35]).

In the 9 mA to 25 mA range, currents may be painful and can make it difficult or impossible to release energized objects grasped by the hand. For still higher currents muscular contractions could make breathing difficult. These effects are not permanent and disappear when the current is interrupted, unless the contraction is very severe and breathing is stopped for minutes rather than seconds. Yet even such cases often respond to resuscitation (Dalziel [B30]).

In the range of 60 mA to 100 mA are reached that ventricular fibrillation, stoppage of the heart, or inhibition of respiration might occur and cause injury or death. A person trained in cardiopulmonary resuscitation (CPR) should administer CPR after the current source is removed and it is safe to do so, until the victim can be treated at a medical facility (Dalziel [B31]; Dalziel and Lee [B32]).

Hence, this guide emphasizes the importance of the fibrillation threshold. If shock currents can be kept below this value by a carefully designed grounding system, injury or death may be avoided.

As shown by Dalziel and others (Dalziel, Lagen, and Thurston [B36]; Dalziel and Massogilia [B35]), the non-fibrillating current of magnitude I_B at durations ranging from 0.03 s to 3.0 s is related to the energy absorbed by the body as described by the following equation:

$$S_B = (I_B)^2 \times t_s \tag{6}$$

where

I_B is the rms magnitude of the current through the body in A

t_s is the duration of the current exposure in *s*

S_B is the empirical constant related to the electric shock energy tolerated by a certain percent of a given population

A more detailed discussion of Equation (6) is provided in Clause 6.

5.3 Importance of high-speed fault clearing

Considering the significance of fault duration both in terms of Equation (6) and implicitly as an accident-exposure factor, high-speed clearing of ground faults can be advantageous for two reasons:

a) The probability of exposure to electric shock can be reduced by fast fault clearing time, in contrast to situations in which fault currents could persist for several minutes or possibly hours.

Copyright © 2015 IEEE. All rights reserved.

Copyright The Institute of Electrical and Electronics Engineers, Inc.
Provided by IHS under license with IEEE
No reproduction or networking permitted without license from IHS

Order Number: 02120914
Sold to:EGAT [700166108393] - VARRIS.Y@EGAT.CO.TH,
Not for Resale,2016-09-15 03:57:51 UTC

b) Tests and experience show that the chance of severe injury or death can be reduced if the duration of a current flow through the body is very brief.

The allowed current value may, therefore, be based on the clearing time of primary protective devices, or that of the backup protection. A good case could be made for using the primary clearing time because of the low combined probability that relay malfunctions will coincide with all other adverse factors necessary for an accident, as described in Clause 4. It is more conservative to choose the backup relay clearing times in Equation (6), because they provide greater safety margin.

An additional incentive to use switching times less than 0.5 s results from the research done by Biegelmeier and Lee [B9]. Their research provides evidence that a human heart becomes increasingly susceptible to ventricular fibrillation when the time of exposure to current is approaching the heartbeat period, but that the danger is smaller if the time of exposure to current is in the region of 0.06 s to 0.3 s.

In reality, high ground gradients from faults are usually infrequent, and shocks from high ground gradients are also infrequent. Further, both events are often of very short duration. Thus, it would not be practical to design against shocks that are merely painful and do not cause serious injury; that is, for currents below the fibrillation threshold.

6. Tolerable body current limit

The magnitude and duration of the current conducted through a human body at 50 Hz or 60 Hz should be less than the value that can cause ventricular fibrillation of the heart.

6.1 Duration formula

The duration for which a 50 Hz or 60 Hz current can be tolerated by most people is related to its magnitude in accordance with Equation (6). Based on the results of Dalziel's studies (Dalziel [B27]; Dalziel and Lee [B33]), it is assumed that 99.5% of all persons can safely withstand, without ventricular fibrillation, the passage of a current with magnitude and duration determined by the following formula:

$$I_B = \frac{k}{\sqrt{t_s}} \tag{7}$$

where, in addition to the terms previously defined for Equation (6)

$$k = \sqrt{S_B}$$

Dalziel found that the shock energy that can be survived by 99.5% of persons weighing approximately 50 kg (110 lb) results in a value of S_B of 0.0135. Thus, $k_{50} = 0.116$ and the formula for the allowable body current becomes

$$I_B = \frac{0.116}{\sqrt{t_s}} \text{ for 50 kg body weight} \tag{8}$$

Equation (8) results in values of 116 mA for $t_s = 1$ s and 367 mA for $t_s = 0.1$ s.

Because Equation (7) is based on tests limited to a range of between 0.03 s and 3.0 s, it obviously is not valid for very short or long durations.

Copyright © 2015 IEEE. All rights reserved.

Copyright The Institute of Electrical and Electronics Engineers, Inc.
Provided by IHS under license with IEEE
No reproduction or networking permitted without license from IHS

Order Number: 02120914
Sold to:EGAT [700166108393] - VARRIS.Y@EGAT.CO.TH,
Not for Resale,2016-09-15 03:57:51 UTC

Over the years, other researchers have suggested other values for I_B. In 1936 Ferris et al. [B67] suggested 100 mA as the fibrillation threshold. The value of 100 mA was derived from extensive experiments at Columbia University. In the experiments, animals having body and heart weights comparable to humans were subjected to maximum shock durations of 3 s. Some of the more recent experiments suggest the existence of two distinct thresholds: one where the shock duration is shorter than one heartbeat period and another one for the current duration longer than one heartbeat. For a 50 kg (110 lb) adult, Biegelmeier [B8][B10] proposed the threshold values at 500 mA and 50 mA, respectively. Other studies on this subject were carried out by Lee [B102] and Kouwenhoven [B98]. The equation for tolerable body current developed by Dalziel is the basis for the derivation of tolerable voltages used in this guide.

6.2 Alternative assumptions

Fibrillation current is assumed to be a function of individual body weight, as illustrated in Figure 4. The figure shows the relationship between the critical current and body weight for several species of animals (calves, dogs, sheep, and pigs), and a 0.5% common threshold region for mammals.

In the 1961 edition of this guide, constants S_B and k in Equation (6) and Equation (7), were given as 0.0272 and 0.165, respectively, and had been assumed valid for 99.5% of all people weighing approximately 70 kg (155 lb). Further studies by Dalziel [B29] and Dalziel and Lee [B33], on which Equation (7) is based, lead to the alternate value of k = 0.157 and S_B = 0.0246 as being applicable to persons weighing 70 kg (155 lb). Thus

$$I_B = \frac{0.157}{\sqrt{t_s}} \text{ for 70 kg body weight} \tag{9}$$

Users of this guide may select k = 0.157 provided that the average population weight can be expected to be at least 70 kg.[5]

[5] Typically, these conditions can be met in places that are not accessible to the public, such as in switchyards protected by fences or walls, etc. Depending on specific circumstances, an assessment should be made if a 50 kg criterion Equation (8) ought to be used for areas outside the fence.

Copyright © 2015 IEEE. All rights reserved.

Copyright The Institute of Electrical and Electronics Engineers, Inc.
Provided by IHS under license with IEEE
No reproduction or networking permitted without license from IHS

Order Number: 02120914
Sold to:EGAT [700166108393] - VARRIS.Y@EGAT.CO.TH,
Not for Resale,2016-09-15 03:57:51 UTC

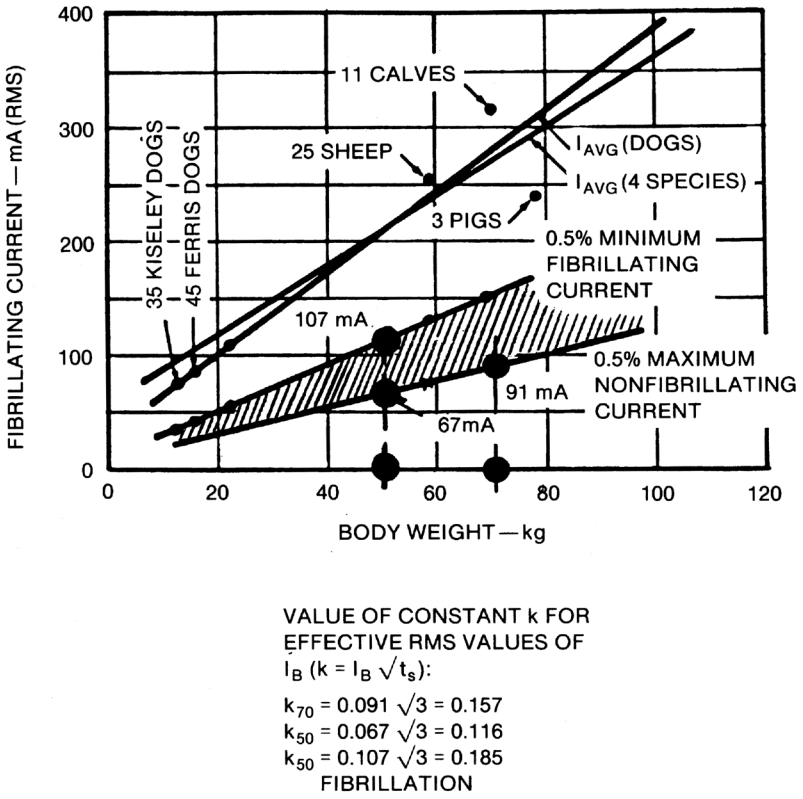

Figure 4—Fibrillating current versus body weight for various animals based on a 3 s duration of the electrical shock

Equation (7) indicates that much higher body currents can be allowed where fast-operating protective devices can be relied upon to limit the fault duration. A judgment decision is needed as to whether to use the clearing time of primary high-speed relays, or that of the back-up protection, as the basis for calculation.

6.3 Comparison of Dalziel's equations and Biegelmeier's curve

The comparison of Equation (8), Equation (9), and the Z-shaped curve of body current versus time developed by Biegelmeier that was published by Biegelmeier and Lee [B9] is shown in Figure 5. The Z curve has a 500 mA limit for short times up to 0.2 s, then decreases to 50 mA at 2.0 s and beyond.

Using Equation (8), the tolerable body current will be less than Biegelmeier's Z curve for times from 0.06 s to 0.7 s.

Copyright © 2015 IEEE. All rights reserved.

Copyright The Institute of Electrical and Electronics Engineers, Inc.
Provided by IHS under license with IEEE
No reproduction or networking permitted without license from IHS

Order Number: 02120914
Sold to:EGAT [700166108393] - VARRIS.Y@EGAT.CO.TH,
Not for Resale,2016-09-15 03:57:51 UTC

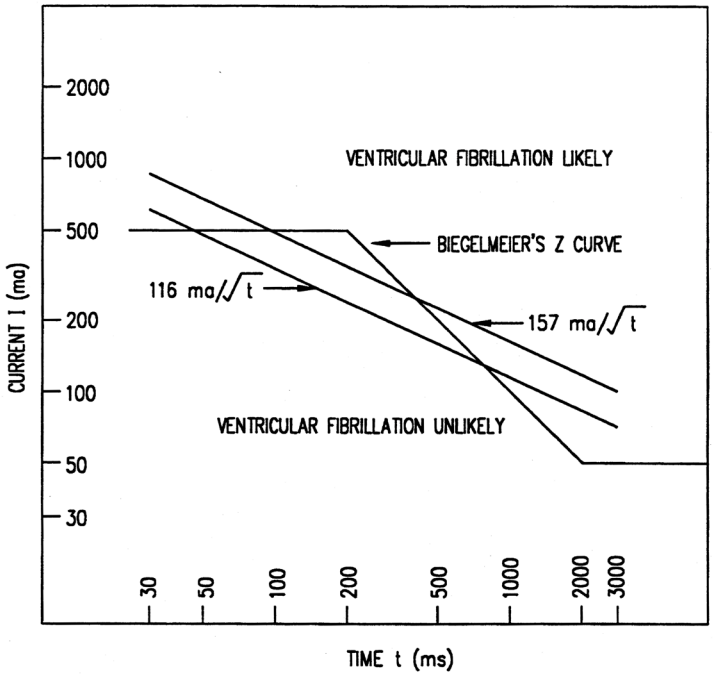

Figure 5—Body current versus time

6.4 Note on reclosing

Reclosure after a ground fault is common in modern operating practice. In such circumstances, a person might be subjected to the first shock without permanent injury. Next, a single instantaneous automatic reclosure could result in a second shock, initiated within less than 0.33 s from the start of the first. It is this second shock, occurring after a relatively short interval of time before the person has recovered, that might cause a serious accident. With manual reclosure, the possibility of exposure to a second shock can be reduced because the reclosing time interval may be substantially greater.

The cumulative effect of two or more closely spaced shocks has not been thoroughly evaluated, but a reasonable allowance can be made by using the sum of individual shock durations as the time of a single exposure.

7. Accidental ground circuit

7.1 Resistance of the human body

For dc and 50 Hz or 60 Hz ac currents, the human body can be approximated by a resistance. The current path typically considered is from one hand to both feet, or from one foot to the other one. The internal resistance of the body is approximately 300 Ω, whereas values of body resistance including skin range from 500 Ω to 3000 Ω, as suggested in Daziel [B27], Geddes and Baker [B75], Gieiges [B76], Kiselev [B97], and Osypka [B121]. The human body resistance is decreased by damage or puncture of the skin at the point of contact.

Copyright © 2015 IEEE. All rights reserved.

Copyright The Institute of Electrical and Electronics Engineers, Inc.
Provided by IHS under license with IEEE
No reproduction or networking permitted without license from IHS

Order Number: 02120914
Sold to:EGAT [700166108393] - VARRIS.Y@EGAT.CO.TH,
Not for Resale,2016-09-15 03:57:51 UTC

As mentioned in 5.2, Dalziel [B35] conducted extensive tests using saltwater to wet hands and feet to determine safe let-go currents, with hands and feet wet. Values obtained using 60 Hz for men were as follows: the current was 9.0 mA; corresponding voltages were 21.0 V for hand-to-hand and 10.2 V for hand-to-feet. Hence, the ac resistance for a hand-to-hand contact is equal to 21.0/0.009 or 2330 Ω, and the hand-to-feet resistance equals 10.2/0.009 or 1130 Ω, based on this experiment.

Thus, for the purposes of this guide, the following resistances, in series with the body resistance, are assumed as follows:

a) Hand and foot contact resistances are equal to zero.

b) Glove and shoe resistances are equal to zero.

A value of 1000 Ω in Equation (10), which represents the resistance of a human body from hand-to-feet and also from hand-to-hand, or from one foot to the other foot, will be used throughout this guide.

$$R_B = 1000\ \Omega \tag{10}$$

7.2 Current paths through the body

It should be remembered that the choice of a 1000 Ω resistance value relates to paths such as those between the hand and one foot or both feet, where a major part of the current passes through parts of the body containing vital organs, including the heart. It is generally agreed that current flowing from one foot to the other is far less dangerous. Referring to tests done in Germany, Loucks [B103] mentioned that much higher foot-to-foot than hand-to-foot currents had to be used to produce the same current in the heart region. He stated that the ratio is as high as 25:1.

Based on these conclusions, resistance values greater than 1000 Ω could possibly be allowed, where a path from one foot to the other foot is concerned. However, the following factors should be considered:

a) A voltage between the two feet, painful but not fatal, might result in a fall that could cause a larger current flow through the chest area. The degree of this hazard would further depend on the fault duration and the possibility of another successive shock, perhaps on reclosure.

b) A person might be working or resting in a prone position when a fault occurs.

The dangers from foot-to-foot contact appear to be less than from the other type. However, since deaths have occurred from case a) above, it is a danger that should not be ignored (Bodier [B15]; Langer [B99]).

7.3 Accidental circuit equivalents

Using the value of tolerable body current established by either Equation (8) or Equation (9) and the appropriate circuit constants, it is possible to determine the tolerable voltage between any two points of contact.

The following notations are used for the accidental circuit equivalent shown in Figure 6:

I_f is the total fault current in A
I_g is the current flowing in the grid in A
I_b is the body current (body is part of the accidental circuit) in A
R_B is the resistance of the body in Ω
U is the total effective voltage of the accidental circuit (touch or step voltage) in V
H and F are points of contact of the body

Copyright © 2015 IEEE. All rights reserved.

Copyright The Institute of Electrical and Electronics Engineers, Inc.
Provided by IHS under license with IEEE
No reproduction or networking permitted without license from IHS

Order Number: 02120914
Sold to:EGAT [700166108393] - VARRIS.Y@EGAT.CO.TH,
Not for Resale,2016-09-15 03:57:51 UTC

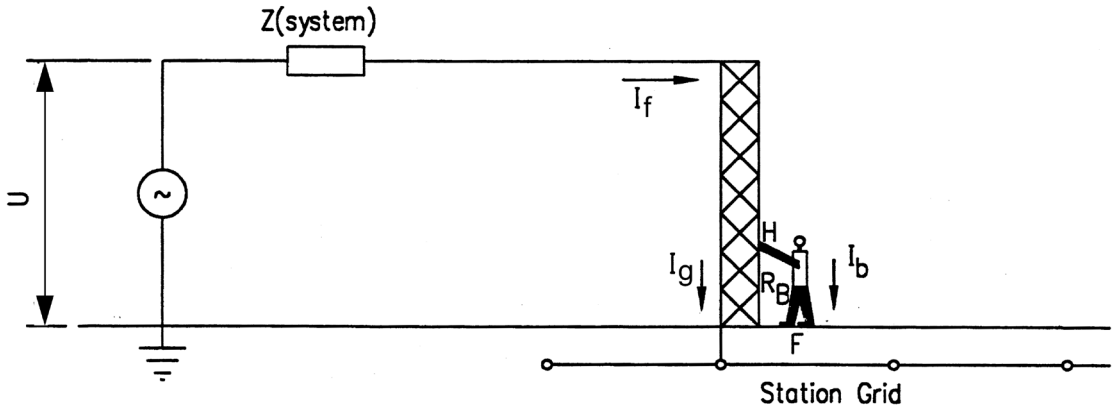

Figure 6—Exposure to touch voltage

The tolerable body current, I_B, defined by Equation (8) or Equation (9), is used to define the tolerable total effective voltage of the accidental circuit (touch or step voltage). The tolerable total effective voltage of the accidental circuit is that voltage that will cause the flow of a body current, I_b, equal to the tolerable body current, I_B .

Figure 6 shows the fault current I_f being discharged to the ground by the grounding system of the substation and a person touching a grounded metallic structure at H. Various impedances in the circuit are shown in Figure 7. Terminal H is a point in the system at the same potential as the grid into which the fault current flows and terminal F is the small area on the surface of the earth that is in contact with the person's two feet. The current, I_b, flows from H through the body of the person to the ground at F. The Thevenin theorem allows us to represent this two terminal (H, F) network of Figure 7 by the circuit shown in Figure 8 (Dawalibi, Southey, and Baishiki [B50]; Dawalibi, Xiong, and Ma [B51]).

The Thevenin voltage V_{Th} is the voltage between terminals H and F when the person is not present. The Thevenin impedance Z_{Th} is the impedance of the system as seen from points H and F with voltage sources of the system short-circuited. The current I_b through the body of a person coming in contact with H and F is given by

$$I_b = \frac{V_{Th}}{Z_{Th} + R_B} \tag{11}$$

where

R_B is the resistance of the human body in Ω

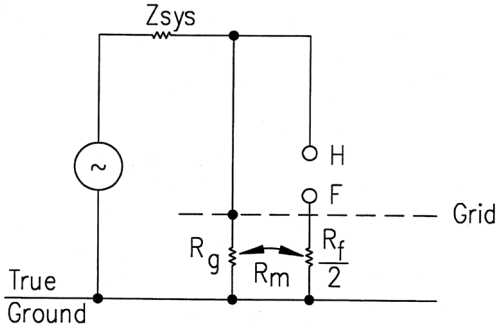

Figure 7—Impedances to touch voltage circuit

Copyright © 2015 IEEE. All rights reserved.
Copyright The Institute of Electrical and Electronics Engineers, Inc.
Provided by IHS under license with IEEE
No reproduction or networking permitted without license from IHS
Order Number: 02120914
Sold to:EGAT [700166108393] - VARRIS.Y@EGAT.CO.TH,
Not for Resale,2016-09-15 03:57:51 UTC

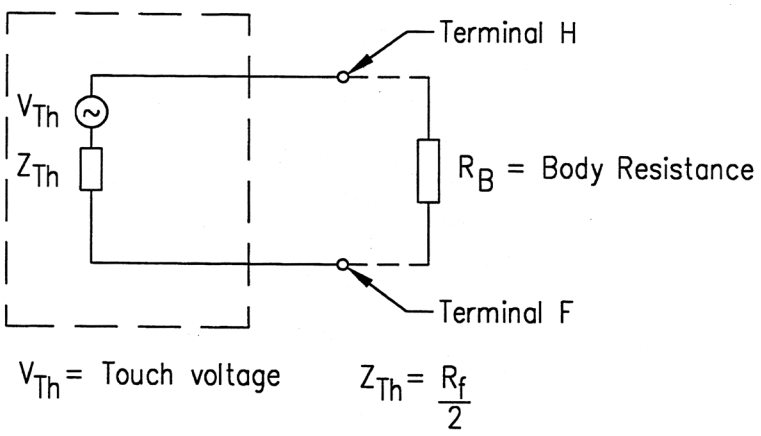

Figure 8—Touch voltage circuit

For most practical cases, the effects of Z_{sys}, grid resistance and the mutual resistance between the grid and the person's feet can be neglected on the total circuit Thevenin equivalent impedance. Thus, Z_{Th} is represented by the equivalent impedance of the person's feet.

Figure 9 shows the fault current I_f being discharged to the ground by the grounding system of the substation. The current, I_b, flows from one foot F_1 through the body of the person to the other foot, F_2. Terminals F_1 and F_2 are the areas on the surface of the earth that are in contact with the two feet, respectively. The Thevenin theorem allows us to represent this two-terminal (F_1, F_2) network in Figure 10. The Thevenin voltage V_{Th} is the voltage between terminals F_1 and F_2 when the person is not present. The Thevenin impedance Z_{Th} is the impedance of the system as seen from the terminals F1 and F2 with the voltage sources of the system short-circuited. The current I_b through the body of a person is given by Equation (11).

The Thevenin equivalent impedance, Z_{Th}, is computable with a number of methods (Dawalibi, Southey, and Baishiki [B50]; Dawalibi, Xiong, and Ma [B51]; ERPI EL-2699 [B61]; Thapar, Gerez, and Kejriwal [B147]; Laurent [B100]).

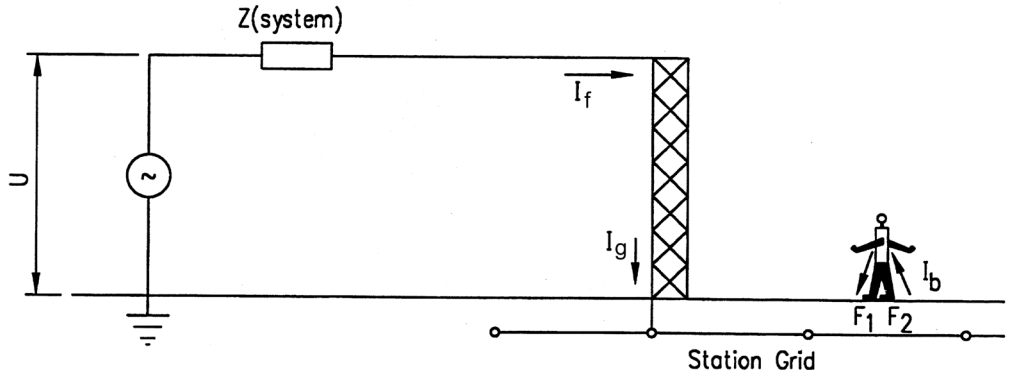

Figure 9—Exposure to step voltage

Copyright © 2015 IEEE. All rights reserved.
Copyright The Institute of Electrical and Electronics Engineers, Inc.
Provided by IHS under license with IEEE
No reproduction or networking permitted without license from IHS
Order Number: 02120914
Sold to:EGAT [700166108393] - VARRIS.Y@EGAT.CO.TH,
Not for Resale,2016-09-15 03:57:51 UTC

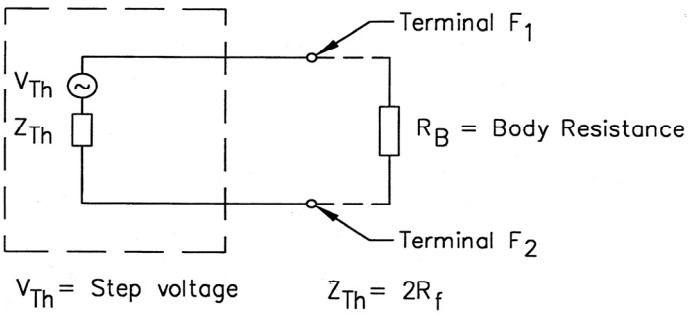

Figure 10—Step voltage circuit

In this guide, the following formulas for the Thevenin equivalent impedance are used.

For touch voltage accidental circuit

$$Z_{Th} = \frac{R_f}{2} \tag{12}$$

And for the step voltage accidental circuit

$$Z_{Th} = 2R_f \tag{13}$$

where

R_f is the ground resistance of one foot (with presence of the substation grounding system ignored) in Ω

For the purpose of circuit analysis, the human foot is usually represented as a conducting metallic disc and the contact resistance of shoes, socks, etc., is neglected. The ground resistance in ohms of a metallic disc of radius b (m) on the surface of a homogeneous earth of resistivity ρ (Ω-m) is given by Laurent [B100].

$$R_f = \frac{\rho}{4b} \tag{14}$$

Traditionally, the metallic disc representing the foot is taken as a circular plate with a radius of 0.08 m. With only slight approximation, equations for Z_{Th} can be obtained in numerical form and expressed in terms of ρ as follows.

For touch voltage accidental circuit

$$Z_{Th} = 1.5\rho \tag{15}$$

And for step voltage accidental circuit

$$Z_{Th} = 6.0\rho \tag{16}$$

Based on investigation reported in Dawalibi, Xiong, and Ma [B51]; Meliopoulos, Xia, Joy, and Cokkonides [B110]; and Thapar, Gerez, and Kejriwal [B147], Equation (15) and Equation (16) are conservative in the sense that they underestimate the Thevenin equivalent impedance for uniform soil and, therefore, will result in higher body currents.

Copyright © 2015 IEEE. All rights reserved.

Copyright The Institute of Electrical and Electronics Engineers, Inc.
Provided by IHS under license with IEEE
No reproduction or networking permitted without license from IHS

Order Number: 02120914
Sold to:EGAT [700166108393] - VARRIS.Y@EGAT.CO.TH,
Not for Resale,2016-09-15 03:57:51 UTC

The permissible total equivalent voltage (i.e., tolerable touch and step voltage), using Equation (15) and Equation (16), is

$$E_{touch} = I_B(R_B + 1.5\rho) \tag{17}$$

and

$$E_{step} = I_B(R_B + 6.0\rho) \tag{18}$$

7.4 Effect of a thin layer of surface material

Equation (14) is based on the assumption of uniform soil resistivity. However, a 0.08 m to 0.15 m (3 in to 6 in) layer of high resistivity material, such as gravel, is often spread on the earth's surface above the ground grid to increase the contact resistance between the soil and the feet of persons in the substation. The relatively shallow depth of the surface material, as compared to the equivalent radius of the foot, precludes the assumption of uniform resistivity in the vertical direction when computing the ground resistance of the feet. However, for a person in the substation area, the surface material can be assumed to be of infinite extent in the lateral direction.

If the underlying soil has a lower resistivity than the surface material, such as clean large rock with wet resistivity in the thousands of Ω-m, only some grid current will go upward into the thin layer of the surface material, and the surface voltage will be very nearly the same as that without the surface material. The current through the body will be lowered considerably with the addition of the surface material because of the greater contact resistance between the earth and the feet. However, this resistance may be considerably less than that of a surface layer thick enough to assume uniform resistivity in all directions. The reduction depends on the relative values of the soil and the surface material resistivities, and on the thickness of the surface material. This reduction effect for surface material resistivity greater than soil resistivity can be represented by a factor C_s, as described below and plotted in Figure 11. For this scenario, the reflection factor K will be negative and the factor C_s will be less than 1.0.

The converse of the derating principle is also true. If the underlying soil has a higher resistivity than the surface material, such as a cured, wet concrete slab or driveway with a resistivity in the range of 100 Ω-m to 200 Ω-m, a small portion of the grid current will go upward into the thin layer of surface material. For this scenario, the reflection factor K will be positive and the factor C_s will be greater than 1.0. This has the effect of increasing, rather than reducing, the effective resistivity of the surface material resistivity. However, unlike the case described in the preceding paragraph, and for typical surface material depths, the surface potentials will be altered by current flowing near the surface. Thus, the effective resistivity of the surface material should not be upgraded without taking into account this change in surface potential. This problem can best be solved using multilayer soil analysis (see 13.4.2.4). Thus, the C_s factor shown in Equation (20) and Equation (27) is not applicable for top layer resistivity lower than the bottom layer resistivity.

An analytical expression for the ground resistance of the foot on a thin layer of surface material can be obtained with the use of the method of images (Sunde [B134]; Thapar, Gerez, and Emmanuel [B146]; Thapar, Gerez, and Kejriwal [B147]).

Equation (19), Equation (20), and Equation (21) give the ground resistance of the foot on the surface material (Thapar, Gerez, and Kejriwal [B147]).

$$R_f = \left[\frac{\rho_s}{4_b}\right] C_s \tag{19}$$

Copyright © 2015 IEEE. All rights reserved.
Copyright The Institute of Electrical and Electronics Engineers, Inc.
Provided by IHS under license with IEEE
No reproduction or networking permitted without license from IHS
Order Number: 02120914
Sold to:EGAT [700166108393] - VARRIS.Y@EGAT.CO.TH,
Not for Resale,2016-09-15 03:57:51 UTC

$$C_s = 1 + \frac{16b}{\rho_s} \sum_{n=1}^{\infty} K^n R_{m(2nh_s)} \tag{20}$$

$$K = \frac{\rho - \rho_s}{\rho + \rho_s} \tag{21}$$

where

R_f is the ground resistance of the foot on a thin layer of surface material
C_s is the surface layer derating factor
K is the reflection factor between different material resistivities
ρ_s is the surface material resistivity in Ω-m
ρ is the resistivity of the earth beneath the surface material in Ω-m
h_s is the thickness of the surface material in m
b is the radius of the circular metallic disc representing the foot in m
$R_{m(2nh_s)}$ is the mutual ground resistance between the two similar, parallel, coaxial plates, separated by a distance ($2nh_s$), in an infinite medium of resistivity, ρ_s, in Ω-m

For the determination of $R_{m(2nh_s)}$, consider a thin circular plate, D1, in the x–y plane with the z axis passing through its center. The radius of the plate is b and it discharges a current I in an infinite uniform medium of resistivity, ρ_s. Using cylindrical coordinates, the potential at any point (r,z) is given by the following equations (Jackson [B92]):

$$r = \sqrt{x^2 + y^2} \tag{22}$$

$$Z = 2nh_s \tag{23}$$

$$V_{r,z} = \frac{I \times \rho_s}{4\pi b} \sin^{-1}\left[\frac{2b}{\sqrt{(r-b)^2 + (z^2)} + \sqrt{(r+b)^2 + z^2}} \right] \tag{24}$$

Consider another similar plate, D2, placed parallel and coaxial to the circular plate, D1, and at a distance ($2nh$) from it. The potential produced on D2 can be determined by evaluating the average potential over the surface of the plate. It is given by

$$V_{D2} = \frac{1}{\pi b^2} \int_0^b \left(2\pi r \times V_{r,z}\right) dr \tag{25}$$

The mutual ground resistance, $R_{m(2nh_s)}$, between the two plates is given by

$$R_{m(2nh_s)} = \frac{V_{D2}}{I} \tag{26}$$

Copyright © 2015 IEEE. All rights reserved.

Copyright The Institute of Electrical and Electronics Engineers, Inc.
Provided by IHS under license with IEEE
No reproduction or networking permitted without license from IHS

Order Number: 02120914
Sold to:EGAT [700166108393] - VARRIS.Y@EGAT.CO.TH,
Not for Resale,2016-09-15 03:57:51 UTC

Comparing Equation (14) and Equation (19), C_s can be considered as a corrective factor to compute the effective foot resistance in the presence of a finite thickness of surface material. Because the quantity C_s is rather tedious to evaluate without the use of a computer, these values have been calculated for b = 0.08 m and are given in the form of graphs in Figure 11.

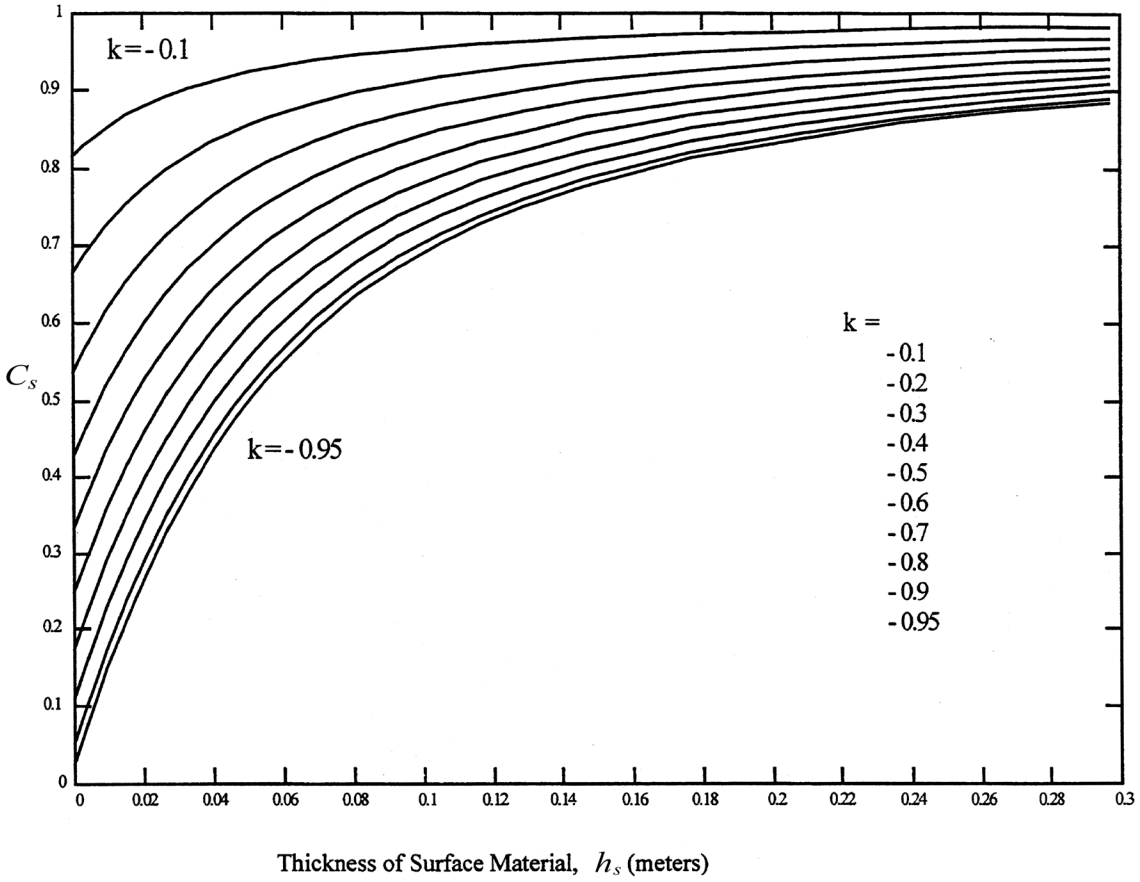

Figure 11—C_s versus h_s

Computer models have also been used to determine the value of C_s (Dawalibi, Xiong, and Ma [B51]; Meliopoulos, Xia, Joy, and Cokkonides [B110]). There is a close match in the values obtained from these computer models with the values given in Figure 11.

The following empirical equation gives the value of C_s. The values of C_s obtained using Equation (27) are within 5% of the values obtained with the analytical method (Thapar, Gerez, and Kejriwal [B147]).

$$C_s = 1 - \frac{0.09\left(1 - \frac{\rho}{\rho_s}\right)}{2h_s + 0.09} \tag{27}$$

Copyright © 2015 IEEE. All rights reserved.

Copyright The Institute of Electrical and Electronics Engineers, Inc.
Provided by IHS under license with IEEE
No reproduction or networking permitted without license from IHS

Order Number: 02120914
Sold to:EGAT [700166108393] - VARRIS.Y@EGAT.CO.TH,
Not for Resale,2016-09-15 03:57:51 UTC

8. Criteria of tolerable voltage

8.1 Criteria of tolerable voltage definitions

NOTE—The following definitions are also listed in Clause 3, but repeated here for the convenience of the reader.

ground potential rise (GPR): The maximum electrical potential that a substation ground grid may attain relative to a distant grounding point assumed to be at the potential of remote earth. This voltage, GPR, is equal to the maximum grid current multiplied by the grid resistance.

NOTE—Under normal conditions, the grounded electrical equipment operates at near zero ground potential. That is, the potential of a grounded neutral conductor is nearly identical to the potential of remote earth. During a ground fault the portion of fault current that is conducted by a substation ground grid into the earth causes the rise of the grid potential with respect to remote earth.

mesh voltage: The maximum touch voltage within a mesh of a ground grid.

metal-to-metal touch voltage: The difference in potential between metallic objects or structures within the substation site that may be bridged by direct hand-to-hand or hand-to-feet contact.

NOTE—The metal-to-metal touch voltage between metallic objects or structures bonded to the ground grid is assumed to be negligible in conventional substations. However, the metal-to-metal touch voltage between metallic objects or structures bonded to the ground grid and metallic objects internal to the substation site, such as an isolated fence, but not bonded to the ground grid may be substantial. In the case of a gas-insulated substation (GIS), the metal-to-metal touch voltage between metallic objects or structures bonded to the ground grid may be substantial because of internal faults or induced currents in the enclosures.

In a conventional substation, the worst touch voltage is usually found to be the potential difference between a hand and the feet at a point of maximum reach distance. However, in the case of a metal-to-metal contact from hand-to-hand or from hand-to-feet, both situations should be investigated for the possible worst reach conditions. Figure 12 and Figure 13 illustrate these situations for air-insulated substations, and Figure 14 illustrates these situations in GIS.

step voltage: The difference in surface potential experienced by a person bridging a distance of 1 m with the feet without contacting any other grounded object.

touch voltage: The potential difference between the ground potential rise (GPR) and the surface potential at the point where a person is standing while at the same time having a hand in contact with a grounded structure. Touch voltage measurements can be “open circuit” (without the equivalent body resistance included in the measurement circuit) or “closed circuit” (with the equivalent body resistance included in the measurement circuit).

transferred voltage: A special case of the touch voltage where a voltage is transferred into or out of the substation from or to a remote point external to the substation site.

Copyright © 2015 IEEE. All rights reserved.

Copyright The Institute of Electrical and Electronics Engineers, Inc.
Provided by IHS under license with IEEE
No reproduction or networking permitted without license from IHS

Order Number: 02120914
Sold to:EGAT [700166108393] - VARRIS.Y@EGAT.CO.TH,
Not for Resale,2016-09-15 03:57:51 UTC

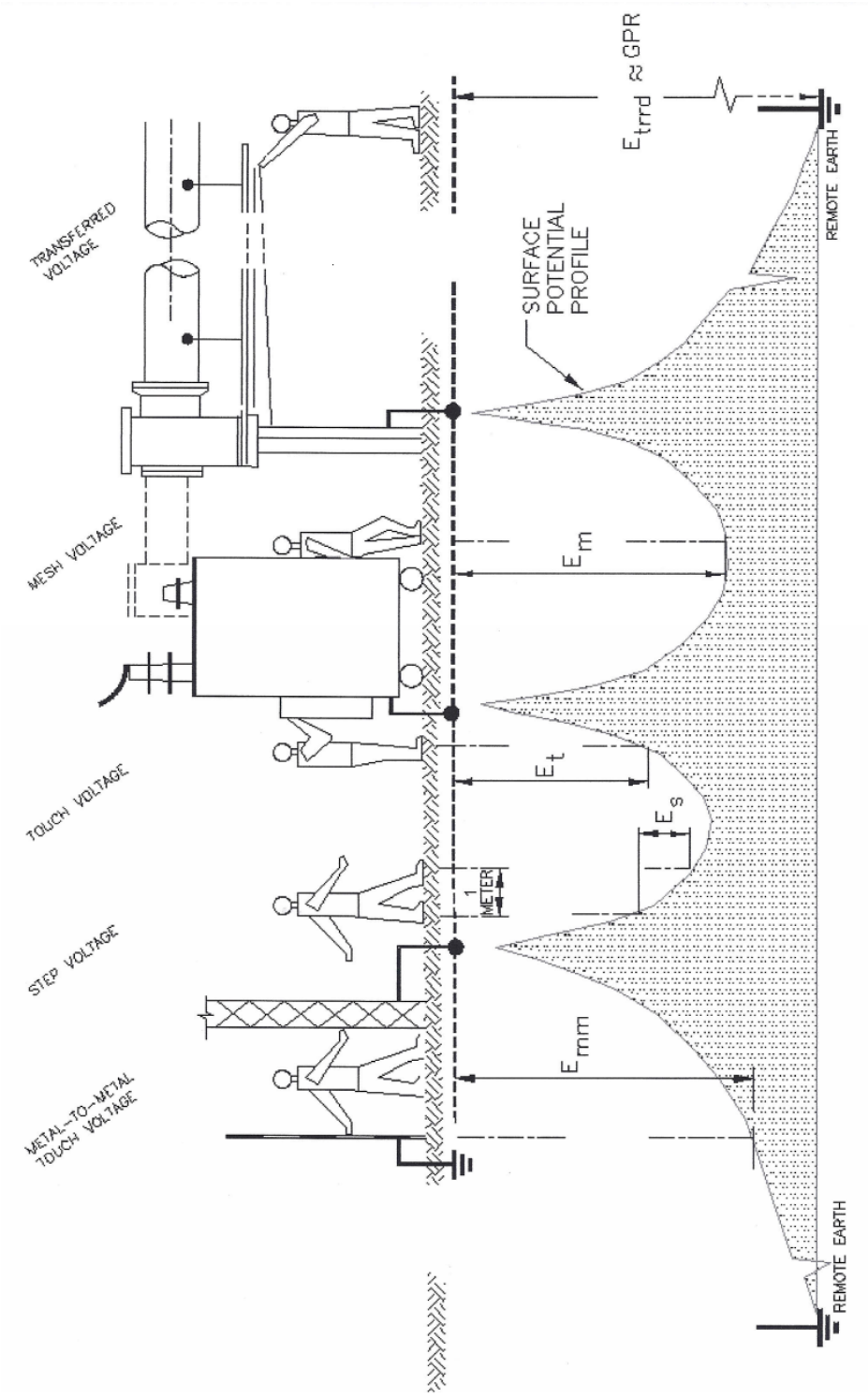

Figure 12—Basic shock situations

Copyright © 2015 IEEE. All rights reserved.

Copyright The Institute of Electrical and Electronics Engineers, Inc.
Provided by IHS under license with IEEE
No reproduction or networking permitted without license from IHS

Order Number: 02120914
Sold to:EGAT [700166108393] - VARRIS.Y@EGAT.CO.TH,
Not for Resale,2016-09-15 03:57:51 UTC

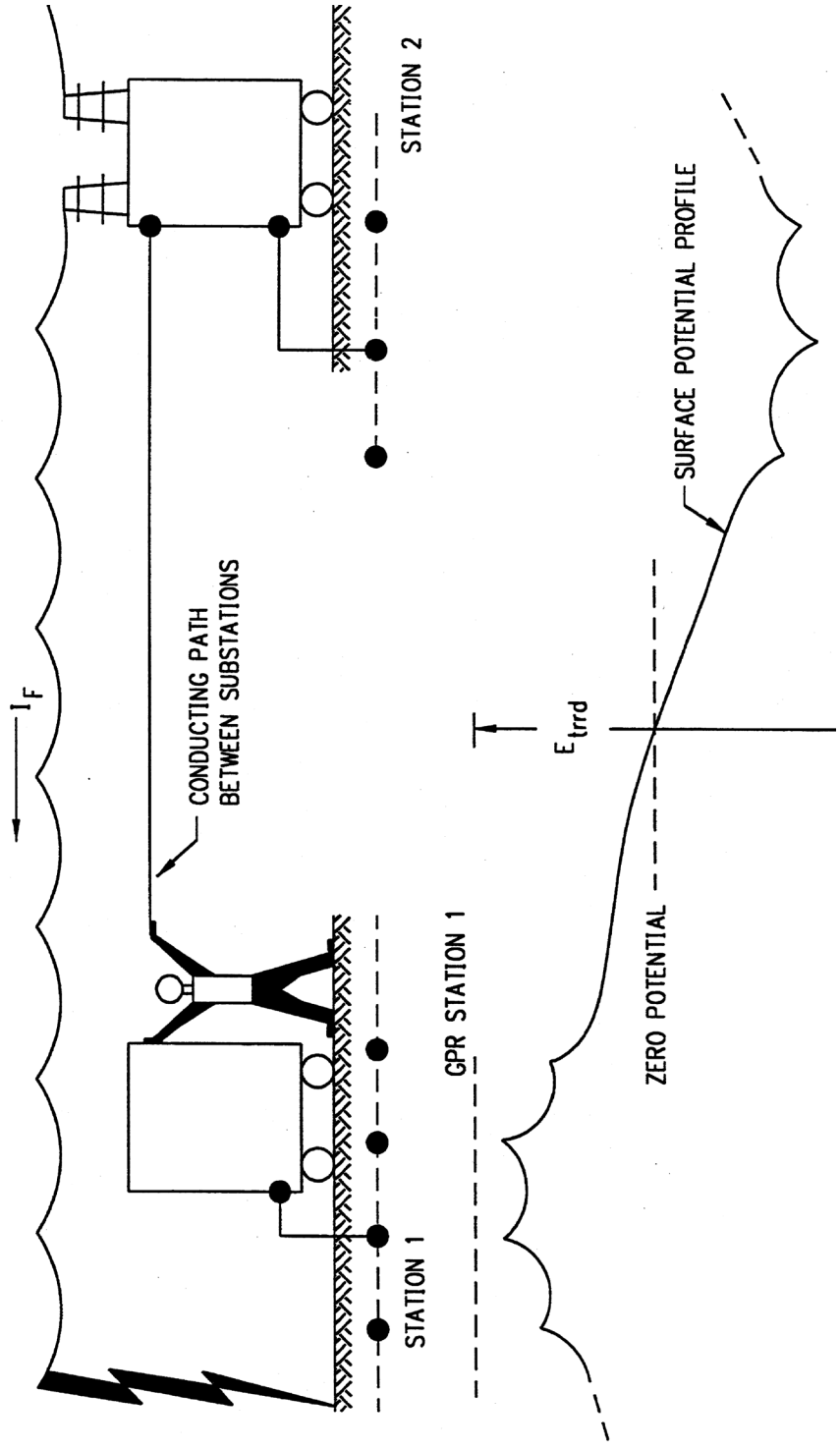

Figure 13—Typical situation of extended transferred potential

Copyright © 2015 IEEE. All rights reserved.

Copyright The Institute of Electrical and Electronics Engineers, Inc.
Provided by IHS under license with IEEE
No reproduction or networking permitted without license from IHS

Order Number: 02120914
Sold to:EGAT [700166108393] - VARRIS.Y@EGAT.CO.TH,
Not for Resale,2016-09-15 03:57:51 UTC

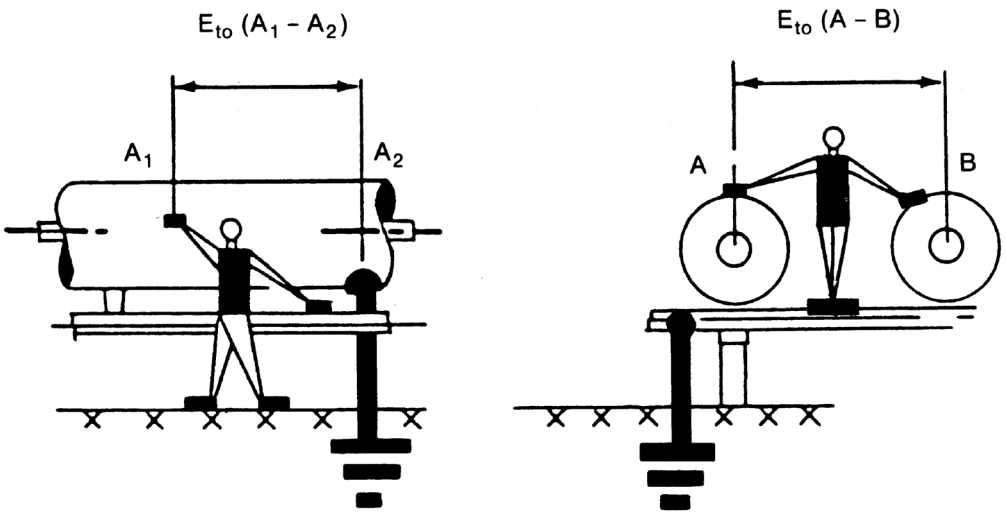

Figure 14—Typical metal-to-metal touch situation in GIS

8.2 Typical shock situations for air-insulated substations

Figure 12 and Figure 13 show five basic situations involving a person and grounded facilities during a fault. For a foot-to-foot contact, the accidental circuit equivalent is that of Figure 9, and its driving voltage U is equal to E_s (step voltage). For the three examples of hand-to-feet contact Figure 12 applies, and U is equal to E_t (touch voltage), E_m (mesh voltage), or E_{trrd} (transferred voltage), respectively. The accidental circuit involving metal-to-metal contact, either hand-to-hand or hand-to-feet, is shown in Figure 14 where U is equal to the metal-to-metal touch voltage, E_{mm}.

During a fault, the earth conducts currents that emanate from the grid and other permanent ground electrodes buried below the earth's surface. The resulting potential gradients have a primary effect on the value of U.

In the case of conventional substations, the typical case of metal-to-metal touch voltage occurs when metallic objects or structures within the substation site are not bonded to the ground grid. Objects such as pipes, rails, or fences that are located within or near the substation ground grid area, and not bonded to the ground grid, meet this criteria. Substantial metal-to-metal touch voltages may be present when a person standing on or touching a grounded object or structure comes into contact with a metallic object or structure within the substation site that is not bonded to the ground grid. Calculation of the actual metal-to-metal touch voltage is complex. In practice, hazards resulting from metal-to-metal contact may best be avoided by bonding potential danger points to the substation grid.

Typically, the case of transferred voltage occurs when a person standing within the substation area touches a conductor grounded at a remote point, or a person standing at a remote point touches a conductor connected to the substation ground grid. During fault conditions, the resulting potential to ground may equal or exceed the full ground potential rise (GPR) of a ground grid discharging the fault current, rather than the fraction of this total voltage encountered in the ordinary touch contact situations (see Figure 13). In fact, as discussed in Clause 17, the transferred voltage may exceed the sum of the GPRs of both substations, due to induced voltages on communication circuits, static or neutral wires, pipes, etc. It is impractical, and often impossible, to design a ground grid based on the touch voltage caused by the external transferred voltages. Hazards from these external transferred voltages are best avoided by using isolating or neutralizing devices and by treating and clearly labeling these circuits, pipes, etc., as being equivalent to energized lines.

Copyright © 2015 IEEE. All rights reserved.

Copyright The Institute of Electrical and Electronics Engineers, Inc.
Provided by IHS under license with IEEE
No reproduction or networking permitted without license from IHS

Order Number: 02120914
Sold to:EGAT [700166108393] - VARRIS.Y@EGAT.CO.TH,
Not for Resale,2016-09-15 03:57:51 UTC

8.3 Typical shock situations for gas-insulated substations

In the grounding analysis of GIS, the touch voltage considerations present several unique problems. Unlike conventional facilities, the GIS equipment features a metal sheath enclosing gas-insulated switchgear and inner high-voltage buses. Each bus is contained within its enclosure and the enclosures are grounded. Because a voltage is induced in the outer sheath whenever a current flows in the coaxial busbar, certain parts of the enclosure might be at different potentials with respect to the substation ground. To evaluate the maximum voltage occurring on the bus enclosure during a fault, it is necessary to determine the inductance of the outer sheath to ground, the inductance of the inner conductor, and the mutual inductances for a given phase configuration of individual buses.

A person touching the outer sheath of a GIS might be exposed to voltages resulting from two basic fault conditions:

a) An internal fault within the gas-insulated bus system, such as a flashover between the bus conductor and the inner wall of the enclosure.

b) A fault external to the GIS in which a fault current flows through the GIS bus and induces currents in the enclosures.

Because the person may stand on a grounded metal grating and the accidental circuit may involve a hand-to-hand and hand-to-feet current path, the analysis of GIS grounding necessitates consideration of metal-to-metal touch voltage (see Figure 14).

8.4 Step and touch voltage criteria

The safety of a person depends on preventing the critical amount of shock energy from being absorbed before the fault is cleared and the system de-energized. The maximum driving voltage of any accidental circuit should not exceed the limits defined as follows. For step voltage the limit is

$$E_{step} = \left(R_B + 2R_f\right)I_B \tag{28}$$

for body weight of 50 kg

$$E_{step50} = \left(1000 + 6C_s \times \rho_s\right)\frac{0.116}{\sqrt{t_s}} \tag{29}$$

for body weight of 70 kg

$$E_{step70} = \left(1000 + 6C_s \times \rho_s\right)\frac{0.157}{\sqrt{t_s}} \tag{30}$$

Similarly, the touch voltage limit is

$$E_{touch} = \left(R_B + \frac{R_f}{2}\right)I_B \tag{31}$$

Copyright © 2015 IEEE. All rights reserved.

Copyright The Institute of Electrical and Electronics Engineers, Inc.
Provided by IHS under license with IEEE
No reproduction or networking permitted without license from IHS

Order Number: 02120914
Sold to:EGAT [700166108393] - VARRIS.Y@EGAT.CO.TH,
Not for Resale,2016-09-15 03:57:51 UTC

for body weight of 50 kg

$$E_{touch50} = (1000 + 1.5C_s \times \rho_s)\frac{0.116}{\sqrt{t_s}} \tag{32}$$

for body weight of 70 kg

$$E_{touch70} = (1000 + 1.5C_s \times \rho_s)\frac{0.157}{\sqrt{t_s}} \tag{33}$$

where

E_{step} is the step voltage in V
E_{touch} is the touch voltage in V
C_s is determined from Figure 11 or Equation (27)
ρ_s is the resistivity of the surface material in Ω-m
t_s is the duration of shock current in seconds

If no protective surface layer is used, then C_s =1 and $\rho_s = \rho$.

The metal-to-metal touch voltage limits are derived from the touch voltage equations, Equation (32) and Equation (33). Metal-to-metal contact, both hand-to-hand and hand-to-feet, will result in ρ_s = 0. Therefore, the total resistance of the accidental circuit is equal to the body resistance, R_B.

With the substitution of ρ_s = 0 in the foot resistance terms of Equation (32) and Equation (33), the metal-to-metal touch voltage limit is

for body weight of 50 kg

$$E_{mm-touch50} = \frac{116}{\sqrt{t_s}} \tag{34}$$

for body weight of 70 kg

$$E_{mm-touch70} = \frac{157}{\sqrt{t_s}} \tag{35}$$

where

E_{mm} is the metal-to-metal touch voltage in V

The actual step voltage, touch voltage, or metal-to-metal touch voltage should be less than the respective maximum allowable voltage limits to ensure safety. Hazards from external transferred voltages are best avoided by isolation or neutralizing devices and labeling these danger points as being equivalent to live lines.

Copyright © 2015 IEEE. All rights reserved.

Copyright The Institute of Electrical and Electronics Engineers, Inc.
Provided by IHS under license with IEEE
No reproduction or networking permitted without license from IHS

Order Number: 02120914
Sold to:EGAT [700166108393] - VARRIS.Y@EGAT.CO.TH,
Not for Resale,2016-09-15 03:57:51 UTC

8.5 Effect of sustained ground currents

After the safe step and touch voltage limits are established, the grounding system can then be designed based on the available fault current and overall clearing time. The designer should also consider sustained low-level (below setting of protective relays) fault magnitudes that may be above the let-go current threshold. Some sustained faults above the let-go current, but below the fibrillation threshold, may cause asphyxiation from prolonged contraction of the chest muscles. However, it would not be practical to design against lesser shocks that are painful, but cause no permanent injury.

9. Principal design considerations

9.1 Definitions

NOTE—The following definitions are also listed in Clause 3, but repeated here for the convenience of the reader.

auxiliary ground electrode: A ground electrode with certain design or operating constraints. Its primary function may be other than conducting the ground fault current into the earth.

ground electrode: A conductor imbedded in the earth and used for collecting ground current from, or dissipating ground current into, the earth.

ground grid: A system of interconnected ground electrodes arranged in a pattern over a specified area and buried below the surface of the earth.

NOTE—Grids buried horizontally near the earth's surface are also effective in controlling the surface potential gradients. A typical grid usually is supplemented by a number of ground rods and may be further connected to auxiliary ground electrodes, to lower its resistance with respect to remote earth.

ground mat: A solid metallic plate or a system of closely spaced bare conductors that are connected to and often placed in shallow depths above a ground grid or elsewhere at the earth surface, in order to obtain an extra protective measure minimizing the danger of the exposure to high step or touch voltages in a critical operating area or places that are frequently used by people. Grounded metal grating, placed on or above the soil surface, or wire mesh placed directly under the surface material, are common forms of a ground mat.

grounding system: Comprises all interconnected grounding facilities in a specific area.

primary ground electrode: A ground electrode specifically designed or adapted for discharging the ground fault current into the ground, often in a specific discharge pattern, as required (or implicitly called for) by the grounding system design.

9.2 General concept

A grounding system should be installed in a manner that will limit the effect of ground potential gradients to such voltage and current levels that will not endanger the safety of people or equipment under normal and fault conditions. The system should also help ensure continuity of service.

In the discussion that follows, it is assumed that the system of ground electrodes has the form of a grid of horizontally buried conductors, supplemented by a number of vertical ground rods connected to the grid. Based on two surveys, the first reported in an AIEE application guide in 1954 [B4], and the second published in 1980 (Dawalibi, Bauchard, and Mukhedkar [B46]), this concept represents the prevailing practice of most utilities both in the United States and in other countries.

Copyright © 2015 IEEE. All rights reserved.

Copyright The Institute of Electrical and Electronics Engineers, Inc.
Provided by IHS under license with IEEE
No reproduction or networking permitted without license from IHS

Order Number: 02120914
Sold to:EGAT [700166108393] - VARRIS.Y@EGAT.CO.TH,
Not for Resale,2016-09-15 03:57:51 UTC

Some of the reasons for using the combined system of vertical rods and horizontal conductors are as follows:

— In substations a single electrode is, by itself, inadequate in providing a safe grounding system. In turn, when several electrodes, such as ground rods, are connected to each other and to all equipment neutrals, frames, and structures that are to be grounded, the result is essentially a grounding system consisting of multiple ground electrodes, regardless of the original objective. If the connecting links happen to be buried in a soil having good conductivity, this network alone may represent an excellent grounding system. Partly for this reason, some utilities depend on the use of a grid alone. However, ground rods are of a particular value, as explained in item 2, below.

— If the magnitude of current dissipated into the earth is high, it seldom is possible to install a grid with resistance so low as to assure that the rise of a ground potential will not generate surface gradients unsafe for human contact. Then, the hazard can be eliminated only by control of local potentials through the entire area. A system that combines a horizontal grid and a number of vertical ground rods penetrating lower soils has the following advantages:

  1) While horizontal (grid) conductors are most effective in reducing the danger of high step and touch voltages on the earth's surface, provided that the grid is installed in a shallow depth (usually 0.3 m to 0.5 m [12 in to 18 in] below grade), sufficiently long ground rods will stabilize the performance of such a combined system. For many installations this is important because freezing or drying of upper soil layers could vary the soil resistivity with seasons, while the resistivity of lower soil layers remains nearly constant.

  2) Rods penetrating the lower resistivity soil are far more effective in dissipating fault currents whenever a two-layer or multilayer soil is encountered and the upper soil layer has higher resistivity than the lower layers. For many GIS and other space-limited installations, this condition becomes in fact the most desirable one to occur, or to be achieved by the appropriate design means (extra-long ground rods, grounding wells, etc.).

  3) If the rods are installed predominantly along the grid perimeter in high-to-low or uniform soil conditions, the rods will considerably moderate the steep increase of the surface gradient near the peripheral meshes. See Clause 16 for details of this arrangement. These details are pertinent to the use of simplified methods in determining the voltage gradient at the earth's surface.

9.3 Primary and auxiliary ground electrodes

In general, most grounding systems utilize two groups of ground electrodes. Primary ground electrodes are specifically designed for grounding purposes. Auxiliary ground electrodes are electrodes that comprise various underground metal structures installed for purposes other than grounding. Typical primary electrodes include such things as ground grids, counterpoise conductors, ground rods, and ground wells. Typical auxiliary electrodes include underground metal structures and reinforcing bars encased in concrete, if connected to the ground grid. Auxiliary ground electrodes may have a limited current carrying capability.

9.4 Basic aspects of grid design

Conceptual analysis of a grid system usually starts with inspection of the substation layout plan, showing all major equipment and structures. To establish the basic ideas and concepts, the following points may serve as guidelines for starting a typical ground grid design:

a) A continuous conductor loop should surround the perimeter to enclose as much area as practical. This measure helps to avoid high current concentration and, hence, high gradients both in the grid area and near the projecting cable ends. Enclosing more area also reduces the resistance of the ground grid.

Copyright © 2015 IEEE. All rights reserved.

Copyright The Institute of Electrical and Electronics Engineers, Inc.
Provided by IHS under license with IEEE
No reproduction or networking permitted without license from IHS

Order Number: 02120914
Sold to:EGAT [700166108393] - VARRIS.Y@EGAT.CO.TH,
Not for Resale,2016-09-15 03:57:51 UTC

b) Within the loop, conductors are typically laid in parallel lines and, where practical, along the structures or rows of equipment to provide for short ground connections.

c) A typical grid system for a substation may include 4/0 bare copper conductors buried 0.3 m to 0.5 m (12 in to 18 in) below grade, spaced 3 m to 7 m (10 ft to 20 ft) apart, in a grid pattern. At cross-connections, the conductors would be securely bonded together. Ground rods may be at the grid corners and at junction points along the perimeter. Ground rods may also be installed at major equipment, especially near surge arresters. In multilayer or high resistivity soils, it might be useful to use longer rods or rods installed at additional junction points.

d) This grid system would be extended over the entire substation switchyard and often beyond the fence line. Multiple ground leads or larger sized conductors would be used where high concentrations of current may occur, such as at a neutral-to-ground connection of generators, capacitor banks, or transformers.

e) The ratio of the sides of the grid meshes usually is from 1:1 to 1:3, unless a precise (computer-aided) analysis warrants more extreme values. Frequent cross-connections have a relatively small effect on lowering the resistance of a grid. Their primary role is to control the surface potentials. The cross-connections are also useful in providing multiple paths for the fault current, reducing the voltage drop in the grid itself, and providing a certain measure of redundancy in the case of a conductor failure.

9.5 Design in difficult conditions

In areas where the soil resistivity is rather high or the substation space is at a premium, it may not be possible to obtain a low impedance grounding system by spreading the grid electrodes over a large area, as is done in more favorable conditions. Such a situation is typical of many GIS installations and industrial substations, occupying only a fraction of the land area normally used for conventional equipment. This often makes the control of surface gradients difficult. Some of the solutions include

a) Connection(s) of remote ground grid(s) and adjacent grounding facilities, a combined system utilizing separate installations in buildings, underground vaults, etc. A predominant use of remote ground electrodes requires careful consideration of transferred potentials, surge arrester locations, and other critical points. A significant voltage drop may develop between the local and remote grounding facilities, especially for high-frequency surges (lightning).

b) Use of deep-driven ground rods and drilled ground wells.

c) Various additives and soil treatments used in conjunction with ground rods and interconnecting conductors are more fully described in 14.5.

d) Use of wire mats. It is feasible to combine both a surface material and fabricated mats made of wire mesh to equalize the gradient field near the surface. A typical wire mat might consist of copper-clad steel wires of No. 6 AWG, arranged in a 0.6 m × 0.6 m (24 in × 24 in) grid pattern, installed on the earth's surface and below the surface material, and bonded to the main ground grid at multiple locations.

e) Where feasible, controlled use of other available means to lower the overall resistance of a ground system, such as connecting static wires and neutrals to the ground (see 15.3). Typical is the use of metallic objects on the site that qualify for and can serve as auxiliary ground electrodes, or as ground ties to other systems. Consequences of such applications, of course, have to be carefully evaluated.

f) Wherever practical, a nearby deposit of low resistivity material of sufficient volume can be used to install an extra (satellite) grid. This satellite grid, when sufficiently connected to the main grid, will lower the overall resistance and, thus, the ground potential rise of the ground grid. The nearby low resistivity material may be a clay deposit or it may be a part of some large structure, such as the concrete mass of a hydroelectric dam (Verma, Merand, and Barbeau [B152]).

Copyright © 2015 IEEE. All rights reserved.

Copyright The Institute of Electrical and Electronics Engineers, Inc.
Provided by IHS under license with IEEE
No reproduction or networking permitted without license from IHS

Order Number: 02120914
Sold to:EGAT [700166108393] - VARRIS.Y@EGAT.CO.TH,
Not for Resale,2016-09-15 03:57:51 UTC

9.6 Connections to grid

Conductors of adequate ampacity and mechanical strength (see Clause 11) should be used for the connections between:

a) All ground electrodes, such as ground grids, rodbeds, ground wells, and, where applicable, metal, water, or gas pipes, water well casings, etc.

b) All above-ground conductive metal parts that might accidentally become energized, such as metal structures, machine frames, metal housings of conventional or gas-insulated switchgear, transformer tanks, guards, etc. Also, conductive metal parts that might be at a different potential relative to other metal parts that have become energized should be bonded together, usually via the ground grid.

c) All fault current sources such as surge arresters, capacitor banks or coupling capacitors, transformers, and, where appropriate, machine neutrals and lighting and power circuits.

Copper cables or straps are usually employed for these ground connections. However, transformer tanks are sometimes used as part of a ground path for surge arresters. Similarly, most steel or aluminum structures may be used for the ground path if it can be established that their conductance, including that of any connections, is and can be maintained as equivalent to that of the conductor that would normally be installed. Where this practice is followed, any paint films that might otherwise introduce a highly resistive connection should be removed, and a suitable joint compound should be applied, or other effective means, such as jumpers across the connections, should be taken to prevent subsequent deterioration of the connection. In the case of GIS installations, extra attention should be paid to the possibility of unwanted circulation of induced currents. Clause 10 covers the subject in more detail.

Equal division of currents between multiple ground leads at cross-connections or similar junction points should not be assumed.

All accessible ground leads should be inspected on a periodic basis. Exothermic weld, brazed, or pressure-type connectors can be used for underground connections (see 11.4). Soldered connections should be avoided because of the possibility of failure under high fault currents.

Open circuits, even in exposed locations, can escape detection, and it obviously is impractical to inspect buried portions of the grounding network once it is installed. More detailed discussion of test methods used to determine the continuity of buried grounding systems is included in 19.4. Those facilities that are most likely to supply or carry a high current, such as transformer and circuit breaker tanks, switch frames, and arrester pads, should be connected to the grid with more than one ground lead. The leads should preferably be run in opposite directions to eliminate common mode failure.[6]

10. Special considerations for gas-insulated substations (GIS)

10.1 Special considerations for GIS definitions

NOTE—The following definitions are also listed in Clause 3, but repeated here for the convenience of the reader.

continuous enclosure: A bus enclosure in which the consecutive sections of the housing along the same phase conductor are bonded together to provide an electrically continuous current path throughout the

[6] One possible exception is grounding of the secondaries of potential and current transformers. The grounding of such devices usually must be restricted to a single point to avoid any parallel path that could cause undesirable circulation of currents affecting the performance of relays and metering devices.

Copyright © 2015 IEEE. All rights reserved.

Copyright The Institute of Electrical and Electronics Engineers, Inc.
Provided by IHS under license with IEEE
No reproduction or networking permitted without license from IHS

Order Number: 02120914
Sold to:EGAT [700166108393] - VARRIS.Y@EGAT.CO.TH,
Not for Resale,2016-09-15 03:57:51 UTC

entire enclosure length. Cross-bondings, connecting the other phase enclosures, are made only at the extremities of the installation and at a few selected intermediate points.

enclosure currents: Currents that result from the voltages induced in the metallic enclosure by the current(s) flowing in the enclosed conductor(s).

gas-insulated substation (GIS): A compact, multi-component assembly, enclosed in a grounded metallic housing in which the primary insulating medium is a gas, and that normally consists of buses, switchgear, and associated equipment (subassemblies).

main ground bus: A conductor or system of conductors provided for connecting all designated metallic components of the gas-insulated substation (GIS) to a substation grounding system.

non-continuous enclosure: A bus enclosure with the consecutive sections of the housing of the same phase conductor electrically isolated (or insulated from each other), so that no current can flow beyond each enclosure section.

transient enclosure voltage (TEV): Very fast transient phenomena, which are found on the grounded enclosure of gas-insulated substation (GIS) systems. Typically, ground leads are too long (inductive) at the frequencies of interest to effectively prevent the occurrence of TEV. The phenomenon is also known as transient ground rise (TGR) or transient ground potential rise (TGPR).

very fast transient (VFT): A class of transients generated internally within a gas-insulated substation (GIS) characterized by short duration and very high frequency. VFT is generated by the rapid collapse of voltage during breakdown of the insulating gas, either across the contacts of a switching device or line-to-ground during a fault. These transients can have rise times in the order of nanoseconds implying a frequency content extending to about 100 MHz. However, dominant oscillation frequencies, which are related to physical lengths of GIS bus, are usually in the 20 MHz to 40 MHz range.

very fast transients overvoltage (VFTO): System overvoltages that result from generation of VFT. While VFT is one of the main constituents of VFTO, some lower frequency (≅ 1 MHz) component may be present as a result of the discharge of lumped capacitance (voltage transformers). Typically, VFTO will not exceed 2.0 per unit, though higher magnitudes are possible in specific instances.

10.2 GIS characteristics

GIS can be subjected to the same magnitude of ground fault current and require the same low-impedance grounding as conventional substations.

Typically, the GIS installation necessitates 10% to 25% of the land area required for conventional equipment. Because of this smaller area, it may be difficult to obtain adequate grounding solely by conventional methods. Particular attention should be given to the bonding of the metallic enclosures of the GIS assembly, as these enclosures carry induced currents of significant magnitude, which must be confined to specific paths. In this respect, grounding recommendations by the manufacturer of a given GIS usually need to be strictly followed.

As a result of the compact nature of GIS and its short distances, electrical breakdown in the insulating gas, either across the contacts of a switching device during operation or under fault conditions can generate very high frequency transients that can couple onto the grounding system [B19]. In general, these transients need to be considered in the overall grounding design. These transients may cause high magnitude, short duration ground rises and are also the source of electromagnetic interference (EMI) in the GIS. While EMI is beyond the scope of this document, the EMI mitigation techniques often involve special considerations in the grounding design (Harvey [B80]).

Copyright © 2015 IEEE. All rights reserved.

Copyright The Institute of Electrical and Electronics Engineers, Inc.
Provided by IHS under license with IEEE
No reproduction or networking permitted without license from IHS

Order Number: 02120914
Sold to:EGAT [700166108393] - VARRIS.Y@EGAT.CO.TH,
Not for Resale,2016-09-15 03:57:51 UTC

10.3 Enclosures and circulating currents

The shielding effectiveness of the bus enclosure is determined by its impedance, which governs the circulation of induced currents.

With separate enclosures for each phase, the magnitude and direction of the enclosure current is influenced by the size of the enclosure and the phase spacing between the buses, as well as by the method of interconnecting the enclosures.

In a continuous enclosure design, a voltage is induced in an enclosure by the current in the conductor that it surrounds, producing a longitudinal current flow in the enclosure. When a continuity of all phase enclosures is maintained through short connections at both ends, the enclosure current is only slightly less than that flowing in the inner bus in the opposite direction. This current returns through the housing (enclosures) of adjacent phases when the load is equalized between phases. This enclosure current contains most of the magnetic field within the enclosure because it cancels out much of the magnetic field outside the enclosure.

In a non-continuous enclosure design, there are no external return paths for enclosure currents. Thus the voltage induced in a non-continuous enclosure by the current of an inner bus(es) that it surrounds cannot produce any longitudinal current flow. Also, voltages might be induced in each enclosure by the currents in the conductors not enclosed by it. Non-uniform voltages result, causing local current flows in each isolated enclosure section, with the currents flowing in non-uniform patterns. Because of these properties, the non-continuous design is generally considered less advantageous than that of the continuous type. As such, it is not currently used by the industry.

10.4 Grounding of enclosures

Normally, the continuous-type enclosures provide a return path for induced currents so that the conductor and enclosure form a concentric pair with effective external shielding of the field internal to the enclosure. However, under asymmetrical faults, the dc component is not shielded and causes an external voltage drop due to enclosure resistance.

Frequent bonding and grounding of GIS enclosures is the best solution to minimize hazardous touch and step voltages within the GIS area. Additional measures[7] include the use of conductive platforms (ground mats) that are connected to GIS structures and grounded.

To limit the undesirable effects caused by circulating currents, the following requirements should be met:

a) All metallic enclosures should normally operate at ground voltage level.

b) When grounded at the designated points, the bus enclosure design should ensure that no significant voltage differences exist between individual enclosure sections and that neither the supporting structures nor any part of the grounding systems is adversely influenced by the flow of induced currents.

c) To avoid the circulation of enclosure currents beyond regular return path within the GIS assembly, power cable sheath grounds should be tied to the grounding system via connections that are separated from the GIS enclosures. To facilitate this isolation, the design of cable terminations should be such that an isolating air gap or proper insulation elements are provided. Very fast transients generated by switching or by faults in the GIS may cause these insulation elements to

[7] Despite all measures described, the presence of circulating currents can cause different parts of the GIS metal housing to have a slightly different potential to ground. Although the resulting voltage differences are small and generally of no concern to a shock hazard, accidental metallic bridging of adjacent enclosures can cause annoying sparks.

Copyright © 2015 IEEE. All rights reserved.

Copyright The Institute of Electrical and Electronics Engineers, Inc.
Provided by IHS under license with IEEE
No reproduction or networking permitted without license from IHS

Order Number: 02120914
Sold to:EGAT [700166108393] - VARRIS.Y@EGAT.CO.TH,
Not for Resale,2016-09-15 03:57:51 UTC

flashover. In such cases, the consequences of such flashovers on current distribution within the grounding system should be considered (Fujimoto, Croall, and Foty [B69]).

d) Enclosure return currents also cannot be permitted to flow through any mounted current transformers.

10.5 Cooperation between GIS manufacturer and user

Usually it is the GIS manufacturer who defines clearly what constitutes the main ground bus of the GIS and specifies what is required of the user for connecting the GIS assembly to the substation ground. Ample documentation is necessary to assure that none of the proposed connections from the main ground bus to the ground grid will interfere with the required enclosure current path or any other operational feature of the GIS design. That may be especially pertinent if the main ground bus consists of a system of interconnections between the GIS components and structures, and no separate busbar (continuous common ground bus loop) is furnished.

Usually the GIS manufacturer also provides, or is responsible for

— Providing the subassembly-to-subassembly bonding to establish safe voltage gradients that meet safety requirements between all intentionally grounded parts of the GIS assembly and between those parts and the main ground bus of the GIS.

— Furnishing readily accessible connectors of sufficient mechanical strength to withstand electromagnetic forces and normal abuse, and that are capable of carrying the anticipated maximum fault current in that portion of the circuit without overheating.

— Providing ground pads or connectors, or both, allowing, at least, for two paths to ground from the main ground bus, or from each metallic enclosure and auxiliary piece of GIS equipment designated for a connection to the substation ground if the main ground bus of the GIS assembly does not actually exist.

— Recommending proper procedures for connections between dissimilar metals, typically between a copper cable or a similar ground conductor and aluminum enclosures.

The user usually provides information on the sources of fault current and the expected magnitudes and durations that should be considered. Moreover, the user should assist the GIS manufacturer in reviewing all proposed grounding provisions for proper interfacing of:

a) Connections for the neutral current of grounded equipment or apparatus and for dissipating surges caused by lightning and switching within the GIS.

b) Devices for dissipating lightning and switching surge currents external to the GIS assembly.

c) Requirements of protective relaying, and satisfying the provisions necessary for telephone and communication facilities.

d) Ground connections to all GIS supporting frames and structures, metallic sheaths, and installation of shielding for cable terminations where applicable.

e) Connections to all pads or connectors furnished by the GIS manufacturer.

f) Safe voltage for step and touch, under both normal and abnormal operating conditions external to the GIS assembly.

g) Compliance with the grounding specifications, related to correct grounding practices, as mutually agreed to by the GIS manufacturer and the user.

Copyright © 2015 IEEE. All rights reserved.

Copyright The Institute of Electrical and Electronics Engineers, Inc.
Provided by IHS under license with IEEE
No reproduction or networking permitted without license from IHS

Order Number: 02120914
Sold to:EGAT [700166108393] - VARRIS.Y@EGAT.CO.TH,
Not for Resale,2016-09-15 03:57:51 UTC

10.6 Other special aspects of GIS grounding

Precautions should be taken to prevent excessive currents from being induced into adjacent frames, structures, or reinforcing steel, and to avoid establishment of current loops via other substation equipment, such as transformers or separate switchgear. If there is the possibility of undesirable current loops via ground connections, or if any sustained current path might partially close or pass through grounded structures, the substation grounding scheme and the physical layout should be carefully reviewed with the GIS manufacturer.

Equal care is needed in the proximity of discontinuities in enclosure grounding paths at the transformer connections to GIS and at the interface points to conventional switchgear to prevent circulating currents in the circuit breaker and transformer tank steel.

Where applicable, all isolating elements should be able to withstand the full potential difference that may occur between the locally grounded system and that external to the GIS. In many cases, the very fast transients generated by switching or by faults in the GIS may cause very high transient voltages to appear at these points. For instance, the isolation of high-pressure oil pipe cables from the GIS grounding system often involves difficulties. Although the individual high-voltage or extra-high-voltage terminators may provide adequate separation from the external grounds (by the virtue of a design that usually includes the use of base plate insulators made of high-voltage rated porcelain or fiberglass), problems sometimes arise if the same level of insulation is also expected at other interface points. One typical problem area is the auxiliary piping between the oil chamber of individual GIS terminators and the oil diffusion chamber at the end of a pipe cable that frequently branches to a variety of oil pressure monitoring instruments and alarm devices (Graybill, Koehler, Nadkarni, and Nicholas [B78]). In these branch areas the isolation of metal parts is often achieved by the means of ceramic or plastic inserts. Adequate creepage distance should be ensured where possible. To protect against transient voltages, other precautions might be necessary (Dick, Fujimoto, Ford, and Harvey [B53]; Ford and Geddes [B68]; Fujimoto, Croall, and Foty [B69]).

The direct effects of transient enclosure voltage (TEV) on humans may not necessarily be fatal, but the secondary effects on humans should be carefully considered by the design engineer and manufacturer.

In these and similar circumstances, close cooperation with the GIS manufacturer at the early stages of design is very important.

10.7 Notes on grounding of GIS foundations

Since the earth path of ground currents is strongly affected by the relative position of conductive objects that are in the ground, more attention should be paid to those portions of the GIS grounding system that include discontinuities, or where the design requires an abrupt change in the pattern of ground electrodes. The following circumstances are of concern.

In the limited space of GIS substations, a substantial part of the substation area is often occupied by concrete foundations, which may cause irregularities in a current discharge path. In this respect, a simple monolithic concrete steel reinforced slab is advantageous both as an auxiliary grounding device and for seismic reasons.

If a continuous floor slab is used, a good adjunct measure is to tie its reinforcing steel mesh to the common ground bus (main ground bus) so that both the GIS enclosures and the structural steel in and above the foundation will be approximately the same potential level. The assumption is that this measure should

Copyright © 2015 IEEE. All rights reserved.

Copyright The Institute of Electrical and Electronics Engineers, Inc.
Provided by IHS under license with IEEE
No reproduction or networking permitted without license from IHS

Order Number: 02120914
Sold to:EGAT [700166108393] - VARRIS.Y@EGAT.CO.TH,
Not for Resale,2016-09-15 03:57:51 UTC

produce a better ground and the reinforcing bars, being considerably closer together than the wires of a typical ground grid, should produce more even potentials within the floor and at the surface.[8]

GIS foundations, which include reinforcing bars and other metals, can act as auxiliary ground electrodes and may be so used provided that under no circumstances would the discharge of current result in a damage of concrete because of local overheating or a gradual erosion of the concrete-steel bonds. For further details, refer to 14.6.

10.8 Touch voltage criteria for GIS

Although the GIS manufacturer generally designs the equipment to meet the already mentioned requirements and usually performs most, if not all, calculations that are necessary for determining the sheath voltages and currents during faults, the user still needs to ascertain that the entire installation is safe. Having this possibility in mind, some of the critical aspects of interconnecting the GIS with a grounding system are briefly discussed next.

A certain paradox, inherent to the GIS design, may occur when one tries to determine the best concept of GIS grounding. In contrast to the general wisdom that a large ground connection necessarily equals a good grounding practice, the circulating currents generated in the GIS enclosures during a fault should also be taken into account. To be considered are: 1) where these currents will circulate, and 2) where and to what degree the design engineer or GIS manufacturer, or both, prefer these currents to circulate.

Typically in a continuous enclosure design, the path of enclosure currents includes some structural members of the GIS frame and the enclosures themselves. With each phase enclosure tied to the enclosures of adjacent phases at both ends, several loops are formed. Because a cross section of the mentioned structural members is usually much smaller than that of the enclosure and comparable to that of the grounding straps that connect the GIS assembly to a ground grid (and for that matter, also to the reinforcing bars of the concrete foundation), several questions need to be asked:

a) If the currents divide and flow via all available metallic paths, what ratio is to be expected between the currents circulating within the GIS assembly and those circulating via a ground connection?

b) How much current circulating via a ground connection loop is too much?

c) Is the GIS being designed to be safe if no circulating current would (at least for an external fault) circulate via ground connections?

d) And finally, how much grounding is needed for the best balance between operational and safety-related requirements?

Presently, there are no clear-cut answers and solutions to the questions listed above. Some manufacturers prefer to supply a special ground bus (main ground bus) as a part of the GIS package, with clearly designated ground connection points. Others do not use any main ground bus at all, but simply designate certain points on the enclosure as grounding pads and let the utility complete the grounding.

In either case, it becomes necessary to limit the body current to some value in a milliampere range, while the fault currents that are of concern range from hundreds to thousands of amperes. Thus, one can assume that the full potential difference existing prior to a contact would not change while forcing the current through an alternate path including the body. Then the case of a person touching the GIS sheath metal can be reduced to the problem of finding the voltage drop between two points of contact along one or between

[8] It might be argued that the concrete slab, being a fairly good conductor itself, could produce a more uniform voltage at the floor level if no current would flow into the reinforcing bars from the ground system. If the bars are connected, the electrical field in the earth between the bars of the slab and the underlying grid would be zero. (As both mats are at the same potential, hardly any current would flow out of the bars into the concrete and toward the ground grid.) Therefore, the concrete with reinforcing bars will produce a substantially uniform potential field across the floor surface.

Copyright © 2015 IEEE. All rights reserved.

Copyright The Institute of Electrical and Electronics Engineers, Inc.
Provided by IHS under license with IEEE
No reproduction or networking permitted without license from IHS

Order Number: 02120914
Sold to:EGAT [700166108393] - VARRIS.Y@EGAT.CO.TH,
Not for Resale,2016-09-15 03:57:51 UTC

two enclosures and a common ground. For the hand-to-feet contact made by a person standing on a non-metallic surface (for instance, a concrete slab or the soil layer above the ground grid), only a minor modification of the application criterion of Equation (32) and Equation (33) is required in order to take into account the maximum inductive voltage drop occurring within the GIS assembly.

The touch voltage criterion for GIS is

$$\sqrt{E_t^2 + \left(E'_{to\max}\right)^2} < E_{touch} \tag{36}$$

where

E_t is the maximum touch voltage, as determined for the point underneath a person's feet

$E'_{to\max}$ is the (predominantly inductive) maximum value of metal-to-metal voltage difference on and between GIS enclosures, or between these enclosures and the supporting structures, including any horizontal or vertical members for which the GIS assembly is designed

In practical situations, as shown in Figure 15, a multiplicity of return paths and considerable cross-coupling occurs. This makes the calculation of longitudinally induced currents difficult and for some remote external faults often outright unpractical, as too many parameters remain undefined. As a rule, because of a great variety in possible physical arrangements of the GIS assembly, the GIS manufacturers perform detailed calculations for determining the basic design parameters, such as spacing and location of bonds.

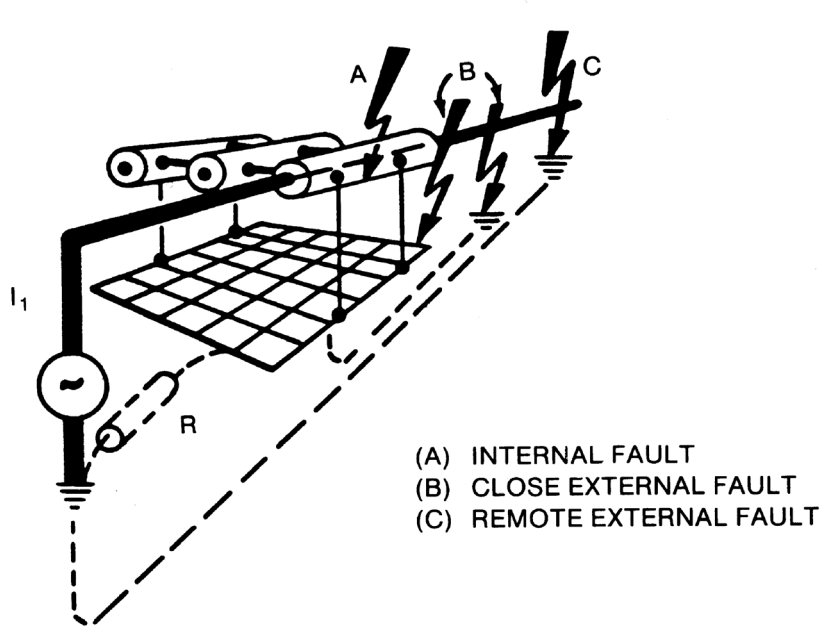

Figure 15—Typical faults in GIS

Copyright © 2015 IEEE. All rights reserved.
Copyright The Institute of Electrical and Electronics Engineers, Inc.
Provided by IHS under license with IEEE
No reproduction or networking permitted without license from IHS
Order Number: 02120914
Sold to:EGAT [700166108393] - VARRIS.Y@EGAT.CO.TH,
Not for Resale,2016-09-15 03:57:51 UTC

10.9 Recommendations

The following recommendations should be considered for GIS installations:

a) When applying the touch voltage criterion Equation (36), the following facts should be considered. The case of an internal fault with ground return requires the addition of the resistive and inductive voltage drop to the resistive drop representing the difference of potentials between the substation ground and the point beneath a person's feet. This generally is not necessary for faults external to the GIS. For an external line-to-ground fault, the voltages induced on the sheath should be checked for a hand-to-hand, metal-to-metal contact, but the calculation of step and touch voltages at the earth's surface is the same as that for conventional installations (i.e., the inductive term in Equation (36) is zero).

b) In evaluating the magnitude of induced voltages caused by faults external to the GIS, only the case of a close-in fault (case (B) in Figure 15) needs to be analyzed because remote external faults will cause less of a problem.

11. Selection of conductors and connections

11.1 Basic requirements

Proper selection of conductor material will maintain the integrity of a grounding system for years if the conductors are of adequate size and the soil conditions are not corrosive to the material used. In assessing which conductor material and what conductor size or what maximum allowable temperature limit needs to be applied in individual design situations, the final choice should always reflect the considerations outlined below.

Each element of the grounding system, including grid conductors, connections, connecting leads, and all primary electrodes, should be so designed that for the expected design life of the installation, the element will:

a) Have sufficient conductivity, so that it will not contribute substantially to local voltage differences.

b) Resist fusing and mechanical deterioration under the most adverse combination of a fault magnitude and duration.

c) Be mechanically reliable and rugged to a high degree.

d) Be able to maintain its function even when exposed to corrosion or physical abuse.

11.2 Choice of material for conductors and related corrosion problems

11.2.1 Copper

Copper is a common material used for grounding systems. Copper conductors, in addition to their high conductivity, have the advantage of being resistant to most underground corrosion because copper is cathodic with respect to most other metals that are likely to be buried in the vicinity.

Copyright © 2015 IEEE. All rights reserved.

Copyright The Institute of Electrical and Electronics Engineers, Inc.
Provided by IHS under license with IEEE
No reproduction or networking permitted without license from IHS

Order Number: 02120914
Sold to:EGAT [700166108393] - VARRIS.Y@EGAT.CO.TH,
Not for Resale,2016-09-15 03:57:51 UTC

11.2.2 Copper-clad and copper-plated steel

Copper-clad and copper-plated steel are common materials used for grounding systems, especially where theft is a problem.

11.2.3 Aluminum

Aluminum has rarely been used for ground grids. Although at first glance the use of aluminum would be a natural choice for GIS equipment with enclosures made of aluminum or aluminum alloys, there are the following disadvantages to consider:

a) Aluminum itself may corrode in certain soils. The layer of corroded aluminum material is non-conductive for all practical grounding purposes.

b) Gradual corrosion caused by alternating currents may also be a problem under certain conditions. It is not recommended to use aluminum conductor underground, despite the fact that, like steel, it would alleviate the problem of contributing to the corrosion of other buried objects. Aluminum is anodic to many other metals, including steel and, if interconnected to one of these metals in the presence of an electrolyte, the aluminum will sacrifice itself to protect the other metal.

11.2.4 Steel

Steel or stainless steel conductors and ground rods may be used in applications where the soil conditions may be detrimental to copper. Of course, such a design requires that attention is paid to the corrosion of the steel or stainless steel. Use of zinc coated steel or stainless steel, in combination with cathodic protection, is typical for steel grounding systems (Mahonar and Nagar [B104]).

11.2.5 Other considerations

A grid of copper or copper-clad steel forms a galvanic cell with buried steel structures, pipes, and any of the lead-based alloys that might be present in cable sheaths. This galvanic cell may hasten corrosion of the latter. Tinning the copper has been tried by some of the utilities. That reduces the cell potential with respect to steel and zinc by about 50% and practically eliminates this potential with respect to lead (tin being slightly sacrificial to lead). The disadvantage of using a tinned copper conductor is that it accelerates and concentrates the natural corrosion, caused by the chemicals in the soil, of the copper in any small bare area. Other often-used methods are

a) Insulation of the sacrificial metal surfaces with a coating such as plastic tape, asphalt compound, or both.

b) Routing of buried metal elements so that any copper-based conductor will cross water pipe lines or similar objects made of other uncoated metals as nearly as possible at right angles, and then applying an insulated coating to one metal or the other where they are in proximity. The insulated coating is usually applied to the pipe.

c) Cathodic protection using sacrificial anodes or impressed current systems.

d) Use of non-metallic pipes and conduits.

In GIS, the use of cathodic protection may also be required for other reasons. Cathodic protection is commonly used to protect facilities that are external to the GIS, such as pressurized pipe-type cables, lead shielded cables, etc. Because of the complexity of GIS installations, it is essential to consider all aspects of corrosion prevention before designing the grounding system. Specific guidelines are difficult to establish because substation conditions may be different due to location and application in the electric power system.

Copyright © 2015 IEEE. All rights reserved.

Copyright The Institute of Electrical and Electronics Engineers, Inc.
Provided by IHS under license with IEEE
No reproduction or networking permitted without license from IHS

Order Number: 02120914
Sold to:EGAT [700166108393] - VARRIS.Y@EGAT.CO.TH,
Not for Resale,2016-09-15 03:57:51 UTC

The subject of underground corrosion and cathodic protection is complex. Many studies have been made and much has been published on this subject. A detailed discussion of these phenomena is beyond the scope of this guide.

11.3 Conductor sizing factors

11.3.1 Symmetrical currents

The short time temperature rise in a ground conductor, or the required conductor size as a function of conductor current, can be obtained from Equation (37) through Equation (42), which are taken from the derivation by Sverak [B137]. These equations are also included as Annex B in IEEE Std 837™ [B89]. These equations evaluate the ampacity of any conductor for which the material constants are known, or can be determined by calculation. Material constants of the commonly used grounding materials are listed in Table 1. Equation (37) through Equation (42) are derived for symmetrical currents (with no dc offset).

$$I = A_{mm^2}\sqrt{\left(\frac{TCAP\times 10^{-4}}{t_c\alpha_r\rho_r}\right)\ln\left(\frac{K_o+T_m}{K_o+T_a}\right)} \tag{37}$$

where

I is the rms current in kA
A_{mm^2} is the conductor cross section in mm^2
K_o $1/\alpha_o$ or $(1/\alpha_r) - T_r$ in °C
T_m is the maximum allowable temperature in °C
T_a is the ambient temperature in °C
T_r is the reference temperature for material constants in °C
α_o is the thermal coefficient of resistivity at 0 °C in 1/°C
α_r is the thermal coefficient of resistivity at reference temperature T_r in 1/°C
ρ_r is the resistivity of the ground conductor at reference temperature T_r in μΩ-cm
t_c is the duration of current in s
$TCAP$ is the thermal capacity per unit volume from Table 1, in J/(cm^3 · °C)

It should be noted that α_r and ρ_r are both to be found at the same reference temperature of T_r °C. Table 1 provides data for α_r and ρ_r at 20 °C.

If the conductor size is given in kcmils ($A_{mm2} \times 1.974 = A_{kcmil}$), Equation (37) becomes

$$I = 5.07\times 10^{-3} A_{kcmil}\sqrt{\left(\frac{TCAP}{t_c\alpha_r\rho_r}\right)\ln\left(\frac{K_o+T_m}{K_o+T_a}\right)} \tag{38}$$

Independent testing shows the actual short-term fusing currents for a copper-clad steel conductor and a copper-bonded steel ground rod can be different than those calculated by Equation (37) because of the phenomenon of variable heat capacity of steel, explained in note (d) of Table 1. Manufacturers of copper-clad steel conductors and copper-plated ground rods may be able to provide test data to help guide decisions as to which product size is appropriate. However, the fusing of bimetallic conductor should refer to the failure of the metal with lower melting temperature because the integrity of the conductor must be maintained throughout the lifetime of the substation.

Copyright © 2015 IEEE. All rights reserved.

Copyright The Institute of Electrical and Electronics Engineers, Inc.
Provided by IHS under license with IEEE
No reproduction or networking permitted without license from IHS

Order Number: 02120914
Sold to:EGAT [700166108393] - VARRIS.Y@EGAT.CO.TH,
Not for Resale,2016-09-15 03:57:51 UTC

11.3.1.1 Calculation of *TCAP*

TCAP can be calculated for materials not listed in Table 1 from the specific heat and density. Specific heat, cp, in cal/(grams × °C) and density, δ, in gram/cm^3 are related to the thermal capacity per unit volume in J/(cm^3) × °C as follows:

4.184 J = 1 calorie

Therefore, *TCAP* is defined by

$$TCAP\ [\text{cal}/(\text{cm}^3 \times °\text{C})] = c_p\ [\text{cal}/(\text{gram} \cdot °\text{C})] \times \delta\ (\text{gram}/\text{cm}^3) \tag{39}$$

or

$$TCAP\ [\text{J}/(\text{cm}^3 \cdot °\text{C})] = 4.184\ (\text{J}/\text{cal}) \times c_p\ [(\text{cal}/(\text{gram} \cdot °\text{C})] \times \delta\ (\text{gram}/\text{cm}^3) \tag{40}$$

Once *TCAP* is determined, Equation (37) and Equation (38) can be used to determine the ampacity of the conductor.

Material constants given in Table 1 for composite materials, such as copper-clad steel, are average values for the conductor.

Specific heat is defined as the amount of energy needed to increase the temperature of one gram of a material by one degree Celsius. Specific heat usually applies to an individual material. However, when the components of a composite conductor stay at the same temperature, an average specific heat can be used. The average specific heat is proportional to the mass fraction. For example, a composite that is 90% material A and 10% material B, the specific heat is the amount of energy required to raise the temperature of 0.9 grams of material A and 0.1 grams of material B by one degree Celsius. The specific heat can be calculated with the following equation.

$$c_{pav} = w_1 c_{p1} + w_2 c_{p2} \tag{41}$$

where

c_{pav} is the average specific heat
w_1 is the mass fraction of material 1
c_{p1} is the specific heat of material 1
w_2 is the mass fraction of material 2
c_{p2} is the specific heat of material 2

The average density is the total mass of the conductor divided by the total volume of the conductor. The average density is calculated using the following equation

$$D_{av} = \frac{m_1 + m_2}{V_1 + V_2} \tag{42}$$

where

D_{av} is the average density
m_1 is the mass of material 1
m_2 is the mass of material 2
V_1 is the volume of material 1
V_2 is the volume of material 2

Copyright © 2015 IEEE. All rights reserved.

Copyright The Institute of Electrical and Electronics Engineers, Inc.
Provided by IHS under license with IEEE
No reproduction or networking permitted without license from IHS

Order Number: 02120914
Sold to:EGAT [700166108393] - VARRIS.Y@EGAT.CO.TH,
Not for Resale,2016-09-15 03:57:51 UTC

Example 1: To calculate the thermal capacity of a 5/8 in nominal copper-clad steel rod with 0.545 in OD, and 0.01 in copper thickness. First the average specific heat and density is calculated from the dimensions of the rod as well as the density and specific heat of the materials

$$Steel\ Area = A_i = \frac{\pi}{4}(0.545)^2 = 0.233\,in^2 = 1.505\,cm^2$$

$$Copper\ Area = A_o = \frac{\pi}{4}\left(0.565^2 - 0.545^2\right) = 0.0174\,in^2 = 0.112\,cm^2$$

$$Mass\,Faction\ \ Steel = w_i = \frac{D_i A_i}{D_i A_i + D_o A_o} = \frac{(7.87)(1.505)}{(7.87)(1.505) + (8.95)(0.112)} = 0.922$$

$$Mass\ \ Faction\ \ Copper = w_i = \frac{D_i A_i}{D_i A_i + D_o A_o} = \frac{(8.95)(0.112)}{(7.87)(1.505) + (8.95)(0.112)} = 0.078$$

$$Average\ \ Specific\ \ Heat = c_{pav} = w_i c_{pi} + w_o c_{po} = (0.922)(0.486) + (0.078)(0.385) = 0.48\frac{J}{g\cdot°C}$$

$$D_{av} = \frac{m_i + m_o}{V_i + V_o} = \frac{D_i A_i L_r + D_o A_o L_r}{A_i L_r + A_o L_r} = \frac{D_i A_i + D_o A_o}{A_i + A_o} = \frac{(7.87)(1.505) + (8.95)(0.112)}{1.505 + 0.112} = 7.9\frac{g}{cm^3}$$

where

A_i is the area of inner layer, cm^2
A_o is the area of outer layer, cm^2
c_{pi} is the specific heat of inner layer, J/(g ·°C)
c_{po} is the specific heat of outer layer, J/(g ·°C)
c_{pav} is the average specific, J/(g ·°C)
D_i is the density of inner layer, g/cm^3
D_o is the density of outer layer, g/cm^3
D_{av} is the average density, g/cm^3
m_i is the mass of inner layer, g
m_o is the mass of outer layer, g
V_i is the volume of the inner layer, cm^3
V_o is the volume of the inner layer, cm^3
w_i is the mass fraction of inner layer
w_o is the mass fraction of outer layer
L_r is the length of the ground rod or wire, m

From the average density and average specific weight the thermal capacity can be calculated.

$$Thermal\ \ Capacity = TCAP = c_{pav} D_{av} = (7.9)(0.48) = 3.8 J/(cm^3 \cdot °C)$$

In this case the thermal capacity in the same as the steel to within rounding error. This is because the volume of steel exceeds the volume of copper by so much that it dominates the thermal capacity.

Copyright © 2015 IEEE. All rights reserved.

Copyright The Institute of Electrical and Electronics Engineers, Inc.
Provided by IHS under license with IEEE
No reproduction or networking permitted without license from IHS

Order Number: 02120914
Sold to:EGAT [700166108393] - VARRIS.Y@EGAT.CO.TH,
Not for Resale,2016-09-15 03:57:51 UTC

Example 2: To calculate the thermal capacity of a 19 No. 9 40% IACS copper-clad steel with 0.572 in OD and 0.1144 in single end diameter. Copper thickness, density, and resistivity, and values are not calculated in this example, but are taken from ASTM B910 as follows:

Minimum copper thickness = 5% of the overall diameter

Density at 20 °C = 8.24 g/cm^3

Maximum resistivity at 20 °C = 4.40 μΩ-cm

$$Steel\ Area = A_i = 19 \times \frac{\pi}{4}(0.103\,in)^2 = 0.158\,in^2 = 1.021\,cm^2$$

$$Copper\ \ Area = A_o = 19 \times \frac{\pi}{4}\left(0.1144^2 - 0.103^2\right)\ in^2 = 0.037\,in^2 = 0.239\,cm^2$$

$$Mass\ Fraction\ Steel = w_i = \frac{D_i A_i}{D_i A_i + D_o A_o} = \frac{(7.87)(1.021)}{(7.87)(1.021) + (8.95)(0.239)} = 0.79$$

$$Mass\ Fraction\ Copper = w_o = \frac{D_i A_i}{D_i A_i + D_o A_o} = \frac{(8.95)(0.239)}{(7.87)(1.021) + (8.95)(0.239)} = 0.21$$

$$Average\ Specific\ Heat = c_{pav} = w_i c_{pi} + w_o c_{po} = (0.79)(0.486) + (0.21)(0.385) = 0.465 \frac{J}{g \cdot °C}$$

$$Thermal\ Capacity = TCAP = c_{pav} \times D_{av} = (0.465 \times \frac{J}{g \cdot °C})(8.24 \frac{g}{cm^3}) = 3.8 \frac{J}{cm^3 \cdot °C}$$

11.3.1.2 Resistivity of clad steel rod

To calculate the resistivity of clad steel rod, it is assumed the metals are electrically in parallel.

$$R_{clad} = \frac{R_i R_o}{R_i + R_o} = \frac{\left(\frac{\rho_i L_r}{A_i}\right)\left(\frac{\rho_o L_r}{A_o}\right)}{\frac{\rho_i L_r}{A_i} + \frac{\rho_o L_r}{A_o}} = \frac{L_r \rho_i \rho_o}{\rho_i A_o + \rho_o A_i} \tag{43}$$

$$\rho_{clad} = \frac{R_{clad} A_{clad}}{L_r} = \frac{\rho_i \rho_o (A_i + A_o)}{\rho_i A_o + \rho_o A_i} \tag{44}$$

where

R_i resistance of inner layer, μΩ
R_o resistance of outer layer, μΩ
R_{clad} resistance of bimetallic rod or wire, μΩ
ρ_i resistivity of inner layer, μΩ-cm
ρ_o resistivity of outer layer, μΩ-cm
ρ_{clad} effective resistivity of bimetallic rod or wire, μΩ-cm
A_i area of inner layer, cm^2

Copyright © 2015 IEEE. All rights reserved.

Copyright The Institute of Electrical and Electronics Engineers, Inc.
Provided by IHS under license with IEEE
No reproduction or networking permitted without license from IHS

Order Number: 02120914
Sold to:EGAT [700166108393] - VARRIS.Y@EGAT.CO.TH,
Not for Resale,2016-09-15 03:57:51 UTC

A_o area of outer layer, cm^2

A_{clad} area of a bimetallic rod or wire, cm^2

Example: A copper-clad 5/8 in nominal steel rod with an outside diameter (OD) of 0.545 in and 0.01 in copper-clad thickness

$$Steel\ Area = A_i = \frac{\pi}{4}(0.545)^2 = 0.233\,\text{in}^2 = 1.505\,cm^2$$

$$Copper\ Area = A_O = \frac{\pi}{4}\left(0.565^2 - 0.545^2\right) = 0.0174\,in^2 = 0.112\ cm^2$$

$$\rho_{clad} = \frac{\rho_i \rho_o \left(A_i + A_o\right)}{\rho_i A_o + \rho_o A_i}$$

$$\rho_{clad} = \frac{15.9(1.72)(1.51 + 0.112)}{15.9(0.112) + 1.72(1.51)} = 10.1\,\mu\Omega\text{-m}$$

Resistivity values are taken from Table 1.

$$\text{Conductivity} = \frac{100(1.72)}{10.1} = 17.0\%$$

Table 1—Material constant

Description	Material[a] conductivity (% IACS)	α_r factor[a] at 20 °C (1/°C)	K_O at 0 °C (0°C)	Fusing[a] temperature T_m (°C)	Resistivity[a] at 20 °C ρ_r (μΩ-cm)	Thermal[a] capacity *TCAP* [J/(cm^3 · °C)]
Copper, annealed soft-drawn	100.0	0.003 93	234	1083	1.72	3.4
Copper, commercial hard-drawn	97.0	0.003 81	242	1084	1.78	3.4
Copper-clad steel wire	40.0	0.003 78	245	1084[e]	4.40	3.8
Copper-clad steel wire	30.0	0.003 78	245	1084[e]	5.86	3.8
Copper-clad steel rod	17.0	0.003 78	245	1084[e]	10.1	3.8
Aluminum-clad steel wire	20.3	0.00360	258	657	8.48	3.561
Steel, 1020	10.8[b]	0.003 77	245	1510	15.90	3.8
Stainless-clad steel rod[c]	9.8	0.003 77	245	1400[e]	17.50	4.4
Zinc-coated steel rod	8.6	0.003 20	293	419[e]	20.10	3.9
Stainless steel, 304	2.4	0.001 30	749	1400	72.00	4.0

[a]Material constants for copper, steel, stainless steel, and zinc are from *The Metals Handbook* by the American Society for Metals.

[b] Copper-clad steel rods based on nominal 5/8 in rod, 0.010 in soft-drawn copper thickness over No. 1020 steel.

[c] Stainless-clad steel rod based on nominal 5/8 in rod, 0.020 in No. 304 stainless steel thickness over No. 1020 steel core.

[d] Unlike most metals, steel has a highly variable heat capacity from 550 °C to 800 °C; however since the heat capacity in this range is much larger than at lower and higher temperatures, calculations using lower values are conservative with respect to conductor heating.

[e] Bi-metallic materials fusing temperature based on metal with lower fusing temperature.

Copyright © 2015 IEEE. All rights reserved.

Copyright The Institute of Electrical and Electronics Engineers, Inc.
Provided by IHS under license with IEEE
No reproduction or networking permitted without license from IHS

Order Number: 02120914
Sold to:EGAT [700166108393] - VARRIS.Y@EGAT.CO.TH,
Not for Resale,2016-09-15 03:57:51 UTC

Equation (37) and Equation (38), in conjunction with Equation (39) and Equation (40) (which defines *TCAP*), reflect two basic assumptions:

a) That all heat will be retained in the conductor (adiabatic process).

b) That the product of specific heat (SH) and density (δ), *TCAP,* is approximately constant because SH increases and δ decreases at about the same rate. For most metals, these premises are applicable over a reasonably wide temperature range, as long as the fault duration is within a few seconds.

$$A_{mm^2} = I \frac{1}{\sqrt{\left(\frac{TCAP \times 10^{-4}}{t_c \alpha_r \rho_r}\right) \ln\left(\frac{K_o + T_m}{K_o + T_a}\right)}} \tag{45}$$

$$A_{kcmil} = I \frac{197.4}{\sqrt{\left(\frac{TCAP}{t_c \alpha_r \rho_r}\right) \ln\left(\frac{K_o + T_m}{K_o + T_a}\right)}} \tag{46}$$

Example: A tabulation can be made, using Equation (46) and Table 1, to get data for 30% and 40% copper-clad steel, and for 100% and 97% copper conductors. For instance, to calculate the 1 s size of a 30% copper-clad steel conductor, one gets

$$t_e = 1.0,\ a_{20} = 0.00378,\ \rho_{20} = 5.86,\ TCAP = 3.85,\ T_m = 1084,\ T_a = 40,\ K_0 = 245$$

Thus, for I = 1 kA and using Equation (46)

$$A_{kcmil} = \frac{197.4}{\sqrt{267.61}} = 12.06 \text{ kcmil}$$

For every 1 kA, 12.06 kcmil is required.

11.3.1.3 Formula simplification

The formula in English units can be simplified to the following:

$$A_{kcmil} = I \times K_f \sqrt{t_c} \tag{47}$$

where

A_{kcmil} is the area of conductor in kcmil
I is the rms fault current in kA
t_c is the current duration in s
K_f is the constant from Table 2 for the material at various values of T_m (fusing temperature or limited conductor temperature based on 11.3.3) and using ambient temperature (T_a) of 40 °C.

Copyright © 2015 IEEE. All rights reserved.

Copyright The Institute of Electrical and Electronics Engineers, Inc.
Provided by IHS under license with IEEE
No reproduction or networking permitted without license from IHS

Order Number: 02120914
Sold to:EGAT [700166108393] - VARRIS.Y@EGAT.CO.TH,
Not for Resale,2016-09-15 03:57:51 UTC

Table 2—Material constants

Material	Conductivity (%)	T_m [a] (^{0}C)	K_f
Copper, annealed soft-drawn	100.0	1083	7.00
Copper, commercial hard-drawn	97.0	1084	7.06
Copper, commercial hard-drawn	97.0	250	11.78
Copper-clad steel wire	40.0	1084	10.45
Copper-clad steel wire	30.0	1084	12.06
Copper-clad steel rod	17.0	1084	14.64
Aluminum-clad steel wire	20.3	657	17.26
Steel 1020	10.8	1510	18.39
Stainless-clad steel rod	9.8	1400	14.72
Zinc-coated steel rod	8.6	419	28.96
Stainless steel 304	2.4	1400	30.05

[a] See 11.3.3 for comments concerning material selection.

Examples: Using Equation (47) for a 20 kA, 3 s fault

a) For soft-drawn copper

$$A_{kcmil} = 20 \times 7\sqrt{3}$$
$$= 242.5 \text{ kcmil}$$
use 250 kcmil

b) For 40% conductivity copper-clad steel conductor

$$A_{kcmil} = 20 \times 10.45\sqrt{3}$$
$$= 362.0 \text{ kcmil}$$
Use 19/No. 7

c) For steel conductor

$$A_{kcmil} = 20 \times 15.95\sqrt{3}$$
$$= 552.5 \text{ kcmil}$$
use 3/4 in diameter conductor

One can also compare the fusing currents of a stated conductor size for various durations of time. Using 4/0 AWG (211.6 kcmil) soft-drawn copper as an example

$$\text{If } t_c = 0.5s;\ I = 211.6/(7.00)\sqrt{0.5} = 42.7 \text{ kA}$$

$$\text{If } t_c = 2.0s;\ I = 211.6/(7.00)\sqrt{2.0} = 30.2 \text{ kA}$$

$$\text{If } t_c = 3.0s;\ I = 211.6/(7.00)\sqrt{3.0} = 17.5 \text{ kA}$$

The conductor size actually selected is usually larger than that based on fusing because of factors such as

a) The conductor should have the strength to withstand any expected mechanical and corrosive abuse during the design life of the grounding installation.
b) The conductor should have a high enough conductance to prevent any possible dangerous voltage drop during a fault, for the life of the grounding installation.
c) The need to limit the conductor temperature (see 11.3.3).
d) A factor of safety should be applied to the grounding system as with other electrical components.

Copyright © 2015 IEEE. All rights reserved.

Copyright The Institute of Electrical and Electronics Engineers, Inc.
Provided by IHS under license with IEEE
No reproduction or networking permitted without license from IHS

Order Number: 02120914
Sold to:EGAT [700166108393] - VARRIS.Y@EGAT.CO.TH,
Not for Resale,2016-09-15 03:57:51 UTC

11.3.2 Asymmetrical currents

11.3.2.1 Using decrement factor

In cases where accounting for a possible dc offset component in the fault current is desired, an equivalent value of the symmetrical current, I_F, representing the effective value of an asymmetrical current integrated over the entire fault duration, t_c, can be determined as a function of *X/R* by using the decrement factor D_f, Equation (84) in 15.10, prior to the application of Equation (37) through Equation (42).

$$I_F = I_f \times D_f \tag{48}$$

The resulting value of I_F is always larger than I_f because the decrement factor is based on a conservative assumption that the ac component does not decay with time but remains constant at its initial subtransient value.

11.3.2.2 Using asymmetrical current tables

Because the dc offset in the fault current will cause the conductor to reach a higher temperature for the same fault conditions (fault current duration and magnitude), Equation (48) determines an equivalent value of the symmetrical current in the presence of dc offset. In addition, if present, dc offset will result in mechanical forces and absorbed energy being almost four times the value than for an equivalent symmetric current case. However, the effect of dc offsets can be neglected if the duration of the current is greater than or equal to 1 s or the *X/R* ratio at the fault location is less than 5.

Fusing characteristics for various sizes of copper conductor with various degree of dc offset are presented in Table 3 Table 4, Table 5, and Table 6. These fusing characteristics have been derived theoretically, and then extensively verified experimentally (Reichman, Vainberg, and Kuffel [B126]).

Table 3—Ultimate current carrying capabilities of copper grounding cables; currents are RMS values, for frequency of 60 Hz, *X/R* = 40; current in kiloamperes

Cable size, AWG	Nominal cross section, mm^2	6 cycles (100 ms)	15 cycles (250 ms)	30 cycles (500 ms)	45 cycles (750 ms)	60 cycles (1 s)	180 cycles (3 s)
No. 2	33.63	22	16	12	10	9	5
No. 1	42.41	28	21	16	13	11	7
1/0	53.48	36	26	20	17	14	8
2/0	67.42	45	33	25	21	18	11
3/0	85.03	57	42	32	27	23	14
4/0	107.20	72	53	40	34	30	17
250 kcmil	126.65	85	62	47	40	35	21
350 kcmil	177.36	119	87	67	56	49	29

Copyright © 2015 IEEE. All rights reserved.

Copyright The Institute of Electrical and Electronics Engineers, Inc.
Provided by IHS under license with IEEE
No reproduction or networking permitted without license from IHS

Order Number: 02120914
Sold to:EGAT [700166108393] - VARRIS.Y@EGAT.CO.TH,
Not for Resale,2016-09-15 03:57:51 UTC

Table 4—Ultimate current carrying capabilities of copper grounding cables; currents are in RMS values, for frequency of 60 Hz, *X/R* = 20; current in kilopamperes

Cable size, AWG	Nominal cross section, mm^2	6 cycles (100 ms)	15 cycles (250 ms)	30 cycles (500 ms)	45 cycles (750 ms)	60 cycles (1 s)	180 cycles (3 s)
No. 2	33.63	25	18	13	11	9	5
No. 1	42.41	32	22	16	13	12	7
1/0	53.48	40	28	21	17	15	9
2/0	67.42	51	36	26	22	19	11
3/0	85.03	64	45	33	27	24	14
4/0	107.20	81	57	42	35	30	18
250 kcmil	126.65	95	67	50	41	36	21
350 kcmil	177.36	134	94	70	58	50	29

Table 5—Ultimate current carrying capabilities of copper grounding cables; currents are in RMS values, for frequency of 60 Hz, *X/R* = 10; current in kiloamperes

Cable size, AWG	Nominal cross section, mm^2	6 cycles (100 ms)	15 cycles (250 ms)	30 cycles (500 ms)	45 cycles (750 ms)	60 cycles (1 s)	180 cycles (3 s)
No. 2	33.63	27	19	13	11	9	5
No. 1	42.41	35	23	17	14	12	7
1/0	53.48	44	30	21	17	15	9
2/0	67.42	56	38	27	22	19	11
3/0	85.03	70	48	34	28	24	14
4/0	107.20	89	60	43	36	31	18
250 kcmil	126.65	105	71	51	42	36	21
350 kcmil	177.36	147	99	72	59	51	30

Copyright © 2015 IEEE. All rights reserved.

Copyright The Institute of Electrical and Electronics Engineers, Inc.
Provided by IHS under license with IEEE
No reproduction or networking permitted without license from IHS

Order Number: 02120914
Sold to:EGAT [700166108393] - VARRIS.Y@EGAT.CO.TH,
Not for Resale,2016-09-15 03:57:51 UTC

Table 6—Ultimate current carrying capabilities of copper grounding cables; currents are in RMS values, for frequency of 60 Hz, *X/R* =0; current in kiloamperes

Cable size, AWG	Nominal cross section, mm^2	6 cycles (100 ms)	15 cycles (250 ms)	30 cycles (500 ms)	45 cycles (750 ms)	60 cycles (1 s)	180 cycles (3 s)
No. 2	33.63	31	19	14	11	9	5
No. 1	42.41	39	24	17	14	12	7
1/0	53.48	49	31	22	18	15	9
2/0	67.42	62	39	28	22	19	11
3/0	85.03	79	50	35	28	25	14
4/0	107.20	99	63	44	36	31	18
250 kcmil	126.65	117	74	52	43	37	21
350 kcmil	177.36	165	104	73	60	52	30

NOTE 1—The current values in Table 3 through Table 6 were computed from the computer program RTGC (Reichman, Vainberg, and Kuffel [B126]). This computer program can be used directly to determine the grounding cable size requirements for known *X/R* ratio and fault clearing time.

NOTE 2—Current is computed for maximum dc offset (see 15.10).

NOTE 3—Initial conductor temperature = 40 °C; final conductor temperature = 1083 °C.

NOTE 4—Metric values are soft conversions. Soft conversion is a direct area calculation, in metric units, from the AWG size.

11.3.3 Additional conductor sizing factors

The designer should take precautions to verify that the temperature of any conductor and connection in the grounding installation does not pose a danger to the safe operation of the substation. For instance

a) Typically, conductors and connections near flammable materials should be subject to more stringent temperature limitations.

b) If the strength of hard-drawn copper is required for mechanical reasons, then it may be prudent not to exceed 250 °C to prevent annealing of the conductors.

The possible exposure to a corrosive environment should be carefully examined. Even when the correct conductor size and the selected joining (connecting) method have satisfied all the IEEE Std 837 [B89] test requirements, it may be prudent to choose a larger conductor size to compensate for some gradual reduction in the conductor cross section during the design life of the installation where the soil environment tends to promote corrosion.

The down leads from the equipment to the grid may be subjected to the total fault current into the grid, while the grid divides this current so that each conductor segment in the grid is only subjected to some fraction of the total fault current. Thus, the down leads may have to be larger than the grid conductors or may have to be multiples from the equipment to the grid to have sufficient ampacity for the total fault current.

Ground lead conductors conducting lightning current seldom require further consideration. The size of the conductor, which is selected according to its fault current requirements, usually is also adequate for carrying short time surges caused by lightning (Bellaschi [B7]).

Copyright © 2015 IEEE. All rights reserved.

Copyright The Institute of Electrical and Electronics Engineers, Inc.
Provided by IHS under license with IEEE
No reproduction or networking permitted without license from IHS

Order Number: 02120914
Sold to:EGAT [700166108393] - VARRIS.Y@EGAT.CO.TH,
Not for Resale,2016-09-15 03:57:51 UTC

In practice, the requirements on mechanical reliability will set the minimum conductor size. While it might seem proper for the designer to establish minimum sizes in light of local conditions, the need for conservatism deserves consideration. Some of the specific reasons are

a) Relay malfunctions can result in fault duration in excess of primary clearing times. The backup clearing time is usually adequate for sizing the conductor. For smaller substations, this may approach 3 s or longer. However, because large substations usually have complex or redundant protection schemes, the fault will generally be cleared in 1 s or less.

b) The ultimate value of current used to determine the conductor size should take into account the possibility of future growth. It is less costly to include an adequate margin in conductor size during the initial design than to try to reinforce a number of ground leads at a later date.

11.4 Selection of connections

All connections made in a grounding network above and below ground should be evaluated to meet the same general requirements of the conductor used; namely, electrical conductivity, corrosion resistance, current carrying capacity, and mechanical strength. These connections should be massive enough to maintain a temperature rise below that of the conductor and to withstand the effect of heating. The connections should also be strong enough to withstand the electromagnetic forces of the maximum expected fault currents and be able to resist corrosion for the intended life of the installation.

IEEE Std 837 [B89] provides detailed information on the application and testing of permanent connections for use in substation grounding. Grounding connections that pass IEEE Std 837 [B89] satisfy all the criteria—electrical conductivity, corrosion resistance, current carrying capacity, and mechanical strength.

12. Soil characteristics

12.1 Soil as a grounding medium

The behavior of a ground electrode buried in soil can be analyzed by means of the circuit in Figure 16. As shown, most soils behave both as a conductor of resistance, r, and as a dielectric. Except for high-frequency and steep-front waves penetrating a very resistive soil material, the charging current is negligible in comparison to the leakage current, and the earth can be represented by a pure resistance.

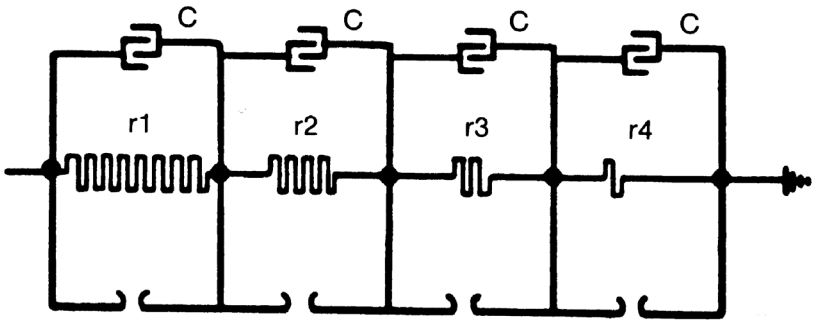

Figure 16—Soil model

Copyright © 2015 IEEE. All rights reserved.

Copyright The Institute of Electrical and Electronics Engineers, Inc.
Provided by IHS under license with IEEE
No reproduction or networking permitted without license from IHS

Order Number: 02120914
Sold to:EGAT [700166108393] - VARRIS.Y@EGAT.CO.TH,
Not for Resale,2016-09-15 03:57:51 UTC

12.2 Effect of voltage gradient

The soil resistivity is not affected by a voltage gradient unless the latter exceeds a certain critical value. The value somewhat varies with the soil material, but it usually has the magnitude of several kilovolts per centimeter. Once exceeded, arcs would develop at the electrode surface and progress into the earth so as to increase the effective size of the electrode, until gradients are reduced to values that the soil material can withstand. This condition is illustrated by the presence of gaps in Figure 16. Because the substation grounding system normally is designed to comply with far more stringent criteria of step and touch voltage limits, the gradient can always be assumed to be below the critical range.

12.3 Effect of current magnitude

Soil resistivity in the vicinity of ground electrodes may be affected by current flowing from the electrodes into the surrounding soil. The thermal characteristics and the moisture content of the soil will determine if a current of a given magnitude and duration will cause significant drying and thus increase the effective soil resistivity. A conservative value of current density, as given by Armstrong [B5], is not to exceed 200 A/m^2 for 1 s.

12.4 Effect of moisture, temperature, and chemical content

Electrical conduction in soils is essentially electrolytic. For this reason the resistivity of most soils rises abruptly whenever the moisture content accounts for less than 15% of the soil weight. The amount of moisture further depends upon the grain size, compactness, and variability of the grain sizes. However, as shown in curve 2 of Figure 17, the resistivity is little affected once the moisture content exceeds approximately 22%, as shown in IEEE Std 142™ [B86].

The effect of temperature on soil resistivity is nearly negligible for temperatures above the freezing point. At 0 °C, the water in the soil starts to freeze and the resistivity increases rapidly. Curve 3 shows this typical variation for a sandy loam soil containing 15.2% of moisture by weight.

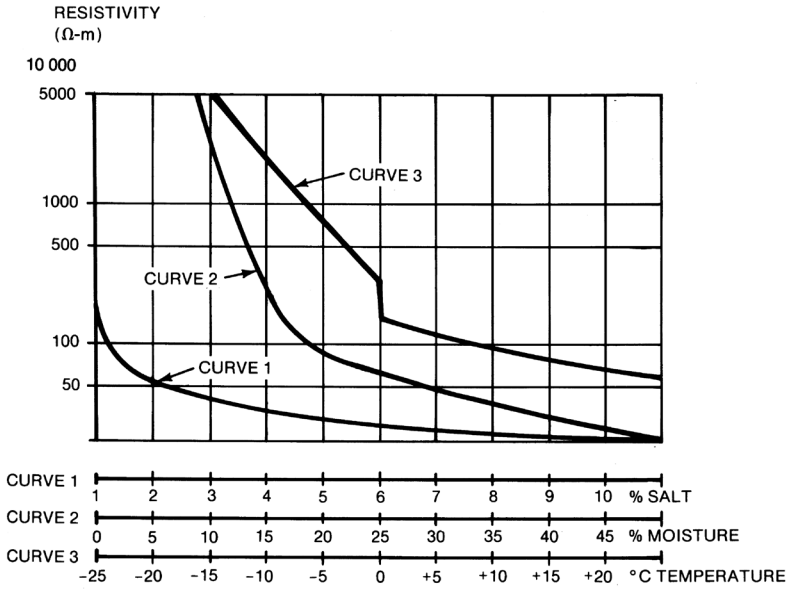

Figure 17—Effects of moisture, temperature, and salt upon soil resistivity

Copyright © 2015 IEEE. All rights reserved.
Copyright The Institute of Electrical and Electronics Engineers, Inc.
Provided by IHS under license with IEEE
No reproduction or networking permitted without license from IHS
Order Number: 02120914
Sold to:EGAT [700166108393] - VARRIS.Y@EGAT.CO.TH,
Not for Resale,2016-09-15 03:57:51 UTC

The composition and the amount of soluble salts, acids, or alkali present in the soil may considerably affect its resistivity. Curve 1 of Figure 18 illustrates a typical effect of salt (sodium chloride) on the resistivity of a soil containing 30% moisture by weight (Towne [B151]).

Figure 17 should not be used for calculation purposes. To determine the actual soil resistivity, tests such as those described in IEEE Std 81™ should be performed at the site.

12.5 Use of surface material layer

Gravel or surface material coverings, usually about 0.08 m to 0.15 m (3 in to 6 in) in depth, are very useful in retarding the evaporation of moisture and, thus, in limiting the drying of topsoil layers during prolonged dry weather periods. Also, as discussed in 7.4, covering the surface with a material of high resistivity is very valuable in reducing shock currents. The value of this layer in reducing shock currents is not always fully realized. Tests by Bodier [B15] at a substation in France showed that the river gravel used as yard surfacing when moistened had a resistivity of 5000 Ω-m. A layer 0.1 m to 0.15 m (4 in to 6 in) thick decreased the danger factor (ratio of body to short-circuit current) by a ratio of 10:1, as compared to the natural moist ground. Tests by Langer [B99] in Germany compared body currents when touching a hydrant while standing on wet coarse gravel of 6000 Ω-m resistivity with body currents while standing on dry sod. The current in the case of dry sod was of the order of 20 times the value for wet coarse gravel. Tests reported by others provide further confirmation of these benefits (Elek [B55]; EPRI TR-100863 [B65]).

In basing calculations on the use of a layer of clean surface material or gravel, consideration should be given to the possibility that insulation may become impaired in part through filling of voids by compression of the lowest ballast layers into the soil beneath by material from subsequent excavations, if not carefully removed, and in some areas by settlement of airborne dust.

The range of resistivity values for the surface material layer depends on many factors, some of which are kinds of stone, size, condition of stone (that is, clean or with fines), amount and type of moisture content, atmospheric contamination, etc. Table 7 indicates that the resistivity of the water with which the rock is wet has considerable influence on the measured resistivity of the surface material layer. Thus, surface material subjected to sea spray may have substantially lower resistivity than surface material utilized in arid environments. As indicated by Table 7, local conditions, size, and type of stone, etc., may affect the value of resistivity. Thus, it is important that the resistivity of rock samples typical of the type being used in a given area be measured.

Table 7 gives typical resistivity values for different types of surface material measured by several different parties in different regions of the United States (Abledu and Laird [B2]; EPRI TR-100863 [B64]; Hammond and Robson [B79]; Thompson [B149][B150]). These values are not valid for all types and sizes of stone in any given region. Tests should be performed to determine the resistivity of the stone typically purchased by the utility.

Copyright © 2015 IEEE. All rights reserved.

Copyright The Institute of Electrical and Electronics Engineers, Inc.
Provided by IHS under license with IEEE
No reproduction or networking permitted without license from IHS

Order Number: 02120914
Sold to:EGAT [700166108393] - VARRIS.Y@EGAT.CO.TH,
Not for Resale,2016-09-15 03:57:51 UTC

Table 7—Typical surface material resistivities

Number	Description of surface material (U.S. state where found)	Resistivity of sample, Ω-m	
		Dry	Wet
1	Crusher run granite with fines (NC)	140×10^6	1300 (ground water, 45 Ω-m)
2	1½ in (0.04 m) crusher run granite (GA) with fines	4000	1200 (rain water, 100 Ω-m)
3	¾ in to1 in (0.02 m to 0.025 m) granite (CA) with fines	---	6513 (10 minutes after 45 Ω-m water drained)
4	No. 4 (1 in to 2 in) (0.025 m to 0.05 m) washed granite (GA)	1.5×10^6 to 4.5×10^6	5000 (rain water, 100 Ω-m)
5	No. 3 (2 in to 4 in) (0.05 m to 0.1 m) washed granite (GA)	2.6×10^6 to 3×10^6	10 000 (rain water, 100 Ω-m)
6	Size unknown, washed limestone (MI)	7×10^6	2000 to 3000 (ground water, 45 Ω-m)
7	Washed granite, similar to ¾ in (0.02 m) gravel	2×10^6	10 000
8	Washed granite, similar to pea gravel	40×10^6	5000
9	No. 57 (¾ in) (0.02 m) washed granite (NC)	190×10^6	8000 (ground water, 45 Ω-m)
10	Asphalt	2×10^6 to 30×10^6	10 000 to 6×10^6
11	Concrete	1×10^6 to 1×10^9 [a]	21 to 200

[a]Oven-dried concrete (Hammond and Robson [B79]). Values for air-cured concrete can be much lower due to moisture content.

13. Soil structure and selection of soil model

13.1 Investigation of soil structure

Resistivity investigations of a substation site are essential for determining both the general soil composition and degree of homogeneity. Boring test samples and other geological investigations often provide useful information on the presence of various layers and the nature of soil material, leading at least to some ideas as to the range of resistivity at the site.

13.2 Classification of soils and range of resistivity

A number of tables exist in the literature showing the ranges of resistivity for various soils and rocks. The tabulation from Rüdenberg [B130] has the advantage of extreme simplicity. More detailed data are available in engineering handbooks and publications (for instance, Sunde [B134] and Wenner [B154]). See Table 8.

Copyright © 2015 IEEE. All rights reserved.
Copyright The Institute of Electrical and Electronics Engineers, Inc.
Provided by IHS under license with IEEE
No reproduction or networking permitted without license from IHS
Order Number: 02120914
Sold to:EGAT [700166108393] - VARRIS.Y@EGAT.CO.TH,
Not for Resale,2016-09-15 03:57:51 UTC

Table 8—Range of earth resistivity

Type of earth	Average resistivity (Ω-m)
Wet organic soil	10
Moist soil	10^2
Dry soil	10^3
Bedrock	10^4

13.3 Resistivity measurements

Estimates based on soil classification yield only a rough approximation of the resistivity. Actual resistivity tests therefore are imperative. These should be made at a number of places within the site. Substation sites where the soil may possess uniform resistivity throughout the entire area and to a considerable depth are seldom found. Typically, there are several layers, each having a different resistivity. Often, lateral changes also occur, but in comparison to the vertical ones, these changes usually are more gradual. Soil resistivity tests should be made to determine if there are any important variations of resistivity with depth. The number of such readings taken should be greater where the variations are large, especially if some readings are so high as to suggest a possible safety problem.

If the resistivity varies appreciably with depth, it is often desirable to use an increased range of probe spacing in order to obtain an estimate of the resistivity of deeper layers. This is possible because, as the probe spacing is increased, the test source current penetrates more and more distant areas, in both vertical and horizontal directions, regardless of how much the current path is distorted due to the varying soil conditions (*Manual on Ground Resistance Testing* [B105]).

A number of measuring techniques are described in detail in IEEE Std 81. The Wenner four-pin method, as shown in Figure 18, is the most commonly used technique. In brief, four probes are driven into the earth along a straight line, at equal distances *a* apart, driven to a depth *b*. The voltage between the two inner (potential) electrodes is then measured and divided by the current between the two outer (current) electrodes to give a value of resistance *R*.

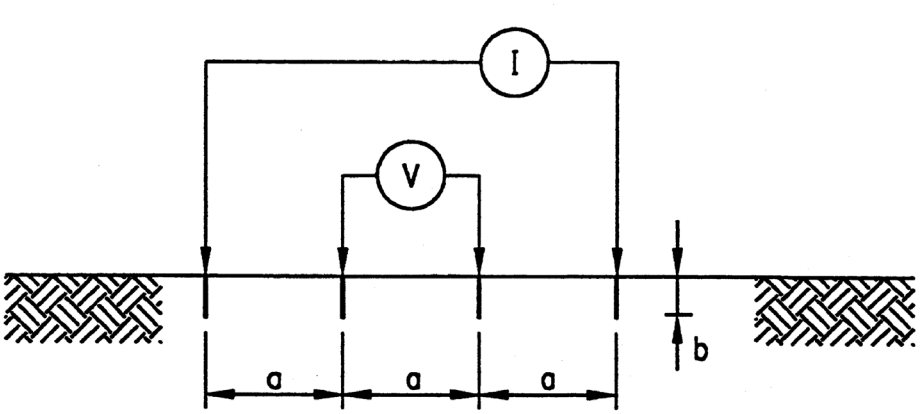

Figure 18—Wenner four-pin method

Copyright © 2015 IEEE. All rights reserved.
Copyright The Institute of Electrical and Electronics Engineers, Inc.
Provided by IHS under license with IEEE
No reproduction or networking permitted without license from IHS
Order Number: 02120914
Sold to:EGAT [700166108393] - VARRIS.Y@EGAT.CO.TH,
Not for Resale,2016-09-15 03:57:51 UTC

Then,

$$\rho_a = \frac{4\pi aR}{1 + \frac{2a}{\sqrt{a^2 + 4b^2}} - \frac{a}{\sqrt{a^2 + b^2}}} \tag{49}$$

where

ρ_a is the apparent resistivity of the soil in Ω-m
R is the measured resistance in Ω
a is the distance between adjacent electrodes in m
b is the depth of the electrodes in m

If b is small compared to a, as is the case of probes penetrating the ground only a short distance, Equation (49) can be reduced to

$$\rho_a = 2\pi aR \tag{50}$$

The current tends to flow near the surface for the small probe spacing, whereas more of the current penetrates deeper soils for large spacing. Thus, it is usually a reasonable approximation to assume that the resistivity measured for a given probe spacing a represents the apparent resistivity of the soil to a depth of a when soil layer resistivity contrasts are not excessive. Equation (49) and Equation (50) thus can be used to determine the apparent resistivity ρ_a at a depth a.

Palmer [B122] is a modified version of the Wenner method. This method gives greater sensitivity for large probe spacing, as described in IEEE Std 81.

Another method of measuring soil resistivity, as shown in Figure 19 and described in IEEE Std 81, is the driven-rod method based on the three-pin or fall-of-potential method (Blattner [B12][B13]; Purdy [B125]).

In this method, the depth L_r of the driven-rod located in the soil to be tested is varied. The other two rods, known as reference rods, are driven to a shallow depth in a straight line. The location of the voltage rod is varied between the test rod and the current rod. Alternately, the voltage rod may be placed on the side opposite the current rod. The apparent resistivity is given by

$$\rho_a = \frac{2\pi L_r R}{\ln\left(\frac{8L_r}{d}\right) - 1} \tag{51}$$

where

L_r is the length of the rod in m
d is the diameter of the rod in m

A plot of the measured apparent resistivity value ρ_a versus the rod length L_r provides a visual aid for determining earth resistivity variations with depth.

Tests conducted by Ohio State University [B63] demonstrated that either the Wenner four-pin method or the driven-rod three-pin method can provide the information needed to develop a soil model.

Copyright © 2015 IEEE. All rights reserved.

Copyright The Institute of Electrical and Electronics Engineers, Inc.
Provided by IHS under license with IEEE
No reproduction or networking permitted without license from IHS

Order Number: 02120914
Sold to:EGAT [700166108393] - VARRIS.Y@EGAT.CO.TH,
Not for Resale,2016-09-15 03:57:51 UTC

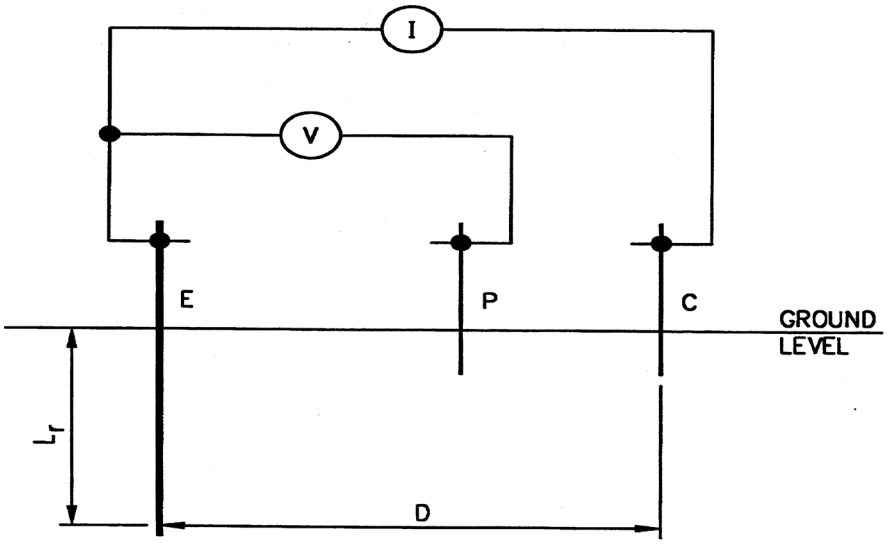

Figure 19—Circuit diagram for three-pin or driven-ground rod method

The Wenner four-pin method is the most popular method in use. There are a number of reasons for this popularity. The four-pin method obtains the soil resistivity data for deeper layers without driving the test pins to those layers. No heavy equipment is needed to perform the four-pin test. The results are not greatly affected by the resistance of the test pins or the holes created in driving the test pins into the soil.

An advantage of the driven-rod method, although not related necessarily to the measurements, is the ability to determine to what depth the ground rods can be driven. Knowing if and how deep rods can be driven into the earth can save the need to redesign the ground grid. Often, because of hard layers in the soil such as rock, hard clay, etc., it becomes practically impossible to drive the test rod any further resulting in insufficient data. A technique for the prediction of the soil resistivity to a depth 10 times the depth of known resistivity value has been developed by Blattner [B12]. This technique can be effectively used in cases where the test rod cannot be driven deep. However, the user is advised to review practical limitations of this technique before using it. A disadvantage of the driven-rod method is that when the test rod is driven deep in the ground, it usually loses contact with the soil due to the vibration and the larger diameter couplers resulting in higher measured resistance values. A ground grid designed with these higher soil resistivity values may be unnecessarily conservative. The driven-rod method presents an uncertainty in the resistance value. The 62% rule is valid only for large electrode separation and uniform soil. In non-uniform soils, this assumption may affect the outcome of the readings, as described in IEEE Std 81. If the flat portion of the curve is used to determine the test rod resistance, this flat portion may not give the correct resistance in non-uniform soil, and the flat portion may not even be obtained unless the test and current rod separation is very large (Dawalibi and Mukhedkar [B40][B45]).

Resistivity measurement records should include temperature data and information on the moisture content of the soil at the time of measurement. All data available on known buried conductive objects in the area studied should also be recorded.

Buried conductive objects in contact with the soil can invalidate readings made by the methods described if they are close enough to alter the test current flow pattern. This is particularly true for large or long objects. For this reason, the soil resistivity measurements are likely to be significantly distorted in an area where grid conductors have already been installed, except for shallow-depth measurements in or near the center of a very large mesh rectangle. In such cases, a few approximate readings might be taken in a short distance outside the grid, with the probes so placed as to minimize the effect of the grid on the current flow pattern.

Copyright © 2015 IEEE. All rights reserved.

Copyright The Institute of Electrical and Electronics Engineers, Inc.
Provided by IHS under license with IEEE
No reproduction or networking permitted without license from IHS

Order Number: 02120914
Sold to:EGAT [700166108393] - VARRIS.Y@EGAT.CO.TH,
Not for Resale,2016-09-15 03:57:51 UTC

Though not conclusive as to conditions inside the grid, such readings may be used for approximation, especially if there is reason to believe that the soil in the entire area is reasonably homogeneous.

13.4 Interpretation of soil resistivity measurements

Interpretation of apparent resistivity obtained in the field is perhaps the most difficult part of the measurement program. The basic objective is to derive a soil model that is a good approximation of the actual soil. Soil resistivity varies laterally and with respect to depth, depending on the soil stratification. Seasonal variations may occur in soil resistivity due to varying weather conditions as described in EPRI TR 100863 [B65]. It must be recognized that the soil model is only an approximation of the actual soil conditions and that a perfect match is unlikely.

The most commonly used soil resistivity models are the uniform soil model and the two-layer soil model. Two-layer soil models are often a good approximation of many soil structures while multilayer soil models may be used for more complex soil conditions. Interpretation of the soil resistivity measurements may be accomplished either manually or by use of computer analysis techniques described in Blattner [B12][B13]; Blattner and Dawalibi [B14]; Endrenyi [B57]; EPRI EL-2699 [B61]; EPRI EL-3982 [B63]; EPRI TR-100622 [B64]; Lazzara and Barbeito [B101]; Meliopoulos and Papelexopoulos [B106]; Meliopoulos, Papelexopoulos, Webb, and Blattner [B108]; Moore [B113]; Nahman and Salamon [B115]; Roman [B127]; and Tagg [B139].

A uniform soil model should be used only when there is a moderate variation in apparent resistivity. In homogeneous soil conditions, which rarely occur in practice, the uniform soil model may be reasonably accurate. If there is a large variation in measured apparent resistivity, the uniform soil model is unlikely to yield accurate results.

A more accurate representation of the actual soil conditions can be obtained by use of a two-layer model. The two-layer model consists of an upper layer of finite depth and with different resistivity than a lower layer of infinite thickness. There are several techniques to determine an equivalent two-layer model from apparent resistivity obtained from field tests. In some instances a two-layer model can be approximated by visual inspection of a plot of the apparent resistivity versus depth from driven rod measurements or apparent resistivity versus probe spacing from Wenner four-pin measurements (Blattner [B11][B13]; IEEE Tutorial Course 86 [B90]).

Computer programs available to the industry may also be used to derive a two-layer soil model and multilayer soil models (Dawalibi and Barbeito [B39]; EPRI EL-2699 [B61]; EPRI TR-100622 [B64]; Orellara and Mooney [B120]).

In some instances the variation in soil resistivity may exhibit minimums and maximums such that an equivalent two-layer model may not yield an accurate model. In such instances a different soil model, such as a multilayer model, may be required as described in Dawalibi, Ma, and Southey [B47] and Dawalibi and Barbeito [B39].

13.4.1 Uniform soil assumption

A uniform soil model can be used instead of the multilayer soil model whenever the two-layer or multilayer computation tools are not available. Unfortunately, an upper bound of the error on all relevant grounding parameters is difficult to estimate in general, but when the contrast between the various layer resistivities is moderate, an average soil resistivity value may be used as a first approximation or to establish order of magnitudes. The approximate uniform soil resistivity may be obtained by taking an arithmetic average of the measured apparent resistivity data as shown in Equation (52).

Copyright © 2015 IEEE. All rights reserved.

Copyright The Institute of Electrical and Electronics Engineers, Inc.
Provided by IHS under license with IEEE
No reproduction or networking permitted without license from IHS

Order Number: 02120914
Sold to:EGAT [700166108393] - VARRIS.Y@EGAT.CO.TH,
Not for Resale,2016-09-15 03:57:51 UTC

$$\rho_{a(av1)} = \frac{\rho_{a(1)} + \rho_{a(2)} + \rho_{a(3)} + \cdots + \rho_{a(n)}}{n} \tag{52}$$

where

$\rho_{a(1)}, \rho_{a(2)}, \rho_{a(3)} \ldots \rho_{a(n)}$ are the measured apparent resistivity data obtained at different spacings in the four-pin method or at different depths in the driven ground rod method in Ω-m

n is total number of measurements

A majority of the soils will not meet the criteria of Equation (52). It is difficult to develop a uniform soil model when the resistivity of a soil varies significantly. Because the step and touch voltage equations of this guide are based on uniform soil models, an attempt was made to develop a guideline to approximate a non-uniform soil to a uniform soil. Apparent soil resistivity data were obtained using the four-pin method from several different geographical locations. The soil data from each location were approximated with three different equivalent soil models. These approximate models consisted of one computer-generated (EPRI TR100622 [B64]) two-layer model and two uniform soil models. The uniform soil models were determined from measured apparent resistivity data using Equation (52) and Equation (53). In the next step, the grid resistance and step/touch voltages for a 76.2 m × 76.2 m (250 ft × 250 ft) grid with a total of 64 uniformly distributed ground rods were computed using a computer program (EPRI TR-100622 [B64]). The depth of the ground rods was dependent on the soil model used. For example, in the case of the two-layer model, the ground rods penetrated the lower layer. Refer to Annex E for more details of this investigation. Finally, the grounding parameters computed for the two-layer model were compared with that computed using the uniform soil models. The grounding parameters computed using the uniform soil model of Equation (48) compared well with that computed using the two-layer model.

$$\rho_{a(av2)} = \frac{\rho_{a(\max)} + \rho_{a(\min)}}{2} \tag{53}$$

where

$\rho_{a(\max)}$ is the maximum apparent resistivity value (from measured data) in Ω-m

$\rho_{a(\min)}$ is the minimum apparent resistivity value (from measured data) in Ω-m

There are a number of assumptions made in the above study. As a result, the Equation (53) should be used with caution. For example, use of Equation (53) is not recommended for a ground grid without ground rods (Dawalibi, Ma, and Southey [B48]). In addition, if the uniform soil resistivity determined using Equation (53) is employed to design a ground grid, the ground rods should at least reach the depth where the measured resistivity corresponds to the computed value of $\rho_{a(av2)}$.

There are several methods suggested by different authors to approximate a non-uniform soil with a uniform soil model. One of these methods includes using the average of upper layer apparent resistivity for the touch and step voltage calculations and the average of lower layer apparent resistivity for the grounding system resistance calculation. Dawalibi and Barbeito [B39]; Dawalibi, Ma, and Southey [B47]; EPRI TR-100622 [B64]; Fujimoto, Dick, Boggs, and Ford [B70]; and Thapar and Gerez [B144] may provide additional information about interpretation of the measured soil data and the influence of multilayer, two-layer, and uniform soil models on grounding parameters.

13.4.2 Non-uniform soil assumptions

Another approach to situations where resistivity varies markedly with depth is suggested by Sunde [B134], and in some of the books on geophysical prospecting to which he refers. For example, it is often possible

Copyright © 2015 IEEE. All rights reserved.

Copyright The Institute of Electrical and Electronics Engineers, Inc.
Provided by IHS under license with IEEE
No reproduction or networking permitted without license from IHS

Order Number: 02120914
Sold to:EGAT [700166108393] - VARRIS.Y@EGAT.CO.TH,
Not for Resale,2016-09-15 03:57:51 UTC

from field readings taken with a wide range of probe spacing to deduce a stratification of the earth into two or more layers of appropriate thickness that will account for the actual test variations (Moore [B113]).

13.4.2.1 Two-layer soil model (general)

A two-layer soil model can be represented by an upper layer soil of a finite depth above a lower layer of infinite depth. The abrupt change in resistivity at the boundaries of each soil layer can be described by means of a reflection factor. The reflection factor, *K*, is defined by Equation (54).

$$K = \frac{\rho_2 - \rho_1}{\rho_1 + \rho_2} \tag{54}$$

where

ρ_1 is the upper layer soil resistivity, in Ω-m

ρ_2 is the lower layer soil resistivity, in Ω-m

While the most accurate representation of a grounding system should certainly be based on the actual variations of soil resistivity present at the substation site, it will rarely be economically justifiable or technically feasible to model all these variations. However, in most cases, the representation of a ground electrode based on an equivalent two-layer earth model is sufficient for designing a safe grounding system.

IEEE Std 81 provides methods for determining the equivalent resistivities of the upper and lower layer of soil and the height of the upper layer for such a model.

There are other methods suggested by authors that include determining a two-layer model and using the upper layer resistivity for touch and step calculations and the lower resistivity for resistance and methods that modify the equations presented in the guide to be used in two-layer soil models. These papers may provide the designer with more information about the interpretation of soils and the impact of multilayer, two-layer, and uniform models (Dawalibi and Barbeito [B39]; Dawalibi, Ma, and Southey [B47]; Thapar and Gerez [B144]).

13.4.2.2 Two-layer soil model by graphical method

A two-layer soil model can be approximated by using graphical methods described in Blattner and Dawalibi [B14]; Endrenyi [B57]; Roman [B127]; Sunde [B134]; and Tagg [B140]. Sunde's graphical method is described in the following paragraphs.

In Sunde's method, the graph shown in Figure 20 is used to approximate a two-layer soil model. The graph in Figure 20, which is based on the Wenner four-pin test data, is reproduced from Figure 2.6 of Sunde [B134], with notations revised to match the symbols used in this guide.

Parameters ρ_1 and ρ_2 are obtained by inspection of plotted resistivity measurements (Figure 21). Only *h* is obtained by Sunde's graphical method, as follows:

a) Plot a graph of apparent resistivity ρ_a on y-axis versus pin spacing on x-axis.

b) Estimate ρ_1 and ρ_2 from the graph plotted in a). ρ_a corresponding to a smaller spacing is ρ_1 and for a larger spacing is ρ_2. Extend the apparent resistivity graph at both ends to obtain these extreme resistivity values if the field data are insufficient.

Copyright © 2015 IEEE. All rights reserved.

Copyright The Institute of Electrical and Electronics Engineers, Inc.
Provided by IHS under license with IEEE
No reproduction or networking permitted without license from IHS

Order Number: 02120914
Sold to:EGAT [700166108393] - VARRIS.Y@EGAT.CO.TH,
Not for Resale,2016-09-15 03:57:51 UTC

c) Determine ρ_2/ρ_1 and select a curve on the Sunde graph in Figure 20, which matches closely, or interpolate and draw a new curve on the graph.

d) Select the value on the y-axis of ρ_a/ρ_1 within the sloped region of the appropriate ρ_2/ρ_1 curve of Figure 20.

e) Read the corresponding value of *a/h* on the x-axis.

f) Compute ρ_a by multiplying the selected value, ρ_a/ρ_1, in d) by ρ_1.

g) Read the corresponding probe spacing from the apparent resistivity graph plotted in a).

h) Compute *h*, the depth of the upper level, using the appropriate probe separation, *a*.

Using the soil data from soil type 1 in Table E.2, a plot of resistivity versus spacing can be drawn. See Figure 23. Both ρ_1 and ρ_2 can be determined by visual inspection. Assuming ρ_1 = 100 Ω-m and ρ_2 = 300 Ω-m, the following example illustrates Sunde's graphical method:

a) Plot Figure 23.

b) Choose ρ_1 = 100 Ω-m, ρ_2 = 300 Ω-m

c) ρ_2/ρ_1 = 300/100 = 3. Draw curve on Figure 20. (See Figure 22 for an example.)

d) Select ρ_a/ρ_1 = 2.

e) Read *a/h* = 2.7 from Figure 22 for ρ_a/ρ_1 = 2.

f) Compute ρ_a: $\rho_a = 2\rho_1 = 2(100) = 200$.

g) Read *a* = 19 on the apparent resistivity curve of Figure 23 for ρ_a = 200.

h) Compute h; $h = \frac{a}{a/h}$ 19/2.7 = 7.0 m or 23 ft.

This compares favorably with the 6.1 m (20 ft) using EPRI TR-100622 [B64].

Copyright © 2015 IEEE. All rights reserved.

Copyright The Institute of Electrical and Electronics Engineers, Inc.
Provided by IHS under license with IEEE
No reproduction or networking permitted without license from IHS

Order Number: 02120914
Sold to:EGAT [700166108393] - VARRIS.Y@EGAT.CO.TH,
Not for Resale,2016-09-15 03:57:51 UTC

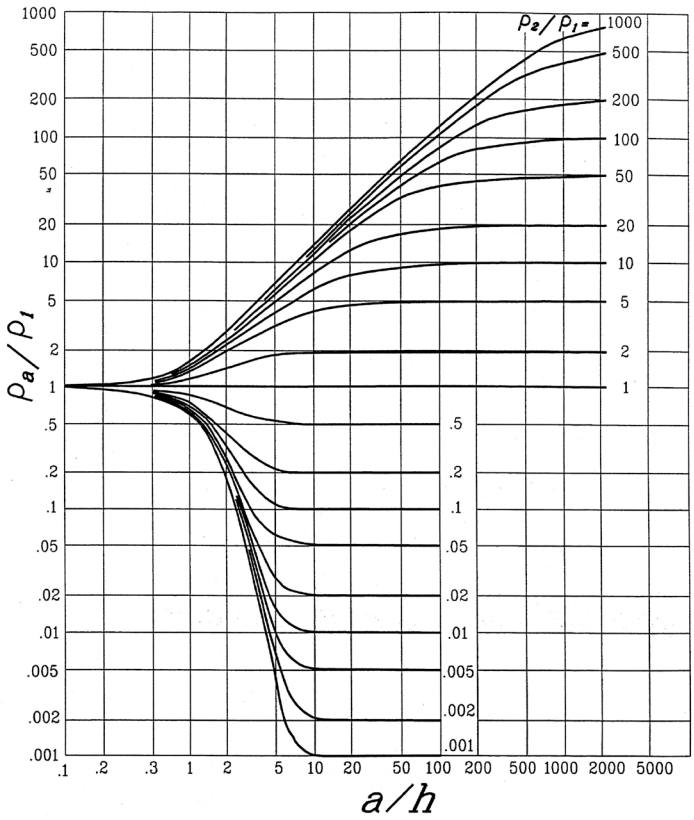

Figure 20—Sunde's graphical method

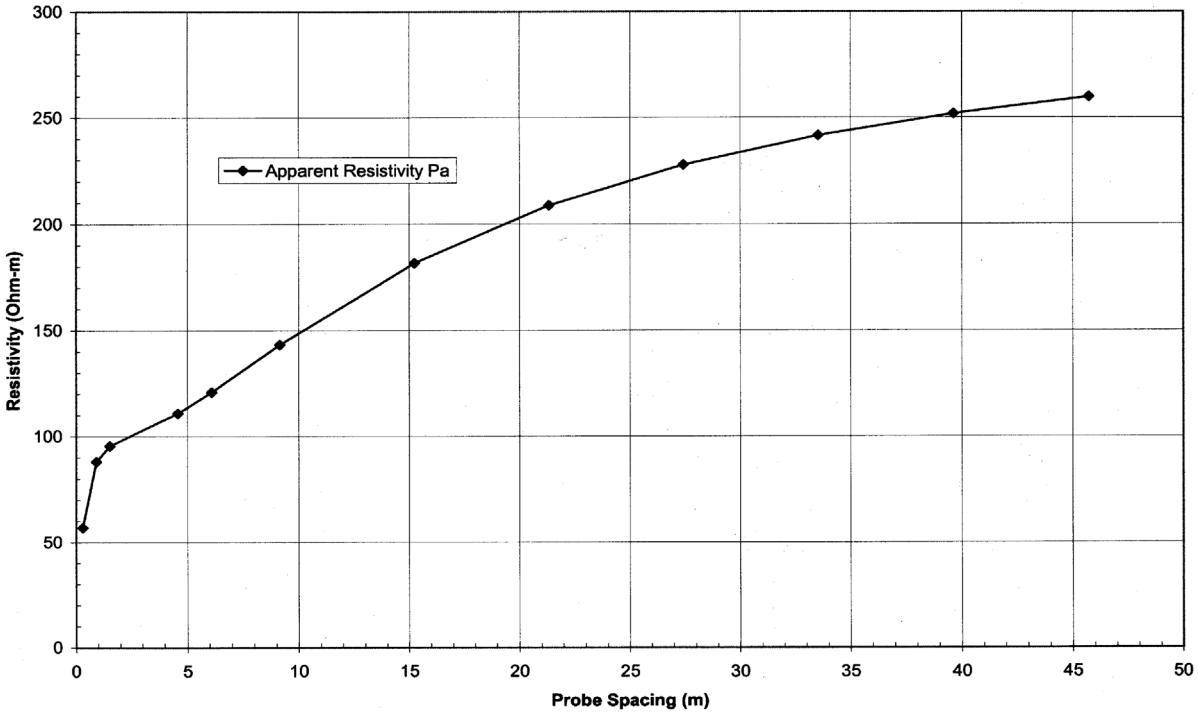

Figure 21—Resistivity plot of data from soil type 1, Table E.2

Copyright © 2015 IEEE. All rights reserved.

Copyright The Institute of Electrical and Electronics Engineers, Inc.
Provided by IHS under license with IEEE
No reproduction or networking permitted without license from IHS

Order Number: 02120914
Sold to:EGAT [700166108393] - VARRIS.Y@EGAT.CO.TH,
Not for Resale,2016-09-15 03:57:51 UTC

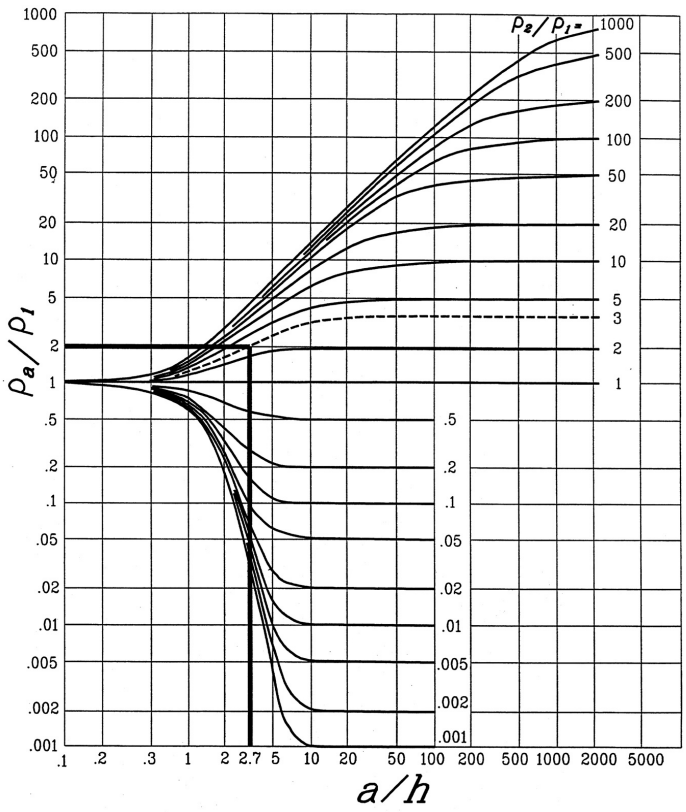

Figure 22—Example of Sunde's graphical method

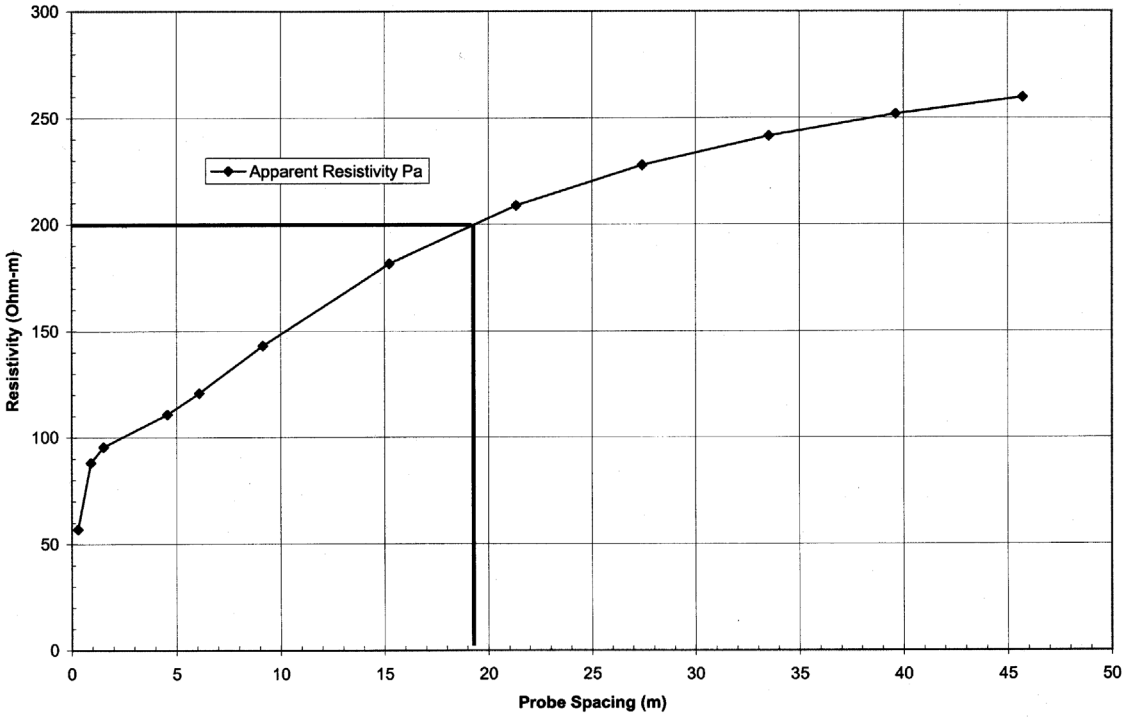

Figure 23—Example to determine *a* from apparent resistivity curve

Copyright © 2015 IEEE. All rights reserved.

Copyright The Institute of Electrical and Electronics Engineers, Inc.
Provided by IHS under license with IEEE
No reproduction or networking permitted without license from IHS

Order Number: 02120914
Sold to:EGAT [700166108393] - VARRIS.Y@EGAT.CO.TH,
Not for Resale,2016-09-15 03:57:51 UTC

13.4.2.3 Comparison of uniform and two-layer soil model on grounding systems

The two-layer model approach has been found to be much more accurate than the uniform soil model. A grounding system in a two-layer soil environment behaves differently in comparison with the same system in uniform soil.

Generally, for a grounding system in uniform soil or in two-layer soil with ρ_1 less than ρ_2 (upper layer soil resistivity less than lower layer soil resistivity, a positive reflection factor), the current density is higher in the conductors at the outer edges of the ground grid. In two-layer soil with ρ_1 greater than ρ_2 (the soil in the upper layer is more resistive than the lower layer soil, a negative reflection factor), the current density is more uniform over all the conductors of the grounding system. This is caused by the tendency of the grid current to go downward into the layer of lower resistivity, rather than up and outward to the more resistive upper layer. Studies by Thapar and Gross [B145] and Dawalibi et al. [B42][B44][B49] provide a wealth of information on this subject.

a) Variations in soil resistivity have considerable influence on the performance of most grounding systems, affecting both the value of ground resistance and ground potential rise, and the step and touch surface voltages. In general, for negative values of K (upper layer more resistive than lower layer), the resistance is less than that of the same grounding system in uniform soil with resistivity ρ_1. In contrast, for positive values of K, the resistance is generally higher than that in uniform soil and resistivity ρ_1. A similar relationship exists for the step and touch voltages produced on the surface of a two-layer earth versus that on the surface of uniform soil. For negative values of K, the step and touch voltages are generally lower than the voltages for the same grounding system in uniform soil of resistivity ρ_1. Also, for positive values of K, the step and touch voltages are generally higher than in uniform soil.

b) Other parameters, such as the upper layer height h, also affect the differences in the performance of ground electrodes in a two-layer environment and in uniform soil conditions. The general rule is that when the upper layer height h becomes significantly larger than the electrode's own dimensions, the performance of the electrode approaches the performance of the same electrode in uniform soil of resistivity ρ_1.

c) Also, it must be recognized that the above characteristics are based on the premise of a constant fault current source. The actual currents in the grounding system will change from case to case as a function of ρ_1 and ρ_2, reflecting the local changes relative to all other ground fault current paths predetermined by the fault location. This current division is discussed in Clause 15. Therefore, in certain cases some of the assumptions given above may not always hold true.

For design applications involving relatively simple grounding arrangements of electrodes buried in a reasonably uniform soil, the approximate methods provided elsewhere in the guide will be suitable for obtaining a realistic design with adequate safety margins. However, for designs involving a large grounded area, odd-shaped grids, etc., or where the resistivity of soil is clearly very non-uniform, the engineer responsible for the design should decide if more sophisticated methods are needed (Zaborszky [B156]).

Annex F provides a parametric analysis of various grid configurations in uniform and two-layer soil models.

13.4.2.4 Multilayer soil model

Highly non-uniform soil conditions may be encountered. Such soil conditions may require the use of multilayer modeling techniques if an equivalent two-layer soil model is not feasible. A multilayer soil model may include several horizontal layers or vertical layers. Techniques to interpret highly non-uniform soil resistivity require the use of computer programs or graphical methods (Dawalibi and Barbeito [B39]; Dawalibi, Ma, and Southey [B47]; EPRI EL-2699 [B61]; EPRI TR-100622 [B64]; Orellara and Mooney [B120]).

Copyright © 2015 IEEE. All rights reserved.

Copyright The Institute of Electrical and Electronics Engineers, Inc.
Provided by IHS under license with IEEE
No reproduction or networking permitted without license from IHS

Order Number: 02120914
Sold to:EGAT [700166108393] - VARRIS.Y@EGAT.CO.TH,
Not for Resale,2016-09-15 03:57:51 UTC

The equations that govern the performance of a grounding system buried in multilayer soil can be obtained by solving Laplace's equations for a point current source, or by the method of images, which gives identical results. The use of either method in determining the earth potential caused by a point current source results in an infinite series of terms representing the contributions of each consequent image of the point current source. Exact formulation of the equations that include these effects is given in Dawalibi and Mukhedkar [B42], Heppe [B81], and Sunde [B134].

14. Evaluation of ground resistance

14.1 Usual requirements

As discussed in 12.5, it is a common practice to have a thin layer of surface material overlaying the grounded area of a substation. It could appear that such a high resistivity layer, having the layer height *h*, much less than the depth of the grounding system, might worsen both the step and touch voltage. However, this is not the case. The surface material is used to increase the contact resistance between a person's foot and the earth surface. Thus, for a given maximum allowable body current, considerably higher step and touch voltages can be allowed if a high resistivity surface material is present.

14.2 Simplified calculations

Estimation of the total resistance to remote earth is one of the first steps in determining the size and basic layout of a grounding system. The resistance depends primarily on the area to be occupied by the grounding system, which is usually known in the early design stage. As a first approximation, a minimum value of the substation grounding system resistance in uniform soil can be estimated by means of the formula of a circular metal plate at zero depth

$$R_g = \frac{\rho}{4}\sqrt{\frac{\pi}{A}} \tag{55}$$

where

R_g is the substation ground resistance in Ω
ρ is the soil resistivity in Ω-m
A is the area occupied by the ground grid in m^2

Next, an upper limit of the substation ground resistance can be obtained by adding a second term to the above formula, as proposed by Laurent [B100] and Nieman [B118].

$$R_g = \frac{\rho}{4}\sqrt{\frac{\pi}{A}} + \frac{\rho}{L_T} \tag{56}$$

where

L_T is the total buried length of conductors in m

In the case of a grid rod combination in uniform soil, a combined length of horizontal conductors and ground rods will yield a slightly conservative estimate of L_T, because ground rods usually are more effective on a per unit length basis.

Copyright © 2015 IEEE. All rights reserved.

Copyright The Institute of Electrical and Electronics Engineers, Inc.
Provided by IHS under license with IEEE
No reproduction or networking permitted without license from IHS

Order Number: 02120914
Sold to:EGAT [700166108393] - VARRIS.Y@EGAT.CO.TH,
Not for Resale,2016-09-15 03:57:51 UTC

The second term recognizes the fact that the resistance of any actual grounding system that consists of a number of conductors is higher than that of a solid metallic plate. The difference will decrease with the increasing length of buried conductors and will approach 0 for infinite L_T, when the condition of a solid plate is reached.

Sverak [B137] expanded Equation (56) to take into account the effect of grid depth

$$R_g = \rho\left[\frac{1}{L_T} + \frac{1}{\sqrt{20A}}\left(1 + \frac{1}{1 + h\sqrt{20/A}}\right)\right] \tag{57}$$

where

h is the depth of the grid in m

For grids without ground rods, this formula has been tested to yield results that are practically identical to those obtained with Equation (61) of Schwarz [B132], described in 14.3.

The following tabulation from Kinyon [B96] offers some idea of how the calculated and actual measured resistance for five different substations compare. Equation (56) was used to compute the grid resistance. See Table 9.

Table 9—Typical grid resistances

Parameter soil texture	Sub 1 sand and gravel	Sub 2 sandy loam	Sub 3 sand and clay	Sub 4 sand and gravel	Sub 5 soil and clay
Resistivity (Ω-m)	2000	800	200	1300	28.0
Grid area (ft^2)	15 159	60 939	18 849	15 759	61 479
Buried length (ft)	3120	9500	1775	3820	3000
R_g (calculated Ω)	25.7	4.97	2.55	16.15	0.19
R_g (measured Ω)	39.0	4.10	3.65	18.20	0.21

An average value of all measured resistivity values is frequently substituted for the uniform soil resistivity in Equation (56). If this average resistivity is used, Equation (56) usually produces a resistance that is higher than the value that would result from a direct resistance measurement. The calculated and measured resistance values shown in Table 9 do not reflect this trend, because Kinyon [B96] based his calculations on the "... lowest average value of resistivity measured on the site." Readers are referred to Kinyon [B96] for further discussion on his choice of resistivity values used in Table 9.

14.3 Schwarz's equations

Schwarz [B132] developed the following set of equations to determine the total resistance of a grounding system in a homogeneous soil consisting of horizontal (grid) and vertical (rods) electrodes. Schwarz's equations extended accepted equations for a straight horizontal wire to represent the ground resistance, R_1, of a grid consisting of crisscrossing conductors, and a sphere embedded in the earth to represent ground rods, R_2. He also introduced an equation for the mutual ground resistance R_m between the grid and rod bed.

Copyright © 2015 IEEE. All rights reserved.

Copyright The Institute of Electrical and Electronics Engineers, Inc.
Provided by IHS under license with IEEE
No reproduction or networking permitted without license from IHS

Order Number: 02120914
Sold to:EGAT [700166108393] - VARRIS.Y@EGAT.CO.TH,
Not for Resale,2016-09-15 03:57:51 UTC

Schwarz used the following equation introduced by Sunde [B134] and Rüdenberg [B131] to combine the resistance of the grid, rods, and mutual ground resistance to calculate the total system resistance, R_g.

$$R_g = \frac{R_1 R_2 - R_m^{\ 2}}{R_1 + R_2 - 2R_m} \tag{58}$$

where

R_1 ground resistance of grid conductors in Ω
R_2 ground resistance of all ground rods in Ω
R_m mutual ground resistance between the group of grid conductors, R_1, and group of ground rods, R_2 in Ω

Ground resistance of the grid

$$R_1 = \frac{\rho}{\pi L_C}\left[\ln\left(\frac{2L_C}{a'}\right) + \frac{k_1 \times L_C}{\sqrt{A}} - k_2\right] \tag{59}$$

where

ρ is the soil resistivity in Ω-m
L_c is the total length of all connected grid conductors in m
a' is $\sqrt{a \times 2h}$ for conductors buried at depth h in m, or
a' is a for conductor on earth surface in m
$2a$ is the diameter of conductor in m
A is the area covered by conductors in m^2
k_1, k_2 are the coefficients (see Figure 24(a) and (b))

Ground resistance of the rod bed

$$R_2 = \frac{\rho}{2\pi n_R L_r}\left[\ln\left(\frac{4L_r}{b}\right) - 1 + \frac{2k_1 \times L_r}{\sqrt{A}}\left(\sqrt{n_R} - 1\right)^2\right] \tag{60}$$

where

L_r is the length of each rod in m
$2b$ is the diameter of rod in m
n_R number of rods placed in area A

Mutual ground resistance between the grid and the rod bed

$$R_m = \frac{\rho}{\pi L_c}\left[\ln\left(\frac{2L_c}{L_r}\right) + \frac{k_1 \times L_c}{\sqrt{A}} - k_2 + 1\right] \tag{61}$$

The combined ground resistance of the grid and the rod bed will be lower than the ground resistance of either component alone, but still higher than that of a parallel combination.

Copyright © 2015 IEEE. All rights reserved.

Copyright The Institute of Electrical and Electronics Engineers, Inc.
Provided by IHS under license with IEEE
No reproduction or networking permitted without license from IHS

Order Number: 02120914
Sold to:EGAT [700166108393] - VARRIS.Y@EGAT.CO.TH,
Not for Resale,2016-09-15 03:57:51 UTC

Schwarz compared the results of his equations to previously published theoretical work and to model tests to verify the accuracy of his equations. Since they were published in 1954, Schwarz's equations have been modified by Kercel [B95] to provide equations for constants k_1 and k_2 and further expanded to include the use of equations in two-layer soil (Nahman and Salamon [B116][B117]).

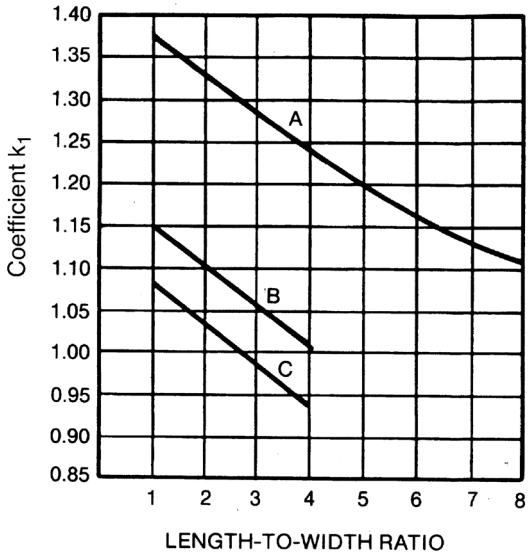

CURVE A — FOR DEPTH h = 0
$\gamma_A = -0.04x + 1.41$
CURVE B — FOR DEPTH h = 1/10 $\sqrt{\text{AREA}}$
$\gamma_B = -0.05x + 1.20$
CURVE C — FOR DEPTH h = 1/6 $\sqrt{\text{AREA}}$
$\gamma_C = -0.05x + 1.13$

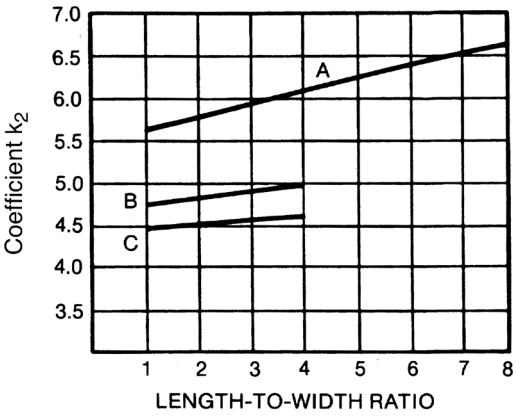

CURVE A — FOR DEPTH h = 0
$\gamma_A = 0.15x + 5.50$
CURVE B — FOR DEPTH h = 1/10 $\sqrt{\text{AREA}}$
$\gamma_B = 0.10x + 4.68$
CURVE C — FOR DEPTH h = 1/6 $\sqrt{\text{AREA}}$
$\gamma_C = -0.05x + 4.40$

Figure 24—Coefficients k_1 and k_2 of Schwarz's formula: (a) coefficient k_1, (b) coefficient k_2

Copyright © 2015 IEEE. All rights reserved.
Copyright The Institute of Electrical and Electronics Engineers, Inc.
Provided by IHS under license with IEEE
No reproduction or networking permitted without license from IHS
Order Number: 02120914
Sold to:EGAT [700166108393] - VARRIS.Y@EGAT.CO.TH,
Not for Resale,2016-09-15 03:57:51 UTC

14.4 Note on ground resistance of primary electrodes

In general, the ground resistance of any primary electrode depends on the soil resistivity and the size and type of arrangement of all individual conductors comprising the ground electrode. In more complex arrangements involving crisscrossed wires and a large number of rods in the same area, the mutual resistance between individual elements plays an important role.

14.5 Soil treatment to lower resistivity

It is often impossible to achieve the desired reduction in ground resistance by adding more grid conductors or ground rods. An alternate solution is to effectively increase the diameter of the electrode by modifying the soil surrounding the electrode. The inner shell of soil closest to the electrode normally comprises the bulk of the electrode ground resistance to remote earth. This phenomenon is often utilized to an advantage, as follows:

a) Use of sodium chloride, magnesium, and copper sulfates, or calcium chloride, to increase the conductivity of the soil immediately surrounding an electrode. State or federal authorities may not permit using this method because of possible leaching to surrounding areas. Further, the salt treatment must be renewed periodically.

b) Use of bentonite, a natural clay containing the mineral montmorillionite, which was formed by volcanic action years ago. It is non-corrosive, stable, and has a resistivity of 2.5 Ω-m at 300% moisture. The low resistivity results mainly from an electrolytic process between water, Na_2O (soda), K_2O (potash), CaO (lime), MgO (magnesia), and other mineral salts that ionize forming a strong electrolyte with pH ranging from 8 to 10. This electrolyte will not gradually leach out, as it is part of the clay itself. Provided with a sufficient amount of water, it swells up to 13 times its dry volume and will adhere to nearly any surface it touches. Due to its hydroscopic nature, it acts as a drying agent drawing any available moisture from the surrounding environment. Bentonite needs water to obtain and maintain its beneficial characteristics. Its initial moisture content is obtained at installation when the slurry is prepared. Once installed, bentonite relies on the presence of ground moisture to maintain its characteristics. Most soils have sufficient ground moisture so that drying out is not a concern. The hydroscopic nature of bentonite will take advantage of the available water to maintain its as installed condition. If exposed to direct sunlight, it tends to seal itself off, preventing the drying process from penetrating deeper. It may not function well in a very dry environment, because it may shrink away from the electrode, increasing the electrode resistance (Jones [B93]).

c) Chemical-type electrodes consist of a copper tube filled with a salt. Holes in the tube allow moisture to enter, dissolve the salts, and allow the salt solution to leach into the ground. These electrodes are installed in an augured hole and typically back-filled with soil treatment.

d) Ground enhancement materials, some with a resistivity of less than 0.12 Ω-m (about 5% of the resistivity of bentonite), are typically placed around the rod in an augured hole or around grounding conductors in a trench, in either a dry form or premixed in a slurry. Some of these enhancement materials are permanent and will not leach any chemicals into the ground. Other available ground enhancement materials are mixed with local soil in varying amounts and will slowly leach into the surrounding soil, lowering the earth resistivity.

14.6 Concrete-encased electrodes

Concrete, being hygroscopic, attracts moisture. Buried in soil, a concrete block behaves as a semiconducting medium with a resistivity of 30 Ω-m to 200 Ω-m depending on the moisture level. This is

Copyright © 2015 IEEE. All rights reserved.

Copyright The Institute of Electrical and Electronics Engineers, Inc.
Provided by IHS under license with IEEE
No reproduction or networking permitted without license from IHS

Order Number: 02120914
Sold to:EGAT [700166108393] - VARRIS.Y@EGAT.CO.TH,
Not for Resale,2016-09-15 03:57:51 UTC

of particular interest in medium and highly resistive soils because a wire or metallic rod encased in concrete has lower resistance than a similar electrode buried directly in the earth. This encasement reduces the resistivity of the most critical portion of material surrounding the metal element in much the same manner as a chemical treatment of soils. However, this phenomenon may often be both a design advantage and disadvantage. Some of the reasons are as follows:

a) On the one hand, it is impractical to build foundations for structures where the inner steel (reinforcing bars) is not electrically connected to the metal of the structure. Even if extreme care were taken with the anchor bolt placement in order to prevent any direct metal-to-metal contact, the semi-conductive nature of concrete would provide an electrical connection.

b) On the other hand, the presence of a small dc current can cause corrosion of rebar material. Although ac current as such does not produce corrosion, approximately 0.01% of the ac current becomes rectified at the interface of the steel bar and concrete (Rosa, McCollum, and Peters [B128]).

c) Splitting of concrete may occur either due to the above phenomenon because corroded steel occupies approximately 2.2 times its original volume, producing pressures approaching 35 MPa or the passage of a very high current, which would vaporize the moisture in the concrete.

Fortunately, there is a certain threshold potential for dc corrosion, approximately 60 V dc, below which no corrosion will occur. A number of field tests concerning the maximum current loading is reported in Bogajewski, Dawalibi, Gervais, and Mukhedkar [B17]; Dick and Holliday [B54]; and Miller, Hart, and Brown [B111]. The short-time current loading capacity, I_{CE}, of concrete-encased electrodes can be estimated by means of Ollendorff's formula[9] for an indefinitely sustainable current I∞, adjusted by a 1.4 multiplying factor, or directly from Figure 25.

$$I_{CE} = 1.4\left(I_{\infty}\right) = \frac{1.4}{R_z}\sqrt{2\lambda_g \rho\left(T_v - T_a\right)} \tag{62}$$

where

λ_g is the thermal conductivity of the earth in W/(m °C)
R_z is the ground resistance of the concrete-encased electrode in Ω
ρ is the soil resistivity in Ω-m
T_a is the ambient temperature in °C
T_v is the maximum allowable temperature to prevent sudden evaporation of moisture in °C
I_{∞} is the indefinitely sustainable current in A

The applicability of this formula has been verified in Bogajewski, Dawalibi, Gervais, and Mukhedkar [B17], which reports on the results of extensive field testing of concrete poles. In general, if damage is to be prevented, the actual current should be less than the value of I_{CE} determined by Equation (62). A 20% to 25% safety margin is reasonable for most practical applications.

[9] Ollendorff [B119] neglects the cooling effect of evaporated moisture in calculating I∞.

Copyright © 2015 IEEE. All rights reserved.

Copyright The Institute of Electrical and Electronics Engineers, Inc.
Provided by IHS under license with IEEE
No reproduction or networking permitted without license from IHS

Order Number: 02120914
Sold to:EGAT [700166108393] - VARRIS.Y@EGAT.CO.TH,
Not for Resale,2016-09-15 03:57:51 UTC

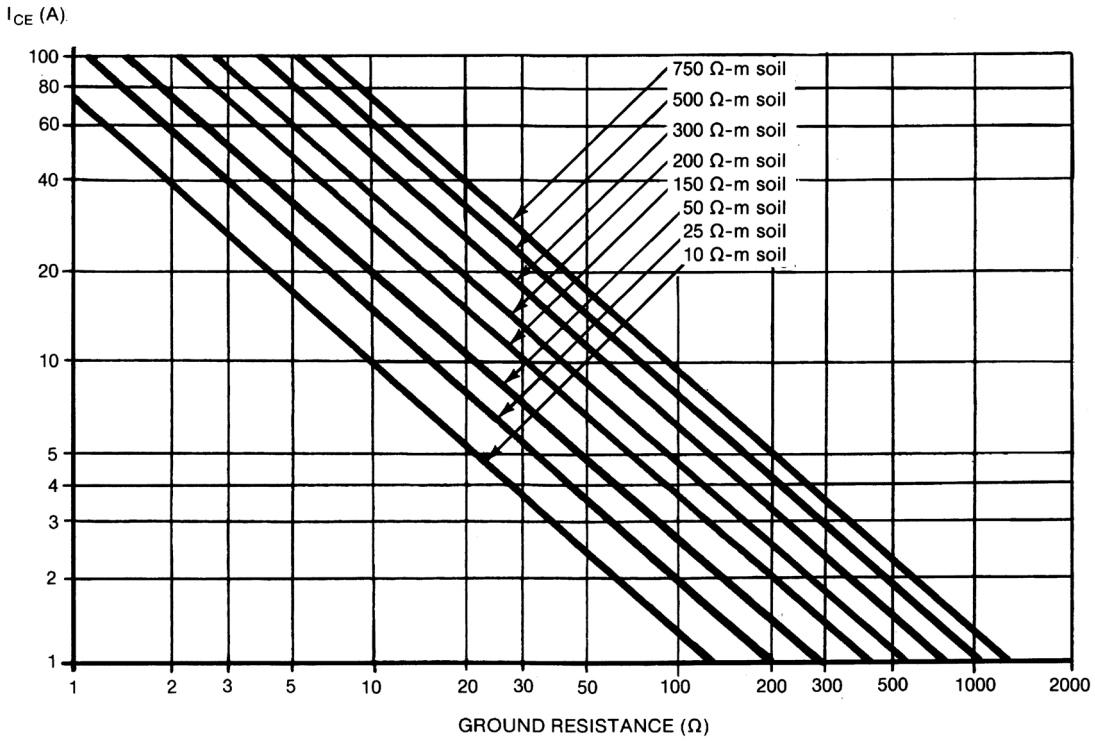

Figure 25—Short-time current loading capability of concrete-encased ground electrodes

Thus, with proper precautions, the concrete-encased electrodes may be used as auxiliary ground electrodes.

Fagan and Lee [B66] use the following equation for obtaining the ground resistance, R_{CE-rod}, of a vertical rod encased in concrete:

$$R_{CE-rod} = \frac{1}{2\pi L_r}\left(\rho_c\left[ln\left(D_C / d\right)\right] + \rho\left[ln\left(8L_r / D_C\right) - 1\right]\right) \tag{63}$$

where

ρ_c is the resistivity of the concrete in Ω-m
ρ is the resistivity of the soil in Ω-m
L_r is the length of the ground rod in m
d is the diameter of the ground rod in m
D_C is the diameter of the concrete shell in m

Equation (63) can be related to the commonly used formula for a ground rod of length L_r and diameter d, as follows:

$$R_{rod} = \frac{\rho}{2\pi L_r}\left[\ln\left(8L_r / d\right) - 1\right] \tag{64}$$

Copyright © 2015 IEEE. All rights reserved.
Copyright The Institute of Electrical and Electronics Engineers, Inc.
Provided by IHS under license with IEEE
No reproduction or networking permitted without license from IHS
Order Number: 02120914
Sold to:EGAT [700166108393] - VARRIS.Y@EGAT.CO.TH,
Not for Resale,2016-09-15 03:57:51 UTC

then Equation (63) can be resolved into

$$R_{CE-rod} = \frac{1}{2\pi L_r}\{\rho[\ln(8L_r / D_C)-1]+\rho_c[\ln(8L_r / d)-1]-\rho_c[\ln(8L_r / D_C)-1]\} \quad (65)$$

representing a *combination* of two resistances in series:

a) Ground resistance calculated by Equation (64) of a concrete cylinder of diameter D_C, directly buried in soil ρ

b) Ground resistance of the inner segment of diameter D_C, containing a metal rod of diameter d

Obviously, the latter term is obtained as a difference of the hypothetical resistance values for a rod in concrete, if d and D_C are entered in the single-medium formula Equation (64), and ρ is replaced by ρ_c.

Such an approach is generally valid for any other electrode having a different shape. Noting, for convenience

$$R_{SM} = F(\rho, S_o, G) \quad (66)$$

$$R_{DM} = F(\rho_C, S_o, G) + F(\rho, S_i, G) - F(\rho, S_i, G) \quad (67)$$

where, in addition to the symbols already mentioned,

R_{SM} is the electrode resistance in single medium in Ω
R_{DM} is the electrode resistance in dual medium in Ω
S_o is the surface area of a given electrode in m^2
S_i is the area of interface in m^2
G is a geometrical factor characterizing the particular shape of a given electrode

The following recommendations should be considered when using concrete-encased electrodes:

a) Connect anchor bolt and angle stubs to the reinforcing steel for a reliable metal-to-metal contact.

b) Reduce the current duty and dc leakage to allowable levels by making sure that enough primary ground electrodes (ground grid and ground rods) will conduct most of the fault current.

c) Ground enhancement material may be used in the areas of a high soil resistivity to reduce the resistance of primary grounding. Augering a 100 mm to 250 mm (4 in to 10 in) hole and backfilling it with a soil enhancement material around a ground rod is a useful method to help prevent the predominance of auxiliary electrodes in dissipating the fault current.

This form is adaptable to a variety of electrodes, buried in soil, and assumed to be surrounded by a concentric shell of a material that has different resistivity than the soil. One possible model of this type, for which Schwarz's formula for a rod bed can easily be modified, is shown in Figure 26.

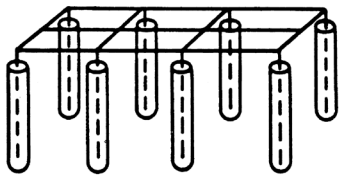

Figure 26—Grid with encased vertical electrodes

Copyright © 2015 IEEE. All rights reserved.
Copyright The Institute of Electrical and Electronics Engineers, Inc.
Provided by IHS under license with IEEE
No reproduction or networking permitted without license from IHS
Order Number: 02120914
Sold to:EGAT [700166108393] - VARRIS.Y@EGAT.CO.TH,
Not for Resale,2016-09-15 03:57:51 UTC

15. Determination of maximum grid current

15.1 Determination of maximum grid current definitions

NOTE—The following definitions are also listed in Clause 3, but repeated here for the convenience of the reader.

dc offset: Difference between the symmetrical current wave and the actual current wave during a power system transient condition. Mathematically, the actual fault current can be broken into two parts, a symmetrical alternating component and a unidirectional (dc) component. The unidirectional component can be of either polarity, but will not change polarity, and will decrease at some predetermined rate.

decrement factor: An adjustment factor used in conjunction with the symmetrical ground fault current parameter in safety-oriented grounding calculations. It determines the rms equivalent of the asymmetrical current wave for a given fault duration, t_f, accounting for the effect of initial dc offset and its attenuation during the fault.

fault current division factor: A factor representing the inverse of a ratio of the symmetrical fault current to that portion of the current that flows between the ground grid and surrounding earth.

$$S_f = \frac{I_g}{3I_o} \tag{68}$$

where

S_f is the fault current division factor
I_g is the rms symmetrical grid current in A
I_0 is the zero-sequence fault current in A

NOTE—In reality, the current division factor would change during the fault duration, based on the varying decay rates of the fault contributions and the sequence of interrupting device operations. However, for the purposes of calculating the design value of maximum grid current and symmetrical grid current per definitions of symmetrical grid current and maximum grid current, the ratio is assumed constant during the entire duration of a given fault.

maximum grid current: A design value of the maximum grid current, defined as follows:

$$I_G = D_f \times I_g \tag{69}$$

where

I_G is the maximum grid current in A
D_f is the decrement factor for the entire duration of fault t_f, given in s
I_g is the rms symmetrical grid current in A

subtransient reactance: Reactance of a generator at the initiation of a fault. This reactance is used in calculations of the initial symmetrical fault current. The current continuously decreases, but it is assumed to be steady at this value as a first step, lasting approximately 0.05 s after a suddenly applied fault.

Copyright © 2015 IEEE. All rights reserved.

Copyright The Institute of Electrical and Electronics Engineers, Inc.
Provided by IHS under license with IEEE
No reproduction or networking permitted without license from IHS

Order Number: 02120914
Sold to:EGAT [700166108393] - VARRIS.Y@EGAT.CO.TH,
Not for Resale,2016-09-15 03:57:51 UTC

symmetrical grid current: That portion of the symmetrical ground fault current that flows between the ground grid and surrounding earth. It may be expressed as

$$I_g = S_f \times I_f \tag{70}$$

where

I_g is the rms symmetrical grid current in A

I_f is the rms value of symmetrical ground fault current in A ($I_f = 3I_0$)

S_f is the fault current division factor

synchronous reactance: Steady-state reactance of a generator during fault conditions used to calculate the steady-state fault current. The current so calculated excludes the effect of the automatic voltage regulator or governor.

transient reactance: Reactance of a generator between the subtransient and synchronous states. This reactance is used for the calculation of the symmetrical fault current during the period between the subtransient and steady states. The current decreases continuously during this period, but is assumed to be steady at this value for approximately 0.25 s.

***X/R* ratio**: Ratio of the system inductive reactance to resistance. It is indicative of the rate of decay of any dc offset. A large *X/R* ratio corresponds to a large time constant and a slow rate of decay.

15.2 Procedure

In most cases, the largest value of grid current will result in the most hazardous condition. For these cases, the following steps are involved in determining the correct design value of maximum grid current I_G for use in substation grounding calculations:

a) Assess the type and location of those ground faults that are likely to produce the greatest flow of current between the ground grid and surrounding earth, and hence the greatest GPR and largest local surface potential gradients in the substation area (see 15.8).

b) Determine, by computation, the fault current division factor S_f for the faults selected in a), and establish the corresponding values of symmetrical grid current I_g (see 15.9).

c) For each fault, based on its duration time, t_f, determine the value of decrement factor D_f to allow for the effects of asymmetry of the fault current wave. Select the largest product $D_f \times I_g$, and hence the worst fault condition (see 15.10).

d) Consider future increases in available fault current (see 15.11).

15.3 Types of ground faults

Many different types of faults may occur in the system. Unfortunately, it may be difficult to determine which fault type and location will result in the greatest flow of current between the ground grid and surrounding earth because no simple rule applies. Figure 27, Figure 28, Figure 29, and Figure 30 show maximum grid current I_G for various fault locations and system configurations.

In determining the applicable fault types, consideration should be given to the probability of occurrence of the fault. Multiple simultaneous faults, even though they may result in higher ground current, need not be considered if their probability of occurrence is negligible. It is thus recommended, for practical reasons, that investigation be confined to single-line-to-ground and line-to-line-to-ground faults.

Copyright © 2015 IEEE. All rights reserved.

Copyright The Institute of Electrical and Electronics Engineers, Inc.
Provided by IHS under license with IEEE
No reproduction or networking permitted without license from IHS

Order Number: 02120914
Sold to:EGAT [700166108393] - VARRIS.Y@EGAT.CO.TH,
Not for Resale,2016-09-15 03:57:51 UTC

In the case of a line-to-line-to-ground fault, the zero sequence fault current is

$$I_0 = \frac{E\left(R_2 + \mathrm{j}X_2\right)}{\left(R_1 + jX_1\right)\left[R_0 + R_2 + 3R_f + j\left(X_0 + X_2\right)\right] + \left(R_2 + jX_2\right)\left(R_0 + 3R_f + jX_0\right)} \tag{71}$$

where

I_0 is the symmetrical rms value of zero sequence fault current in A
E is the phase-to-neutral voltage in V
R_f is the estimated resistance of the fault in Ω (normally $R_f = 0$ is assumed)
R_1 is the positive sequence equivalent system resistance in Ω
R_2 is the negative sequence equivalent system resistance in Ω
R_0 is the zero sequence equivalent system resistance in Ω
X_1 is the positive sequence equivalent system reactance (subtransient) in Ω
X_2 is the negative sequence[10] equivalent system reactance in Ω
X_0 is the zero sequence equivalent system reactance in Ω

The values R_1, R_2, R_0, X_1, X_2, and X_0 are computed looking into the system from the point of fault.

In the case of a single-line-to-ground fault, the zero sequence fault current is

$$I_0 = \frac{E}{3R_f + R_1 + R_2 + R_0 + j\left(X_1 + X_2 + X_0\right)} \tag{72}$$

In many cases, however, the effect of the resistance terms in Equation (72) is negligible. For practical purposes, the following simplified equations are sufficiently accurate and more convenient.

Zero sequence current for line-to-line-to-ground fault:

$$I_0 = \frac{E \times X_2}{X_1\left(X_0 + X_2\right) + \left(X_2 \times X_0\right)} \tag{73}$$

Zero sequence current for line-to-ground fault:

$$I_0 = \frac{E}{X_1 + X_2 + X_0} \tag{74}$$

[10] In most calculations it is usually permissible to assume a ratio of X_2/X_1 equal to unity, and, hence, $X_1 = X_2$, especially if an appreciable percentage of the positive-sequence reactance to the point of fault is that of static apparatus and transmission lines.

Copyright © 2015 IEEE. All rights reserved.
Copyright The Institute of Electrical and Electronics Engineers, Inc.
Provided by IHS under license with IEEE
No reproduction or networking permitted without license from IHS
Order Number: 02120914
Sold to:EGAT [700166108393] - VARRIS.Y@EGAT.CO.TH,
Not for Resale,2016-09-15 03:57:51 UTC

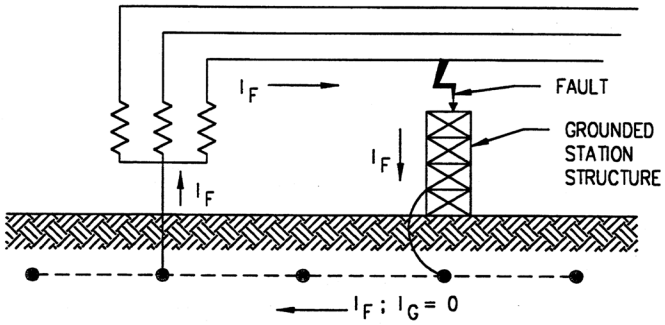

Figure 27—Fault within local substation; local neutral grounded

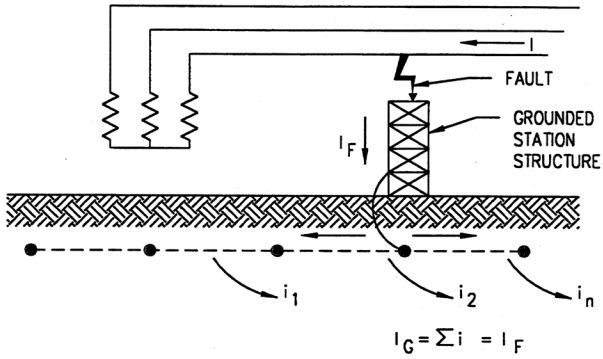

Figure 28—Fault within local substation; neutral grounded at remote location

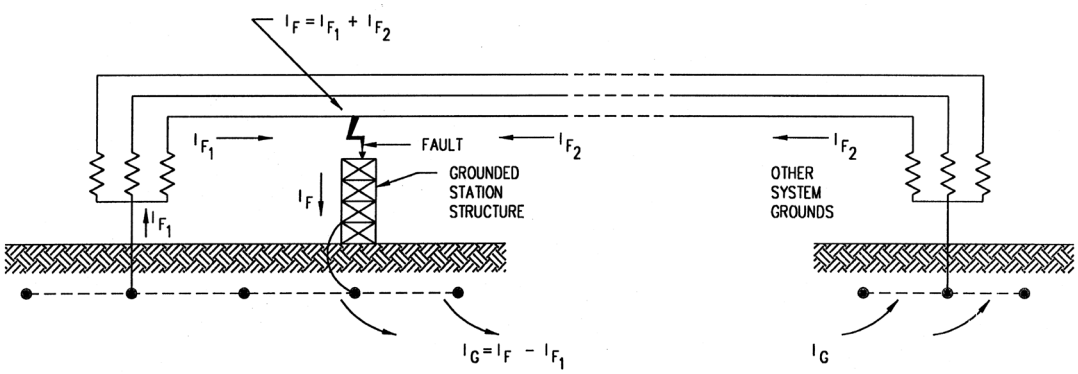

Figure 29—Fault in substation; system grounded at local substation and also at other points

Copyright © 2015 IEEE. All rights reserved.

Copyright The Institute of Electrical and Electronics Engineers, Inc.
Provided by IHS under license with IEEE
No reproduction or networking permitted without license from IHS

Order Number: 02120914
Sold to:EGAT [700166108393] - VARRIS.Y@EGAT.CO.TH,
Not for Resale,2016-09-15 03:57:51 UTC

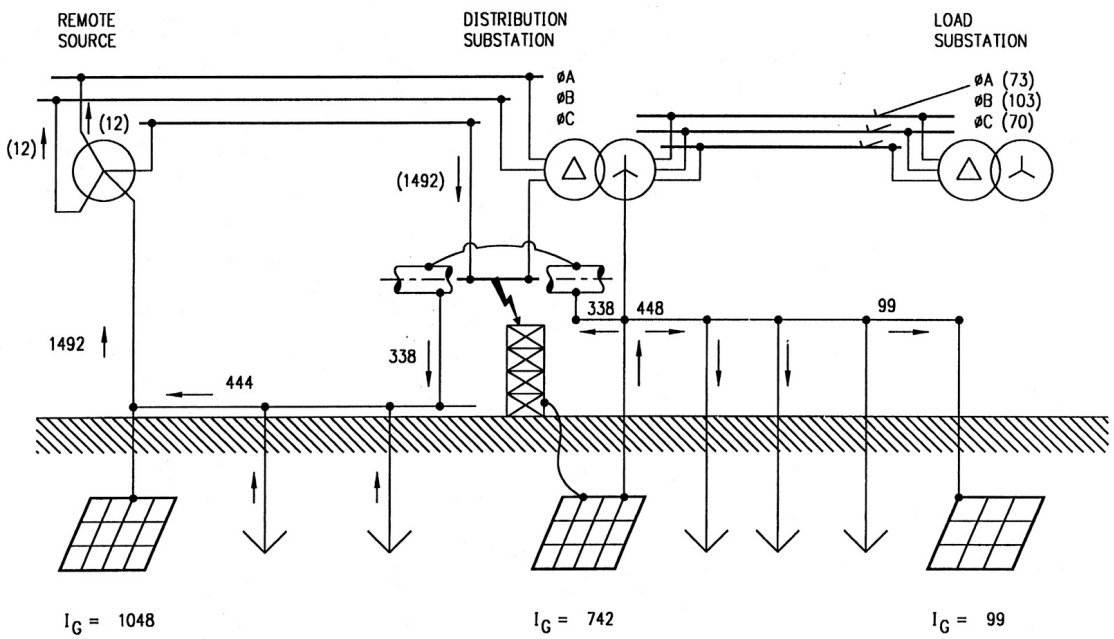

Figure 30—Typical current division for a fault on high side of distribution substation

15.4 Effect of substation ground resistance

In most cases it is sufficient to derive the maximum grid current I_G, as described in 15.2 and 15.3, by neglecting the system resistance, the substation ground resistance, and the resistance at the fault. The error thus introduced is usually small, and is always on the side of safety. However, there may be unusual cases where the predicted substation ground resistance is so large, in relation to system reactance, that it is worthwhile to take the resistance into account by including it into the more exact Equation (71) or Equation (72). This poses a problem because the substation ground system is not yet designed and its resistance is not known. However, the resistance can be estimated by the use of the approximate formulas of 14.2 or 14.3. This estimated resistance generally gives sufficient accuracy for determining the current I_g, and hence I_G.

15.5 Effect of fault resistance

If the fault is an insulation breakdown within the local substation, the only safe assumption is that the resistance of the fault be assumed zero (see Figure 27, Figure 28, Figure 29, and Figure 30).

In the case of a fault outside of the local substation area, on a line connected to the substation bus (Figure 30), it is permissible, if a conservative (minimum) value of fault resistance R_f can be assigned, to use this in the ground fault current calculations. This is done by multiplying R_f by three and adding it to the other resistance terms as indicated in the denominator of Equation (71) or Equation (72). If, however, the actual fault resistance does not maintain a value at least as great as the value of R_f used in the calculations, then the fault resistance should be neglected. Any error from neglecting R_f will, of course, be on the side of safety.

Copyright © 2015 IEEE. All rights reserved.

Copyright The Institute of Electrical and Electronics Engineers, Inc.
Provided by IHS under license with IEEE
No reproduction or networking permitted without license from IHS

Order Number: 02120914
Sold to:EGAT [700166108393] - VARRIS.Y@EGAT.CO.TH,
Not for Resale,2016-09-15 03:57:51 UTC

15.6 Effect of overhead ground wires and neutral conductors

Where transmission line overhead ground wires or neutral conductors are connected to the substation ground, a substantial portion of the ground fault current is diverted away from the substation ground grid. Where this situation exists, the overhead ground wires or neutral conductors should be taken into consideration in the design of the ground grid. Connecting the substation ground to overhead ground wires or neutral conductors, or both, and through them to transmission line structures or distribution poles, will usually have the overall effect of increasing the GPR at tower bases, while lessening it at the substation. This is because each of the nearby towers will share in voltage rise of the substation ground mat, whatever the cause, instead of being affected only by a local insulation failure or flashover at one of the towers. Conversely, when such a tower fault does occur, the effect of the connected substation ground system should decrease the magnitude of gradients near the tower bases.

15.7 Effect of direct buried pipes and cables

Buried cables with their sheaths or armor in effective contact with the earth, and buried metallic pipes bonded to the substation ground system and extending beyond its perimeter will have an effect similar to that of overhead ground wires and neutrals. By conducting part of the ground fault current away from the substation, the potential rise of the grid during the fault, and the local gradients in the substation will be somewhat lessened. As discussed in Clause 17, external hazards may sometimes be introduced (Bodier [B16]; Rüdenberg [B131]).

Because of the complexities and uncertainties in the pattern of current flow, the effect is often difficult to calculate. Some guidelines to the computation of the input impedance of such current paths leaving the substation are supplied by Rüdenberg [B131] and Laurent [B100]. A more recent study of this problem is presented in EPRI EL-904 [B60], which provides methods for computing the impedance of both above-ground and buried pipes. From these values an approximate calculation can determine the division of ground current between these paths, the substation ground system, and any overhead ground wires that are present and connected.

15.8 Worst fault type and location

The worst fault type for a given grounding system is usually the one resulting in the highest value of the maximum grid current I_G. Because this current is proportional to the zero sequence or ground fault current and the current division factor, and because the current division is almost independent of the fault type, the worst fault type can be defined as the one resulting in the highest zero sequence or ground fault current flow into the earth, $3I_0$. In a given location, a single-line-to-ground fault will be the worst fault type if $Z_1 Z_0 > Z_2^2$ at the point of fault, and a line-to-line-to-ground fault will be the worst type if $Z_1 Z_0 < Z_2^2$. In the usual case where Z_2 is assumed equal to Z_1, the above comparisons reduce to $Z_0 > Z_1$, and $Z_0 < Z_2$, respectively.

Z_1, Z_2, Z_0 are defined as

$$Z_1 = R_1 + jX_1 \tag{75}$$

$$Z_2 = R_2 + jX_2 \tag{76}$$

$$Z_0 = R_0 + jX_0 \tag{77}$$

The question of the fault location producing the maximum grid current I_G involves several considerations. The worst fault location may be either on the high-voltage side or on the low-voltage side, and in either

Copyright © 2015 IEEE. All rights reserved.

Copyright The Institute of Electrical and Electronics Engineers, Inc.
Provided by IHS under license with IEEE
No reproduction or networking permitted without license from IHS

Order Number: 02120914
Sold to:EGAT [700166108393] - VARRIS.Y@EGAT.CO.TH,
Not for Resale,2016-09-15 03:57:51 UTC

case may be either inside the substation or outside on a line, at a certain distance from the substation. A fault is classified as inside the substation if it is related to a metallic structure that is electrically connected to the substation ground grid via negligible impedance. There are no universal rules for the determination of the worst fault location. The following discussion relates to some, but by no means all, possibilities.

For distribution substations with the transformer grounded only on the distribution side, the maximum grid current I_G usually occurs for a ground fault on the high-side terminals of the transformer. However, if the source of ground fault current on the high side is weak, or if a parallel operation of several transformers results in a strong ground fault current source on the low side, the maximum grid current may occur for a ground fault somewhere on the distribution circuit.

For ground faults on the low-side terminals of such a secondary grounded transformer, the transformer's contribution to the fault circulates in the substation grid conductor with negligible leakage current into the earth and, thus, has no effect on the substation GPR, as shown in Figure 28.

For ground faults outside the substation on a distribution feeder (far enough to be at remote earth with respect to the ground grid), a large portion of the fault current will return to its source (the transformer neutral) via the substation grid, thus contributing to the substation GPR.

In transmission substations with three-winding transformers or autotransformers, the problem is more complex. The maximum grid current I_G may occur for a ground fault on either the high or low side of the transformer; both locations should be checked. In either case, it can be assumed that the worst fault location is at the terminals of the transformer inside the substation, if the system contribution to the fault current is larger than that of the transformers in the substation. Conversely, the worst fault location may be outside the substation on a transmission line, if the transformer contribution dominates.

Exceptions to the above generalities exist. Therefore, for a specific system, several fault location candidates for the maximum grid current should be considered. For each candidate, the applicable value of zero sequence current I_0 (ground fault current) should be established in this step.

In a few cases, a further complication arises. The duration of the fault depends on the type of protection scheme used, the location of the fault, and the choice of using primary or back-up clearing times for the fault (shock) duration. The fault duration not only affects the decrement factor, D_f, but also the tolerable voltages, as discussed in Clause 8. If the fault clearing time for a particular fault is relatively long, the corresponding tolerable voltages may be reduced to values that make this fault condition the worst case, even though the grid current for this case is not the maximum value. This situation generally occurs where a delta-wye grounded transformer is fed from a relatively weak source of fault current and the fault occurs some distance down a rural distribution feeder. In this case, the high (delta) side fault current may be relatively low, and the low (wye grounded) side feeder faults are determined primarily by the transformer and feeder impedances. If backup clearing is considered, a feeder fault several kilometers down the feeder, depending on the high side clearing device to back-up the failure of the feeder breaker, could take several seconds to clear. The tolerable voltage for this case may be significantly lower than that for a high side fault, making the low side feeder fault the worst case for the grid design. Thus, the worst fault type and location must take into consideration not only the maximum value of grid current I_G, but also the tolerable voltages based on the fault clearing time.

15.9 Computation of current division

For the assumption of a sustained flow of the initial ground fault current, the symmetrical grid current can be expressed as

$$I_g = S_f \times (3I_0) \tag{78}$$

Copyright © 2015 IEEE. All rights reserved.

Copyright The Institute of Electrical and Electronics Engineers, Inc.
Provided by IHS under license with IEEE
No reproduction or networking permitted without license from IHS

Order Number: 02120914
Sold to:EGAT [700166108393] - VARRIS.Y@EGAT.CO.TH,
Not for Resale,2016-09-15 03:57:51 UTC

To determine I_g, the current division factor S_f must be computed.

The process of computing consists of deriving an equivalent representation of the overhead ground wires, neutrals, etc., connected to the grid and then solving the equivalent to determine what fraction of the total fault current flows between the grid and earth, and what fraction flows through the ground wires or neutrals. S_f is dependent on many parameters, some of which are

a) Location of the fault, as described in 15.8.

b) Magnitude of substation ground grid impedance, as discussed in Clause 4.

c) Buried pipes and cables in the vicinity of or directly connected to the substation ground system, as discussed in 15.7.

d) Overhead ground wires, neutrals, or other ground return paths, as discussed in 15.6.

Because of S_f, the symmetrical grid current I_g, and therefore also I_G, are closely related to the location of the fault. If the additional ground paths of items c) and d) above are neglected, the current division ratio (based on remote versus local current contributions) can be computed using traditional symmetrical components. However, the current I_g, computed using such a method might be overly conservative.

The remaining discussion refers only to overhead ground wires and neutral conductors, although the principles involved also apply to buried pipes, cables, or any other conducting path connected to the grid. High-voltage transmission lines are commonly provided with overhead static wires, either throughout their length or for short distances from each substation. They may be grounded at each tower along the line or they may be insulated from the towers and used for communication purposes. There are many sources that provide assistance in determining the effective impedance of a static wire as seen from the fault point (see, for instance, Carson [B18]; Clem [B20]; EEI and Bell Telephone Systems [B21]; CCITT Study Group V [B25]; Desieno, Marchenko, and Vassel [B52]; Laurent [B100]; Patel [B123]; and Verma and Mukhedkar [B153]). Many of these methods may, however, be difficult to apply by the design engineer. Because it is beyond the scope of this guide to discuss in detail the applicability of each method to all possible system configurations, only a brief description of some of the more recent methods will be given.

Endrenyi [B56][B58] presents an approach in which, for a series of identical spans, the tower impedances and overhead ground wires or neutrals are reduced to an equivalent lumped impedance. Except for estimating purposes, Endrenyi recommends including the mutuals between multiple ground conductors and introduces a coupling factor to account for the mutual impedance between the neutral conductors and the phase conductors. This technique is developed further by Verma and Mukhedkar [B153].

In the cascaded matrix method of Sebo [B133], an impedance matrix is derived for each span of the line, and the individual span matrices are cascaded into a resulting matrix representing the entire line. This technique allows a person to take into account all self and mutual impedances (except between the tower footing grounds), and the location and type of fault. A correction for the end effects of the line is suggested, using a modified screening factor.

With some limitations in applicability and accuracy, the span-by-span calculation technique can be considerably simplified. A typical approach, in which all mutual couplings between the neutral conductor and phase conductors and between neutral conductors are ignored, has been described by Garrett [B71]. In this technique, each neutral conductor is modeled by the impedance of each span and the equivalent ground impedance of each tower to form a network resembling a ladder. This ladder network is then reduced, using simple network reduction techniques, to the input impedance as seen from the fault point. The input impedance of each circuit is combined with the grid resistance and three times this resulting value is included in the zero-sequence equivalent fault impedance. The current division factor S_f is computed by applying Kirchoff's current law to obtain the current division between the grid resistance and the input impedance of each circuit. Although this, or similar approximate approaches, is limited in applicability and

Copyright © 2015 IEEE. All rights reserved.

Copyright The Institute of Electrical and Electronics Engineers, Inc.
Provided by IHS under license with IEEE
No reproduction or networking permitted without license from IHS

Order Number: 02120914
Sold to:EGAT [700166108393] - VARRIS.Y@EGAT.CO.TH,
Not for Resale,2016-09-15 03:57:51 UTC

accuracy, in many cases it may provide a reasonable estimate of the influence of overhead ground wires and neutrals on both the resistance of the grounding system and the current division ratio.

Dawalibi [B38], [B41] provides algorithms for deriving simple equations to solve for the currents in the grid and in each tower. These equations are obtained from one or both ends of each line and do not require the large computer storage requirements of the techniques that model each span individually. Dawalibi also addresses the effects of the soil structure (that is, multilayer earth resistivities) on the self and mutual impedances of the conductors and on the current division ratio.

Meliopoulos et al. [B107] introduced an equivalent conductor to represent the effects of earth using Carson's formula. Every span in each line is modeled and the resulting network is solved for current flows. From this solution, the current division ratio is computed. The number of lines and substations modeled are limited only by the computer used to solve the network (EPRI TR-100622 [B64]).

Garrett, Meyers, and Patel [B74] used the method of Meliopoulos, [B107] to perform a parametric analysis of the parameters affecting S_f, and to develop a set of curves of S_f versus grid resistance for some of the most critical parameters. This provides a quick and simple method to estimate the current division that avoids the need for some of the simplifying assumptions of the other approximate methods, though the results are still only approximate. These curves, along with a few new curves and an impedance table added for this guide, are included in Annex C. Refer to Annex C for limitations on this method.

Obviously, the techniques that model the static wires, phase conductors, towers, etc., in detail will give the best evaluation of the current division factor S_f. However, the approximate methods discussed above have been compared with the detailed methods and found to give comparable answers for many simple examples. Thus, the choice of the method used to determine S_f will depend on the complexity of the system connected to the substation and the desired degree of accuracy. A simple example follows, showing the results of four of the methods described in the preceding paragraphs. In the following example, the approximate methods of Endrenyi and Garrett and Patel are compared with the results of Dawalibi's and Meliopoulos's more accurate methods.

As an example, Figure 31 shows a one-feeder distribution substation fed by single transmission line connecting the substation to a remote equivalent source (next adjacent substation). The transmission line is 20 km long and the distance between tower grounds is 0.5 km. The feeder is 4 km long and the distance between pole grounds is 0.122 km. The soil is assumed to be uniform with a resistivity of 200 Ω-m. Carson's equations are used to compute the self-impedances of the phase conductors and overhead static wire, and the mutual impedance between these (transmission line only) for use with Endrenyi's formula and Garrett and Patel's split-factor curves. Annex C shows the equations used to calculate the line impedances necessary for the current split computations. The various impedances for each line section tower footing resistance, remote terminal ground resistance, and substation grid resistance are

R_{tg} = 10.0 + j0.0 Ω/section

R_{dg} = 25.0 + j0.0 Ω/section

R_s = 3.0 + j0.0 Ω

R_g = 2.5 + j0.0 Ω

Z_1 = 3.82 + j9.21 Ω for the 115 kV line

$Z_{0(a)}$ = 7.37 + j35.86 Ω for the 115 kV line

$Z_{0(g)}$ = 148.24 + j66.44 Ω for the 115 kV line

$Z_{0(ag)}$ = 3.56 + j33.34 Ω for the 115 kV line

Z_0 = 12.54 + j39.72 Ω for the 115 kV line

Z_{s-l} = 1.24 + j0.55 Ω/span for the 115 kV overhead static wire

Z_{s-f} = 0.11 + j0.11 Ω/span for the 12.47 kV feeder neutral

Copyright © 2015 IEEE. All rights reserved.

Copyright The Institute of Electrical and Electronics Engineers, Inc.
Provided by IHS under license with IEEE
No reproduction or networking permitted without license from IHS

Order Number: 02120914
Sold to:EGAT [700166108393] - VARRIS.Y@EGAT.CO.TH,
Not for Resale,2016-09-15 03:57:51 UTC

where

R_{tg} is the impedance to remote earth of each transmission ground electrode in Ω
R_{dg} is the impedance to remote earth of each distribution ground electrode in Ω
R_s is the remote terminal ground impedance (equivalent) in Ω
R is the station ground impedance to remote earth in Ω
Z_1 is the equivalent positive sequence impedance for the 115 kV line in Ω
$Z_{0(a)}$ is the zero sequence self-impedance for the 115 kV phase conductors in Ω
$Z_{0(g)}$ is the zero sequence self-impedance for the 115 kV ground wire in Ω
$Z_{0(ag)}$ is the zero sequence mutual impedance between phase and ground conductors for the 115 kV line in Ω
Z_0 is the equivalent zero sequence impedance for the 115 kV line in Ω
Z_{s-l} is the self-impedance of the 115 kV overhead static wire in Ω/span
Z_{s-f} is the self-impedance of the 12.47 kV feeder neutral in Ω/span

Adding the 115 kV line impedances to the source impedances gives the following equivalent fault impedance at the 115 kV bus:

$$Z_{1(eq)} = 3.82 + j19.01 \ \Omega$$

$$Z_{0(eq)} = 12.54 + j46.32 \ \Omega$$

Thus, for a 115 kV single-line-to-ground fault

$$\left|3I_0\right| = \left|\frac{3\times 115\ 000/\sqrt{3}}{2(3.82 + j19.01) + (12.54 + j46.32)}\right| = \left|534.5 - j2233.8\right| = 2297$$

Using the circuit shown in Figure 31, assume a single-line-to-ground fault occurs at the substation from the phase conductor bus to the substation neutral.

Using Endrenyi's [B58] method, the equivalent impedance of the overhead static wire (as seen from the fault point and ignoring the effects of coupling) is

$$Z_{eq-l} = 0.5\times(1.24 + j0.55) + \sqrt{10\times(1.24 + j0.55)} = 4.22 + j1.04 \ \Omega$$

The equivalent impedance of the feeder neutral (as seen from the substation) is

$$Z_{eq-f} = 0.5\times(0.11 + j0.11) + \sqrt{25\times(0.11 + j0.11)} = 1.88 + j0.89 \ \Omega$$

Copyright © 2015 IEEE. All rights reserved.
Copyright The Institute of Electrical and Electronics Engineers, Inc.
Provided by IHS under license with IEEE
No reproduction or networking permitted without license from IHS
Order Number: 02120914
Sold to:EGAT [700166108393] - VARRIS.Y@EGAT.CO.TH,
Not for Resale,2016-09-15 03:57:51 UTC

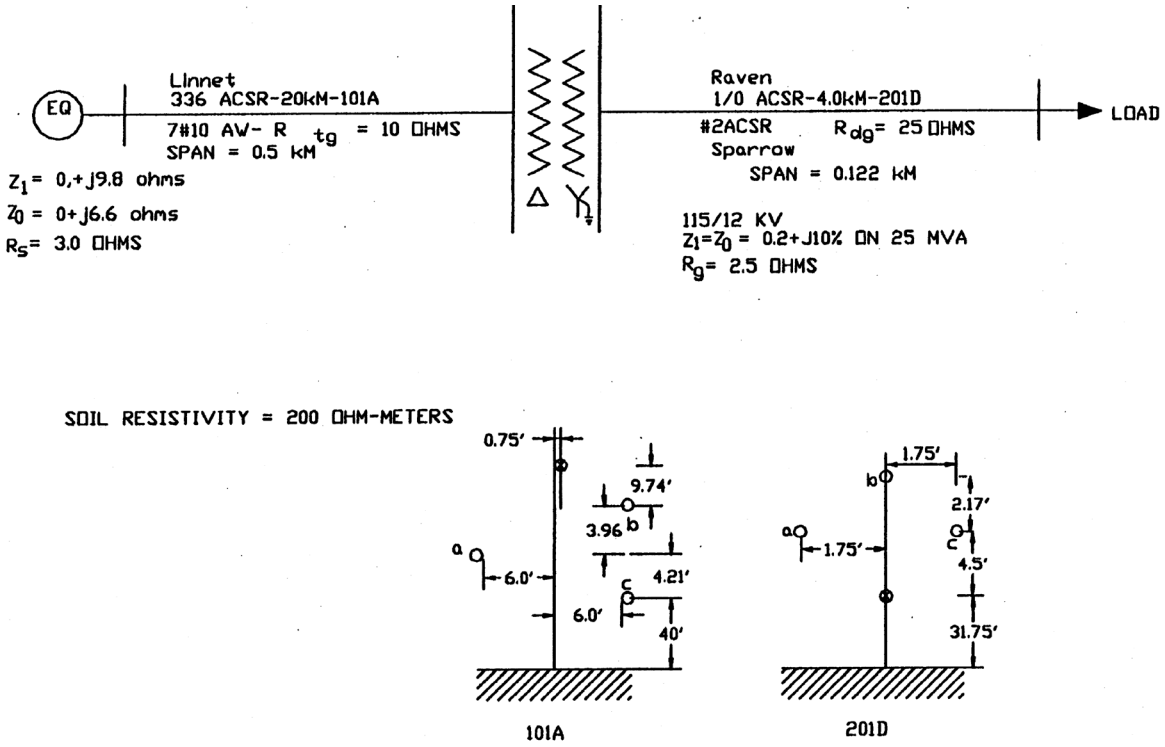

Figure 31—Example system for computation of current division factor S_f

The resulting equivalent of the overhead static wire and feeder neutral is found by paralleling the above equivalent impedances:

$$Z_{eq} = \frac{1}{\frac{1}{Z_{eq-l}} + \frac{1}{Z_{eq-f}}} = 1.31 + j0.52\ \Omega$$

The current division factor, S_f, is Z

$$S_f = \left| \frac{Z_{eq}}{Z_{eq} + R_g} \right| = \left| \frac{1.31 + j0.52}{(1.31 + j0.52) + 2.5} \right| = 0.37$$

and the resulting grid current I_g is

$$I_g = S_f \times 3I_0 = 0.37 \times 2297 = 850\ \text{A}$$

Using Garrett and Patel's table of split factor equivalents (Annex C), the equivalent of the overhead static wire and feeder neutral is

$$Z = 0.91 + j0.485\ \Omega$$

and the split factor is

Copyright © 2015 IEEE. All rights reserved.
Copyright The Institute of Electrical and Electronics Engineers, Inc.
Provided by IHS under license with IEEE
No reproduction or networking permitted without license from IHS
Order Number: 02120914
Sold to:EGAT [700166108393] - VARRIS.Y@EGAT.CO.TH,
Not for Resale,2016-09-15 03:57:51 UTC

$$S_f = \left| \frac{Z_{eq}}{Z_{eq} + R_g} \right| = \left| \frac{0.91 + j0.485}{(0.91 + j0.485) + 2.5} \right| = 0.30$$

Thus, the grid current is

$$I_g = S_f \times 3I_0 = 0.30 \times 2297 = 689 \text{ A}$$

Using Garret and Patel's split factor curves (Figure C.3), the approximate split factor S_f = 0.28. Thus, the grid current is

$$I_g = S_f \times 3I_0 = 0.28 \times 2297 = 643 \text{ A}$$

Using EPRI TR-100622 [B64], the total fault current $3I_0$ is 2472 A. Approximately 34% (I_g = 836 A) of the fault current flows through grid to remote earth, so the current division factor equals 0.34. Similar results are obtained using Dawalibi [B38].

As shown above, the approximate and detailed methods are in close agreement for this example. However, for more complex systems, with both local and remote ground sources and with dissimilar lines and sources, the results may not be in close agreement (see Annex C).

15.10 Effect of asymmetry

The design of a ground grid must consider the asymmetrical current. A decrement factor, D_f, will be derived to take into account the effect of dc current offset. In general, the asymmetrical fault current includes the subtransient, transient, and steady-state ac components, and the dc offset current component. Both the subtransient and transient ac components and the dc offset decay exponentially, each having a different attenuation rate.

However, in typical applications of this guide, it is assumed that the ac component does not decay with time, but remains at its initial value. Thus, as a periodic function of time, t, the asymmetrical fault current may be expressed as

$$i_f(t) = \sqrt{2} \times E \times Y_{ac} \left[\sin(\omega t + \alpha - \theta) - e^{-t/T_a} \times \sin(\alpha - \theta) \right] \quad (79)$$

where

$i_f(t)$ is the asymmetrical fault current, in A, at any instant t, t in s
E is the prefault rms voltage, line-to-neutral V
ω is the system frequency in radians/s
α is the voltage angle at current initiation in radians
θ is the circuit phase angle in radians
Y_{ac} is the equivalent ac system admittance in mhos
T_a is the dc offset time constant in s [T_a = X/(ωR), for 60 Hz, T_a = X/(120πR)]

The *X/R* ratio to be used here is the system *X/R* ratio at the fault location for a given fault type. The *X* and *R* components of the system subtransient fault impedance should be used to determine the *X/R* ratio.

Copyright © 2015 IEEE. All rights reserved.

Copyright The Institute of Electrical and Electronics Engineers, Inc.
Provided by IHS under license with IEEE
No reproduction or networking permitted without license from IHS

Order Number: 02120914
Sold to:EGAT [700166108393] - VARRIS.Y@EGAT.CO.TH,
Not for Resale,2016-09-15 03:57:51 UTC

In reality, faults occur at random with respect to the voltage wave. However, the shock contact may exist at the moment the fault is initiated. Hence, to allow for the most severe condition, it is necessary to assume that the maximum possible dc offset will be present at the moment of an accidental shock contact.

Maximum dc offset occurs when: $(\alpha - \theta) = -\pi/2$

Then Equation (79) becomes

$$i_f(t) = \sqrt{2}E \times Y_{ac}\left[e^{-t/T_a} - \cos(\omega t)\right] \tag{80}$$

Because the experimental data in the fibrillation threshold are based on the energy content of a symmetrical sine wave of constant amplitude, it is necessary to establish an equivalent rms value of the asymmetrical current wave for the maximum time of possible shock exposure. This value, in accordance with the definition of the effective asymmetrical fault current I_F, can be determined by integration of Equation (80) squared over the entire duration of fault t_f in s.

$$I_F = \sqrt{\frac{1}{t_f}\int_0^{t_f}\left[i_f(t)\right]^2 dt} \tag{81}$$

where

I_F is the effective rms value of approximate asymmetrical current for the entire duration of a fault in A

t_f is the time duration of fault in s

t is the time (variable) after the initiation of fault in s

Evaluating the integral of Equation (81) in terms of Equation (80), it follows that

$$I_F = I_f \times \sqrt{\frac{2}{t_f}\int_0^{t_f}\left[e^{-t/T_a} - \cos(\omega t)\right]^2 dt} \tag{82}$$

Therefore, the decrement factor D_f is determined by the ratio I_F/I_f, yielding

$$D_f = \frac{I_F}{I_f} \tag{83}$$

$$D_f = \sqrt{1 + \frac{T_a}{t_f}\left(1 - e^{\frac{-2t_f}{T_a}}\right)} \tag{84}$$

Equation (84) can be used to compute the decrement factor for specific *X/R* ratios and fault durations. Typical values of the decrement factor for various fault durations and *X/R* ratios are shown in Table 10.

For relatively long fault durations, the effect of the dc offset current can be assumed to be more than compensated by the decay of the subtransient component of ac current. A decrement factor of 1.0 can be used for fault durations of 30 cycles or more.

Copyright © 2015 IEEE. All rights reserved.

Copyright The Institute of Electrical and Electronics Engineers, Inc.
Provided by IHS under license with IEEE
No reproduction or networking permitted without license from IHS

Order Number: 02120914
Sold to:EGAT [700166108393] - VARRIS.Y@EGAT.CO.TH,
Not for Resale,2016-09-15 03:57:51 UTC

For closely spaced successive shocks (possibly from reclosures), early editions of this guide suggested a decrement factor computed using the shortest single fault duration, even if the time, t_s, used elsewhere in the calculations is based on the sum of the individual shock durations. However, the preceding discussion of the asymmetrical fault current decrement factor suggests that the use of the shortest fault duration in conjunction with the longest shock duration, or sum of the shock durations, may result in an overdesigned grounding system. This is especially true for faults of intermediate duration (that is, 6 to 30 cycles), where the decrement factor is relatively large and the ac component of current is assumed to remain at its subtransient value. Crawford and Griffith [B23] suggest that the shock duration and fault duration be assumed identical, which will result in sufficient grid design for cases involving no automatic reclosures or successive (high-speed) shocks. However, because little or no testing has been done on the effects of repetitive shocks separated by only a few cycles, the design engineer should judge whether or not to use the longest shock duration for time t_s elsewhere in the calculations and the shortest fault duration for the time t_f in computing the decrement factor with Equation (84).

It is important that the values of the decrement factor given in Table 10 not be confused with the multiplying factors given by IEEE Std C37.010™-1979 [B85]. The decrement factor is D_f, and is used to determine the effective current during a given time interval after inception of a fault, whereas the multiplying factors given by IEEE Std C37.010-1979 [B85] are used to determine the rms current at the end of this interval. Because of the decay of ac and dc transient components with time, the decrement factors determined by Equation (84) are slightly higher than the factors given by IEEE Std C37.010-1979 [B85] for short fault and shock durations.

Table 10—Typical values of D_f

Fault duration, t_f		Decrement factor, D_f			
Seconds	**Cycles at 60 Hz**	***X/R* = 10**	***X/R* = 20**	***X/R* = 30**	***X*/R = 40**
0.008 33	0.5	1.576	1.648	1.675	1.688
0.05	3	1.232	1.378	1.462	1.515
0.10	6	1.125	1.232	1.316	1.378
0.20	12	1.064	1.125	1.181	1.232
0.30	18	1.043	1.085	1.125	1.163
0.40	24	1.033	1.064	1.095	1.125
0.50	30	1.026	1.052	1.077	1.101
0.75	45	1.018	1.035	1.052	1.068
1.00	60	1.013	1.026	1.039	1.052

15.11 Effect of future changes

It is a common experience for maximum fault currents at a given location to increase as system capacity is added or new connections are made to the grid. While an increase in system capacity will increase the maximum expected fault current I_F, new connections may increase or decrease the maximum grid current I_G. One case in which the grid current may decrease with new connections is when new transmission lines are added with ground or neutral wires, or both. In general, if no margin for increase in I_G is included in the original ground system design, the design may become unsafe. Also, subsequent additions will usually be much less convenient and more expensive to install. It has been a widely accepted practice to assume the total fault current, I_F, between the grid and surrounding earth (that is, ignoring any current division) in an attempt to allow for system growth. While this assumption would be overly pessimistic for present-year conditions, it may not exceed the current I_G computed considering current division and system growth. If

Copyright © 2015 IEEE. All rights reserved.

Copyright The Institute of Electrical and Electronics Engineers, Inc.
Provided by IHS under license with IEEE
No reproduction or networking permitted without license from IHS

Order Number: 02120914
Sold to:EGAT [700166108393] - VARRIS.Y@EGAT.CO.TH,
Not for Resale,2016-09-15 03:57:51 UTC

the system growth is taken into account and current division is ignored, the resulting grid will be overdesigned. An estimate of the future system conditions can be obtained by including all system additions forecasted.

Caution should be exercised when future changes involve such design changes as disconnection of overhead ground wires coming into the substations. Such changes may have an effect on ground fault currents and may result in an inadequate grounding system. However, future changes, such as additions of incoming overhead ground wires, may decrease the current division ratio, resulting in the existing ground system being overdesigned.

16. Design of grounding system

16.1 Design criteria

As stated in 4.1, there are two main design goals to be achieved by any substation ground system under normal as well as fault conditions. These goals are

a) To provide means to dissipate electric currents into the earth without exceeding any operating and equipment limits.

b) To assure that a person in the vicinity of grounded facilities is not exposed to the danger of critical electric shock.

The design procedures described in the following subclauses are aimed at achieving safety from dangerous step and touch voltages within a substation. It is pointed out in 8.2 that it is possible for transferred potentials to exceed the GPR of the substation during fault conditions. Clause 17 discusses some of the methods used to protect personnel and equipment from these transferred potentials. Thus, the design procedure described here is based on assuring safety from dangerous step and touch voltages within, and immediately outside, the substation fenced area. Because the mesh voltage is usually the worst possible touch voltage inside the substation (excluding transferred potentials), the mesh voltage will be used as the basis of this design procedure.

Step voltages are inherently less dangerous than mesh voltages. If, however, safety within the grounded area is achieved with the assistance of a high resistivity surface layer (surface material), which does not extend outside the fence, then step voltages may be dangerous. In any event, the computed step voltages should be compared with the permissible step voltage after a grid has been designed that satisfies the touch voltage criterion.

For equally spaced ground grids, the mesh voltage will increase along meshes from the center to the corner of the grid. The rate of this increase will depend on the size of the grid, number and location of ground rods, spacing of parallel conductors, diameter and depth of the conductors, and the resistivity profile of the soil. In a computer study of three typical ground grids in uniform soil resistivity, the data shown in Table 11 were obtained. These grids were all symmetrically shaped square grids with no ground rods and equal parallel conductor spacing. The corner E_m was computed at the center of the corner mesh. The actual worst case E_m occurs slightly off-center (toward the corner of the grid), but is only slightly higher than the E_m at the center of the mesh.

As indicated in Table 11, the corner mesh voltage is generally much higher than that in the center mesh. This will be true unless the grid is unsymmetrical (has projections, is L-shaped, etc.), has ground rods located on or near the perimeter, or has extremely non-uniform conductor spacing. Thus, in the equations for the mesh voltage E_m given in 16.5, only the mesh voltage at the center of the corner mesh is used as the basis of the design procedure. Analysis based on computer programs, described in 16.8, may use this

Copyright © 2015 IEEE. All rights reserved.

Copyright The Institute of Electrical and Electronics Engineers, Inc.
Provided by IHS under license with IEEE
No reproduction or networking permitted without license from IHS

Order Number: 02120914
Sold to:EGAT [700166108393] - VARRIS.Y@EGAT.CO.TH,
Not for Resale,2016-09-15 03:57:51 UTC

approximate corner mesh voltage, the actual corner mesh voltage, or the actual worst-case touch voltage found anywhere within the grounded area as the basis of the design procedure. In either case, the initial criterion for a safe design is to limit the computed mesh or touch voltage to below the tolerable touch voltage from Equation (32) or Equation (33).

Unless otherwise specified, the remainder of the guide will use the term mesh voltage (E_m) to mean the touch voltage at the center of the corner mesh. However, the mesh voltage may not be the worst-case touch voltage if ground rods are located near the perimeter, or if the mesh spacing near the perimeter is small. In these cases, the touch voltage at the corner of the grid may exceed the corner mesh voltage.

Table 11—Typical ratio of corner-to-corner mesh voltage

Grid number	Number of meshes	E_m corner/center
1	10 × 10	2.71
2	20 × 20	5.55
3	30 × 30	8.85

16.2 Critical parameters

The following site-dependent parameters have been found to have substantial impact on the grid design: maximum grid current I_G, fault duration t_f, shock duration t_s, soil resistivity ρ, surface material resistivity ρ_s, and grid geometry. Several parameters define the geometry of the grid, but the area of the grounding system, the conductor spacing, and the depth of the ground grid have the most impact on the mesh voltage, while parameters such as the conductor diameter and the thickness of the surfacing material have less impact (AIEE Working Group [B4]; Dawalibi and Mukhedkar [B43]; Dawalibi, Bauchard, and Mukhedkar [B46]; EPRI EL-3099 [B62]). A brief discussion or review of the critical parameters is given in 16.2.1 through 16.2.5.

16.2.1 Maximum grid current (I_G)

The evaluation of the maximum design value of ground fault current that flows through the substation ground grid into the earth, I_G, has been described in Clause 15. In determining the maximum current I_G, by means of Equation (69), consideration should be given to the resistance of the ground grid, division of the ground fault current between the alternate return paths and the grid, and the decrement factor.

16.2.2 Fault duration (t_f) and shock duration (t_s)

The fault duration and shock duration are normally assumed equal, unless the fault duration is the sum of successive shocks, such as from reclosures. The selection of t_f should reflect fast clearing time for transmission substations and slow clearing times for distribution and industrial substations. The choices t_f and t_s should result in the most pessimistic combination of fault current decrement factor and allowable body current. Typical values for t_f and t_s range from 0.25 s to 1.0 s. More detailed information is given in 5.2 through 6.4 and 15.10 on the selection of t_f and t_s.

Copyright © 2015 IEEE. All rights reserved.

Copyright The Institute of Electrical and Electronics Engineers, Inc.
Provided by IHS under license with IEEE
No reproduction or networking permitted without license from IHS

Order Number: 02120914
Sold to:EGAT [700166108393] - VARRIS.Y@EGAT.CO.TH,
Not for Resale,2016-09-15 03:57:51 UTC

16.2.3 Soil resistivity (ρ)

The grid resistance and the voltage gradients within a substation are directly dependent on the soil resistivity. Because in reality soil resistivity will vary horizontally as well as vertically, sufficient data must be gathered for a substation yard. The Wenner method described in 13.3 is widely used (James J. Biddle Co. [B105]; Wenner [B154]).

Because the equations for E_m and E_s given in 16.5 assume uniform soil resistivity, the equations can employ only a single value for the resistivity. Refer to 13.4.1 for guidance in determining an approximate uniform soil resistivity.

16.2.4 Resistivity of surface layer (ρ_s)

A layer of surface material helps in limiting the body current by adding resistance to the equivalent body resistance. Refer to 7.4 and 12.5 for more details on the application of this parameter.

16.2.5 Grid geometry

In general, the limitations on the physical parameters of a ground grid are based on economics and the physical limitations of the installation of the grid. The economic limitation is obvious. It is impractical to install a copper plate grounding system. Clause 18 describes some of the limitations encountered in the installation of a grid. For example, the digging of the trenches into which the conductor material is laid limits the conductor spacing to approximately 2 m or more. Typical conductor spacings range from 3 m to 15 m, while typical grid depths range from 0.5 m to 1.5 m. For the typical conductors ranging from 2/0 AWG (67 mm^2) to 500 kcmil (253 mm^2), the conductor diameter has negligible effect on the mesh voltage. The area of the grounding system is the single most important geometrical factor in determining the resistance of the grid. The larger the area grounded, the lower the grid resistance and, thus, the lower the GPR.

16.3 Index of design parameters

Table 12 contains a summary of the design parameters used in the design procedure.

16.4 Design procedure

The block diagram of Figure 32 illustrates the sequences of steps to design the ground grid. The parameters shown in the block diagram are identified in the index presented in Table 12. The following describes each step of the procedure:

- Step 1: The property map and general location plan of the substation should provide good estimates of the area to be grounded. A soil resistivity test, described in Clause 13, will determine the soil resistivity profile and the soil model needed (that is, uniform or two-layer model).
- Step 2: The conductor size is determined by equations given in 11.3. The fault current $3I_0$ should be the maximum expected future fault current that will be conducted by any conductor in the grounding system, and the time, t_c, should reflect the maximum possible clearing time (including backup).

Copyright © 2015 IEEE. All rights reserved.

Copyright The Institute of Electrical and Electronics Engineers, Inc.
Provided by IHS under license with IEEE
No reproduction or networking permitted without license from IHS

Order Number: 02120914
Sold to:EGAT [700166108393] - VARRIS.Y@EGAT.CO.TH,
Not for Resale,2016-09-15 03:57:51 UTC

— Step 3: The tolerable touch and step voltages are determined by equations given in 8.4. The choice of time, t_s, is based on the judgment of the design engineer, with guidance from 5.2 through 6.3.

— Step 4: The preliminary design should include a conductor loop surrounding the entire grounded area, plus adequate cross-conductors to provide convenient access for equipment grounds, etc. The initial estimates of conductor spacing and ground rod locations should be based on the current I_G and the area being grounded.

— Step 5: Estimates of the preliminary resistance of the grounding system in uniform soil can be determined by the equations given in 14.2 and 14.3. For the final design, more accurate estimates of the resistance may be desired. Computer analysis based on modeling the components of the grounding system in detail can compute the resistance with a high degree of accuracy, assuming the soil model is chosen correctly.

— Step 6: The current I_G is determined by the equations given in Clause 15. To prevent overdesign of the grounding system, only that portion of the total fault current, $3I_0$, that flows through the grid to remote earth should be used in designing the grid. The current I_G should, however, reflect the worst fault type and location, the decrement factor, and any future system expansion.

— Step 7: If the GPR of the preliminary design is below the tolerable touch voltage, no further analysis is necessary. Only additional conductor required to provide access to equipment grounds is necessary.

— Step 8: The calculation of the mesh and step voltages for the grid as designed can be done by the approximate analysis techniques described in 16.5 for uniform soil, or by the more accurate computer analysis techniques, as demonstrated in 16.8. Further discussion of the calculations is reserved for those sections.

— Step 9: If the computed mesh voltage is below the tolerable touch voltage, the design may be complete (see Step 10). If the computed mesh voltage is greater than the tolerable touch voltage, the prelimiry design should be revised (see Step 11).

— Step 10: If both the computed touch and step voltages are below the tolerable voltages, the design needs only the refinements required to provide access to equipment grounds. If not, the preliminary design must be revised (see Step 11).

— Step 11: If either the step or touch tolerable limits are exceeded, revision of the grid design is required. These revisions may include smaller conductor spacings, additional ground rods, etc. More discussion on the revision of the grid design to satisfy the step and touch voltage limits is given in 16.6.

— Step 12: After satisfying the step and touch voltage requirements, additional grid and ground rods may be required. The additional grid conductors may be required if the grid design does not include conductors near equipment to be grounded. Additional ground rods may be required at the base of surge arresters, transformer neutrals, etc. The final design should also be reviewed to eliminate hazards due to transferred potential and hazards associated with special areas of concern. See Clause 17.

Copyright © 2015 IEEE. All rights reserved.
--`,,,,,,`,```,,`-`-`,,`,,`,`,,-`-`,,`,,`,`---
Copyright The Institute of Electrical and Electronics Engineers, Inc.
Provided by IHS under license with IEEE
No reproduction or networking permitted without license from IHS
Order Number: 02120914
Sold to:EGAT [700166108393] - VARRIS.Y@EGAT.CO.TH,
Not for Resale,2016-09-15 03:57:51 UTC

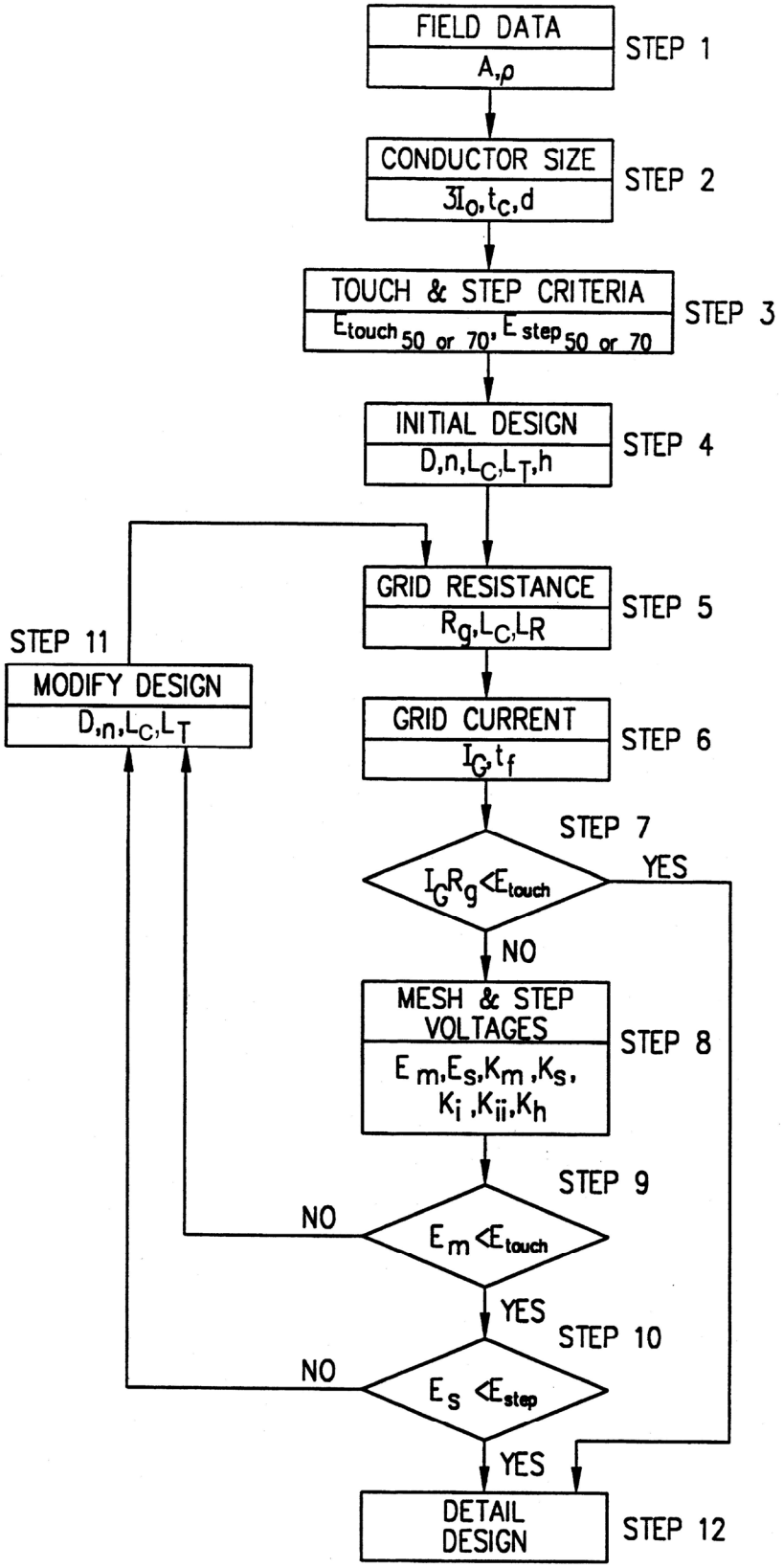

Figure 32—Design procedure block diagram

Copyright © 2015 IEEE. All rights reserved.

Copyright The Institute of Electrical and Electronics Engineers, Inc.
Provided by IHS under license with IEEE
No reproduction or networking permitted without license from IHS

Order Number: 02120914
Sold to:EGAT [700166108393] - VARRIS.Y@EGAT.CO.TH,
Not for Resale,2016-09-15 03:57:51 UTC

Table 12—Index of design parameters

Symbol	Description	Clause numbers
ρ	Soil resistivity, Ω-m	13
ρ_S	Surface layer resistivity, Ω-m	7.4, 12.5
$3I_0$	Symmetrical fault current in substation for conductor sizing, A	15.3
A	Total area enclosed by ground grid, m^2	14.2
C_s	Surface layer derating factor	7.4
d	Diameter of grid conductor, m	16.5
D	Spacing between parallel conductors, m	16.5
D_f	Decrement factor for determining I_G (see: *maximum grid current*)	15.1, 15.10
D_m	Maximum distance between any two points on the grid, m	16.5
E_m	Mesh voltage at the center of the corner mesh for the simplified method, V	16.5
E_s	Step voltage between a point above the outer corner of the grid and a point 1 m diagonally outside the grid for the simplified method, V	16.5
E_{step50}	Tolerable step voltage for human with 50 kg body weight, V	8.3
E_{step70}	Tolerable step voltage for human with 70 kg body weight, V	8.3
$E_{touch50}$	Tolerable touch voltage for human with 50 kg body weight, V	8.3
$E_{touch70}$	Tolerable touch voltage for human with 70 kg body weight, V	8.3
$E_{mm\text{-}touch50}$	Tolerable metal-metal touch voltage for human with 50 kg body weight, V	8.4
$E_{mm\text{-}touch70}$	Tolerable metal-metal touch voltage for human with 70 kg body weight, V	8.4
h	Depth of ground grid conductors, m	14.2
h_s	Surface layer thickness, m	7.4
I_G	Maximum grid current that flows between ground grid and surrounding earth (including dc offset), A (see: *maximum grid current*)	15.1
I_g	Symmetrical grid current, A (see: *symmetrical grid current*)	15.1
K	Reflection factor between different resistivities	7.4
K_h	Corrective weighting factor that emphasizes the effects of grid depth, simplified method	16.5
K_i	Correction factor for grid geometry, simplified method	16.5
K_{ii}	Corrective weighting factor that adjusts for the effects of inner conductors on the corner mesh, simplified method	16.5
K_m	Spacing factor for mesh voltage, simplified method	16.5
K_s	Spacing factor for step voltage, simplified method	16.5
L_c	Total length of grid conductor, m	14.3
L_M	Effective length of $L_c + L_R$ for mesh voltage, m	16.5
L_R	Total length of ground rods, m	16.5
L_r	Length of ground rod at each location, m	14.3, 16.5
L_S	Effective length of $L_c + L_R$ for step voltage, m	16.5
L_T	Total effective length of grounding system conductor, including grid and ground rods, m	14.2
L_x	Maximum length of grid conductor in x direction, m	16.5
L_y	Maximum length of grid conductors in y direction, m	16.5
n	Geometric factor composed of factors n_a, n_b, n_c, and n_d	16.5
n_R	Number of rods placed in area, A	14.3
R_g	Resistance of grounding system, Ω	14.1 through 14.4
S_f	Fault current division factor (split factor) (see: *fault current division factor*)	15.1
t_c	Duration of fault current for sizing ground conductor, s	11.3
t_f	Duration of fault current for determining decrement factor, s	15.10
t_s	Duration of shock for determining allowable body current, s	5.2 through 6.3

Copyright © 2015 IEEE. All rights reserved.

Copyright The Institute of Electrical and Electronics Engineers, Inc.
Provided by IHS under license with IEEE
No reproduction or networking permitted without license from IHS

Order Number: 02120914
Sold to:EGAT [700166108393] - VARRIS.Y@EGAT.CO.TH,
Not for Resale,2016-09-15 03:57:51 UTC

16.5 Calculation of maximum step and mesh voltages

Computer algorithms for determining the grid resistance and the mesh and step voltages have been developed in Dawalibi and Mukhedkar [B43]; EPRI TR-100622 [B64]; Garrett and Holley [B72]; Heppe [B82]; and Joy, Meliopoulos, and Webb [B94]. These algorithms required considerable storage capability and were relatively expensive to execute, but improvements in the solution algorithms and the proliferation of powerful desktop computers have alleviated most of these concerns.

In some cases, it is not economically justifiable to use these computer algorithms, or the designer may not have access to a computer with the required capabilities. This subclause, in conjunction with Annex D, describes approximate equations for determining the design parameters and establishing corresponding values of E_m and E_s without the necessity of using a computer.

16.5.1 Mesh voltage (E_m)

The mesh voltage values are obtained as a product of the geometrical factor, K_m; a corrective factor, K_i, which accounts for some of the error introduced by the assumptions made in deriving K_m; the soil resistivity, ρ; and the average current per unit of effective buried length of the grounding system conductor (I_G/L_M).

$$E_m = \frac{\rho \times K_m \times K_i \times I_G}{L_M} \tag{85}$$

The geometrical factor K_m (Sverak [B136]), is as follows:

$$K_m = \frac{1}{2\times\pi} \times \left[\ln\left[\frac{D^2}{16\times h\times d} + \frac{(D+2\times h)^2}{8\times D\times d} - \frac{h}{4\times d} \right] + \frac{K_{ii}}{K_h} \times \ln\left[\frac{8}{\pi(2\times n-1)} \right] \right] \tag{86}$$

For grids with ground rods along the perimeter, or for grids with ground rods in the grid corners, as well as both along the perimeter and throughout the grid area

$$K_{ii} = 1$$

For grids with no ground rods or grids with only a few ground rods, none located in the corners or on the perimeter.

$$K_{ii} = \frac{1}{(2\times n)^{\frac{2}{n}}} \tag{87}$$

$$K_h = \sqrt{1+\frac{h}{h_o}} \qquad h_o = 1 \text{ m (grid reference depth)} \tag{88}$$

Using four grid shape components developed in Thapar, Gerez, Balakrishnan, and Blank [B148], the effective number of parallel conductors in a given grid, n, can be made applicable to rectangular or irregularly shaped grids that represent the number of parallel conductors of an equivalent rectangular grid.

$$n = n_a \times n_b \times n_c \times n_d \tag{89}$$

Copyright © 2015 IEEE. All rights reserved.

Copyright The Institute of Electrical and Electronics Engineers, Inc.
Provided by IHS under license with IEEE
No reproduction or networking permitted without license from IHS

Order Number: 02120914
Sold to:EGAT [700166108393] - VARRIS.Y@EGAT.CO.TH,
Not for Resale,2016-09-15 03:57:51 UTC

where

$$n_a = \frac{2 \times L_C}{L_p} \tag{90}$$

n_b = 1 for square grids

n_c = 1 for square and rectangular grids

n_d = 1 for square, rectangular and L-shaped grids

otherwise

$$n_b = \sqrt{\frac{L_p}{4 \times \sqrt{A}}} \tag{91}$$

$$n_c = \left[\frac{L_x \times L_y}{A} \right]^{\frac{0.7 \times A}{L_x \times L_y}} \tag{92}$$

$$n_d = \frac{D_m}{\sqrt{L_x^2 + L_y^2}} \tag{93}$$

L_C is the total length of the conductor in the horizontal grid in m

L_p is the peripheral length of the grid in m

A is the area of the grid in m^2

L_x is the maximum length of the grid in the x direction in m

L_y is the maximum length of the grid in the y direction in m

D_m is the maximum distance between any two points on the grid in m

and D, h, and d are defined in Table 12.

The irregularity factor, K_i, used in conjunction with the above defined n is

$$K_i = 0.644 + 0.148 \times n \tag{94}$$

grids with no ground rods, or grids with only a few ground rods scattered throughout the grid, but none located in the corners or along the perimeter of the grid, the effective buried length, L_M, is

$$L_M = L_C + L_R \tag{95}$$

where

L_R is the total length of all ground rods in m

Copyright © 2015 IEEE. All rights reserved.

Copyright The Institute of Electrical and Electronics Engineers, Inc.
Provided by IHS under license with IEEE
No reproduction or networking permitted without license from IHS

Order Number: 02120914
Sold to:EGAT [700166108393] - VARRIS.Y@EGAT.CO.TH,
Not for Resale,2016-09-15 03:57:51 UTC

For grids with ground rods in the corners, as well as along the perimeter and throughout the grid, the effective buried length, L_M, is

$$L_M = L_C + \left[1.55 + 1.22\left(\frac{L_r}{\sqrt{L_x^2 + L_y^2}}\right)\right] L_R \tag{96}$$

where

L_r is the length of each ground rod in m

16.5.2 Step voltage (Es)

The step voltage values are obtained as a product of the geometrical factor, K_s; the corrective factor, K_i; the soil resistivity, ρ; and the average current per unit of buried length of grounding system conductor (I_G/L_S).

$$E_s = \frac{\rho \times K_s \times K_i \times I_G}{L_s} \tag{97}$$

For grids with or without ground rods, the effective buried conductor length, L_S, is

$$L_S = 0.75 \times L_C + 0.85 \times L_R \tag{98}$$

The maximum step voltage is assumed to occur over a distance of 1 m, beginning at and extending outside of the perimeter conductor at the angle bisecting the most extreme corner of the grid. For the usual burial depth of 0.25 m < h < 2.5 m (Sverak [B136]), K_s is

$$K_s = \frac{1}{\pi}\left[\frac{1}{2 \times h} + \frac{1}{D + h} + \frac{1}{D}\left(1 - 0.5^{n-2}\right)\right] \tag{99}$$

16.6 Refinement of preliminary design

If calculations based on the preliminary design indicate that dangerous potential differences can exist within the substation, the following possible remedies should be studied and applied where appropriate:

a) *Decrease total grid resistance:* A decrease in total grid resistance will decrease the maximum GPR and, hence, the maximum transferred voltage. The most effective way to decrease ground grid resistance is by increasing the area occupied by the grid. Deep driven rods or wells may be used if the available area is limited and the rods penetrate lower resistivity layers. A decrease in substation resistance may or may not decrease appreciably the local gradients, depending on the method used.

b) *Closer grid spacings:* By employing closer spacing of grid conductors, the condition of the continuous plate can be approached more closely. Dangerous potentials within the substation can thus be eliminated at a cost. The problem at the perimeter may be more difficult, especially at a small substation where resistivity is high. However, it is usually possible, by burying the grid ground conductor outside the fence line, to ensure that the steeper gradients immediately outside this grid perimeter do not contribute to the more dangerous touch contacts. Another effective and economical way to control gradients is to increase the density of ground rods at the perimeter. This density may be decreased toward the center of the grid. Another approach to controlling perimeter

Copyright © 2015 IEEE. All rights reserved.

Copyright The Institute of Electrical and Electronics Engineers, Inc.
Provided by IHS under license with IEEE
No reproduction or networking permitted without license from IHS

Order Number: 02120914
Sold to:EGAT [700166108393] - VARRIS.Y@EGAT.CO.TH,
Not for Resale,2016-09-15 03:57:51 UTC

gradients and step potentials is to bury two or more parallel conductors around the perimeter at successively greater depth as distance from the substation is increased. Another approach is to vary the grid conductor spacing with closer conductors near the perimeter of the grid (AIEE Working Group [B4]; Biegelmeier and Rotter [B10]; Laurent [B100]; Sverak [B136]).

c) *Diverting a greater part of the fault current to other paths:* By connecting overhead ground wires of transmission lines or by decreasing the tower footing resistances in the vicinity of the substation, part of the fault current will be diverted from the grid. In connection with the latter, however, the effect on fault gradients near tower footings should be weighed (Yu [B155]).

d) *Limiting total fault current:* If feasible, limiting the total fault current will decrease the GPR and all gradients in proportion. Other factors, however, will usually make this impractical. Moreover, if accomplished at the expense of greater fault clearing time, the change may be increased rather than diminished.

e) *Barring access to limited areas:* Barring access to certain areas, where practical, will reduce the probability of hazards to personnel.

f) *Increase the tolerable touch and step voltages:* The tolerable touch and step voltages can be increased by reducing the fault clearing time, use a surface material with a higher resistivity or increase the thickness of the surface material. See Table 7.

16.7 Application of equations for E_m and E_s

Several simplifying assumptions are made in deriving the equations for E_m and E_s. The equations were compared with more accurate computer results from cases with various grid shapes, mesh sizes, numbers of ground rods, and lengths of ground rods, and found to be consistently better than the previous equations. These cases included square, rectangular, triangular, T-shaped, and L-shaped grids. Cases were run with and without ground rods. The total ground rod length was varied with different numbers of ground rod locations and different ground rod lengths. The area of the grids was varied from 6.25 m^2 to 10 000 m^2. The number of meshes along a side was varied from 1 to 40. The mesh size was varied from 2.5 m to 22.5 m. All cases assumed a uniform soil model and uniform conductor spacing. Most practical examples of grid design were considered. The comparisons found the equations to track the computer results with acceptable accuracy.

16.8 Use of computer analysis in grid design

Dawalibi and Mukhedkar [B43]; EPRI TR-100622 [B64]; and Heppe [B81] describe computer algorithms for modeling grounding systems. In general, these algorithms are based on

a) Modeling the individual components comprising the grounding system (grid conductors, ground rods, etc.).

b) Forming a set of equations describing the interaction of these components.

c) Solving for the ground-fault current flowing from each component into the earth.

d) Computing the potential at any desired surface point due to all the individual components.

e) The accuracy of the computer algorithm is dependent on how well the soil model and physical layout reflect actual field conditions.

Copyright © 2015 IEEE. All rights reserved.

Copyright The Institute of Electrical and Electronics Engineers, Inc.
Provided by IHS under license with IEEE
No reproduction or networking permitted without license from IHS

Order Number: 02120914
Sold to:EGAT [700166108393] - VARRIS.Y@EGAT.CO.TH,
Not for Resale,2016-09-15 03:57:51 UTC

There are several reasons that justify the use of more accurate computer algorithms in designing the grounding system. These reasons include

- Parameters exceed the limitations of the equations.
- A two-layer or multilayer soil model is preferred due to significant variations in soil resistivity.
- Uneven grid conductor or ground rod spacings cannot be analyzed using the approximate methods of 16.5.
- More flexibility in determining local danger points may be desired.
- Presence of buried metallic structures or conductor not connected to the grounding system, which introduces complexity to the system.

17. Special areas of concern

Before the final ground grid design calculations are completed, there still remains the important task of investigating possible special areas of concern in the substation grounding network. This includes an investigation of grounding techniques for substation fence, switch operating shafts, rails, pipelines, and cable sheaths. The effects of transferred potentials should also be considered.

17.1 Service areas

The problems associated with step and touch voltage exposure to persons outside a substation fence are much the same as those to persons within fenced substation areas.

Occasionally, a fence will be installed to enclose a much larger area than initially utilized in a substation and a ground grid will be constructed only in the utilized area and along the substation fence. The remaining unprotected areas within the fenced area are often used as storage, staging, or general service areas. Step and touch voltages should be checked to determine if additional grounds are needed in these areas.

A reduced substation grid, which does not include the service area, has both initial cost advantages and future savings resulting from not having the problems associated with "working around" a previously installed total area grid system when future expansion is required into the service area. However, a reduced grid provides less personnel protection compared to a complete substation grid that includes the service area. Also, because of the smaller area and less conductor length, a service area grid and reduced substation grid will have a higher overall resistance compared to a complete substation grid that includes the service area.

The service area might be enclosed by a separate fence that is not grounded and bonded to the substation grid. Possible transfer voltage issues are addressed in 17.3.

17.2 Switch shaft and operating handle grounding

Operating handles of switches represent a significant concern if the handles are not adequately grounded. Because the manual operation of a switch requires the presence of an operator near a grounded structure, several things could occur that might result in a fault to the structure and subject the operator to an electrical shock. This includes the opening of an energized circuit, mechanical failure, electrical breakdown of a switch insulator, or attempting to interrupt a greater value of line-charging current or transformer magnetizing current than the switch can safely interrupt.

Copyright © 2015 IEEE. All rights reserved.

Copyright The Institute of Electrical and Electronics Engineers, Inc.
Provided by IHS under license with IEEE
No reproduction or networking permitted without license from IHS

Order Number: 02120914
Sold to:EGAT [700166108393] - VARRIS.Y@EGAT.CO.TH,
Not for Resale,2016-09-15 03:57:51 UTC

It is relatively easy to protect against these hazards when the operating handle is within a reasonably extensive substation ground grid area. If the grounding system has been designed in accordance with this standard, touch and step voltages near the operating handle should be within safe limits. However, quite often additional means are taken to provide a greater safety factor for the operator. For example, the switch operating shaft can be connected to a ground mat (as described in 9.1) on which the operator stands when operating the switch. The ground mat is connected directly to the ground grid and the switch operating shaft. This technique provides a direct bypass to ground across the person operating the switch. The grounding path from the switch shaft to the ground grid must be adequately sized to carry the ground fault current for the required duration. Refer to Figure 33 for a typical switch shaft grounding practice.

The practices for grounding switch operating shafts are varied. The results of a worldwide survey conducted in 2009 indicated that 82% of the utilities that responded required grounding of substation air switch operating shafts to the grounding grid. The survey also showed 100% of the respondents took extra precautions to reduce surface gradients where the switch operator stands. The methodology to ground the operating shaft was almost equally divided among those responding to the questionnaire. Approximately half of the utilities provided a direct jumper between the switch shaft and the ground mat, while the other half provided a jumper from the switch shaft to the adjacent grounded structural steel. The steel is used as part of the conducting path. Approximately 90% of the utilities utilized a braid for grounding the switch shaft. The remaining 10% utilized a braidless grounding device. A typical braided ground is shown in Figure 34 and a braidless grounding device is shown in Figure 35. The methodology for reducing the surface gradients where the switch operator would be standing was divided between utilizing: a grounded platform, a closely spaced wire mesh under the surface material, or closer spacing of the primary grid.

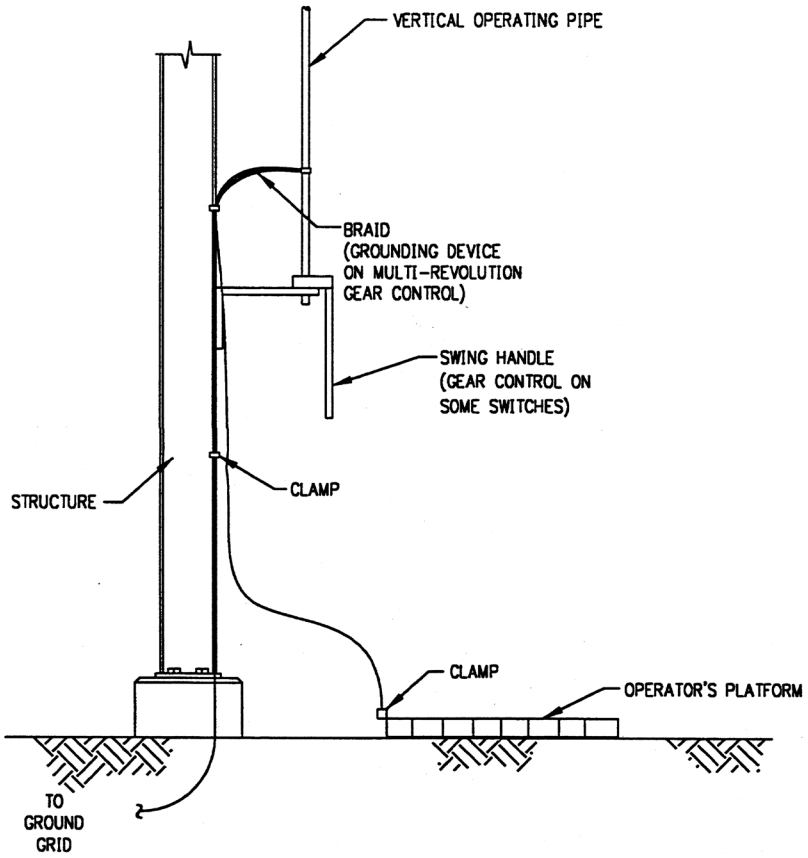

Figure 33—Typical switch shaft grounding

Copyright © 2015 IEEE. All rights reserved.

Copyright The Institute of Electrical and Electronics Engineers, Inc.
Provided by IHS under license with IEEE
No reproduction or networking permitted without license from IHS

Order Number: 02120914
Sold to:EGAT [700166108393] - VARRIS.Y@EGAT.CO.TH,
Not for Resale,2016-09-15 03:57:51 UTC

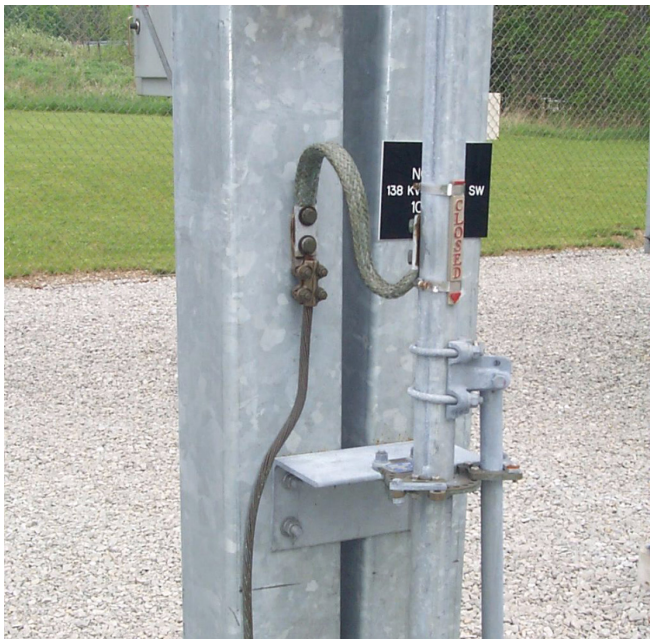

Figure 34—Typical braided ground

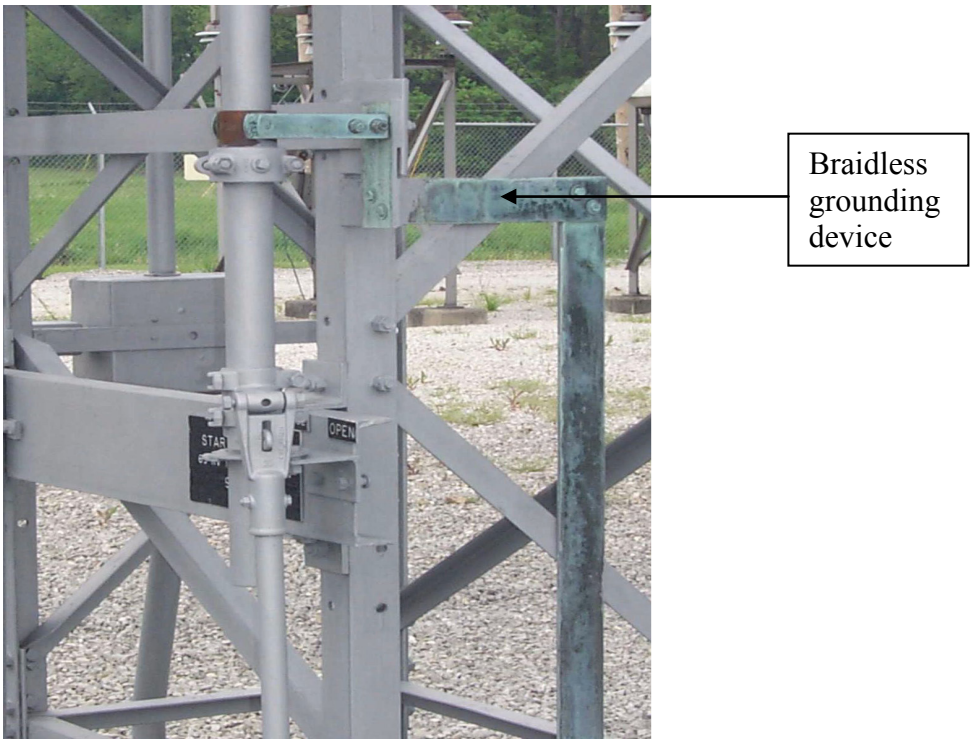

Figure 35—Typical braidless grounding device

Copyright © 2015 IEEE. All rights reserved.

Copyright The Institute of Electrical and Electronics Engineers, Inc.
Provided by IHS under license with IEEE
No reproduction or networking permitted without license from IHS

Order Number: 02120914
Sold to:EGAT [700166108393] - VARRIS.Y@EGAT.CO.TH,
Not for Resale,2016-09-15 03:57:51 UTC

17.3 Grounding of substation fence

Fences around substations are usually metallic. In some cases, the fence might be made of masonry materials or non-conductive materials. For those cases, the fence is not grounded, except possibly at exposed metallic hardware or sections, such as gates. The following discussion pertains to metallic fence grounding.

Fence grounding is of major importance because the fence is usually accessible to the general public. The substation grounding design should be such that the touch voltage on the fence is within the calculated tolerable limit of touch voltage. Step voltage should also be checked to verify that a problem does not exist, though step voltage is rarely a problem when the touch voltage is below the tolerable level.

Several philosophies exist with regard to grounding of substation fence. As an example, the National Electrical Safety Code® (NESC®) [B3] requires grounding metal fences used to enclose electric supply substations having energized electrical conductors or equipment. This metal fence grounding requirement may be accomplished by bonding the fence to the substation ground grid or to a separate ground electrode(s), which might consist of one or more ground rods and a buried conductor inside or outside the fence using the methods described in the NESC. The various fence grounding practices are:

— Fence is within the substation ground grid area and is connected to the substation ground grid.

— Fence is outside of the substation ground grid area and is connected to the substation ground grid.

— Fence is outside of the substation ground grid area, but is not connected to the substation ground grid. The fence is connected to a separate grounding electrode.

— Fence is outside of the substation ground grid area, but is not connected to the substation ground grid. The fence is not connected to a separate grounding electrode. The contact of the fence post through the fence post concrete to earth is relied on for an effective ground.

If the latter two practices on fence grounding are to be followed, i.e., if the fence and its associated grounds are not to be coupled in any way to the main ground grid (except through the soil), then three factors require consideration:

Is the falling of an energized line on the fence a danger that must be considered?

Construction of transmission lines over private fences is common and reliable. The number of lines crossing a substation fence may be greater, but the spans are often shorter and dead-ended at one or both ends. Hence, the danger of a line falling on a fence is usually not of great concern. If one is to design against this danger, then very close coupling of the fence to adjacent ground throughout its length is necessary. Touch and step potentials on both sides of the fence must be within the acceptable limit for a fault current of essentially the same maximum value as for the substation. This is somewhat impractical because the fence is not tied to the main ground grid in the substation and the adjacent earth would be required to dissipate the fault current through the local fence grounding system. In addition, the fault current would cause significant damage to the fence, and predicting the actual clearing time and touch and step voltages might be impossible.

May hazardous potentials exist at the fence during other types of faults because the fence line crosses the normal equipotential contours?

Fences do not follow the normal equipotential lines on the surface of the earth which result from fault current flowing to and from the substation ground grid. If coupling of the fence to ground is based solely on the contact between the fence posts and the surrounding earth, the fence might, under a fault condition, attain the potential of the ground where the coupling was relatively good, and thereby attain a high voltage in relation to the adjacent ground surface at locations where the coupling was not as good. The current flowing in the earth and fence, and the subsequent touch voltage on the fence are less than would result from an energized line falling on the fence; however, the touch voltage may exceed the allowable value and would, hence, be unsafe.

Copyright © 2015 IEEE. All rights reserved.

Copyright The Institute of Electrical and Electronics Engineers, Inc.
Provided by IHS under license with IEEE
No reproduction or networking permitted without license from IHS

Order Number: 02120914
Sold to:EGAT [700166108393] - VARRIS.Y@EGAT.CO.TH,
Not for Resale,2016-09-15 03:57:51 UTC

In practice, can complete metallic isolation of the fence and substation ground grid be assured at all times?

It may be somewhat impractical to expect complete metallic isolation of the fence and the substation ground grid. The chance of an inadvertent electrical connection between the grid and the fence areas may exist. This inadvertent electrical connection may be from metallic conduits, water pipes, etc. These metallic items could transfer main grid potential to the fence and hence dangerous local potential differences could exist on the fence during a fault. If the fence is not closely coupled to the nearby ground by its own adequate ground system then any such inadvertent connections to the main grid could create a hazard along the entire fence length under a fault condition. This hazard could be only partially negated by utilizing insulated joints in the fence at regular intervals. However, this does not appear to be a practical solution to the possible hazard.

Several different practices are followed in regard to fence grounding. Some ground only the fence posts, using various types of connectors as described elsewhere in this guide and depend on the fence fabric fasteners (often simple metallic wire ties) to provide electrical continuity along the fence. Others ground the fence posts, fabric, and barbed wire. The ground grid should extend to cover the swing of all substation gates. The gate posts should be securely bonded to the adjacent fence post utilizing a flexible connection.

To illustrate the effect of various fence grounding practices on fence touch potential, five fence grounding examples were analyzed using computer analysis. The fence grounding techniques analyzed were

— Case 1: Inclusion of fence within the ground grid area. The outer ground wire is 0.91 m (3 ft) outside of the fence perimeter. The fence is connected to the ground grid. Refer to Figure 36 and Figure 37 for grid layout.

— Case 2: Ground grid and fence perimeter approximately coincide. The outer ground wire is directly alongside the fence perimeter. The fence is connected to the ground grid. Refer to Figure 38 and Figure 39 for grid layout.

— Case 3: The outer ground grid wire is 0.91 m (3 ft) inside the fence perimeter. The fence is connected to the ground grid. Refer to Figure 40 and Figure 41 for grid layout.

— Case 4: Ground grid is inside of fence area. The outer ground grid wire is 6.7 m (22 ft) inside the fence perimeter. The fence is connected to the ground grid. Refer to Figure 42 and Figure 43 for grid layout.

— Case 5: Ground grid is inside of fence area. The outer ground grid wire is 6.7 m (22 ft) inside the fence perimeter. The fence is locally grounded but not connected to the ground grid. Refer to Figure 44 and Figure 45 for grid layout.

The fenced area for each case is a square having sides of 43.9 m (144 ft). The test calculations are based on the following parameters:

ρ = 60 Ω-m

I_G = 5000 A

h_s = 0.076 m

ρ_s = 3000 Ω-m, extending 0.91 m (3 ft) beyond the fence

R = 0.66 Ω for cases 1 through 4

R = 0.98 Ω for case 5

t_s = 0.5 s

D_f = 1.0

Copyright © 2015 IEEE. All rights reserved.
Copyright The Institute of Electrical and Electronics Engineers, Inc.
Provided by IHS under license with IEEE
No reproduction or networking permitted without license from IHS
Order Number: 02120914
Sold to:EGAT [700166108393] - VARRIS.Y@EGAT.CO.TH,
Not for Resale,2016-09-15 03:57:51 UTC

The factor C_s for derating the nominal value of surface layer resistivity is dependent on the thickness and resistivity of the surface material and the soil resistivity, and is computed using Equation (27) or Figure 11:

$$K = \frac{\rho - \rho_s}{\rho + \rho_s}$$

$$K = \frac{60 - 3000}{60 + 3000} = -0.961$$

$$C_s = 0.636$$

The allowable step and touch voltages are calculated using Equation (29) and Equation (32). For test cases 1 through 5:

$$E_{step50} = (1000 + 6C_s \times \rho_s)0.116/\sqrt{t_s} = 2042 \text{ V}$$

$$E_{touch50} = (1000 + 1.5C_s \times \rho_s)0.116/\sqrt{t_s} = 634 \text{ V}$$

The actual step voltage E_s and actual mesh voltage E_m are calculated as a function of the GPR in percent, using the following equations:

$$E_S = R_g \times I_g \frac{E_S(\%)}{100} D_f$$

$$E_m = R_g \times I_g \frac{E_m(\%)}{100} D_f$$

where

$E_s(\%)$ is the step voltage in terms of percent of GPR
$E_m(\%)$ is the mesh voltage in terms of percent of GPR

Equating the actual step and mesh voltage equations to the tolerable step and touch voltage values ($E_{step} = E_s$ and $E_{touch} = E_m$) and solving for $E_s(\%)$ and $E_m(\%)$, the equations become

$$E_s(\%) = \frac{E_{step}(100)}{R_g \times I_g \times D_f}$$

$$E_m(\%) = \frac{E_{touch}(100)}{R_g \times I_g \times D_f}$$

Substituting the assumed parameters for these test cases yields the following:

For cases 1 through 4

$$E_s(\%) = 61.9$$

$$E_m(\%) = 19.2$$

Copyright © 2015 IEEE. All rights reserved.
Copyright The Institute of Electrical and Electronics Engineers, Inc.
Provided by IHS under license with IEEE
No reproduction or networking permitted without license from IHS
Order Number: 02120914
Sold to:EGAT [700166108393] - VARRIS.Y@EGAT.CO.TH,
Not for Resale,2016-09-15 03:57:51 UTC

For case 5

$$E_s(\%) = 41.7$$

$$E_m(\%) = 12.9$$

The actual step and mesh voltages as a percent of GPR must be less than 61.9% and 19.2%, respectively, for cases 1 through 4 and less than 41.7% and 12.9%, respectively, for case 5.

For each test case, two voltage profiles were computed at the following locations:

— A line parallel to and 0.91 m (3 ft) outside of fence

— A line through the grid from one side to the other, parallel to the grid wires

17.4 Results of voltage profiles for fence grounding

The results of the voltage profiles along the surface of the earth for test case 1 are shown in Figure 36 and Figure 37. The results for both profiles indicate that the touch voltage on the fence for a person standing 0.91 m (3 ft) from the fence (approximately one arm's length) is less than the tolerable touch voltage and hence safe. The voltage profiles illustrate how the voltage above remote earth decreases rapidly as one leaves the substation ground grid area. As seen in Figure 36, the step voltage is no greater than 3% to 4% and is far below the tolerable step voltage percent of 61.9% of GPR. Because step voltage is usually not the concern in regard to fence grounding, it will not be analyzed in the remaining test cases.

The results of the voltage profiles for test case 2 are shown in Figure 38 and Figure 39. The voltage profile in Figure 39 for a line through the grid from one side to the other indicates that the touch voltage 0.91 m (3 ft) outside of the fence is very nearly equal to the allowable touch voltage. However, as seen in Figure 38 for a voltage profile along the fence and 0.91 m (3 ft) away from it, it is clear that the touch voltages on certain areas of the fence are not safe for a person to contact. By comparing Figure 36 and Figure 38, one can clearly see the effect of having a ground grid wire 0.91 m (3 ft) outside of the fence and around the fence perimeter.

The results of the voltage profiles for test case 3 are shown in Figure 40 and Figure 41. These results are very similar to those of test case 2 and illustrate that the touch voltage on the fence is generally not safe in several areas for a person to contact.

The results of the voltage profiles for test case 4 are shown in Figure 42 and Figure 43. These results again illustrate that the touch voltage on the fence during a fault condition is not safe to contact. It can be seen by comparing Figure 36, Figure 38, Figure 40, and Figure 42 that the touch voltage along the length of the fence increases as the outer ground grid wire is moved inward toward the substation.

The results of the voltage profiles for test case 5 are shown in Figure 44 and Figure 46. The tolerable touch voltage has decreased from 19.2% to 12.9% because of an increase in the substation grid resistance. The grid resistance increase is a result of less wire and reduced area in the grid for test case 5. According to the computer program results, the potential rise on the isolated, separately grounded fence during a ground fault condition is 43.7% of GPR, which is shown as a horizontal line on the graphs. The potential rise on the fence is caused by the coupling through the earth from the ground grid to the fence. As shown in Figure 44, the potential rise on the earth 0.91 m (3 ft) beyond the fence corner caused by a ground fault condition is 30.5% of GPR. The largest difference in voltage between the fence and the earth occurs at the corner and is 13.2% of GPR, which is 0.3% greater than the allowable touch voltage of 12.9%. It is also important to note that if the fence should ever inadvertently become metallically connected to the ground grid, the

Copyright © 2015 IEEE. All rights reserved.
Copyright The Institute of Electrical and Electronics Engineers, Inc.
Provided by IHS under license with IEEE
No reproduction or networking permitted without license from IHS
Order Number: 02120914
Sold to:EGAT [700166108393] - VARRIS.Y@EGAT.CO.TH,
Not for Resale,2016-09-15 03:57:51 UTC

potential on the fence could reach 100% of GPR and the results would be similar to those shown in case 4 (Figure 42 and Figure 43).

Test cases studied for an isolated ungrounded fence yield very similar results as the test cases run for an isolated, separately grounded fence shown in Figure 44 and Figure 46.

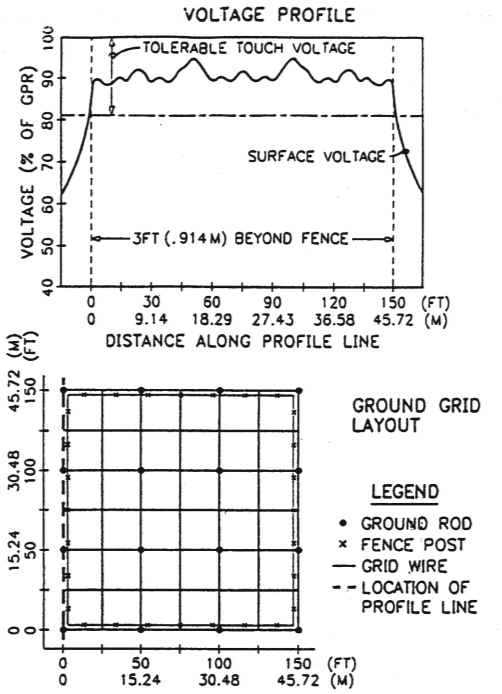

Figure 36—Case 1, plot 1

Copyright © 2015 IEEE. All rights reserved.
Copyright The Institute of Electrical and Electronics Engineers, Inc.
Provided by IHS under license with IEEE
No reproduction or networking permitted without license from IHS
Order Number: 02120914
Sold to:EGAT [700166108393] - VARRIS.Y@EGAT.CO.TH,
Not for Resale,2016-09-15 03:57:51 UTC

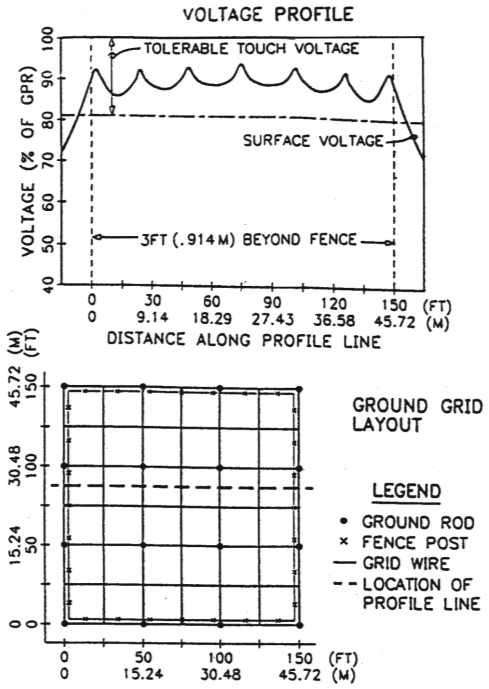

Figure 37—Case 1, plot 2

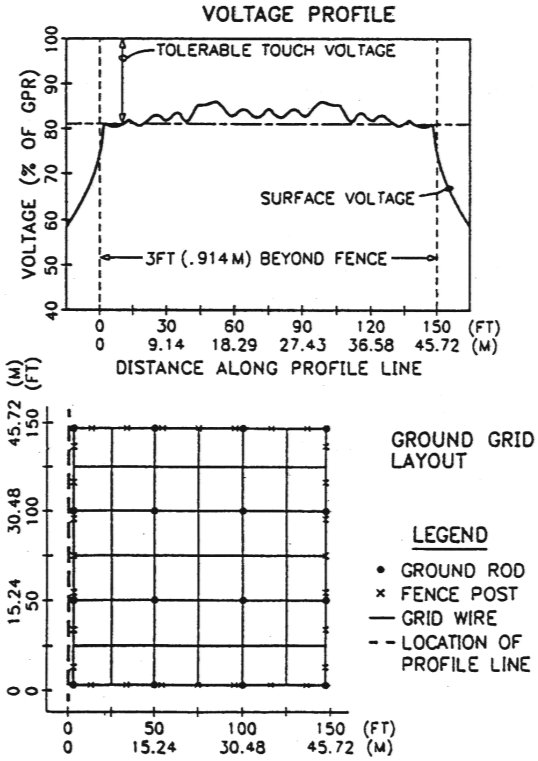

Figure 38—Case 2, plot 1

Copyright © 2015 IEEE. All rights reserved.

Copyright The Institute of Electrical and Electronics Engineers, Inc.
Provided by IHS under license with IEEE
No reproduction or networking permitted without license from IHS

Order Number: 02120914
Sold to:EGAT [700166108393] - VARRIS.Y@EGAT.CO.TH,
Not for Resale,2016-09-15 03:57:51 UTC

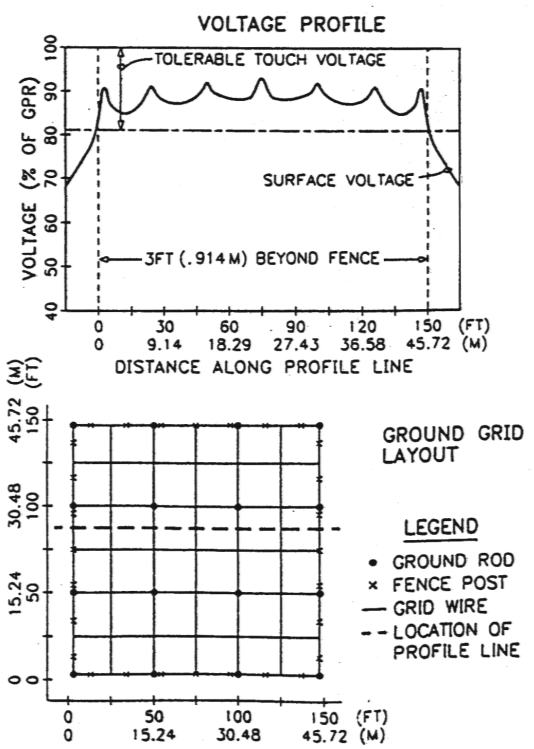

Figure 39—Case 2, plot 2

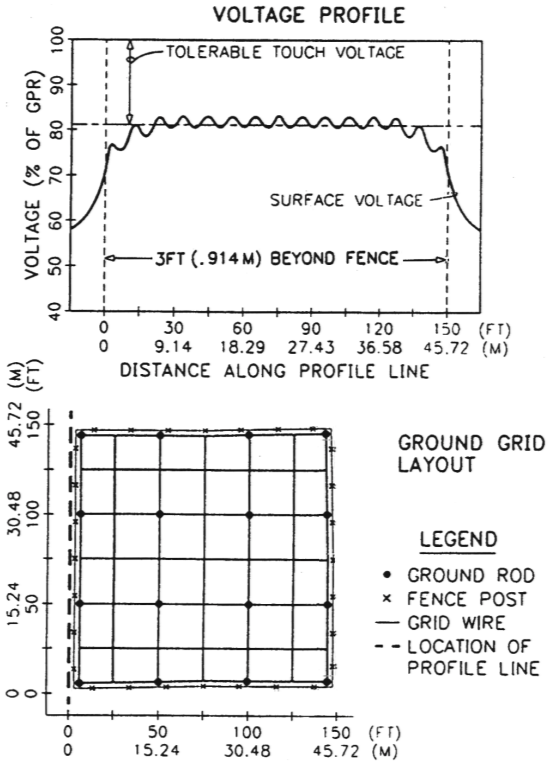

Figure 40—Case 3, plot 1

Copyright © 2015 IEEE. All rights reserved.

Copyright The Institute of Electrical and Electronics Engineers, Inc.
Provided by IHS under license with IEEE
No reproduction or networking permitted without license from IHS

Order Number: 02120914
Sold to:EGAT [700166108393] - VARRIS.Y@EGAT.CO.TH,
Not for Resale,2016-09-15 03:57:51 UTC

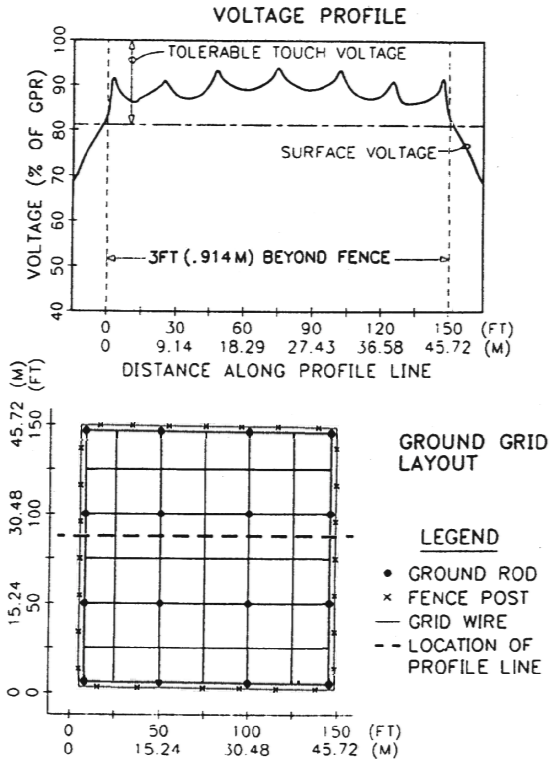

Figure 41—Case 3, plot 2

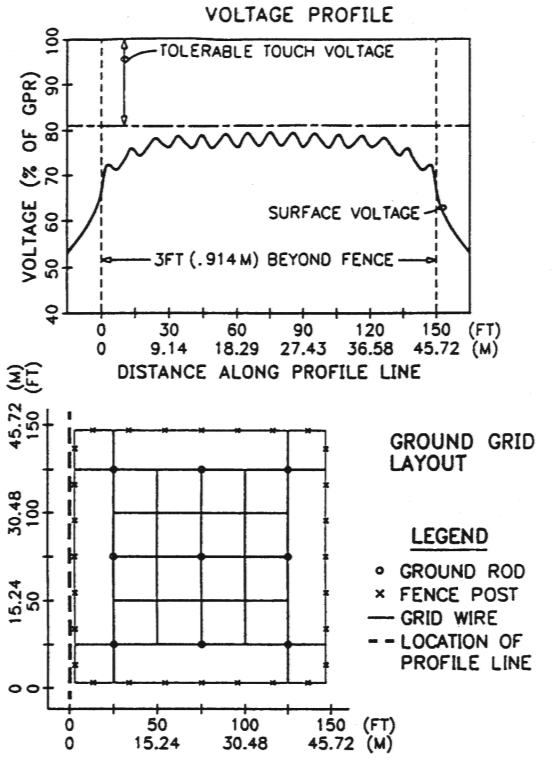

Figure 42—Case 4, plot 1

Copyright © 2015 IEEE. All rights reserved.

Copyright The Institute of Electrical and Electronics Engineers, Inc.
Provided by IHS under license with IEEE
No reproduction or networking permitted without license from IHS

Order Number: 02120914
Sold to:EGAT [700166108393] - VARRIS.Y@EGAT.CO.TH,
Not for Resale,2016-09-15 03:57:51 UTC

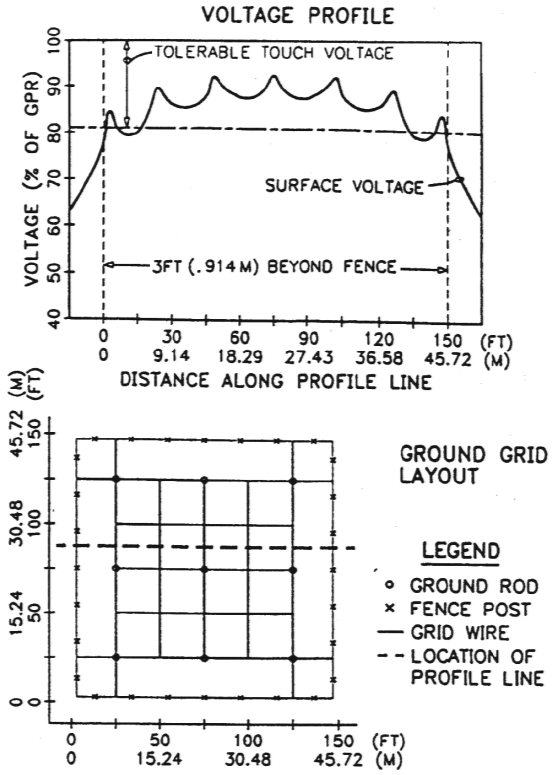

Figure 43—Case 4, plot 2

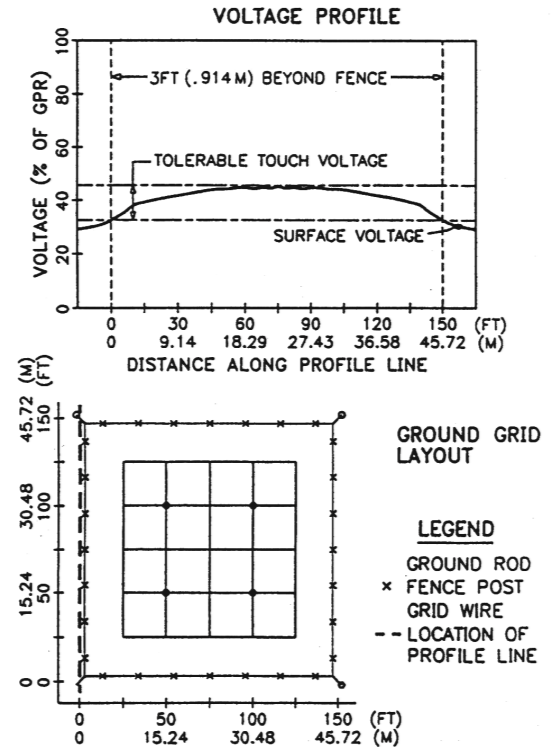

Figure 44—Case 5, plot 1

Copyright © 2015 IEEE. All rights reserved.

Copyright The Institute of Electrical and Electronics Engineers, Inc.
Provided by IHS under license with IEEE
No reproduction or networking permitted without license from IHS

Order Number: 02120914
Sold to:EGAT [700166108393] - VARRIS.Y@EGAT.CO.TH,
Not for Resale,2016-09-15 03:57:51 UTC

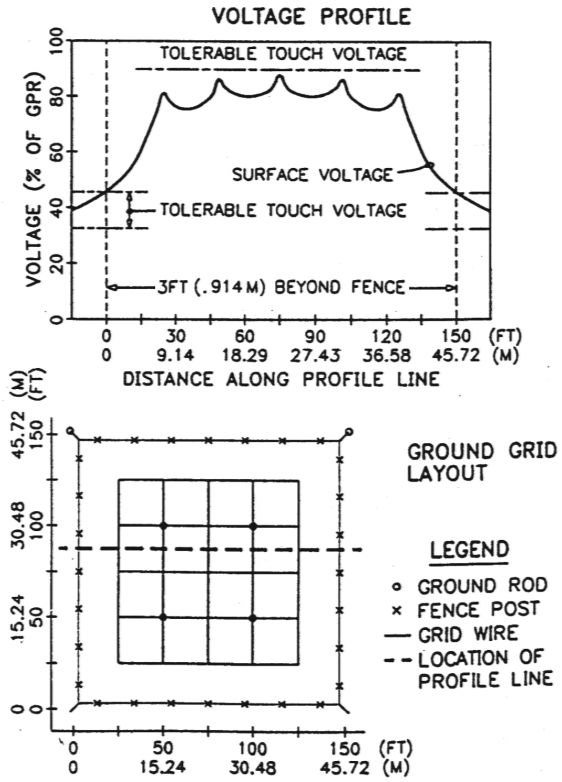

Figure 45—Case 5, plot 2

17.5 Control cable sheath grounding

Metallic cable sheaths, unless effectively grounded, may attain dangerous voltages with respect to ground. These voltages may result from insulation failure, charges due to electrostatic induction, flow of currents in the sheath, or from the voltage rise during faults discharging to the substation ground system to which the sheaths are connected. All grounding connections should be made to the shield in such a way as to provide a permanent low-resistance bond, and have a continuous short-circuit ampacity equal to or greater than the cable sheath.

Unless recommended to eliminate circulating currents in low-voltage or current control circuits, the sheaths of shielded control cables should be grounded at both ends to reduce electromagnetically induced potentials on and currents in the control cable. If the control cable sheath is grounded at widely separated points, large potential gradients in the ground grid during faults may cause excessive sheath currents to flow. One solution is to run a separate conductor in parallel with the control cable connected to the two sheath ground points. The induced current in the separate conductor will induce an opposing voltage on the control cable sheath, thereby minimizing the current in the sheath. This separate conductor (usually bare copper) is typically routed along the top of the inside wall of the cable trench or above direct-buried conductors. Refer to IEEE Std 525™ [B87].

Non-shielded cables are subject to transient induced voltage magnitudes of 190% or more than the induced voltages on shielded cables (Mitani [B112], Patel [B124]). Induced voltages in non-shielded cables can be reduced by as much as 60% by grounding both ends of an unused wire, or by installing parallel ground conductors grounded at both ends, as described above. The effects of fault currents on the conditions to be encountered with any of these grounding arrangements can only be determined by careful analysis of each specific case.

Copyright © 2015 IEEE. All rights reserved.

Copyright The Institute of Electrical and Electronics Engineers, Inc.
Provided by IHS under license with IEEE
No reproduction or networking permitted without license from IHS

Order Number: 02120914
Sold to:EGAT [700166108393] - VARRIS.Y@EGAT.CO.TH,
Not for Resale,2016-09-15 03:57:51 UTC

17.6 GIS bus extensions

A number of unique problems are encountered in the grounding of a GIS vis-a-vis conventional substations. The grounded metal enclosure of GIS equipment can be a source of dangerous touch voltages during fault conditions. Refer to Clause 10 for techniques of evaluating touch voltages in GIS.

17.7 Surge arrester grounding

Surge arresters should always be provided with a reliable low-impedance ground connection. Arresters should be connected as close as possible to the terminals of the apparatus to be protected and have the phase and neutral leads as short and straight as possible. For equipment such as transformers, breakers, and regulators, connecting the arresters from phase to the tank will minimize the surge voltage across the equipment's insulation to ground. For equipment and all other applications, the arrester neutral lead should also be as short and direct a path to the grounding system as practical to dissipate the surge energy to the earth. Bends in the arrester phase or neutral end leads can add significant impedance and reduce the protective level of the arrester. While many utilities provide separate ground leads from arresters mounted on metal structures, other utilities use the arrester mounting structures or the tank for the protected equipment as the surge arrester ground path because the large cross section of the steel members provides a lower resistance path than the usual size copper cable. In these cases it is important to ensure adequate electric connections from the structure to both arrester ground lead and ground grid. Also verify the steel cross-sectional area has adequate conductivity, and that no high resistance is introduced into joints from paint film, rust, etc.

17.8 Separate grounds

The practice of having separate grounds within a substation area is rarely used for the following reasons:

a) Higher resistances for separate safety and system grounds are produced than would be the case for a single uniform ground system.
b) In the event of insulation failures in the substation, high currents could still flow in the safety ground.
c) Because of a high degree of coupling between separate electrodes in the same area, the safety objective of keeping the GPR of the safety grounds low for line faults would not be accomplished.
d) Often dangerous potentials would be possible between nearby grounded points because decoupling of the separate grounds is possible, at least to some extent.
e) Separate grounds can result in large transient potential differences between components of electrical equipment during lightning or other surge events, causing equipment misoperation or damage.

17.9 Transferred potentials

A serious hazard may result during a ground fault from the transfer of potential between the substation ground grid area and outside locations. This transferred potential may be transmitted by communication circuits, conduit, pipes, metallic fences, low-voltage neutral wires, etc. The danger is usually from contact of the touch type. A transferred potential problem generally occurs when a person standing at a remote location away from the substation area touches a conductor connected to the substation ground grid. It might also occur when a person within the substation touches a conductor that leaves the substation and is remotely grounded. The importance of the problem results from the very high magnitude of potential difference, which is often possible. This potential difference may equal or exceed (due to induced voltage on unshielded communication circuits, pipes, etc.) the GPR of the substation during a fault condition. The basic shock situation for transferred potential is shown in Figure 12.

Copyright © 2015 IEEE. All rights reserved.

Copyright The Institute of Electrical and Electronics Engineers, Inc.
Provided by IHS under license with IEEE
No reproduction or networking permitted without license from IHS

Order Number: 02120914
Sold to:EGAT [700166108393] - VARRIS.Y@EGAT.CO.TH,
Not for Resale,2016-09-15 03:57:51 UTC

An investigation into possible transferred potential hazards is essential in the design of a substation grounding network. Various means can be taken to help protect against the danger of transferred potentials. The following subclauses offer a brief discussion of the various transferred potential hazards and means to eliminate the hazard.

17.9.1 Communication circuits

For communications circuits, methods have been developed involving protective devices to safeguard personnel and communications terminal equipment. These will not be discussed here except to emphasize the importance of adequate insulation and isolation from accidental contact of any of these devices and their wiring, which may reach a high voltage with respect to local ground. Fiber optics and optical isolators are now more commonly used to isolate the substation communications terminal from the remote terminal to eliminate the transfer of high potentials. Refer to IEEE Std 487™ for more detailed information.

17.9.2 Rails

Rails entering the substation can create a hazard at a remote point by transferring all or a portion of the GPR from the substation to a remote point during a ground fault. Similarly, if grounded remotely, a hazard can be introduced into the substation area by transferring remote earth potential to within the substation. These hazards can be eliminated by removing the track sections into the substation after initial use, or by using removable track sections where the rails leave the ground grid area. However, insulating flanges, as discussed in the following paragraphs, should also be utilized to provide as much protection as possible when the railroad track is intact for use.

Insulating splices or flanges are manufactured by a variety of vendors. The general practice is to install two or three sets of these devices such that a rail car would not shunt a single set. Investigation of these insulating splices has shown that they are primarily designed for electrical isolation of one track from another for signal scheme purposes. The typical insulated joint consists of a section of track made from an insulated material called an end post, installed between rail ends. The side members bolting the joint are also insulated from the rail sections. The breakdown voltage of the insulating joints should be considered in each application. The insulating joints must be capable of withstanding the potential difference between remote earth and the potential transferred to the joint.

It should be noted, however, that insulating flanges are not recommended as the primary means of protection, as they may create their own hazardous situations (Garrett and Wallace [B73]). If the track sections outside the substation and beyond the insulating flange are in contact with the soil, a hazardous voltage may exist between that rail section and a rail section or perimeter fence grounded to the substation grid during a fault. If the rails are not bonded to the substation grid, a hazardous voltage may exist between the rails and grounded structures within the substation during a fault. Other situations are discussed in Garrett and Wallace [B73] that may result in hazardous voltages. Thus, removal of rail sections at the perimeter of the grounding system is recommended.

17.9.3 Low-voltage neutral wires

Hazards are possible where low-voltage feeders or secondary circuits, serving points outside the substation area, have their neutrals connected to the substation ground. When the potential of the substation ground grid rises as the result of ground-fault current flow, all or a large part of this potential rise may then appear at remote points as a dangerous voltage between this “grounded” neutral wire and the adjacent earth. Moreover, where other connections to earth are also provided, the flow of fault current through these may, under unfavorable conditions, create gradient hazards at points remote from the substation.

To avoid these difficulties, the low-voltage neutral may be isolated from ground at the substation itself; always provided, however, that this does not result in slowing down the clearing time for low-voltage faults to the point where the total hazard is increased rather than diminished. This is often done by utilizing an

--`,,,,,,`,```,,`,`,,`,-`-`,,`,,,`---
Copyright © 2015 IEEE. All rights reserved.

Copyright The Institute of Electrical and Electronics Engineers, Inc.
Provided by IHS under license with IEEE
No reproduction or networking permitted without license from IHS

Order Number: 02120914
Sold to:EGAT [700166108393] - VARRIS.Y@EGAT.CO.TH,
Not for Resale,2016-09-15 03:57:51 UTC

isolation transformer to separate the substation neutral from the neutral of the circuit to the remote service point. If the low-voltage neutral is isolated from that substation ground, it then becomes necessary to avoid hazards at the substation due to the introduction, via the neutral wire, of remote earth potential. This implies that this neutral, in and near the substation, should be treated as a "live" conductor. It should be insulated from the substation ground system by insulation adequate to withstand the GPR; and it should be located to minimize the danger of being contacted by personnel.

Alternately, the remote service point can be treated as an extension of the grid. In this case, additional grounding, such as a loop of grounding and ground rods, or an equipotential ground mat, is installed around the remote service point to help control hazardous touch and step voltages in that area.

17.9.4 Portable equipment and tools supplied from substation

Transferred voltage hazards need to be considered in the case of portable mining, excavating, or material handling equipment, or portable tools, which are supplied electrically from the substation and are used outside of the area of the grid where the mesh potential is held within safe limits. Such loads are often supplied by temporary pole lines or long portable cables. An example is often seen when an addition to an existing substation is being constructed.

A hazardous transferred potential might appear between equipment and the nearby earth during a fault, if the neutral or grounding wire to the equipment is also connected to the substation ground. In cases such as these, it is common to isolate the supply circuits from the substation ground using an isolation transformer with a minimum insulation withstand rating greater than the anticipated ground potential difference; to ground the neutrals and equipment to earth at the site of the work; and to make sure that the maximum fault current to the local ground is limited to a low value that will not itself cause gradient hazards. Another option is to provide power to the external work site using portable generators.

17.9.5 Piping

Pipelines and metallic conduits should always be connected to the substation grounding system to reduce hazards within the substation area. Transferred potentials may be reduced or stopped at the substation boundary by inserting insulating sections of sufficient length to reduce shunting by the adjacent soil. The insulating sections must be capable of withstanding the potential difference between remote earth and the substation.

17.9.6 Auxiliary buildings

Auxiliary buildings can be treated as part of the substation for grounding purposes, or as separate installations, depending on circumstances. If the buildings and substation are relatively close, and especially if the buildings are linked directly to the substation by water pipes, cable sheaths, phone lines, etc., it is appropriate to treat such buildings and their immediate area as part of the substation. As such, the buildings should be grounded using the same safety criteria as the substation. If the buildings are not as close, and if such conducting links are lacking, it may be decided to treat such buildings as separate units with their own local safety grounds. If served electrically from the substation, they should have their own distribution transformers of a type to provide adequate insulation against transfer of the substation GPR. Secondary neutrals would, in this case, be connected to the local ground at the auxiliary buildings only.

17.9.7 Fences

Substation fences have been extended to other areas of a site at some locations. This also presents a possible transferred potential hazard if the fence is connected to the substation ground grid.

Copyright © 2015 IEEE. All rights reserved.

Copyright The Institute of Electrical and Electronics Engineers, Inc.
Provided by IHS under license with IEEE
No reproduction or networking permitted without license from IHS

Order Number: 02120914
Sold to:EGAT [700166108393] - VARRIS.Y@EGAT.CO.TH,
Not for Resale,2016-09-15 03:57:51 UTC

To lessen this hazard, the substation fence should be insulated from the fence leaving the substation area. It is recommended that insulating sections be installed to prevent the transfer of potential through the soil and be long enough to prevent someone from bridging the insulating section.

An example of the potential profile of a fence connected to a substation ground grid and leaving the substation area is shown in Figure 46. As can be seen, the touch voltage on the fence after it leaves the substation grid area of influence is not safe to contact.

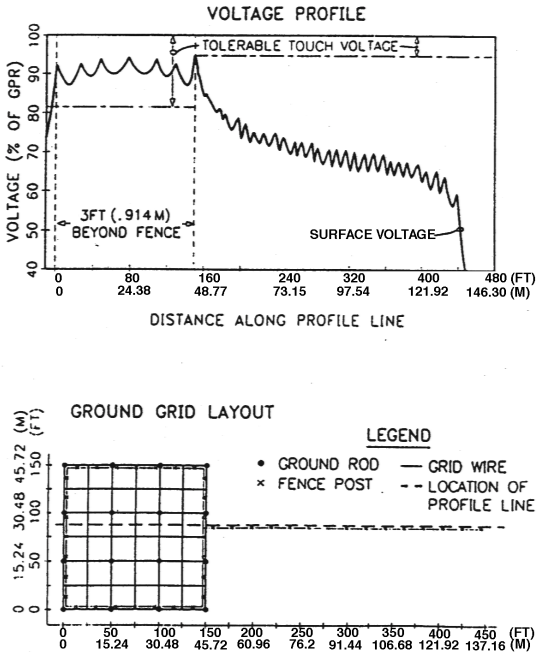

Figure 46—Transfer potential on a fence

18. Construction of a grounding system

The method of construction, or combination of methods chosen, will depend on a number of factors, such as size of a grid, type of soil, size of conductor, depth of burial, availability of equipment, cost of labor, and any physical or safety restrictions due to nearby existing structures or energized equipment.

There are two commonly employed methods to install the ground grid. These are the trench method and the cable plowing method. Both of these methods employ machines. Where these machines are not employed due to lack of space to move them or small size of the job site, the ground grid is installed by hand digging.

18.1 Ground grid construction—trench method

Flags might be staked on the perimeter along two sides to identify the spacing between parallel conductors. These markers also serve as a guide for the trenching machine. The trenches are dug using a trenching machine usually along the side having the larger number of parallel conductors. These trenches are dug to the specified depth (usually about 0.5 m or 1.5 ft). Conductors are installed in these ditches and ground rods are driven and connected to the conductors. Pigtails for equipment grounds may also be placed at this time. These initial ditches are then backfilled with dirt up to the location of the cross-connections.

Copyright © 2015 IEEE. All rights reserved.

Copyright The Institute of Electrical and Electronics Engineers, Inc.
Provided by IHS under license with IEEE
No reproduction or networking permitted without license from IHS

Order Number: 02120914
Sold to:EGAT [700166108393] - VARRIS.Y@EGAT.CO.TH,
Not for Resale,2016-09-15 03:57:51 UTC

The next step is to dig cross-conductor ditches (often to a shallower depth), once again using markers as a guide. Care must be taken when digging these ditches to avoid snagging the conductor laid in the backfilled ditches at cross points. The conductors are installed in the ditches and any remaining ground rods are driven and connected to the conductors. Remaining pigtails are also connected to these conductors. Cross-type connections are made between perpendicular conductor runs. The ditches are then backfilled with dirt.

An alternative method consists of digging all the trenches at the same depth at the same time. This might be done in small sections of the substation (so as not to hinder other construction activities) or over the entire substation. Installation of conductors and ground rods are the same as described in the preceding paragraphs.

18.2 Ground grid construction—conductor plowing method

Another procedure for the installation of ground conductors, which may prove economical and quick when conditions are favorable and proper equipment is available, is to plow the conductors in. A special narrow plow is used, which may be either attached to, or drawn by, a tractor or four-wheel drive truck, if there is sufficient maneuvering room. The plow may also be drawn by a winch placed at the edge of the yard. The conductor may be laid on the ground in front of the plow, or a reel of conductor may be mounted on the tractor or truck, or on a sled pulled ahead of the plow. The conductor is then fed into the ground along the blade of the plow to the bottom of the cut. Another method is to attach the end of the conductor to the bottom of the plow blade, and pull it along the bottom of the cut as the plow progresses. In this case, care should be taken to ensure that the conductor does not work its way upward through the loosened soil.

The cross-conductors are plowed in at slightly less depth to avoid damage to previously laid conductors. The points of crossing, or points where ground rods are to be installed, are then uncovered, and connections are made as described in 18.3.

With adequate equipment, and the absence of heavy rock, this method is suitable for all of the conductor sizes and burial depths normally used. The reader can find additional information in IEEE Std 590™ [B88].

18.3 Installation of connections, pigtails, and ground rods

Once the conductors are placed in their trenches, the required connections are then made. Types of connections are many and varied and depend on the joint, the material being joined, and the standard practice of the utility concerned (see 11.4). During installation, avoid damage to the outer layer of any bimetallic material used. Consideration also needs to be given to the corrosion at the exposed conductor ends where connections are used. Extending the exposed conductor end past the connection might mitigate problems associated with this issue.

Pigtails are left at appropriate locations for grounding connections to structures or equipment. These pigtails may be the same cable size as the underground grid or a different size depending on the number of grounds per device, the magnitude of the ground fault current, and the design practices of the utility concerned. The pigtails are then readily accessible after backfilling to make above-grade connections.

The installation of the ground rods is usually accomplished by using a hydraulic hammer, air hammer, or other mechanical device. The joining of two ground rods is done by using the exothermic method, swaged connection, or a threaded or threadless coupler. The connection between the ground rod and grid conductor can be made using various methods.

Copyright © 2015 IEEE. All rights reserved.

Copyright The Institute of Electrical and Electronics Engineers, Inc.
Provided by IHS under license with IEEE
No reproduction or networking permitted without license from IHS

Order Number: 02120914
Sold to:EGAT [700166108393] - VARRIS.Y@EGAT.CO.TH,
Not for Resale,2016-09-15 03:57:51 UTC

18.4 Construction sequence consideration for ground grid installation

A ground grid is normally installed after the yard is graded, foundations are poured, and deeper underground pipes and conduits are installed and backfilled. The security fence may be installed before or after the ground grid installation. In cases where deeper underground pipes and conduits are not installed before ground grid installation, an attempt should be made to coordinate the trenching procedure in a logical manner.

18.5 Safety considerations during subsequent excavations

As shown in 7.4, the insulating value of a layer of clean surface material or gravel is an aid to safety under ground fault conditions. Therefore, when an excavation is necessary after a rock surfacing has been applied, care should be taken to avoid mixing the lower resistivity soil from the excavation with the surrounding rock surfacing material.

During subsequent excavations there are more chances to snag the ground conductor. In such a case a check should be made to determine if there is a break in the conductor and joints. A break in the conductor or joints, or both, must be immediately repaired. A temporary protective ground (TPG) connection should be placed around the break before it is repaired. The TPG connection should be suitable for the application and installed according to safe grounding practices, because a voltage may exist between the two ground conductor ends. The same precautions should be used when expanding or making additions to an existing grounding system. TPGs should be installed between the old and new grid conductors before handling the conductors to make connections.

19. Field measurements of a constructed grounding system

19.1 Measurements of grounding system impedance

A careful measurement of the impedance of the installation as constructed might be desirable, especially when soil resistivity measurements or interpretation of the appropriate soil model were questionable. However, this measurement is not always practical if the grid is connected to or influenced by other buried metallic structures.

In this clause only general methods are discussed. For more detailed information refer to IEEE Std 81. Several important points of this guide have been used here, where applicable. While in this clause the ohmic value is referred to as resistance, it should be remembered that there is a reactive component that should be taken into consideration when the ohmic value of the ground under test is less than 0.5 Ω and the area is relatively large. This reactive component has little effect on grounds with impedances higher than 0.5 Ω.

19.1.1 Fall-of-potential method

This method has several variations and is applicable to all types of ground resistance measurements (see Figure 47). Basically, the ground resistance measurement consists of measuring the resistance of the grounding system with respect to a remote ground electrode. The remote electrode is theoretically at an infinite distance from the grounding system where the earth current density approaches zero. Although the fall-of-potential method is universally used, it presents many difficulties and sources of error when used to

Copyright © 2015 IEEE. All rights reserved.

Copyright The Institute of Electrical and Electronics Engineers, Inc.
Provided by IHS under license with IEEE
No reproduction or networking permitted without license from IHS

Order Number: 02120914
Sold to:EGAT [700166108393] - VARRIS.Y@EGAT.CO.TH,
Not for Resale,2016-09-15 03:57:51 UTC

measure the resistance of large grounding systems usually encountered in practice. These difficulties occur mainly because of the size and configuration of the grounding system and soil heterogeneity.

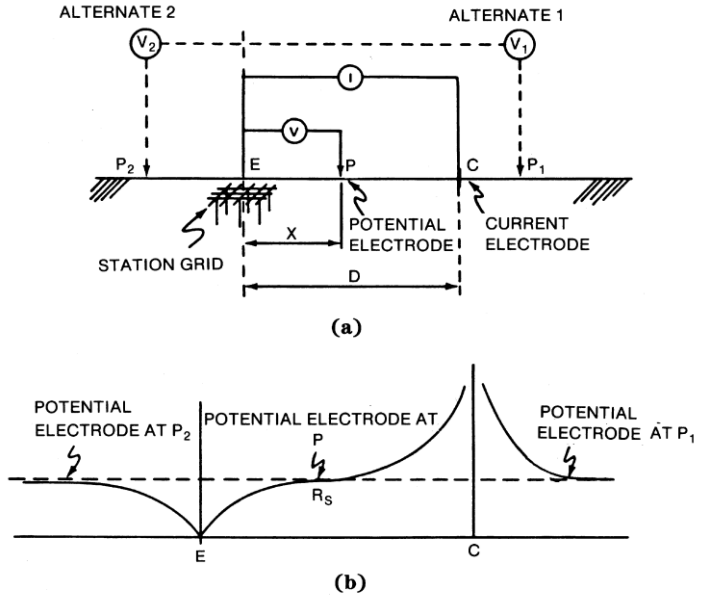

Figure 47—(a) Fall of potential method and (b) Earth surface potentials for various spacings "X"

If the distance D is large enough with respect to the grounding system, the center part of the fall-of-potential curve tends to be nearly horizontal, but it may appear to do so also because of lack of sensitivity of the instruments used. It is usually accepted, although not always correctly, that the nearly horizontal section of the curve gives the resistance R_g. For large grounding systems, large distances D may not be practical or even possible, and as a result the nearly horizontal section of the curve will not exist. In this case, accurate measurements will not be obtained unless one has already a good idea of the exact probe position P. In other cases with non-homogeneous soil, the appropriate probe P position cannot be determined by simple observation of the shape of the curve. Rather, a computer simulation of the grounding system and test circuit needs to be performed to predict the appropriate probe P position.

For measuring resistance, the current source is connected between the substation ground mat E and a current electrode located at a distance of several hundred meters from the substation. The potential-measuring circuit is then connected between the substation mat E and a potential electrode P, with measurements being made at various locations of the electrode outside the substation. This potential electrode may be moved toward the current electrode in equal increments of distance and the resistance readings obtained at the various locations may be plotted against distance from the substation. The resulting graph should resemble curve EPC of Figure 47(b). From E to P, the voltage per ampere of test current rises, but the voltage gradient decreases reaching a minimum at P. Continuing toward C, the effect of current converging on the current test probe becomes apparent and a rising voltage gradient is observed as the current probe is approached. The slowly rising, nearly horizontal portion of the graph, if any, is deemed to represents a zone where the interaction of the tested and return electrodes is small. When the return electrode is placed at a finite distance from the grounding system and the potential probe is driven at a specific location, then an accurate measurement of the resistance is obtained. Unfortunately, the exact location of the potential electrode is well defined only for some ideal cases such as hemispherical or very small electrodes buried in uniform or two-layer soils (Dawalibi and Mukhedkar [B40][B45]). The case of a large grounding system buried in uniform soil assuming uniform current density distribution in the

Copyright © 2015 IEEE. All rights reserved.
Copyright The Institute of Electrical and Electronics Engineers, Inc.
Provided by IHS under license with IEEE
No reproduction or networking permitted without license from IHS
Order Number: 02120914
Sold to:EGAT [700166108393] - VARRIS.Y@EGAT.CO.TH,
Not for Resale,2016-09-15 03:57:51 UTC

conductors has been analyzed by Curdts [B24] and Tagg [B141][B142][B143]. In practice, however, grounding systems consist of a complex arrangement of vertical ground rods and horizontal conductors, usually buried in non-uniform soils.

For large ground grids the spacing required may not be practical or even possible, especially where the transmission line overhead ground wires and feeder neutrals connected to substation ground effectively extend the area of influence. Consequently, the so-called flat portion of the curve will not be obtained and other methods of interpretation must be used. Previous work has shown that when soil is not uniform and separation is not large compared to ground system dimensions, the 61.8% rule, which corresponds to the so called flat portion of the curve, may no longer apply (Dawalibi and Mukhedkar [B40][B45]). Locations varying from 10% to 90% were found to be quite possible.

It should be noted that placement of the potential probe P at the opposite side with respect to electrode C (that is, at P_2) will always result in a measured apparent resistance smaller than the actual resistance. In addition, when P is located on the same side as electrode C (that is, at P_1), there is a particular location that gives the actual resistance.

The primary advantage of the fall-of-potential method is that the potential and current electrodes may have substantially higher resistance than the ground system being tested without significantly affecting the accuracy of the measurements.

19.2 Field survey of potential contours and touch and step voltages

Actual field tests of step and touch voltages by injecting current into the ground mat can be performed to help confirm safe conditions at the substation. Because of the expense, few utilities are likely to make these tests as a routine practice. If, however, large discrepancies between calculated and measured resistance or known anomalies in the ground resistivities throw doubt on the calculated step and touch voltages, then such tests may be considered. This is especially true when the computed values are close to tolerable limits, and further improvement of the ground to provide a larger safety factor would be difficult or costly.

In such situations, it may be worthwhile to load the grounding system with a test current (preferably in the order of 100 A) and actually take measurements of potential gradients at selected locations throughout the substation and around its perimeter. An EPRI project (EPRI TR-100622 [B64]) included such a field test. The project included comparisons of the field test results with a computer solution. The method of measurement was found to be quite feasible and gives good results (EPRI TR-100622 [B64]; Meliopoulos, Patel, and Cokkonides [B109]; Patel [B123]).

The basic method for such gradient measurements involves passing a test current through the substation ground via a remote current electrode, as in substation ground resistance measurements, and measuring the resulting touch and step voltages. To obtain the potentials existing under actual fault conditions, the test values are multiplied by the ratio of actual ground-fault current to test current. Since the potentials of interest are those existing at the surface of the earth, the potential probe used is of a type that makes a surface contact.

The relatively high contact resistances involved generally rule out the use of instruments designed for ground resistance measurements since they operate over a limited range of potential probe resistance. To use a voltmeter-ammeter method, it is usually necessary to have a high-impedance voltmeter, and use test currents high enough to overcome the effects of residual ground currents.

Several methods of measuring and recording voltages may be used. Using a high-impedance voltmeter, profiles and contours of open-circuit contact voltages may be plotted for the entire substation. By assuming suitably conservative values of body-and-foot-to-ground resistances, and safe body current, the maximum

Copyright © 2015 IEEE. All rights reserved.

Copyright The Institute of Electrical and Electronics Engineers, Inc.
Provided by IHS under license with IEEE
No reproduction or networking permitted without license from IHS

Order Number: 02120914
Sold to:EGAT [700166108393] - VARRIS.Y@EGAT.CO.TH,
Not for Resale,2016-09-15 03:57:51 UTC

safe value to open-circuit contact voltage can be determined and hazardous touch and step voltages can be located on the potential map.

Langer [B99] and Bodier [B16] have described measurement techniques in which the effect of actual contact and body resistances are simulated. The operator wears rubber gloves and rubber-soled boots equipped with metallic-mesh contact surfaces. Voltages between these metal contact surfaces are measured by a high impedance voltmeter shunted by a resistance equal to an assumed value of body resistance and current is measured with a milliammeter. The ratio of shock current to total ground current is thus determined. More recent test and results are described in EPRI TR-100863 [B65].

By including foot-to-earth contact resistances as a part of the test procedure, the effect of variations in surface conductivity is taken into account. Thus, the additional safety factor provided by surface coverings of surface material, pavement, etc., is included in the test results.

Additional information on making field measurements of potentials is available in IEEE Std 81.

19.3 Assessment of field measurements for safe design

With the value for measured resistance available, the maximum GPR can be recalculated. If substantially different from that based on the computed resistance, the precautions taken against transferred potentials may need review.

The measured resistance does not provide a direct means of re-checking the computed step and touch voltages, as these are derived from the resistivity. However, if the difference between the computed and measured substation grid resistance is very large, the resistance or resistivity values may come under suspicion. Each case will have to be judged on its merits to determine whether the discrepancy is such as to warrant further investigation, employment of larger safety factors, or direct measurement of danger voltages or shock currents as described in 19.2.

19.4 Ground grid integrity test

Many times, solid-state relays, telephone equipment, event recorder circuits, or power supply units in the control house get damaged due to a lightning surge or a fault if the substation has a poor grounding system. The ground grid integrity test might be performed following such an event. Evaluation of older ground grids using this test is also common in the utility industry. Sometimes the ground grid integrity test is performed to ensure the integrity before the substation is approved for operation. The integrity test is a necessity to detect any open circuit or isolated structure or equipment in a substation.

A typical test set comprises a variable voltage source (0 V to 35 V, 0 A to 300 A), voltage and current measuring devices, and two test leads. One of the two test leads is connected to a reference ground riser, generally a transformer case ground. The other test lead then connects to the ground riser to be tested. The test consists of flowing 10 A to 300 A (typically) between the connected risers and measuring the voltage drop across the ground circuit including the test leads. The measurement of the current division at the riser being tested using a clamp-on ammeter provides additional data to evaluate the ground path. Keeping the reference riser connected, the second test lead is moved around to test risers at other equipment and structures until the entire substation ground grid is tested. The impedance between the reference point and each test point is computed by dividing the current into the measured voltage drop. Often, a cable tracer is employed to locate the unknown or broken ground conductor. The cable tracer detects the magnetic field produced by the test current and generates an electrical noise, which can be heard through headphones. Absence of the noise is indicative of a broken ground wire, open connection or missing conductor.

Copyright © 2015 IEEE. All rights reserved.

Copyright The Institute of Electrical and Electronics Engineers, Inc.
Provided by IHS under license with IEEE
No reproduction or networking permitted without license from IHS

Order Number: 02120914
Sold to:EGAT [700166108393] - VARRIS.Y@EGAT.CO.TH,
Not for Resale,2016-09-15 03:57:51 UTC

It is necessary to determine the voltage drop of the test leads. This is done by shorting the leads across the test set and measuring the voltage drop by circulating current in the loop. This one-time measurement yields the series impedance of the test leads. To obtain a correct impedance value, the test lead impedance is subtracted from the measured impedance between the risers. Though the integrity test is the most practical and convenient test to perform, its results can only be analyzed subjectively. One way to evaluate a ground grid is to compare the impedance values with each other and determine the test risers, which have abnormally high impedance values. Generally, test points farther away from the reference point should have increasing values of impedance, compared to test points close to the reference point. One can also evaluate a ground grid by comparing the voltage drop with a known reference value (typically 1.5 V/50 ft, for 300 A test current between risers) and determining the weak ties between the risers. However, this rule of thumb might not apply where there is significant overhead metallic structure that could conduct the test current from point to point. Measured current divisions can indicate if there is a high impedance or open path in either direction. More information on integrity testing can be found in Gill [B77] and IEEE Std 81.

19.5 Periodic checks of installed grounding system

Some utilities re-check substation ground resistance periodically after completion of construction. It is also well advised to review the ground system from time to time for possible changes in system conditions that might affect the maximum value of ground current, as well as extensions to the substation itself that might affect the maximum current, the substation ground resistance, or local potential differences. It is suggested that records be kept of the total bus fault current used as the design basis, and periodic checks as system short-circuit current increases.

20. Physical scale models

It often is difficult to draw valid conclusions concerning a general grounding problem solely from actual field data. The lack of consistent results caused by the inability to control the test, such as weather conditions, and other variables affecting the condition of the soil, and difficulties in data collecting, all hamper the ability to run and duplicate tests. Because it is helpful to have verification of theoretical assumptions or computer techniques, or both, scale models have been used to bridge the gap. The use of small models can be used to determine the resistance and potential profiles of ground grid arrangements.

The early scale model tests used water to represent uniform soil. The use of small models in large tanks gave consistent results and enabled various models and conditions to be tested and the effects of different parameters to be observed (Armstrong and Simpkin [B6]).

In the late 1960s, a two-layer laboratory model was developed at École Polytechnique to verify computer techniques. This method used concrete blocks to represent the lower layer of soil (Mukhedkar, Gervais, and Dejean [B114]). A technique later developed by Ohio State University used agar, a gelatin-like substance frequently used in biological studies, to simulate the lower levels of soil. In this project, accurate uniform and two-layer soil models were used to study the effects of many parameters on resistance and surface potentials (EPRI EL-3099 [B62]).

Although model tests have inherit measurement in accuracies, scale models can be effectively used for parametric studies for ground grid design and for verifying computer simulations of ground grid parameters (Sverak, Booream, and Kasten [B138]).

Copyright © 2015 IEEE. All rights reserved.

Copyright The Institute of Electrical and Electronics Engineers, Inc.
Provided by IHS under license with IEEE
No reproduction or networking permitted without license from IHS

Order Number: 02120914
Sold to:EGAT [700166108393] - VARRIS.Y@EGAT.CO.TH,
Not for Resale,2016-09-15 03:57:51 UTC

Annex A

(informative)

Bibliography

Bibliographical references are resources that provide additional or helpful material but do not need to be understood or used to implement this standard. Reference to these resources is made for informational use only.

[B1] ABB Power Systems, Inc., *Electrical Transmission and Distribution Reference Book,* 4th Edition, 12th printing, 1964.

[B2] Abledu, K. O., and Laird, D. N., "Measurement of substation rock resistivity," *IEEE Transaction on Power Delivery,* vol. 7, no. 1, pp. 295–300, Jan. 1992.

[B3] Accredited Standards Committee C2-2012, National Electrical Safety Code® (NESC®).[11, 12]

[B4] AIEE Working Group on Substation Grounding Practices, "Application guide on methods of substation grounding," *AIEE Transactions on Power Apparatus and Systems,* no. 11, pp. 271–278, Apr. 1954.

[B5] Armstrong, H. R., "Grounding electrode characteristics from model tests," *AIEE Transactions on Power Apparatus and Systems,* pp. 1301–1306, Dec. 1953.

[B6] Armstrong, H. R., and Simpkin, L. J., "Grounding electrode potential gradients from model tests," *IEEE Transactions on Power Apparatus and Systems,* pp. 618–623, Oct. 1960.

[B7] Bellaschi, P. L., "Lightning currents in field and laboratory," *AIEE Transactions,* vol. 54, pp. 837–843, 1935.

[B8] Biegelmeier, U. G., "Die Bedeatung der Z-Schwelle des Herzkammerfilim-merns fur die Festlegung von Beruhrunggsspanungs greuzeu bei den Schutzma Bradhmer gegen elektrische Unfate," *E&M,* vol. 93, no. 1, pp. 1–8, 1976.

[B9] Biegelmeier, U. G., and Lee, W. R., "New considerations on the threshold of ventricular fibrillation for AC shocks at 50–60 Hz," *Proceedings of the IEEE,* vol. 127, pp. 103–110, 1980.

[B10] Biegelmeier, U. G., and Rotter, K., "Elektrische Widerstrande und Strome in Merischlicken Korper," *E&M,* vol. 89, pp. 104–109, 1971.

[B11] Blattner, C. J., "Analysis of soil resistivity test methods in two-layer earth," *IEEE Transactions on Power Apparatus and Systems,* vol. PAS-104, no. 12, pp. 3603–3608, Dec. 1985.

[B12] Blattner, C. J., "Prediction of soil resistivity and ground rod resistance for deep ground electrodes," *IEEE Transactions on Power Apparatus and Systems,* vol. PAS-99, no. 5, pp. 1758–1763, Sept/Oct. 1980.

[B13] Blattner, C. J., "Study of driven ground rods and four point soil resistivity data," *IEEE Transactions on Power Apparatus and Systems,* vol. PAS 101, no. 8, pp. 2837–2850, Aug. 1982.

[B14] Blattner, C. J., and Dawalibi, F., "Earth resistivity measurement interpretation techniques," *IEEE Transactions on Power Apparatus and Systems,* vol. PAS 103, no. 2, pp. 374–382, Feb. 1984.

[B15] Bodier, M. G., "La Secrites des Personnes et la Question des Mises a la Terre dans les Postes de Distribution," *Bulletin de la Societé Francaise des Electriciens,* ser. 6th, vol. VII, no. 74, pp. 545–562, Oct. 1947.

[B16] Bodier, M. G., "Systematic investigation of potential gradients in and around a transformation substation," *Bulletin de la Societe Francaise des Electriciens,* July 1951.

[11] National Electrical Safety Code and NESC are both registered trademarks and service marks of The Institute of Electrical and Electronics Engineers, Inc.
[12] The NESC is available from The Institute of Electrical and Electronics Engineers at http://standards.ieee.org/.

Copyright © 2015 IEEE. All rights reserved.

Copyright The Institute of Electrical and Electronics Engineers, Inc.
Provided by IHS under license with IEEE
No reproduction or networking permitted without license from IHS

Order Number: 02120914
Sold to:EGAT [700166108393] - VARRIS.Y@EGAT.CO.TH,
Not for Resale,2016-09-15 03:57:51 UTC

[B17] Bogajewski, W., Dawalibi, F., Gervais, Y., and Mukhedkar, D., "Effects of sustained ground fault current on concrete poles," *IEEE Transactions on Power Apparatus and Systems,* vol. PAS-101, no. 8, pp. 2686–2693, Aug. 1982.

[B18] Carson, J. R., "Wave propagation in overhead wires with ground return," *Bell Systems Technical Journal,* vol. 5, 1926.

[B19] CIGRÉ Working Group 33/13-09, "Very fast phenomena associated with gas-insulated substations," 1988 Session of CIGRÉ, paper 33-13, 1988.

[B20] Clem, J. E., "Reactance of transmission lines with ground return," *AIEE Transactions on Power Apparatus and Systems,* vol. PAS-50, pp. 901–918, Sept. 1931.

[B21] "Computation of zero sequence impedances of power lines and cables," *Engineering Report no 37,* Joint Subcommittee on Development and Research of EEI and Bell Telephone Systems, July 22, 1936.

[B22] Conversion Subcommittee of AIEE Substations Committee, "Recommended grounding practices for single polarity DC structures," Paper no. 57-719, *AIEE Transactions on Power Apparatus and Systems,* vol. 76, part III, 1957.

[B23] Crawford, E., and Griffith, M., "A closer look at 'The facts of life' in ground mat design," *IEEE Transactions an Industry Applications,* vol. IA-15, no. 3, pp. 241–250, May/June 1979.

[B24] Curdts, E. B., "Some of the fundamental aspects of ground resistance measurements," *AIEE Transaction on Power Apparatus and Systems,* Part I, vol. 77, pp. 767–770, Nov. 1958.

[B25] "Currents in earth wires at the top of pylons and their effect on the potentials of the pylons and stations in the neighborhood of a point of short-circuit to earth," Contribution no. 78, CCITT, Study Group V, Nov. 1963.

[B26] Dalziel, C. F., "A study of the hazards of impulse currents," *AIEE Transactions on Power Apparatus and Systems,* vol. 72, part III, pp. 1032–1043, Oct. 1953.

[B27] Dalziel, C. F., "Dangerous electric currents," *AIEE Transactions on Power Apparatus and Systems,* vol. 65, pp. 579–585, 1123–1124, 1946.

[B28] Dalziel, C. F., "Effect of wave form on let-go currents," *AIEE Transactions on Power Apparatus and Systems,* vol. 62, pp. 739–744, 1943.

[B29] Dalziel, C. F., "Electric shock hazard," *IEEE Spectrum,* pp. 41–50, Feb. 1972.

[B30] Dalziel, C. F., "Temporary paralysis following freezing to a wire," *AIEE Transactions on Power Apparatus and Systems,* vol. 79, part III, pp. 174–175, 1960.

[B31] Dalziel, C. F., "Threshold 60-cycle fibrillating currents," *AIEE Transactions on Power Apparatus and Systems,* vol. 79, part III, pp. 667–673, 1960.

[B32] Dalziel, C. F., and Lee, W. R., "Lethal electric currents," *IEEE Spectrum,* pp. 44–50, Feb. 1969.

[B33] Dalziel, C. F., and Lee, W. R., "Reevaluation of lethal electric currents," *IEEE Transactions on Industry and General Applications,* vol. IGA-4, no. 5, pp. 467–476, Oct. 1968.

[B34] Dalziel, C. F., and Mansfield, T. H., "Effect of frequency on perception currents," *AIEE Transactions on Power Apparatus and Systems,* vol. 69, pp. 1161–1168, 1950.

[B35] Dalziel, C. F., and Massogilia, F. P., "Let-go currents and voltages," *AIEE Transactions on Power Apparatus and Systems,* vol. 75, part II, pp. 49–56, 1956.

[B36] Dalziel, C. F., Lagen, J. B., and Thurston, J. L., "Electric shock," *AIEE Transactions on Power Apparatus and Systems,* vol. 60, pp. 1073–1079, 1941.

[B37] Dalziel, C. F., Ogden, E., and Abbott, C. E., "Effect of frequency on let-go currents," *AIEE Transactions on Power Apparatus and Systems,* vol. 62, pp. 745–750 and 1000, Dec. 1943.

[B38] Dawalibi, F., "Ground fault current distribution between soil and neutral conductors," *IEEE Transactions on Power Apparatus and Systems,* vol. PAS-99, no. 2, pp. 452–461, Mar./Apr. 1980.

Copyright © 2015 IEEE. All rights reserved.

Copyright The Institute of Electrical and Electronics Engineers, Inc.
Provided by IHS under license with IEEE
No reproduction or networking permitted without license from IHS

Order Number: 02120914
Sold to:EGAT [700166108393] - VARRIS.Y@EGAT.CO.TH,
Not for Resale,2016-09-15 03:57:51 UTC

[B39] Dawalibi, F. P., and Barbeito, N., "Measurements and computations of the performance of grounding systems buried in multilayer soils," *IEEE Transactions on Power Delivery,* vol. 6, no. 4, pp. 1483–1490, Oct. 1992.

[B40] Dawalibi F. P., and Mukhedkar, D., "Ground electrode resistance measurements in non-uniform soils," *IEEE Transactions on Power Apparatus and Systems,* vol. PAS-93, no.1, pp. 109–116, Jan. 1974.

[B41] Dawalibi, F. P., and Mukhedkar, D., "Ground fault current distribution in power systems—The necessary link," Abstract A77 754-5, *Transactions on Power Apparatus and Systems,* vol. PAS-97, no. 2, pp. 332–333, Mar./Apr. 1978.

[B42] Dawalibi, F. P., and Mukhedkar, D., "Influence of ground rods on grounding systems," *IEEE Transactions on Power Apparatus and Systems,* vol. PAS-98, no. 6, pp. 2089–2098, Nov./Dec. 1979.

[B43] Dawalibi, F. P., and Mukhedkar, D., "Optimum design of substation grounding in two-layer earth structure; Part I—Analytical study, Part II—Comparison between theoretical and experimental results, and Part III—Study of grounding grids performance and new electrodes configuration," *IEEE Transactions on Power Apparatus and Systems,* vol. PAS-94, no. 2, pp. 252–261, 262–266, 267–272, Mar./Apr. 1975.

[B44] Dawalibi, F. P., and Mukhedkar, D., "Parametric analysis of grounding systems," *IEEE Transactions on Power Apparatus and Systems,* vol. PAS-98, no. 5, pp. 1659–1668, Sept./Oct. 1979.

[B45] Dawalibi F. P., and Mukhedkar, D., "Resistance measurement of large grounding systems," *IEEE Transactions on Power Apparatus and Systems,* vol. PAS-98, no. 6, pp. 2348–2354, Nov./Dec. 1979.

[B46] Dawalibi, F. P., Bauchard, M., and Mukhedkar, D., "Survey on power system grounding design practices," *IEEE Transactions on Power Apparatus and Systems,* vol. PAS-99, no. 4, pp. 1396–1405, July/Aug. 1980.

[B47] Dawalibi, F. P., Ma, J., and Southey, R. D., "Behavior of grounding systems in multilayer soils: A parametric analysis," *IEEE Transaction on Power Delivery,* vol. 9, no. 1, pp. 334–342, Jan. 1994.

[B48] Dawalibi, F. P., Ma, J., and Southey, R. D., "Equivalence of uniform and two-layer soils to multilayer soils in the analysis of grounding systems," *IEE Proceedings—Generation, Transmission, Distribution,* vol. 143, no. 1, pp. 49–55, Jan. 1996.

[B49] Dawalibi, F. P., Mukhedkar, D., and Bensted, D., "Soil effects on ground fault currents," *IEEE Transactions on Power Apparatus and Systems,* vol. PAS-100, pp. 3442, July 1982.

[B50] Dawalibi, F. P., Southey, R. D, and Baishiki, R. S., "Validity of conventional approaches for calculating body currents resulting from electric shocks," *IEEE Transactions on Power Delivery,* vol. 5, no. 2, pp. 613–626, 1990.

[B51] Dawalibi, F. P., Xiong, W., and Ma, J., "Effects of deteriorated and contaminated substation surface covering layers on foot resistance calculations," *IEEE Transactions on Power Delivery,* vol. 8, no. 1, pp. 104–113, Jan. 1993.

[B52] Desieno, C. F., Marchenko, P. P., and Vassel, G. S., "General equations for fault currents in transmission line ground wires," *IEEE Transactions on Power Apparatus and Systems,* vol. PAS-89, pp. 1891–1900, Nov./Dec. 1970.

[B53] Dick, E. P., Fujimoto, N., Ford, G. L., and Harvey, S., "Transient ground potential rise in gas-insulated substations—Problem identification and mitigation," *IEEE Transactions on Power Apparatus and Systems,* vol. PAS 101, no. 10, pp. 3610–3619, Oct. 1982.

[B54] Dick, W. K., and Holliday, H. R., "Impulse and alternating current tests on grounding electrodes in soil environment," *IEEE Transactions on Power Apparatus and Systems,* vol. PAS-97, no. 1, pp. 102–108, Jan./Feb. 1978.

[B55] Elek, A., "Hazards of electric shock at stations during fault and method of reduction," *Ontario Hydro Research News,* vol. 10, no. 1, pp. 1–6, 1958.

[B56] Endrenyi, J., "Analysis of transmission tower potentials during ground faults," *IEEE Transactions on Power Apparatus and Systems,* vol. PAS-86, pp. 1274–1283, Oct. 1967.

Copyright © 2015 IEEE. All rights reserved.

Copyright The Institute of Electrical and Electronics Engineers, Inc.
Provided by IHS under license with IEEE
No reproduction or networking permitted without license from IHS

Order Number: 02120914
Sold to:EGAT [700166108393] - VARRIS.Y@EGAT.CO.TH,
Not for Resale,2016-09-15 03:57:51 UTC

[B57] Endrenyi, J., "Evaluation of resistivity test for design of station grounds in non-uniform soil," *IEEE Transactions on Power Apparatus and Systems,* vol. 84, pp. 996–970, Dec. 1963.

[B58] Endrenyi, J., "Fault current analysis for substation grounding design," *Ontario Hydro Research Quarterly,* 2nd Quarter, 1967.

[B59] EPRI, *EPRI transmission line reference book 345 kV and above,* Electric Power Research Institute, Palo Alto, Calif., 1975.

[B60] EPRI EL-904, *Mutual design considerations for overhead AC transmission lines and gas transmission pipelines,* vols. 1 and 2, Sept. 1978.

[B61] EPRI EL-2699, *Transmission line grounding,* Chapter 4, (Resistivity) and Chapter 9 (Field Measurement Techniques), Safe Engineering Services, Oct. 1982.

[B62] EPRI EL-3099, *Substation grounding scale model tests,* Ohio State University, May 1983.

[B63] EPRI EL-3982, *Soil resistivity tests using modeling techniques,* Ohio State University, May 1985.

[B64] EPRI TR-100622, *Substation grounding programs,* vols. 1–5, May 1992.

[B65] EPRI TR-100863, *Seasonal variations of grounding parameters by field tests,* SEI/Georgia Power Research Center, July 1992.

[B66] Fagan, E. J., and Lee, R. H., "The use of concrete-enclosed reinforcing rods as grounding electrodes," *IEEE Transactions on Industry and General Applications,* vol. IGA-6, no. 4, pp. 337–348, July/Aug. 1970.

[B67] Ferris, L. P., King, B. G., Spence, P. W., and Williams, H., "Effect of electric shock on the heart," *AIEE Transactions on Power Apparatus and Systems,* vol. 55, pp. 498–515 and 1263, May 1936.

[B68] Ford, G. L., and Geddes, L. A., "Transient ground potential rise in gas-insulated substations—Assessment of shock hazard," *IEEE Transactions on Power Apparatus and Systems,* vol. PAS-101, no. 10, pp. 3620–3629, Oct. 1982.

[B69] Fujimoto, N., Croall, S. J., and Foty, S. M., "Techniques for the protection of gas-insulated substation to cable interfaces," *IEEE Transactions on Power Delivery,* vol. 3, no. 4, pp. 1650–1655, Oct. 1988.

[B70] Fujimoto, N., Dick, E. P., Boggs, S. A., and Ford, G. L, "Transient ground potential rise in gas-insulated substations: Experimental studies," *IEEE Transactions on Power Apparatus and Systems,* vol. PAS101, no. 10, pp. 3603–3609, Oct. 1982.

[B71] Garrett, D. L., "Determination of maximum ground fault current through substation grounding system considering effects of static wires and feeder neutrals," *Proceedings of Southeastern Electric Exchange,* Atlanta, Ga., 1981.

[B72] Garrett, D. L., and Holley, H. J., "Calculation of substation ground resistance using matrix techniques," *IEEE Transactions on Power Apparatus and Systems,* vol. PAS-99, no. 5, pp. 2008–2011, Sept./Oct. 1980.

[B73] Garrett, D. L., and Wallace, K. A., "A critical analysis of grounding practices for railroad tracks in electric utility substations," *IEEE Transactions on Power Delivery,* vol. 8, no. 1, pp. 90–96, Jan., 1993.

[B74] Garrett, D. L., Meyers, J., and Patel, S., "Determination of maximum substation grounding system fault current using graphical analysis," *IEEE Transactions on Power Delivery,* vol. POWRD-2, no. 3, pp. 725–732, July 1987.

[B75] Geddes, L. A., and Baker, L. E., "Response of passage of electric current through the body," *Journal of Association for the Advancement of Medical Instruments,* vol. 2, pp. 13–18, Feb. 1971.

[B76] Gieiges, K. S., "Electric shock hazard analysis," *AIEE Transactions on Power Apparatus and Systems,* vol. 75, part III, pp. 1329–1331, 1956.

Copyright © 2015 IEEE. All rights reserved.

Copyright The Institute of Electrical and Electronics Engineers, Inc.
Provided by IHS under license with IEEE
No reproduction or networking permitted without license from IHS

Order Number: 02120914
Sold to:EGAT [700166108393] - VARRIS.Y@EGAT.CO.TH,
Not for Resale,2016-09-15 03:57:51 UTC

[B77] Gill, A. S., "High-current method of testing ground grid integrity," *NETA WORLD,* International Testing Association, vol. 10, no. 2, Winter 1988–1989.

[B78] Graybill, H. W., Koehler, H. C., Nadkarni, J. D., and Nicholas, J. H., "Termination of high-pressure oil cables in gas-insulated minisubstation equipment," *IEEE Transactions on Power Apparatus and Systems,* vol. PAS-93, no. 5, pp. 1669–1674, Sept./Oct. 1974.

[B79] Hammond, E., and Robson, T. D., "Comparison of electrical properties of various cements and concretes," *The Engineer,* 199, no. 5165, pp. 78–80, Jan. 1955.

[B80] Harvey, S. M., "Control wiring transients and electromagnetic compatibility in GIS," in S. A. Boggs, F. Y. Chu, and Fujimoto, N., eds., *Gas-insulated substations—Technology & practice,* New York: Pergamon Press, 1986.

[B81] Heppe, R. J., "Computation of potential at surface above an energized grid or other electrode, allowing for nonuniform current distribution," *IEEE Transactions on Power Apparatus and Systems,* vol. PAS-98, no. 6, pp. 1978–1989, Nov./Dec. 1979.

[B82] Heppe, R. J., "Step potentials and body currents for near grounds in two-layer earth," *IEEE Transactions on Power Apparatus and Systems,* vol. PAS-98, no. 1, pp. 45–59, Jan./Feb. 1979.

[B83] IEC 60479-1 (1994-09), Effect of current passing through human body—Part I: General aspects.

[B84] IEC 60479-2 (1987-03), Effect of current passing through human body—Part II: Special aspects.

[B85] IEEE Std C37.010™-1979, IEEE Application Guide for AC High-Voltage Circuit Breakers Rated on a Symmetrical Current Basis.[13]

[B86] IEEE Std 142™-1991, IEEE Recommended Practice for Grounding of Industrial and Commercial Power Systems (IEEE Green Book).

[B87] IEEE Std 525™-1992 (Reaff 1999), IEEE Guide for the Design and Installation of Cable Systems in Substations.

[B88] IEEE Std 590™-1992, IEEE Cable Plowing Guide.[14]

[B89] IEEE Std 837™-1989 (Reaff 1996), IEEE Standard for Qualifying Permanent Connections Used in Substation Grounding.

[B90] IEEE Tutorial Course 86 EH0253-5-PWR, "Practical Applications of ANSI/IEEE Standard 80-1986, IEEE Guide for Safety, Chapter 2, (Soil Resistivity Analysis)."

[B91] IEEE Working Group on Electrostatic Effects of Transmission Lines, General Systems Subcommittee, "Electrostatic effects of overhead transmission lines, Part I—Hazards and effects," *IEEE Transactions on Power Apparatus and Systems,* vol. PAS-91, pp. 422–426, Mar./Apr. 1972.

[B92] Jackson, J. D., *Classical electrodynamics,* New York: John Wiley & Sons, Inc., 1975.

[B93] Jones, W. R., "Bentonite rods assure ground rod installation in problem soils," *IEEE Transactions on Power Apparatus,* vol. PAS-99, no. 4, pp. 1343–1346, July/Aug. 1980.

[B94] Joy, E. B., Meliopoulos, A. P., and Webb, R. P., "Touch and step calculations for substation grounding systems," Abstract Paper A 79-052-2, *IEEE Transactions on Power Apparatus and Systems,* vol. PAS 98, no. 4, pp. 1143, July/Aug. 1979.

[B95] Kercel, S. W., "Design of switchyard grounding systems using multiple grids," *IEEE Transactions on Power Apparatus and Systems,* vol. PAS-100, no. 3, pp. 1341–1350, Mar. 1981.

[B96] Kinyon, A. L., "Earth resistivity measurements for grounding grids," *AIEE Transactions on Power Apparatus and Systems,* vol. 20, pp. 795–800, Dec. 1961.

[13] IEEE publications are available from The Institute of Electrical and Electronics Engineers (http://standards.ieee.org/).
[14] IEEE Std 590-1992 has been withdrawn; however, copies can be obtained from Global Engineering, 15 Inverness Way East, Englewood, CO 80112-5704, USA, tel. (303) 792-2181 (http://global.ihs.com/).

Copyright © 2015 IEEE. All rights reserved.

Copyright The Institute of Electrical and Electronics Engineers, Inc.
Provided by IHS under license with IEEE
No reproduction or networking permitted without license from IHS

Order Number: 02120914
Sold to:EGAT [700166108393] - VARRIS.Y@EGAT.CO.TH,
Not for Resale,2016-09-15 03:57:51 UTC

[B97] Kiselev, "Research into electric shock," *Electrical Review,* vol. 31, Dec. 1965.

[B98] Kouwenhoven, W. B., et al., "AC shocks of varying parameters affecting the heart," *AIEE Transactions on Power Apparatus and Systems,* vol. 78, part I, pp. 163–169, 1959.

[B99] Langer, H., "Messungen von Erderspannungen in einem 220 kV Umspanwerk," *Electrotechnische Zietschrift,* vol. 75, no. 4, pp 97–105, Feb. 1954 (English translation available in AIEE No. 80-1961, Appendix V, pp. 91–102).

[B100] Laurent, P. G., "Les Bases Generales de la Technique des Mises a la Terre dans les Installations Electriques," *Bulletin de la Societe Francaise des Electriciens,* vol. 1, ser. 7, pp. 368–402, July 1951.

[B101] Lazzara, J., and Barbeito, N., "Simplified two-layer model substation ground grid design methodology," *IEEE Transactions on Power Delivery,* vol. 5, no. 4, pp. 1741–1750, Nov. 1990.

[B102] Lee, W. R., "Death from electrical shock," *Proceedings of the IEEE,* vol. 113, no. 1, pp. 144–148, Jan. 1966.

[B103] Loucks, W. W., "A new approach to substation grounding," *Electrical News and Engineering,* May 15, 1954.

[B104] Mahonar, V. N., and Nagar, R. P., "Design of steel earthing grids in India," *IEEE Transactions on Power Apparatus and System,* vol. PAS-98, no. 6, pp. 2126–2134, Nov./Dec. 1979.

[B105] *Manual on ground resistance testing,* Publication no. 25-J, James G. Biddle Co., 1970.

[B106] Meliopoulos, A. P., and Papelexopoulos, A. D., "Interpretations of soil resistivity measurement experience with the model SOMIP," *IEEE Transactions on Power Apparatus and Systems,* vol. PAS-1, no. 4, pp. 142–151, Oct. 1986.

[B107] Meliopoulos, A. P., Papalexopoulos, A., and Webb, R. P., "Current division in substation grounding system," *Proceedings of the 1982 Protective Relaying Conference,* Georgia Institute of Technology, Atlanta, Ga., May 1982.

[B108] Meliopoulos, A. P., Papelexopoulos, A. D., Webb, R., and Blattner, C. J., "Estimation of soil parameters from driven-rod measurements," *IEEE Transactions on Power Delivery,* vol. 103, no. 9, Sept. 1994.

[B109] Meliopoulos, A. P., Patel, S., and Cokkonides, G. J., "A new method and instrument for touch and step voltage measurements," *IEEE Transactions on Power Delivery,* vol. 9., no. 4, pp. 1850–1860, Oct. 1994.

[B110] Meliopoulos, A. P., Xia, F., Joy, E. B., Cokkonides, G. J., "An advanced computer model for grounding system analysis," *IEEE Transactions on Power Delivery,* vol. 8, no. 1, pp. 13–23, Jan. 1993.

[B111] Miller, Hart, and Brown, "Stray current and galvanic corrosion of reinforced steel in concrete," *Material Performance,* vol. 15, no. 5, pp. 20–27, May 1976.

[B112] Mitani, H., "Magnitude and frequency of transient induced voltage in low-voltage control circuits of power stations and substations," *IEEE Transactions on Power Apparatus and Systems,* vol. PAS-99, no. 5, pp. 555–570, Sept./Oct. 1980.

[B113] Moore, R., "An empirical method of interpretation of earth resistivity measurements," *American Institute of Mining Engineering,* Column 164, pp. 197–231, 1945.

[B114] Mukhedkar, D., Gervais, Y., and Dejean, J. P., "Modeling a grounding electrode," *IEEE Transactions on Power Apparatus and System,* vol. PAS-92, no. 1, pp. 295–297, Jan. 1973.

[B115] Nahman, J. M., and Salamon, D. D., "A practical method for the interpretation of earth resistivity data obtained from driven rod tests," *IEEE Transactions on Power Apparatus and Systems,* vol. 3, no. 4, pp. 1375–1379, Oct. 1988.

[B116] Nahman, J. M., and Salamon, D. D., "Analytical expressions for the resistance of grounding grids in nonuniform soil," *IEEE Transactions on Power Apparatus and Systems,* vol. PAS-103, pp. 880–885, Apr. 1984.

Copyright © 2015 IEEE. All rights reserved.

Copyright The Institute of Electrical and Electronics Engineers, Inc.
Provided by IHS under license with IEEE
No reproduction or networking permitted without license from IHS

Order Number: 02120914
Sold to:EGAT [700166108393] - VARRIS.Y@EGAT.CO.TH,
Not for Resale,2016-09-15 03:57:51 UTC

[B117] Nahman, J. M., and Salamon, D. D., "Analytical expressions for the resistance of rodbeds and of combined grounding system in nonuniform soil," *IEEE Transactions on Power Apparatus and Systems,* vol. PWRD-1, no. 3, pp. 90–96, July 1986.

[B118] Nieman, J., "Unstellung von Hochstspannungs-Erdungsalagen Aufden Betrieb Mit Starr Geerdetem Sternpunkt," *Electrotechnische Zeitschrift,* vol. 73, no. 10, pp. 333–337, May 1952.

[B119] Ollendorff, F., *Erdstrome (Ground currents),* Stuttgart, Germany: Springer-Verlag, 1928; Burkhauser-Verlag-Baselund, 1969.

[B120] Orellara, E., and Mooney, H. M., "Two and three layer master curves and auxiliary point diagrams for vertical electrical sounding using Wenner arrangement," *Interciencia,* Madrid, Spain, 1972.

[B121] Osypka, P., "Quantitative investigation of current strength and routing in AC electrocution accident involving human beings and animals," *Technische Hochschule Braunschweig,* Brunswick, West Germany, 1966/SLA Translation Center TT-6611470.

[B122] Palmer, L. S., "Examples of geotechnical surveys," *Proceedings of the IEE,* Paper 2791-M, vol. 106, pp. 231–244, June 1959.

[B123] Patel, S. G., "A complete field analysis of substation ground grid by applying continuous low voltage fault," *IEEE Transactions on Power Apparatus and Systems,* vol. PAS-104, no. 8, pp. 2238–2243, Aug. 1985.

[B124] Patel, S. G., Hildreth, J. and Garrett, L., "Protection of electronic equipment in a substation environment," *Power Engineering Society Summer Meeting,* vol. 1, pp. 207–211. 2002.

[B125] Purdy, A. B., "Accurate equations for the characteristics of rod electrodes in a homogeneous medium," Abstract A 79-027-4, *IEEE Transactions on Power Apparatus and Systems,* vol. 98, no. 4, pp. 1141, July/Aug. 1979.

[B126] Reichman, J., Vainberg, M., and Kuffel, J., "Short-circuit capacity of temporary grounding cables," *IEEE Transactions on Power Delivery,* vol. 4, no. 1, pp. 260–271, Jan. 1989.

[B127] Roman, I., "Some interpretations of earth resistivity data," *American Institute of Mining and Metallurgical Engineering,* vol. 110, pp. 183–200, 1934.

[B128] Rosa, E. B., McCollum, B., and Peters, O. S., "Electrolysis in concrete," *Department of Commerce, Technical Paper of Bureau of Standards,* no. 18, pp. 1–137, Mar. 1913.

[B129] Rüdenberg, R., "Basic considerations concerning systems," *Electrotechnische Zeitschrift,* vols. 11 and 12, 1926.

[B130] Rüdenberg, R., "Distribution of short-circuit currents in ground," *Electrotechnische Zeitschrift,* vol. 31, 1921.

[B131] Rüdenberg, R., "Grounding principles and practices—Part 1, Fundamental considerations on grounding currents," *Electrical Engineering,* vol. 64, no. 1, pp. 1–13, Jan. 1945.

[B132] Schwarz, S. J., "Analytical expression for resistance of grounding systems," *AIEE Transactions on Power Apparatus and Systems,* vol. 73, no. 13, part III-B, pp. 1011–1016, Aug. 1954.

[B133] Sebo, S. A., "Zero sequence current distribution along transmission lines," *IEEE Transactions on Power Apparatus and Systems,* vol. PAS-88, pp. 910–919, June 1969.

[B134] Sunde, E. D., *Earth conduction effects in transmission systems,* New York: McMillan, 1968.

[B135] Sverak, J. G., "Optimized grounding grid design using variable spacing technique," *IEEE Transactions on Power Apparatus and Systems,* vol. PAS-95, no. 1, pp. 362–374, Jan./Feb. 1976.

[B136] Sverak, J. G., "Simplified analysis of electrical gradients above a ground grid; Part I—How good is the present IEEE method?" *IEEE Transactions on Power Apparatus and Systems,* vol. PAS-103, no. 1, pp. 7–25, Jan. 1984.

Copyright © 2015 IEEE. All rights reserved.

Copyright The Institute of Electrical and Electronics Engineers, Inc.
Provided by IHS under license with IEEE
No reproduction or networking permitted without license from IHS

Order Number: 02120914
Sold to:EGAT [700166108393] - VARRIS.Y@EGAT.CO.TH,
Not for Resale,2016-09-15 03:57:51 UTC

[B137] Sverak, J. G., "Sizing of ground conductors against fusing," *IEEE Transactions on Power Apparatus and Systems,* vol. PAS-100, no. 1, pp. 51–59, Jan. 1981.

[B138] Sverak, J. G., Booraem, C. H., and Kasten, D. G., "Post-design analysis and scale model tests for a two grid earthing system serving the 345 kV GIS facilities at Seabrook Power Plant," Paper 410-06, *Proceedings of the CIGRÉ Symposium on High Currents in Power Systems Under Normal, Emergency and Fault Conditions,* Brussels, June 3–5, 1985.

[B139] Tagg, G. F., *Earth resistances,* New York: Pitman, 1964.

[B140] Tagg, G. F., "Interpretation of resistivity measurements," *American Institute of Mining and Metallurgical Engineering Transactions,* vol. 110, pp. 135–147, 1934.

[B141] Tagg, G. F., "Measurement of earth-electrode resistance with particular reference to earth-electrode systems covering large area," *Proceedings of IEE,* vol. 111, no. 12, pp. 2118–2130, 1964.

[B142] Tagg, G. F., "Measurement of the resistance of an earth-electrode system covering large area," *Proceedings of IEE,* vol. 116, no. 3, pp. 475–479, Mar. 1969.

[B143] Tagg, G. F., "Measurement of the resistance of physically large earth-electrode systems," *Proceedings of IEE,* vol. 117, no. 11, pp. 2185–2190, Nov. 1970.

[B144] Thapar, B., and Gerez, V., "Equivalent resistivity of non-uniform soil for grounding design," *IEEE Transactions on Power Delivery,* vol. 10, no. 2, pp. 759–767, Apr. 1995.

[B145] Thapar, B., and Gross, E. T. B., "Grounding grids for high voltage stations—Part IV: Resistance of grounding grids in nonuniform soil," *IEEE Transactions on Power Apparatus and Systems,* vol. PAS-82, pp. 782–788, Oct. 1963.

[B146] Thapar, B., Gerez, V., and Emmanuel, P., "Ground resistance of the foot in substation yards," *IEEE Transactions on Power Delivery,* vol. 8, no. 1, pp. 1–6, Jan. 1993.

[B147] Thapar, B., Gerez, V., and Kejriwal, H., "Reduction factor for the ground resistance of the foot in substation yards," *IEEE Transactions on Power Delivery,* vol. 9, no. 1, pp. 360–368, Jan. 1994.

[B148] Thapar, B., Gerez, V., Balakrishnan, A., and Blank, D., "Simplified equations for mesh and step voltages in an AC substation," *IEEE Transactions on Power Delivery,* vol. 6, no. 2, pp. 601–607, Apr. 1991.

[B149] Thompson, P., "Resistivity tests on electric station ground coverings," Internal Report, Los Angeles Department of Water and Power, July 12, 1983.

[B150] Thompson, P., "Resistivity tests on soil and concrete," Internal Report, Los Angeles Department of Water and Power, Aug. 8, 1977.

[B151] Towne, H. M., "Lightning arrester grounds—Parts I, II, and III," *General Electric Review,* vol. 35, pp. 173–280, Mar.–May 1932.

[B152] Verma, R., Merand, A., and Barbeau, P., "Design of low resistance grounding system for hydroelectric plant located on highly resistive soils," *IEEE Transactions on Power Apparatus and Systems,* vol. PAS-97, no. 5, pp. 1760–1768, Sept./Oct. 1978.

[B153] Verma, R., and Mukhedkar, D., "Ground fault current distribution in substation, towers and ground wire," *IEEE Transactions on Power Apparatus and Systems,* vol. PAS-98, pp. 724–730, May/June 1979.

[B154] Wenner, F., "A method of measuring earth resistances," *Bulletin of the Bureau of Standards,* Report no 258, vol. 12, no. 3, pp. 469–482, Feb. 1916.

[B155] Yu, L., "Determination of induced currents and voltages in earth wires during faults," *Proceedings of IEE,* vol. 120, no. 6, pp. 689–692, June 1973.

[B156] Zaborszky, J., "Efficiency of grounding grids with nonuniform soil," *AIEE Transactions on Power Apparatus and Systems,* vol. 74, pp. 1230–1233, Dec. 1955.

Copyright © 2015 IEEE. All rights reserved.

Copyright The Institute of Electrical and Electronics Engineers, Inc.
Provided by IHS under license with IEEE
No reproduction or networking permitted without license from IHS

Order Number: 02120914
Sold to:EGAT [700166108393] - VARRIS.Y@EGAT.CO.TH,
Not for Resale,2016-09-15 03:57:51 UTC

Annex B

(informative)

Sample calculations

This annex illustrates the application of equations, tables, and graphs for designing a substation grounding system. The specific objectives are as follows:

a) To show the application of principal equations of this guide for several refinements of the design concept toward a satisfactory final design solution.

b) To illustrate the typical differences to be expected between results obtained using the simplified calculations of this guide and the more rigorous computer solutions.

c) To illustrate such design conditions for which the use of simplified calculations of this guide would not be appropriate for a safe design, as some of the equations may only be used with caution.

In view of these objectives, the following series of examples (B.1 through B.4) neither represents, nor is intended to be, the best or most efficient way to design a grounding system.

A computer-based grounding program described in EPRI TR-100622 [B64] was used to model the grids in these examples.

For the series of examples (B.1 through B.4), the design data are as follows:

— Fault duration $t_f = 0.5$ s

— Positive sequence equivalent system impedance $Z_1 = 4.0 + j10.0\ \Omega$ (115 kV side)

— Zero sequence equivalent system impedance $Z_0 = 10.0 + j40.0\ \Omega$ (115 kV side)

— Current division factor $S_f = 0.6$

— Line-to-line voltage at worst-fault location = 115 000 V

— Soil resistivity $\rho = 400\ \Omega$-m

— Crushed-rock resistivity (wet) $\rho_s = 2500\ \Omega$-m

— Thickness of crushed-rock surfacing $h_s = 0.102$ m (4 in)

— Depth of grid burial $h = 0.5$ m

— Available grounding area $A = 63\ \text{m} \times 84\ \text{m}$

— Transformer impedance, (Z_1 and Z_0) $= 0.034 + j1.014\ \Omega$ (13 kV) ($Z = 9\%$ at 15 MVA, 115/13 kV)

The crushed-rock resistivity is assumed to be a conservative estimate based on actual measurements of typical rock samples. The equivalent system fault impedances and current division factor S_f are determined for the worst-fault type and location, including any conceivable system additions over the next 25 years. Thus, no additional safety factor for system growth is added. In addition, it is assumed that the substation will not be cleared by circuit breakers with an automatic reclosing scheme. Thus, the fault duration and shock duration are equal.

Copyright © 2015 IEEE. All rights reserved.

Copyright The Institute of Electrical and Electronics Engineers, Inc.
Provided by IHS under license with IEEE
No reproduction or networking permitted without license from IHS

Order Number: 02120914
Sold to:EGAT [700166108393] - VARRIS.Y@EGAT.CO.TH,
Not for Resale,2016-09-15 03:57:51 UTC

B.1 Square grid without ground rods—Example 1

Using the step-by-step procedure as described in 16.4 and illustrated in Figure 32, the following design evaluations can be made.

Step 1: Field data. Although the substation ground grid is to be located within a rectangle of 63 m ×84 m (5292 m^2), for the initial design assessment it may be expedient to assume a square 70 m × 70 m grid with no ground rods. Consequently, the area occupied by such a grid is A = 4900 m^2. An average soil resistivity of 400 Ω-m is assumed, based on soil resistivity measurements.

Step 2: Conductor size. Ignoring the station resistance, the symmetrical ground fault current $I_f \approx 3I_0$, is computed using Equation (72)

$$I_0 = \frac{E}{3 \times R_f + (R_1 + R_2 + R_0) + j(X_1 + X_2 + X_0)} \tag{B.1}$$

For the 115 kV bus fault

$$3I_0 = \frac{(3)(115\ 000/\sqrt{3})}{3(0) + (4.0 + 4.0 + 10.0) + j(10.0 + 10.0 + 40.0)}$$

and, hence

$|3I_0|$ = 3180 A, and the X/R ratio = 3.33

For the 13 kV bus fault, the 115 kV equivalent fault impedances must be transferred to the 13 kV side of the transformer. It should be noted that, due to the delta-wye connection of the transformer, only the positive sequence 115 kV fault impedance is transferred. Thus

$$Z_1 = \left(\frac{13}{115}\right)^2 [4.0 + j10.0] + 0.034 + j1.014 = 0.085 + j1.142$$

$$Z_0 = 0.034 + j1.014$$

$$3I_0 = \frac{(3)\left(13\ 000/\sqrt{3}\right)}{3(0) + (0.085 + 0.085 + 0.034) + j(1.142 + 1.142 + 1.014)}$$

and, hence

$|3I_0|$ = 6814 A, and the X/R ratio is 16.2

The 13 kV bus fault value of 6814 A should be used to size the grounding conductor.

Using Table 10 for fault duration of 0.5 s, the decrement factor D_f is approximately 1.0; thus, the rms asymmetrical fault current is also 6814 A. This current magnitude will be used to determine the minimum diameter of ground conductors.

Copyright © 2015 IEEE. All rights reserved.

Copyright The Institute of Electrical and Electronics Engineers, Inc.
Provided by IHS under license with IEEE
No reproduction or networking permitted without license from IHS

Order Number: 02120914
Sold to:EGAT [700166108393] - VARRIS.Y@EGAT.CO.TH,
Not for Resale,2016-09-15 03:57:51 UTC

Assuming the use of copper wire and an ambient temperature of 40 °C, Equation (47) and Table 2 are used to obtain the required conductor cross-sectional area. For 0.5 s and a melting temperature of 1084 °C for hard-drawn copper, the required cross-sectional area in circular mils is

$$A_{kcmil} = I \times K_f \sqrt{t_c} \tag{B.2}$$

$$A_{kcmil} = 6.814 \times 7.06\sqrt{0.5} = 34.02 \text{ kcmil}$$

34.02 kcmil = 17.2 mm^2

Because $A_{mm^2} = \pi d^2 / 4$, the conductor diameter is approximately 4.7 mm, or 0.0047 m if it is solid conductor.

Based on this computation, a copper wire as small as size No. 4 AWG could be used, but due to the mechanical strength and ruggedness requirements, a larger 2/0 AWG stranded conductor with diameter d = 0.0105 m (0.414 in) is usually preferred as a minimum.

Consequently, at this stage, the designer may opt to check if, alternately, the use of a less conductive (30%) copper-clad steel wire and the imposition of a more conservative maximum temperature limit of 700 °C will still permit the use of a conductor with diameter d = 0.01 m.

Using Equation (46) and Table 1 gives

$$A_{kcmil} = I \frac{197.4}{\sqrt{\left(\frac{TCAP}{t_c \alpha_r \rho_r}\right) \ln\left(\frac{K_o + T_m}{K_o + T_a}\right)}} \tag{B.3}$$

$$A_{kcmil} = 6.814 \frac{197.4}{\sqrt{\left(\frac{3.85}{(0.5)(0.00378)(5.862)}\right) \ln\left(\frac{245 + 700}{245 + 40}\right)}} = 59.81 \text{ kcmils or } 30.24 \text{ mm}^2$$

In this case, $d_{\min}$ = 6.2 mm, or 0.0062 m solid conductor, which is less than d = 0.01 m desired. Hence, a 30% copper-clad steel wire of approximately 2/0 AWG size is a viable alternative for grid wires, even if a conservative maximum temperature limit of 700 °C is imposed.

Step 3: Touch and step criteria. For a 0.102 m (4 in) layer of surface layer material, with a wet resistivity of 2500 Ω-m, and for an earth with resistivity of 400 Ω-m, the reflection factor K is computed using Equation (21)

$$K = \frac{\rho - \rho_s}{\rho + \rho_s} \tag{B.4}$$

$$K = \frac{400 - 2500}{400 + 2500} = -0.72$$

Figure 11 indicates for K = –0.72 the resistivity of the surface layer material is to be derated by a reduction factor $C_s \approx 0.74$. The reduction factor C_s can also be approximated using Equation (27)

Copyright © 2015 IEEE. All rights reserved.

Copyright The Institute of Electrical and Electronics Engineers, Inc.
Provided by IHS under license with IEEE
No reproduction or networking permitted without license from IHS

Order Number: 02120914
Sold to:EGAT [700166108393] - VARRIS.Y@EGAT.CO.TH,
Not for Resale,2016-09-15 03:57:51 UTC

$$C_s = 1 - \frac{0.09\left(1 - \frac{\rho}{\rho_s}\right)}{2h_s + 0.09} \tag{B.5}$$

$$C_s = 1 - \frac{0.09\left(1 - \frac{400}{2500}\right)}{2(0.102) + 0.09} = 0.74$$

Assuming that for the particular station the location of grounded facilities within the fenced property[15] is such that the person's weight can be expected to be at least 70 kg, Equation (30) and Equation (33) may be used to compute the tolerable step and touch voltages, respectively, as follows:

$$E_{step70} = (1000 + 6C_s\rho_s)0.157 / \sqrt{t_s} \tag{B.6}$$

$$E_{step70} = [(1000 + 6(0.74)2500)]0.157/\sqrt{0.5} = 2686.6$$

$$E_{touch70} = (1000 + 1.5C_s\rho_s)0.157 / \sqrt{t_s} \tag{B.7}$$

$$E_{touch70} = [(1000 + 1.5(0.74)2500)]0.157/\sqrt{0.5} = 838.2$$

Step 4: Initial design. Assume a preliminary layout of 70 m × 70 m grid with equally spaced conductors, as shown in Figure B.1, with spacing D = 7 m, grid burial depth h = 0.5 m, and no ground rods. The total length of buried conductor, L_T, is 2 × 11 × 70 m = 1540 m.

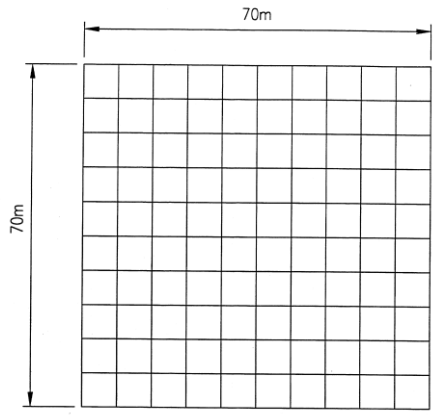

Figure B.1—Square grid without ground rods

[15] That is, not accessible to the general public.

Copyright © 2015 IEEE. All rights reserved.
Copyright The Institute of Electrical and Electronics Engineers, Inc.
Provided by IHS under license with IEEE
No reproduction or networking permitted without license from IHS
Order Number: 02120914
Sold to:EGAT [700166108393] - VARRIS.Y@EGAT.CO.TH,
Not for Resale,2016-09-15 03:57:51 UTC

Step 5: Determination of grid resistance. Using Equation (57) for L = 1540 m, and grid area A = 4900 m^2, the resistance is

$$R_g = \rho\left[\frac{1}{L_T} + \frac{1}{\sqrt{20A}}\left(1 + \frac{1}{1 + h\sqrt{20 / A}}\right)\right] \tag{B.8}$$

$$R_g = 400\left[\frac{1}{1540} + \frac{1}{\sqrt{20 \times 4900}}\left(1 + \frac{1}{1 + 0.5\sqrt{20/4900}}\right)\right] = 2.78 \ \ \Omega$$

Step 6: Maximum grid current I_G. Per the procedure and definitions of 15.1, the maximum grid current I_G is determined by combining Equation (68) and Equation (69). Referring to Step 2, for D_f = 1.0, and the given current division factor S_f = 0.6,

$$S_f = \frac{I_g}{3 \times I_o} \tag{B.9}$$

and

$$I_G = D_f \times I_g \tag{B.10}$$

Though the 13 kV bus fault value of 6814 A is greater than the 115 kV bus fault value of 3180 A, it is recalled from Clause 15 that the wye-grounded 13 kV transformer winding is a "local" source of fault current and does not contribute to the GPR. Thus, the maximum grid current is based on 3180 A.

$$I_G = D_f \times S_f \times 3 \times I_0 \tag{B.11}$$

$$I_G = (1)(0.6)(3180) = 1908 \text{ A}$$

Step 7: GPR. Now it is necessary to compare the product of I_G and R_g, or GPR, to the tolerable touch voltage, $E_{touch70}$

$$GPR = I_G \times R_g \tag{B.12}$$

$$GPR = 1908 \times 2.78 = 5304 \text{ V}$$

which far exceeds 838 V, determined in Step 3 as the safe value of $E_{touch70}$. Therefore, further design evaluations are necessary.

Step 8: Mesh voltage. Using Equation (86), Equation (87), Equation (88), K_m is computed

$$K_m = \frac{1}{2 \times \pi} \times \left[\ln\left[\frac{D^2}{16 \times h \times d} + \frac{(D + 2 \times h)^2}{8 \times D \times d} - \frac{h}{4 \times d}\right] + \frac{K_{ii}}{K_h} \times \ln\left[\frac{8}{\pi(2 \times n - 1)}\right]\right] \tag{B.13}$$

Copyright © 2015 IEEE. All rights reserved.

Copyright The Institute of Electrical and Electronics Engineers, Inc.
Provided by IHS under license with IEEE
No reproduction or networking permitted without license from IHS

Order Number: 02120914
Sold to:EGAT [700166108393] - VARRIS.Y@EGAT.CO.TH,
Not for Resale,2016-09-15 03:57:51 UTC

where

$$K_{ii} = \frac{1}{(2 \times n)^{\frac{2}{n}}} \tag{B.14}$$

$$K_{ii} = \frac{1}{(2 \times 11)^{\frac{2}{11}}} = 0.57$$

and

$$K_h = \sqrt{1 + \frac{h}{h_0}} \tag{B.15}$$

$$K_h = \sqrt{1 + \frac{0.5}{1.0}} = 1.225$$

$$Km = \frac{1}{2\pi}\left[\ln\left[\frac{7^2}{16 \times 0.5 \times 0.01} + \frac{(7 + 2 \times 0.5)^2}{8 \times 7 \times 0.01} - \frac{0.5}{4 \times 0.01}\right] + \frac{0.57}{1.225}\ln\left[\frac{8}{\pi(2 \times 11 - 1)}\right]\right] = 0.89$$

The factor K_i is computed using Equation (89) through Equation (94)

$$K_i = 0.644 + 0.148 \times n \tag{B.16}$$

where

$$n = n_a \times n_b \times n_c \times n_d \tag{B.17}$$

$$n_a = \frac{2 \times L_C}{L_p} \tag{B.18}$$

$$n_a = \frac{2 \times 1540}{280} = 11$$

n_b = 1 for square grid

n_c = 1 for square grid

n_d = 1 for square grid

and therefore

$$n = 11 \times 1 \times 1 \times 1 = 11$$

$$K_i = 0.644 + 0.148 \times 11 = 2.272$$

Finally, E_m is computed using Equation (85) and Equation (95)

Copyright © 2015 IEEE. All rights reserved.

Copyright The Institute of Electrical and Electronics Engineers, Inc.
Provided by IHS under license with IEEE
No reproduction or networking permitted without license from IHS

Order Number: 02120914
Sold to:EGAT [700166108393] - VARRIS.Y@EGAT.CO.TH,
Not for Resale,2016-09-15 03:57:51 UTC

$$E_m = \frac{\rho \times I_G \times K_m \times K_i}{L_C + L_R} \tag{B.19}$$

$$E_m = \frac{400 \times 1908 \times 0.89 \times 2.272}{1540} = 1002.1 \text{ V}$$

Step 9: E_m versus E_{touch}. The mesh voltage is higher than the tolerable touch voltage (that is, 1002.1 V versus 838.2 V). The grid design must be modified.

For comparison, the EPRI TR-100622 [B64] computer program resulted in 2.67 Ω and 984.3 V for the grid resistance and touch voltage, respectively, for this example.

B.2 Square grid with ground rods—Example 2

In the previous example, B.1, Step 10 of the design procedure has not been reached due to the failure to meet the criterion of Step 9. Generally, there are two approaches to modifying the grid design to meet the tolerable touch voltage requirements

a) Reduce the GPR to a value below the tolerable touch voltage or to a value low enough to result in a value of E_m below the tolerable touch voltage.

b) Reduce the available ground fault current.

Usually reduction of the available ground fault current is difficult or impractical to achieve, so the grid is modified by changing any or all of the following: grid conductor spacing, total conductor length, grid depth, addition of ground rods, etc. In this example, the preliminary design will be modified to include 20 ground rods, each 7.5 m (24.6 ft) long, around the perimeter of the grid, as shown in Figure B.2.

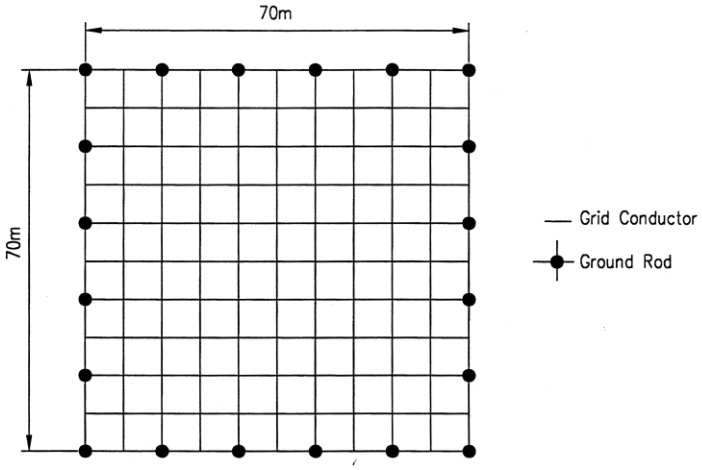

Figure B.2—Square grid with twenty 7.5 m rods

Copyright © 2015 IEEE. All rights reserved.
Copyright The Institute of Electrical and Electronics Engineers, Inc.
Provided by IHS under license with IEEE
No reproduction or networking permitted without license from IHS
Order Number: 02120914
Sold to:EGAT [700166108393] - VARRIS.Y@EGAT.CO.TH,
Not for Resale,2016-09-15 03:57:51 UTC

Step 5. Using Equation (57) for L_T = 1540 + 20 × 7.5 = 1690 m, and A = 4900 m^2 yields the following value of grid resistance R_g:

$$R_g = \rho\left[\frac{1}{L_T} + \frac{1}{\sqrt{20A}}\left(1 + \frac{1}{1 + h\sqrt{20/A}}\right)\right] \tag{B.20}$$

$$R_g = 400\left[\frac{1}{1690} + \frac{1}{\sqrt{20 \times 4900}}\left(1 + \frac{1}{1 + 0.5\sqrt{20/4900}}\right)\right] = 2.75\ \Omega$$

Steps 6 and 7. The revised GPR is (1908)(2.75) = 5247 V, which is still much greater than 838.2 V.

Step 8. Using Equation (80) and Equation (82), K_m is computed

$$K_m = \frac{1}{2 \times \pi}\left[\ln\left[\frac{D^2}{16 \times h \times d} + \frac{(D + 2 \times h)^2}{8 \times D \times d} - \frac{h}{4 \times d}\right] + \frac{K_{ii}}{K_h} \times \ln\left[\frac{8}{\pi(2 \times n - 1)}\right]\right] \tag{B.21}$$

where

K_{ii} = 1.0 with rods

and

$$K_h = \sqrt{1 + \frac{h}{h_0}} \tag{B.22}$$

$$K_h = \sqrt{1 + \frac{0.5}{1.0}} = 1.225$$

$$K_m = \frac{1}{2\pi}\left[\ln\left[\frac{7^2}{16 \times 0.5 \times 0.01} + \frac{(7 + 2 \times 0.5)^2}{8 \times 7 \times 0.01} - \frac{0.5}{4 \times 0.01}\right] + \frac{1.0}{1.225}\ln\left[\frac{8}{\pi(2 \times 11 - 1)}\right]\right] = 0.77$$

This time, E_m is computed using Equation (85) and Equation (96)

$$E_m = \frac{\rho \times I_G \times K_m \times K_i}{L_C + \left[1.55 + 1.22\left(\frac{L_r}{\sqrt{L_x^2 + L_y^2}}\right)\right] \times L_R} \tag{B.23}$$

$$E_m = \frac{400 \times 1908 \times 0.77 \times 2.272}{1540 + \left[1.55 + 1.22\left(\frac{7.5}{\sqrt{70^2 + 70^2}}\right)\right]150} = 747.4\ \text{V}$$

Copyright © 2015 IEEE. All rights reserved.

Copyright The Institute of Electrical and Electronics Engineers, Inc.
Provided by IHS under license with IEEE
No reproduction or networking permitted without license from IHS

Order Number: 02120914
Sold to:EGAT [700166108393] - VARRIS.Y@EGAT.CO.TH,
Not for Resale,2016-09-15 03:57:51 UTC

Because the step voltage has not been calculated yet, Equation (94) and Equation (97), Equation (98), and Equation (99) are used to compute K_i, E_s, L_S, and K_s, respectively. Note that the value for K_i is still 2.272 (same as for mesh voltage).

$$K_s = \frac{1}{\pi}\left[\frac{1}{2\times h} + \frac{1}{D+h} + \frac{1}{D}\left(1-0.5^{n-2}\right)\right] \tag{B.24}$$

$$K_s = \frac{1}{\pi}\left[\frac{1}{2\times 0.5} + \frac{1}{7+0.5} + \frac{1}{7}\left(1-0.5^{11-2}\right)\right] = 0.406$$

Then

$$E_s = \frac{\rho \times I_G \times K_s \times K_i}{0.75\times L_C + 0.85\times L_R} \tag{B.25}$$

$$E_s = \frac{400\times 1908\times 0.406\times 2.272}{0.75\times 1540 + 0.85\times 150} = 548.9 \text{ V}$$

Step 9: E_m versus E_{touch}. Now the calculated corner mesh voltage is lower than the tolerable touch voltage (747.4 V versus 838.2 V), and we are ready to proceed to Step 10.

Step 10: E_s versus E_{step}. The computed E_s is well below the tolerable step voltage determined in Step 3 of Example 1. That is, 548.9 V is much less than 2686.6 V.

Step 11: Modify design. Not necessary for this example.

Step 12: Detailed design. A safe design has been obtained. At this point, all equipment pigtails, additional ground rods for surge arresters, etc., should be added to complete the grid design details.

For comparison, the computer program of EPRI TR-100622 [B64] resulted in 2.52 Ω, 756.2 V, and 459.1 V for the grid resistance, touch voltage, and step voltage, respectively, for this example.

B.3 Rectangular grid with ground rods—Example 3

In this example the preliminary grid design will be reconciled in terms of the actual shape of the grounding area as an alternative design. Realizing that the full grounding area is only about 8% larger than that used in the previous calculations, most of the conclusions from Example 2 can be used for arriving at a suitable final design solution.

Choosing, again, spacing D = 7 m, for a rectangular 63 m × 84 m grid, the grid wire pattern is 10 × 13, and the grid conductor combined length is 13 × 63 m + 10 × 84 m = 1659 m. Assume the use of 38 ground rods, each 10 m long, as shown in Figure B.3.

--`,,,,,,`,```,,`,`,,`,-`-`,,`,,`,`---
Copyright © 2015 IEEE. All rights reserved.
Copyright The Institute of Electrical and Electronics Engineers, Inc.
Provided by IHS under license with IEEE
No reproduction or networking permitted without license from IHS
Order Number: 02120914
Sold to:EGAT [700166108393] - VARRIS.Y@EGAT.CO.TH,
Not for Resale,2016-09-15 03:57:51 UTC

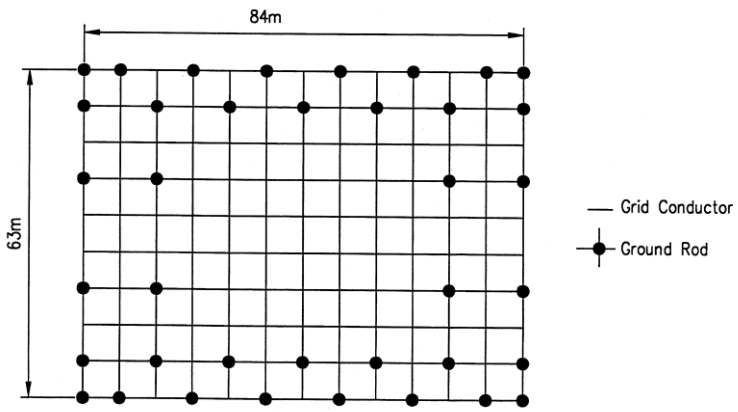

Figure B.3—Rectangular grid with thirty-eight 10 m ground rods

Step 5. Again, using Equation (57), but for L_T = 1659 m + (38)(10 m) = 2039 m and A = 63 m × 84 m = 5292 m^2, gives

$$R_g = \rho\left[\frac{1}{L_T} + \frac{1}{\sqrt{20A}}\left(1 + \frac{1}{1 + h\sqrt{20/A}}\right)\right] \tag{B.26}$$

$$R_g = 400\left[\frac{1}{2039} + \frac{1}{\sqrt{20 \times 5292}}\left(1 + \frac{1}{1 + 0.5\sqrt{20/5292}}\right)\right] = 2.62\ \Omega$$

Steps 6 and 7. Using I_G = 1908 A as before, and R_g = 2.62 Ω, the GPR = (1908)(2.62) = 4998.96 V, which is much greater than 838.2 V.

Step 8. For the particular design arrangement shown in Figure B.3, the equations of 16.5.1 can again be used to estimate the corner mesh voltage. However, because the grid is rectangular, the value of n to be used in the mesh voltage computation will be different, based on the factors determined using Equation (89) through Equation (93).

$$n = n_a \times n_b \times n_c \times n_d \tag{B.27}$$

$$n_a = \frac{2 \times L_C}{L_p} \tag{B.28}$$

$$n_a = \frac{2 \times 1659}{294} = 11.29$$

$$n_b = \sqrt{\frac{L_p}{4 \times \sqrt{A}}} \tag{B.29}$$

$$n_b = \sqrt{\frac{294}{4 \times \sqrt{5292}}} = 1.005$$

Copyright © 2015 IEEE. All rights reserved.

Copyright The Institute of Electrical and Electronics Engineers, Inc.
Provided by IHS under license with IEEE
No reproduction or networking permitted without license from IHS

Order Number: 02120914
Sold to:EGAT [700166108393] - VARRIS.Y@EGAT.CO.TH,
Not for Resale,2016-09-15 03:57:51 UTC

n_c = 1 for rectangular grid

n_d = 1 for rectangular grid

$$n = 11.29 \times 1.005 \times 1 \times 1 = 11.35$$

Now K_m is computed using Equation (86) and Equation (88)

$$K_m = \frac{1}{2 \times \pi} \times \left[\ln\left[\frac{D^2}{16 \times h \times d} + \frac{(D + 2 \times h)^2}{8 \times D \times d} - \frac{h}{4 \times d} \right] + \frac{K_{ii}}{K_h} \times \ln\left[\frac{8}{\pi(2 \times n - 1)} \right] \right] \tag{B.30}$$

where

$K_{ii} = 1$ for a grid with ground rods

$$K_h = \sqrt{1 + \frac{0.5}{1.0}} = 1.225$$

$$K_m = \frac{1}{2\pi} \left[\ln\left[\frac{7^2}{16 \times 0.5 \times 0.01} + \frac{(7 + 2 \times 0.5)^2}{8 \times 7 \times 0.01} - \frac{0.5}{4 \times 0.01} \right] + \frac{1.0}{1.225} \ln\left[\frac{8}{\pi(2 \times 11.35 - 1)} \right] \right] = 0.77$$

Equation (94) is used to compute K_i

$$K_i = 0.644 + 0.148 \times n \tag{B.31}$$

$$K_i = 0.644 + 0.148 \times 11.35 = 2.324$$

Finally, E_m is computed using Equation (85) and Equation (96)

$$E_m = \frac{\rho \times I_G \times K_m \times K_i}{L_C + \left[1.55 + 1.22 \left(\frac{L_r}{\sqrt{L_x^2 + L_y^2}} \right) \right] L_R} \tag{B.32}$$

$$E_m = \frac{400 \times 1908 \times 0.77 \times 2.324}{1659 + \left[1.55 + 1.22 \left(\frac{10}{\sqrt{63^2 + 84^2}} \right) \right] 380} = 595.8 \text{ V}$$

Step 9. This calculated mesh voltage is well below the $E_{touch70}$ limit of 838.2, but uses 119 m of additional conductor and 230 m of additional ground rods, as compared with the previous example. Thus, the mesh spacing could be increased, the number and/or length of ground rods could be reduced, or both to achieve the same margin of safety as Example 2.

The remaining steps are the same as demonstrated in Example 2 and will not be repeated here.

Copyright © 2015 IEEE. All rights reserved.

Copyright The Institute of Electrical and Electronics Engineers, Inc.
Provided by IHS under license with IEEE
No reproduction or networking permitted without license from IHS

Order Number: 02120914
Sold to:EGAT [700166108393] - VARRIS.Y@EGAT.CO.TH,
Not for Resale,2016-09-15 03:57:51 UTC

For comparison, the computer program of EPRI TR-100622 [B64] resulted in 2.28 Ω, 519.4 V, and 349.7 V for the grid resistance, touch voltage, and step voltage, respectively, for this example.

B.4 L-shaped grid with ground rods—Example 4

In this example the design of Example 2 is modified to illustrate the use of the equations for an L-shaped grid with ground rods. The total area and mesh spacing are the same as that of Example 2, and the ground rods are located only around the perimeter of the grid, as shown in Figure B.4. All other parameters are the same as Example 2, except the number of rods (24). Thus, Steps 1 through 4 are the same as Example 2, and this example begins with Step 5.

Step 5. Using Equation (57) for L_T = 1575 m + (24)(7.5 m) = 1755 m and A = 4900 m^2, gives

$$R_g = \rho\left[\frac{1}{L_T} + \frac{1}{\sqrt{20A}}\left(1 + \frac{1}{1 + h\sqrt{20/A}}\right)\right] \tag{B.33}$$

$$R_g = 400\left[\frac{1}{1755} + \frac{1}{\sqrt{20 \times 4900}}\left(1 + \frac{1}{1 + 0.5\sqrt{20/4900}}\right)\right] = 2.74\ \Omega$$

Steps 6 and 7. The revised GPR is (1908)(2.74) = 5228 V, which is much greater than the tolerable touch voltage of 838.2 V.

Step 8. Using Equation (89) through Equation (93), and Equation (86) and Equation (94), n, K_m, and K_i are computed

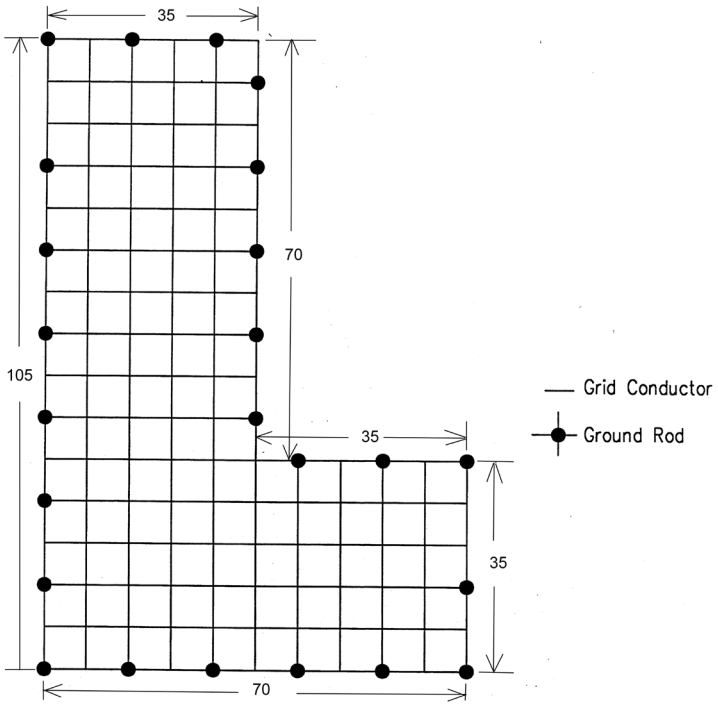

Figure B.4—L-shaped grid with twenty-four 7.5 m ground rods

Copyright © 2015 IEEE. All rights reserved.
Copyright The Institute of Electrical and Electronics Engineers, Inc.
Provided by IHS under license with IEEE
No reproduction or networking permitted without license from IHS
Order Number: 02120914
Sold to:EGAT [700166108393] - VARRIS.Y@EGAT.CO.TH,
Not for Resale,2016-09-15 03:57:51 UTC

$$n = n_a \times n_b \times n_c \times n_d \tag{B.34}$$

$$n_a = \frac{2 \times L_C}{L_P} \tag{B.35}$$

$$n_a = \frac{2 \times 1575}{350} = 9$$

$$n_b = \sqrt{\frac{L_P}{4 \times \sqrt{A}}} \tag{B.36}$$

$$n_b = \sqrt{\frac{350}{4 \times \sqrt{4900}}} = 1.12$$

$$n_c = \left[\frac{L_x \times L_y}{A} \right]^{\frac{0.7 \times A}{L_x \times L_y}} \tag{B.37}$$

$$n_c = \left[\frac{70 \times 105}{4900} \right]^{\frac{0.7(4900)}{70(105)}} = 1.21$$

$n_d = 1$ for L-shaped grid

$$n = (9)(1.12)(1.21)(1) = 12.2$$

Now K_m is computed using Equation (86) and Equation (88)

$$K_{ii} = 1$$

$$K_h = \sqrt{1 + \frac{0.5}{1.0}} = 1.225$$

$$K_m = \frac{1}{2 \times \pi} \times \left[\ln\left[\frac{D^2}{16 \times h \times d} + \frac{(D + 2 \times h)^2}{8 \times D \times d} - \frac{h}{4 \times d} \right] + \frac{K_{ii}}{K_h} \times \ln\left[\frac{8}{\pi(2 \times n - 1)} \right] \right] \tag{B.38}$$

$$K_m = \frac{1}{2\pi} \left[\ln\left[\frac{7^2}{16(0.5)0.01} + \frac{(7 + 2(0.5))^2}{8(7)0.01} - \frac{0.5}{4(0.01)} \right] + \frac{1.0}{1.225} \ln\left[\frac{8}{\pi(2(12.2) - 1)} \right] \right] = 0.76$$

Equation (88) is used to compute K_i

$$K_i = 0.644 + 0.148 \times n \tag{B.39}$$

Copyright © 2015 IEEE. All rights reserved.

Copyright The Institute of Electrical and Electronics Engineers, Inc.
Provided by IHS under license with IEEE
No reproduction or networking permitted without license from IHS

Order Number: 02120914
Sold to:EGAT [700166108393] - VARRIS.Y@EGAT.CO.TH,
Not for Resale,2016-09-15 03:57:51 UTC

$$K_i = 0.644 + 0.148 \times 12.2 = 2.45$$

Finally, E_m is computed using Equation (86) and Equation (96)

$$E_m = \frac{\rho \times I_G \times K_m \times K_i}{L_C + \left[1.55 + 1.22\left(\frac{L_r}{\sqrt{L_x^2 + L_y^2}}\right)\right] L_R} \tag{B.40}$$

$$E_m = \frac{(400)(1908)(0.76)(2.45)}{1575 + \left[1.55 + 1.22\left(\frac{7.5}{\sqrt{70^2 + 105^2}}\right)\right] 180} = 761.1 \text{ V}$$

Equation (97), Equation (98), and Equation (99) are used to compute E_s, L_s and K_s, respectively. It should be noted that the value for K_i is still 2.45 (same as for mesh voltage).

$$K_s = \frac{1}{\pi}\left[\frac{1}{2 \times h} + \frac{1}{D + h} + \frac{1}{D}\left(1 - 0.5^{n-2}\right)\right] \tag{B.41}$$

$$K_s = \frac{1}{\pi}\left[\frac{1}{2(0.5)} + \frac{1}{7 + 0.5} + \frac{1}{7}\left(1 - 0.5^{12.2-2}\right)\right] = 0.41$$

Then

$$E_s = \frac{\rho \times I_G \times K_s \times K_i}{0.75 \times L_C + 0.85 \times L_R} \tag{B.42}$$

$$E_s = \frac{(400)(1908)(0.41)(2.45)}{0.75(1575) + 0.85(180)} = 574.6 \text{ V}$$

Step 9. Note that this is close to the results of Example 2, and is lower than the tolerable $E_{touch70}$ limit of 838.2 V. Proceed to Step 10.

Step 10. The computed E_s is well below the tolerable step voltage determined in Step 3 of Example 1. That is, 574.6 V is much less than 2686.6 V.

Step 11. Not required for this example.

Step 12. A safe design has been obtained and final details can now be added to the design.

For comparison, a computer program of EPRI TR-100622 [B64] gives results of 2.34 Ω, 742.9 V, and 441.8 V for the grid resistance, touch voltage, and step voltage, respectively, for this example.

Copyright © 2015 IEEE. All rights reserved.

Copyright The Institute of Electrical and Electronics Engineers, Inc.
Provided by IHS under license with IEEE
No reproduction or networking permitted without license from IHS

Order Number: 02120914
Sold to:EGAT [700166108393] - VARRIS.Y@EGAT.CO.TH,
Not for Resale,2016-09-15 03:57:51 UTC

B.5 Equally spaced grid with ground rods in two-layer soil—Exhibit 1

Using the computer program of EPRI TR-100622 [B64], an equally spaced grid in two-layer soil was modeled.

As shown in Figure B.5, the 61 m × 61 m (200 ft × 200 ft) grid consisted of four meshes per side, and had nine ground rods, each 9.2 m (30 ft) long. The diameter of ground rods was 0.0127 m (0.5 in). The diameter of the grid wire was 0.01 m diameter, buried 0.5 m below the earth's surface. The depth of the upper layer 300 Ω-m soil was 4.6 m (15 ft); the lower soil had resistivity of 100 Ω-m.

The computer-calculated values of resistance, corner mesh voltage, and maximum step voltage, are as follows:

R_g = 1.353 Ω E_m = 49.66% of GPR E_s = 18.33% of GPR

As can be determined from Figure B.6, the mesh voltage coordinates were X = –75.00 ft, and Y= –75.00 ft, that is, near the center of the corner mesh. The maximum step voltage (not shown) was calculated outside the grid, between the grid corner (X, Y = –100 ft) and the point at X, Y = –102.12 ft, that is, approximately over 1 m distance in a diagonal direction away from the grid corner.

B.6 Unequally spaced grid with ground rods in uniform soil—Exhibit 2

Using the computer program of EPRI TR-100622 [B64], a square grid with unequally spaced conductors was modeled as shown in Figure B.7.

The computer output included the grid resistance, a surface voltage profile, the step voltage, and the corner mesh voltage.

As shown in Figure B.8, the corner mesh voltage is only 9.29% of the GPR, while the maximum touch voltage, occurring above the largest interior mesh, is 17.08% of the GPR.

The maximum touch voltage, thus, did not occur in the corner mesh. For other choices of conductor spacings, the maximum touch voltage may occur above some other meshes. Therefore, for unequal spacings, the touch voltages must be investigated over the entire grid, and the simplified criterion for checking the corner mesh voltage alone is not sufficient. On the other hand, the resistance R_g is not too dependent on the exact configuration of grid conductors and ground rods. For instance, were R_g estimated by Equation (58) for a combined length of grid conductors and ground rods L_T = 18 × 91.44 m + 25 × 9.2 m = 1876 m, the calculated value of 1.61 Ω would be less than 14% higher than the value of 1.416 Ω calculated by the computer program of EPRI TR-100622 [B64].

Copyright © 2015 IEEE. All rights reserved.
--`,,,,,,`,```,,`,`,,`,-`-`,,`,,`,`---
Copyright The Institute of Electrical and Electronics Engineers, Inc.
Provided by IHS under license with IEEE
No reproduction or networking permitted without license from IHS
Order Number: 02120914
Sold to:EGAT [700166108393] - VARRIS.Y@EGAT.CO.TH,
Not for Resale,2016-09-15 03:57:51 UTC

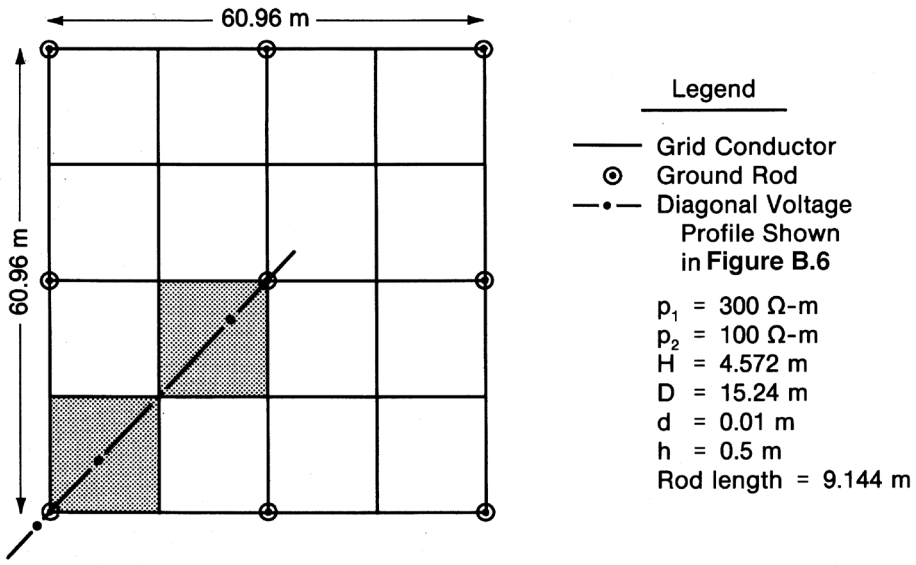

Figure B.5—Equally spaced square grid with nine rods in two-layer soil

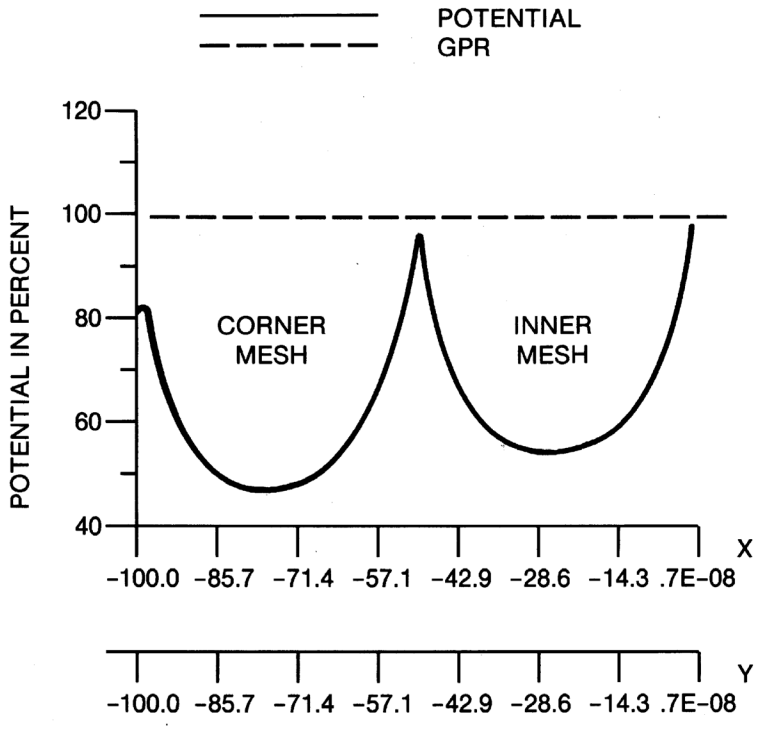

Figure B.6—Diagonal voltage profile for the grid of Figure B.5 in two-layer soil

Copyright © 2015 IEEE. All rights reserved.

Copyright The Institute of Electrical and Electronics Engineers, Inc.
Provided by IHS under license with IEEE
No reproduction or networking permitted without license from IHS

Order Number: 02120914
Sold to:EGAT [700166108393] - VARRIS.Y@EGAT.CO.TH,
Not for Resale,2016-09-15 03:57:51 UTC

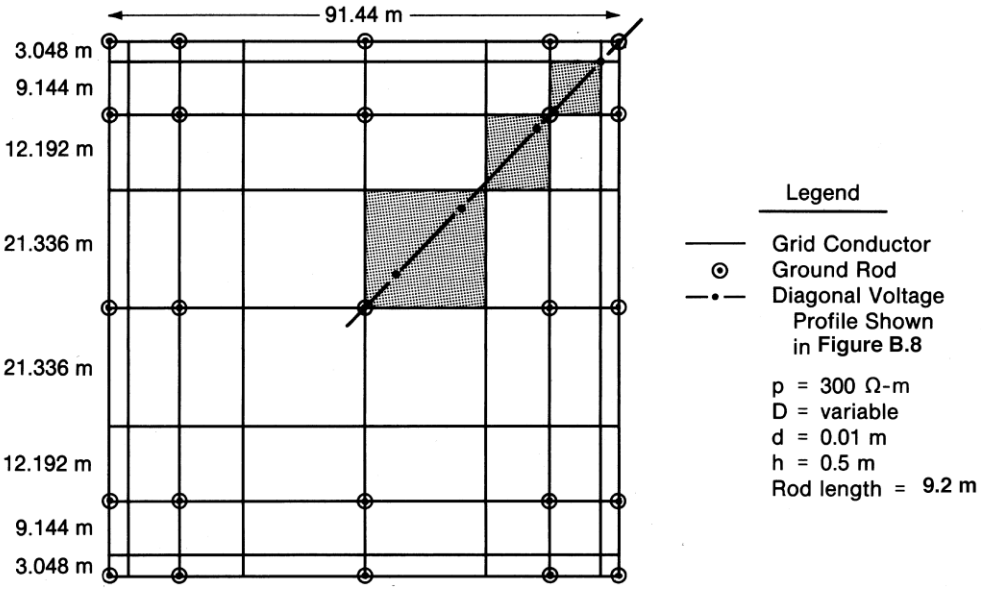

Figure B.7—Unequally spaced square grid with twenty-five 9.2 m rods

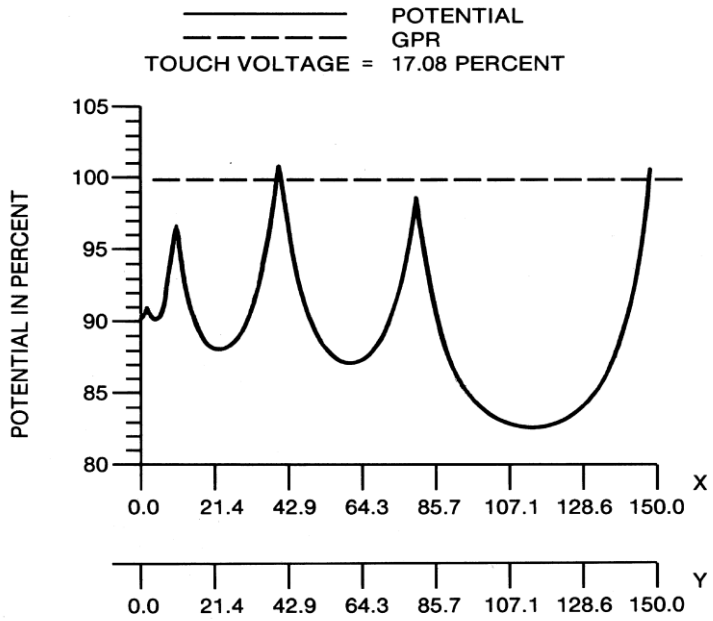

Figure B.8—Diagonal voltage profile for an unequally spaced grid of Figure B.7

Copyright © 2015 IEEE. All rights reserved.
Copyright The Institute of Electrical and Electronics Engineers, Inc.
Provided by IHS under license with IEEE
No reproduction or networking permitted without license from IHS
Order Number: 02120914
Sold to:EGAT [700166108393] - VARRIS.Y@EGAT.CO.TH,
Not for Resale,2016-09-15 03:57:51 UTC

Annex C

(informative)

Graphical and approximate analysis of current division

C.1 Introduction

A graphical method for determining the maximum grid current, based on results obtained using a computer program of EPRI TR-100622 [B64] has been developed. This method attempts to correlate the substation zero sequence fault obtained from a standard short-circuit study to the actual current flowing between the grounding system and surrounding earth. The original presentation of this concept was published in Garrett, Myers, and Patel [B74]. That paper describes the parametric analysis performed and the resulting basis for the assumptions used to develop the curves. Additional curves have since been developed to address other system configurations. The following is an explanation of the use of the graphs shown in Figure C.1 through Figure C.22.

The graphs are divided into the following four categories:

- Category A: 100% remote and 0% local fault current contribution, representing typical distribution substations with delta-wye transformer, with X transmission lines and Y feeders (Figure C.1 through Figure C.16)
- Category B: 75% remote and 25% local ground fault current contribution (Figure C.17 and Figure C.18)
- Category C: 50% remote and 50% local ground fault current contribution (Figure C.19 and Figure C.20)
- Category D: 25% remote and 75% local ground fault current contribution (Figure C.21 and Figure C.22)

Categories B through D represent typical transmission substations or generating plants with X transmission lines (feeders are considered to be transmission lines in these cases), and with local sources of zero sequence current, such as auto transformers, three winding transformers, generators (grounded-wye generator step-up transformers), etc. Category A works well for practical cases. Categories B through D are rough approximations, and the accuracy depends on several system parameters (particularly the source of the local ground fault current).

The following assumptions were used to obtain the graphs:

a) Transmission line length of 23.5 mi (37.82 km) and a distance between grounds of 500 ft (152 m)
b) Transmission tower footing resistance of 15 or 100 Ω
c) Transmission line structure single pole with 7 No. 10 Alumoweld shield wire and 336.4 kcmil, 26/7 ACSR conductor
d) Distribution line length of 2.5 mi (4 km) and a distance between grounds of 400 ft (122 m)
e) Distribution pole footing resistance of 25 Ω or 200 Ω
f) Distribution pole three-phase triangular layout, with one 336.4 kcmil, 26/7 ACSR phase and 1/0 ACSR neutral conductor
g) Soil resistivity of 100 Ω-m

Copyright © 2015 IEEE. All rights reserved.

Copyright The Institute of Electrical and Electronics Engineers, Inc.
Provided by IHS under license with IEEE
No reproduction or networking permitted without license from IHS

Order Number: 02120914
Sold to:EGAT [700166108393] - VARRIS.Y@EGAT.CO.TH,
Not for Resale,2016-09-15 03:57:51 UTC

h) Substation grounding system resistances of 0.1 Ω, 0.5 Ω, 1.0 Ω, 5.0 Ω, 10.0 Ω, and 25.0 Ω

i) Number of transmission lines varied from 0, 1, 2, 4, 8, 12, and 16

j) Number of distribution lines varied from 0, 1, 2, 4, 8, 12, and 16

k) One remote source for each two transmission lines

C.2 How to use the graphs and equivalent impedance table

Referring to Figure C.1 through Figure C.22, a family of curves is plotted, with each curve representing a different number of transmission lines or distribution feeders. The abscissa is a range of grounding system resistances from 0.1 Ω to 25.0 Ω. The ordinate is the percent of the total zero sequence substation bus ground fault current which flows between the grounding system and surrounding earth (i.e., the grid current I_g).

When using Category A curves and Table C.1, only the delta-connected bus fault current should be used as the multiplier of the split factor because this fault current is the one that is from remote sources and is the basis of these curves. When using Category B through D curves, the fault current and contributions should be determined for all transmission voltage levels and the case resulting in the highest grid current should be used. In addition, the following steps must be used to determine the local and remote contributions:

a) Obtain the total single-phase-to-ground fault current at the fault location being studied, in amperes.

b) For the studied fault location, obtain the phase currents for the contributions from each transmission line on all transmission voltage levels at the substation, in amperes on the voltage of each transmission line.

c) With no adjustments for the voltage level of the transmission lines, add the phase a (faulted phase) currents of all transmission lines "crossing the substation fence.", in amperes. This is the remote contribution.

d) Subtract this remote contribution from the total current, in amperes. This is the local contribution.

e) Choose the curves from Categories B-D that most closely match the remote and local contributions. For conservatism, it is suggested that the category with the next higher remote current contribution be used. For example, if the actual remote contribution is 60%, it is suggested to use the Category B (25% local, 75% remote) curves be used.

f) Using the curve with the closest number of transmission lines and the grounding system resistance, determine the split factor S_f. Multiply this split factor by the total fault current to determine the grid current for this fault location.

g) Repeat steps a-f for single-phase-to-ground faults at each transmission level bus in the substation.

h) The design grid current is the maximum of all grid currents computed using steps a) through-g).

Table C.1 shows the equivalent transmission and distribution ground system impedance at 1 Ω for 100% remote contribution with X transmission lines and Y distribution feeders. The first column of impedances is for transmission line ground electrode resistance R_{tg} of 15 Ω and distribution feeder ground electrode resistance R_{dg} of 25 Ω. The second column of impedances is for R_{tg} of 100 Ω and R_{dg} of 200 Ω. To determine the GPR with current splits, parallel the grid resistance with the appropriate impedance from the

Copyright © 2015 IEEE. All rights reserved.

Copyright The Institute of Electrical and Electronics Engineers, Inc.
Provided by IHS under license with IEEE
No reproduction or networking permitted without license from IHS

Order Number: 02120914
Sold to:EGAT [700166108393] - VARRIS.Y@EGAT.CO.TH,
Not for Resale,2016-09-15 03:57:51 UTC

table and multiply this value by the total fault current. For example, a substation with one transmission line and two distribution feeders has a ground grid resistance of 5 Ω, a total fault current of 1600 A, R_{tg} of 15 Ω, and R_{dg} of 25 Ω. From Table C.1, the equivalent impedance of the transmission and distribution ground system is 0.54 + *j*0.33 Ω. The magnitude of the equivalent total ground impedance is

$$\left|Z_g\right| = \left|\frac{(5.0)(0.54 + j0.33)}{5.0 + 0.54 + j0.33}\right| = 0.57\,\Omega \tag{C.1}$$

and the GPR is

$$\text{GPR} = (0.57)(1600) = 912 \text{ V} \tag{C.2}$$

To calculate the grid current, divide the GPR by the ground grid resistance.

$$I_g = \frac{912}{5} = 182 \text{ A} \tag{C.3}$$

The grid current may also be computed directly by current division.

$$\left|I_g\right| = 1600 \times \left|\frac{(0.54 + j0.33)}{5.0 + 0.54 + j0.33}\right| = 182 \text{ A} \tag{C.4}$$

C.3 Examples

To illustrate the use of the graphical analysis, consider a substation with two transmission lines and three distribution feeders, and a ground grid resistance of 1 Ω, as shown in Figure C.23. Using EPRI TR-100622 [B64], the maximum grid current is 2354.6 A, and the total bus ground fault is 9148.7 A. The system in question has two transmission lines with R_{tg} of 15 Ω and three distribution lines with R_{dg} of 25 Ω. Figure C.3 shows curves for two lines/two feeders and two lines/four feeders. Thus, interpolation is necessary for this example. From Figure C.3, we see that the approximate split factor S_f is (32+23)/2 or 27.5%. The maximum grid current is

$$I_g = (9148.7)(0.275) = 2516 \text{ A} \tag{C.5}$$

Using Table C.1, the equivalent impedance of the transmission and distribution ground system for two lines and two distribution feeders is 0.455 + *j*0.241 Ω, and for two lines and four distribution feeders is 0.27 + *j*0.165 Ω. The average of the split factors for these two cases will be used.

$$S_f = \left|\frac{0.455 + j0.241}{1.0 + 0.455 + j0.241}\right| = 0.349$$

$$S_f = \left|\frac{0.27 + j0.165}{1.0 + 0.27 + j0.165}\right| = 0.247$$

Thus, $S_f = (0.349 + 0.247)/2 =$ 0.298 or 28.9%

The resulting grid current using this method is

Copyright © 2015 IEEE. All rights reserved.
Copyright The Institute of Electrical and Electronics Engineers, Inc.
Provided by IHS under license with IEEE
No reproduction or networking permitted without license from IHS
Order Number: 02120914
Sold to:EGAT [700166108393] - VARRIS.Y@EGAT.CO.TH,
Not for Resale,2016-09-15 03:57:51 UTC

$$I_g = (9148.7)(0.298) = 2726 \text{ A}$$

Both methods compare favorably with the value of 2354.6 A or 26% of $3I_0$ from the computer program, though the equivalent impedance method is generally more conservative.

Next consider the more complex system shown in Figure C.24. This example is similar to the first, except that the distribution substation is replaced with a local source of generation, such as a cogeneration plant. For this example, there are both local and remote sources of ground fault current, so the percent of local versus remote ground fault current contribution must be computed. The computer program of EPRI TR-100622 [B64] computed a total fault current of 19 269.6 A at the 115 kV bus, with 48.7% contributed by the local source and 51.3% contributed by the remote sources. The closest curves are for 50/50 split (Figure C.19). For a grid resistance of 0.9 Ω, the split factor is determined from the curve for two lines and no feeders, S_f = 29%. The maximum grid current is

$$I_g = (19269.6)(0.29) = 5588 \text{ A}$$

For this case, the computer program results in a value of 4034.8 A, or 21% of $3I_0$. This does not compare as well as the case with 100% remote contribution, but is still closer than using the total fault current, or even the remote or local contribution. The equivalent impedance method (Table C.1) does not work as well for cases other than 100% remote contribution, and is not included in Table C.1.

C.4 Equations for computing line impedances

The following equations are found in the *Electrical Transmission and Distribution Reference Book* [B1]. The definitions of the terms used in the equations are

GMD is the geometric mean distance between the phase conductors in ft
GMR is the geometric mean radius of the conductor in ft
d_{ab} is the distance between conductors *a* and *b* in ft
r_a is the ac resistance of the conductor at frequency *f*
x_a is the inductive reactance of the conductor to one foot spacing at frequency *f*
f is the frequency in Hz
D_e is the equivalent depth of earth return in ft
ρ is the soil resistivity in Ω-m

The positive sequence impedance, Z_1, of a transmission line (with earth return), ignoring the effects of overhead shield wires, is

$$Z_1 = r_a + jx_a + jx_d \ \ \Omega/\text{mi} \tag{C.6}$$

where

$$x_a = 0.2794 \times \frac{f}{60} \times \log_{10} \frac{1}{GMR}$$

$$x_d = 0.2794 \times \frac{f}{60} \times \log_{10} GMD$$

Copyright © 2015 IEEE. All rights reserved.
Copyright The Institute of Electrical and Electronics Engineers, Inc.
Provided by IHS under license with IEEE
No reproduction or networking permitted without license from IHS
Order Number: 02120914
Sold to:EGAT [700166108393] - VARRIS.Y@EGAT.CO.TH,
Not for Resale,2016-09-15 03:57:51 UTC

and

$$GMD = \sqrt[3]{d_{ab} \times d_{bc} \times d_{ca}}$$

The zero sequence self-impedance, $Z_{0(a)}$, of the transmission line (with earth return), with no overhead shield wires is

$$Z_{o(a)} = r_a + r_e + jx_a + jx_e - 2 \times x_d \ \Omega/\text{mi} \tag{C.7}$$

where

$$r_e = 0.00477 \times f \tag{C.8}$$

and

$$x_e = 0.006985 \times f \times \log_{10}\left(4.6655 \times 10^6 \times \frac{\rho}{f}\right)$$

and r_a, x_a, and x_d are as defined above using characteristics of the phase conductors.

The zero sequence self-impedance, $Z_{0(g)}$, of one overhead shield wire (with earth return) is

$$Z_{0(g)} = 3 \times r_a + r_e + j3 \times x_a + jx_e \ \Omega/\text{mi} \tag{C.9}$$

where r_a and x_a are as defined above using characteristics of the overhead shield wire, and r_e and x_e are as defined above.

The zero sequence self-impedance, $Z_{0(g)}$, of two overhead shield wires (with earth return) is

$$Z_{0(g)} = \frac{3}{2} \times r_a + r_e + j\frac{3}{2} \times x_a + jx_e - j\frac{3}{2} \times x_d \ \Omega/\text{mi} \tag{C.10}$$

where

$$x_d = 0.2794 \times \frac{f}{60} \times \log_{10} d_{xy} \tag{C.11}$$

d_{xy} is the distance between the two overhead shield wires, r_a and x_a are as defined above using characteristics of the overhead shield wire, and r_e and x_e are as defined above.

The zero sequence mutual impedance, $Z_{0(ag)}$ between one circuit and n shield wires (with earth return) is

$$Z_{0(ag)} = r_e + jx_e - j3 \times x_d \ \Omega/\text{mi} \tag{C.12}$$

where

$$x_d = 0.2794 \times \frac{f}{60} \times \log_{10}\left(\sqrt[3n]{d_{ag1} \times d_{bg1} \times d_{cg1} \ldots d_{agn} \times d_{bgn} \times d_{cgn}}\right) \tag{C.13}$$

Copyright © 2015 IEEE. All rights reserved.
Copyright The Institute of Electrical and Electronics Engineers, Inc.
Provided by IHS under license with IEEE
No reproduction or networking permitted without license from IHS
Order Number: 02120914
Sold to:EGAT [700166108393] - VARRIS.Y@EGAT.CO.TH,
Not for Resale,2016-09-15 03:57:51 UTC

d_{ag1} is the distance between phase *a* and the first overhead shield wire, etc., and r_e and x_e are as defined above.

Then, the zero sequence impedance of one circuit with *n* shield wires (and earth return) is

$$Z_0 = Z_{0(a)} - \frac{Z_{0(ag)}^2}{Z_{0(g)}} \ \Omega/\text{mi} \tag{C.14}$$

These equations for Z_1 and Z_0 are used, along with appropriate impedances for transformers, generators, etc., to compute the equivalent fault impedance.

To compute the impedance of an overhead shield wire or feeder neutral for use in Endrenyi's formula, the simple self-impedance (with earth return) of the conductor is used.

$$Z_s = r_c + \frac{r_e}{3} + jx_a + j\frac{x_e}{3} \ \Omega/\text{mi} \tag{C.15}$$

where

r_a and x_a are as defined above using characteristics of the overhead shield wire or feeder neutral, and r_e and x_e are as defined above.

Copyright © 2015 IEEE. All rights reserved.

Copyright The Institute of Electrical and Electronics Engineers, Inc.
Provided by IHS under license with IEEE
No reproduction or networking permitted without license from IHS

Order Number: 02120914
Sold to:EGAT [700166108393] - VARRIS.Y@EGAT.CO.TH,
Not for Resale,2016-09-15 03:57:51 UTC

Table C.1—Approximate equivalent impedance of transmission line overhead shield wires and distribution feeder neutrals

Number of transmission lines	Number of distribution neutrals	$R_{tg} = 15$; $R_{dg} = 25$; $R + jx$ (Ω)	$R_{tg} = 100$; $R_{dg} = 200$; $R + jx$ (Ω)
1	1	0.91 + *j*0.485	3.27 + *j*0.652
1	2	0.54 + *j*0.33	2.18 + *j*0.412
1	4	0.295 + *j*0.20	1.32 + *j*0.244
1	8	0.15 + *j*0.11	0.732 + *j*0.133
1	12	0.10 + *j*0.076	0.507 + *j*0.091
1	16	0.079 + *j*0.057	0.387 + *j*0.069
2	1	0.685 + *j*0.302	2.18 + *j*0.442
2	2	0.455 + *j*0.241	1.63 + *j*0.324
2	4	0.27 + *j*0.165	1.09 + *j*0.208
2	8	0.15 + *j*0.10	0.685 + *j*0.122
2	12	0.10 + *j*0.07	0.47 + *j*0.087
2	16	0.08 + *j*.055	0.366 + *j*0.067
4	1	0.45 + *j*0.16	1.30 + *j*0.273
4	2	0.34 + *j*0.15	1.09 + *j*0.22
4	4	0.23 + *j*0.12	0.817 + *j*0.16
4	8	0.134 + *j*0.083	0.546 + *j*0.103
4	12	0.095 + *j*0.061	0.41 + *j*0.077
4	16	0.073 + *j*0.05	0.329 + *j*0.06
8	1	0.27 + *j*0.08	0.72 + *j*0.152
8	2	0.23 + *j*0.08	0.65 + *j*0.134
8	4	0.17 + *j*0.076	0.543 + *j*0.11
8	8	0.114 + *j*0.061	0.408 + *j*0.079
8	12	0.085 + *j*0.049	0.327 + *j*0.064
8	16	0.067 + *j*0.041	0.273 + *j*0.052
12	1	0.191 + *j*0.054	0.498 + *j*0.106

Copyright © 2015 IEEE. All rights reserved.

Copyright The Institute of Electrical and Electronics Engineers, Inc.
Provided by IHS under license with IEEE
No reproduction or networking permitted without license from IHS

Order Number: 02120914
Sold to:EGAT [700166108393] - VARRIS.Y@EGAT.CO.TH,
Not for Resale,2016-09-15 03:57:51 UTC

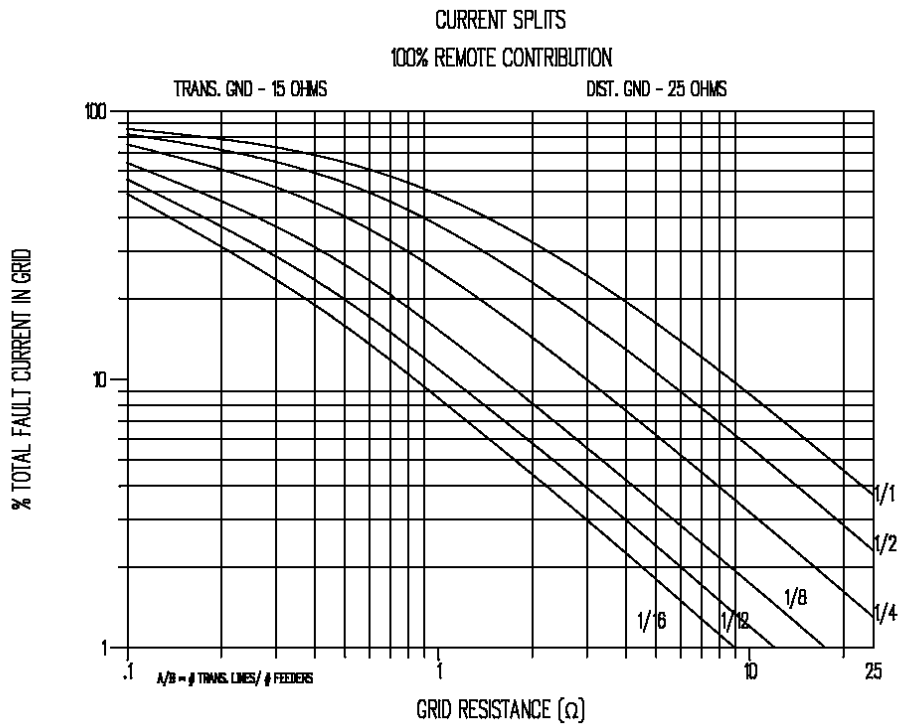

Figure C.1—Curves to approximate split factor S_f

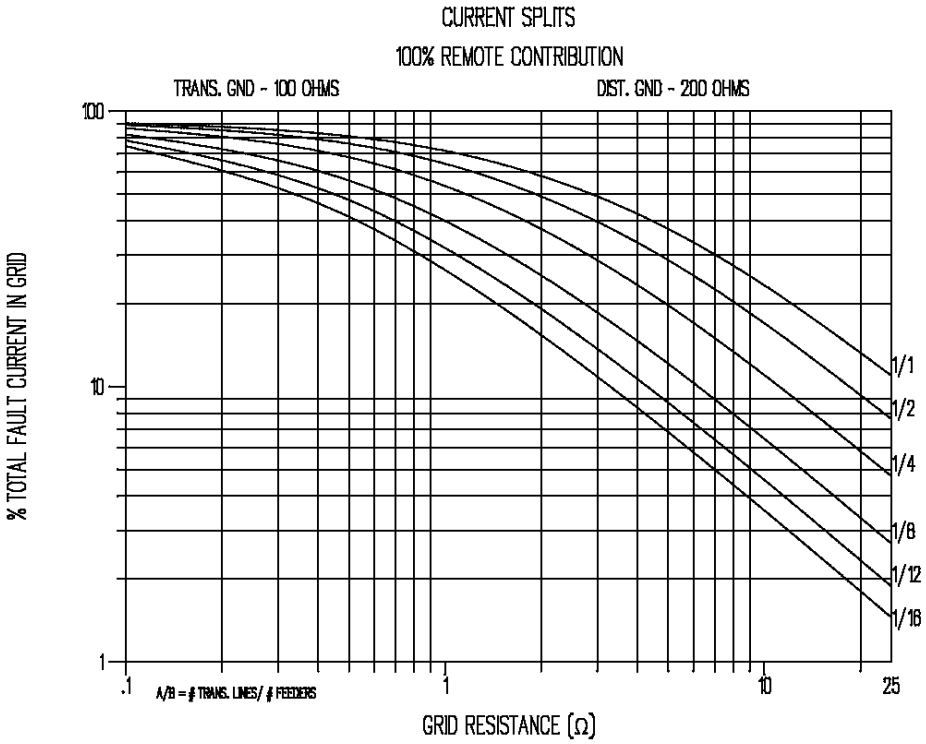

Figure C.2—Curves to approximate split factor S_f

Copyright © 2015 IEEE. All rights reserved.

Copyright The Institute of Electrical and Electronics Engineers, Inc.
Provided by IHS under license with IEEE
No reproduction or networking permitted without license from IHS

Order Number: 02120914
Sold to:EGAT [700166108393] - VARRIS.Y@EGAT.CO.TH,
Not for Resale,2016-09-15 03:57:51 UTC

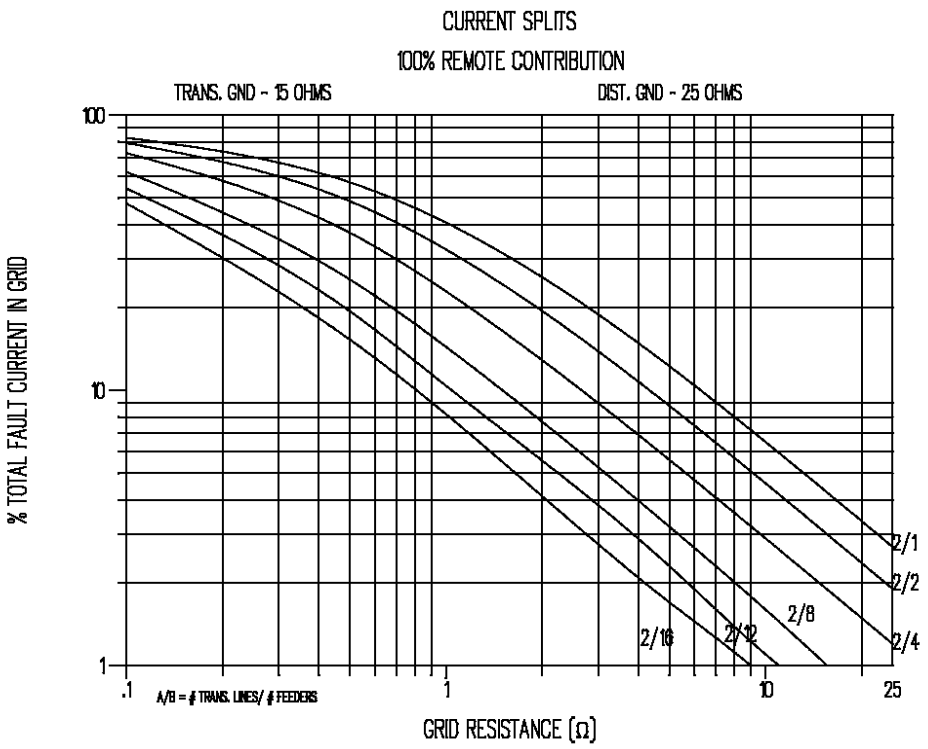

Figure C.3—Curves to approximate split factor S_f

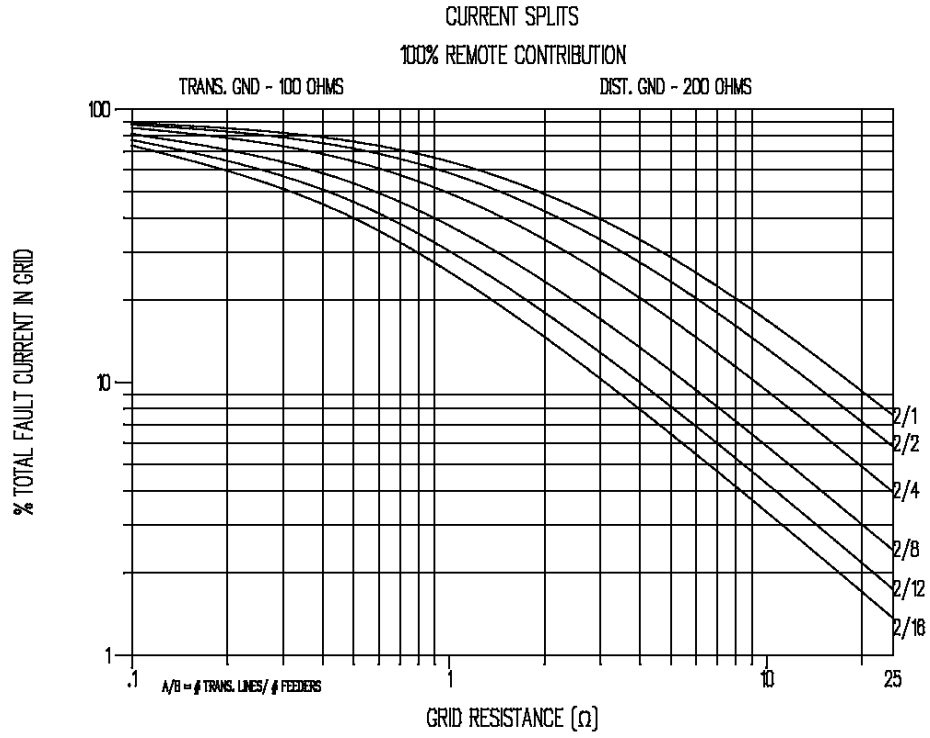

Figure C.4—Curves to approximate split factor S_f

Copyright © 2015 IEEE. All rights reserved.

Copyright The Institute of Electrical and Electronics Engineers, Inc.
Provided by IHS under license with IEEE
No reproduction or networking permitted without license from IHS

Order Number: 02120914
Sold to:EGAT [700166108393] - VARRIS.Y@EGAT.CO.TH,
Not for Resale,2016-09-15 03:57:51 UTC

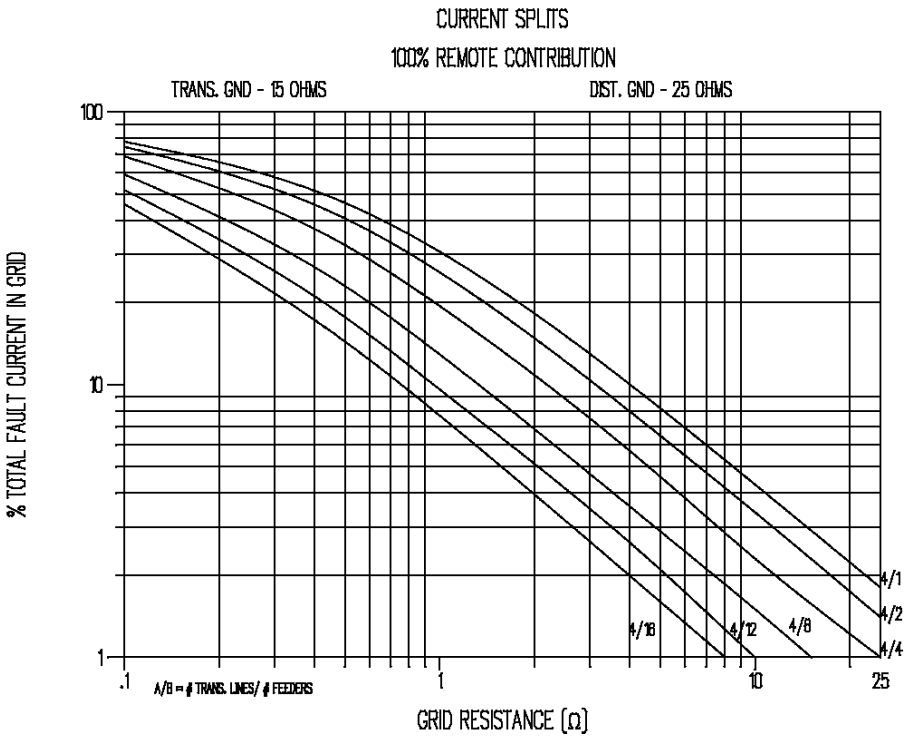

Figure C.5—Curves to approximate split factor S_f

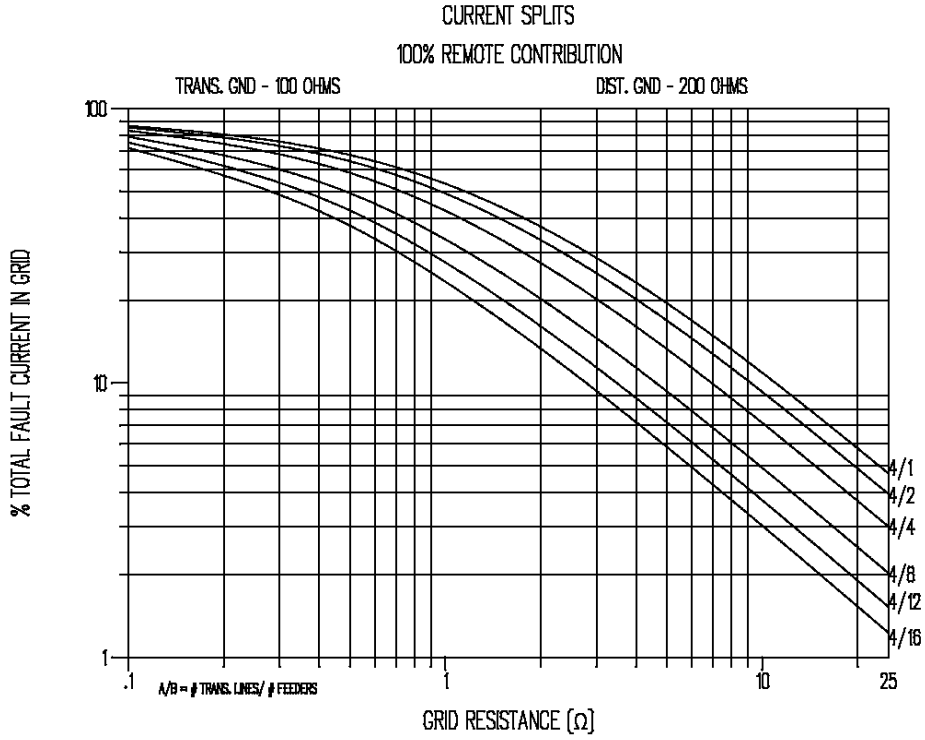

Figure C.6—Curves to approximate split factor S_f

Copyright © 2015 IEEE. All rights reserved.

Copyright The Institute of Electrical and Electronics Engineers, Inc.
Provided by IHS under license with IEEE
No reproduction or networking permitted without license from IHS

Order Number: 02120914
Sold to:EGAT [700166108393] - VARRIS.Y@EGAT.CO.TH,
Not for Resale,2016-09-15 03:57:51 UTC

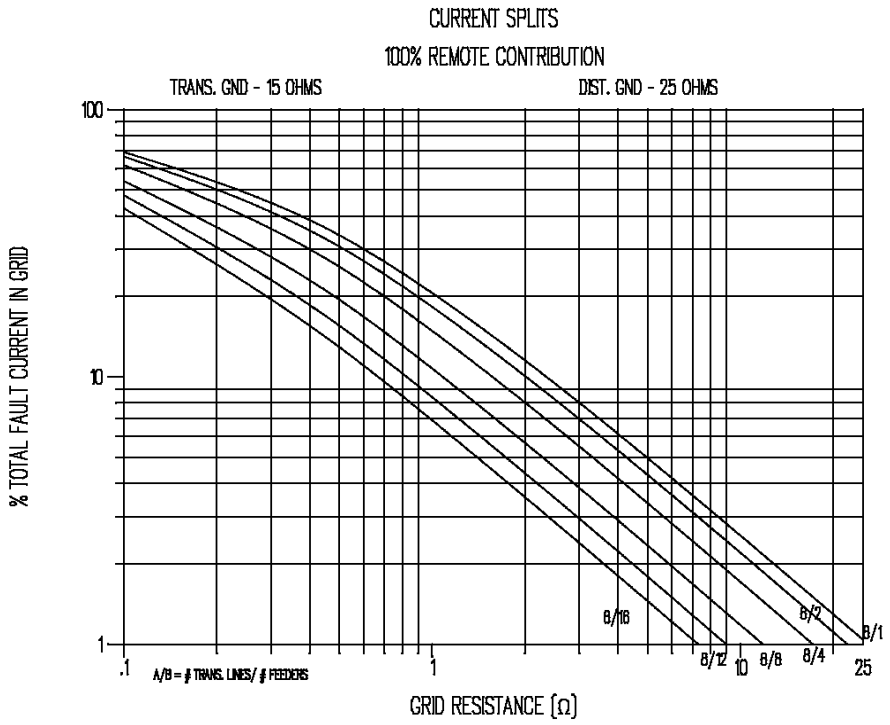

Figure C.7—Curves to approximate split factor S_f

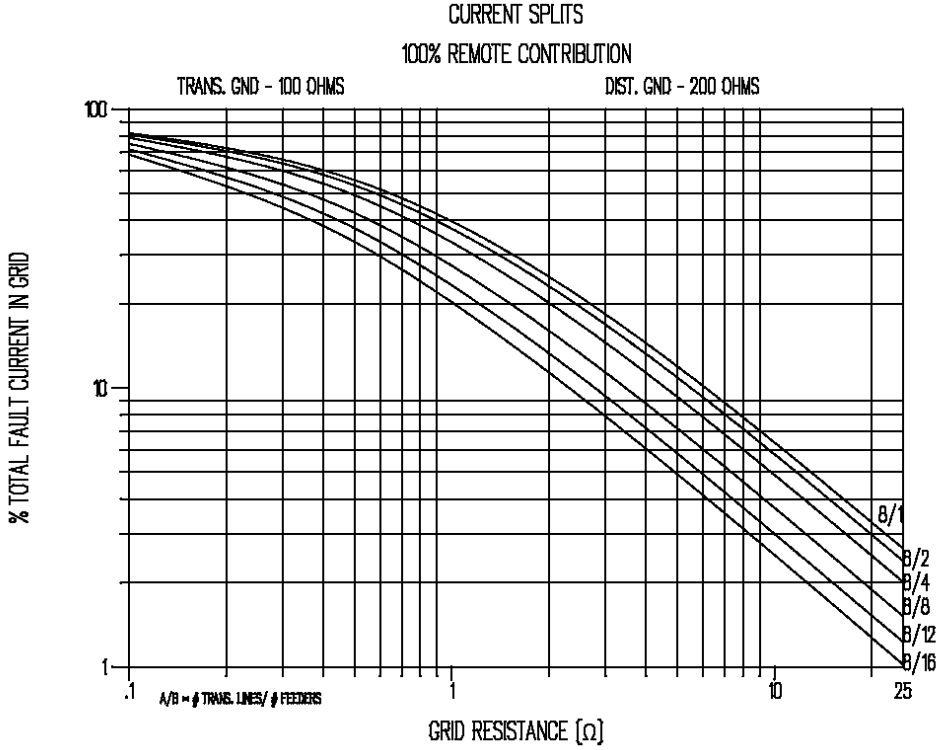

Figure C.8—Curves to approximate split factor S_f

Copyright © 2015 IEEE. All rights reserved.

Copyright The Institute of Electrical and Electronics Engineers, Inc.
Provided by IHS under license with IEEE
No reproduction or networking permitted without license from IHS

Order Number: 02120914
Sold to:EGAT [700166108393] - VARRIS.Y@EGAT.CO.TH,
Not for Resale,2016-09-15 03:57:51 UTC

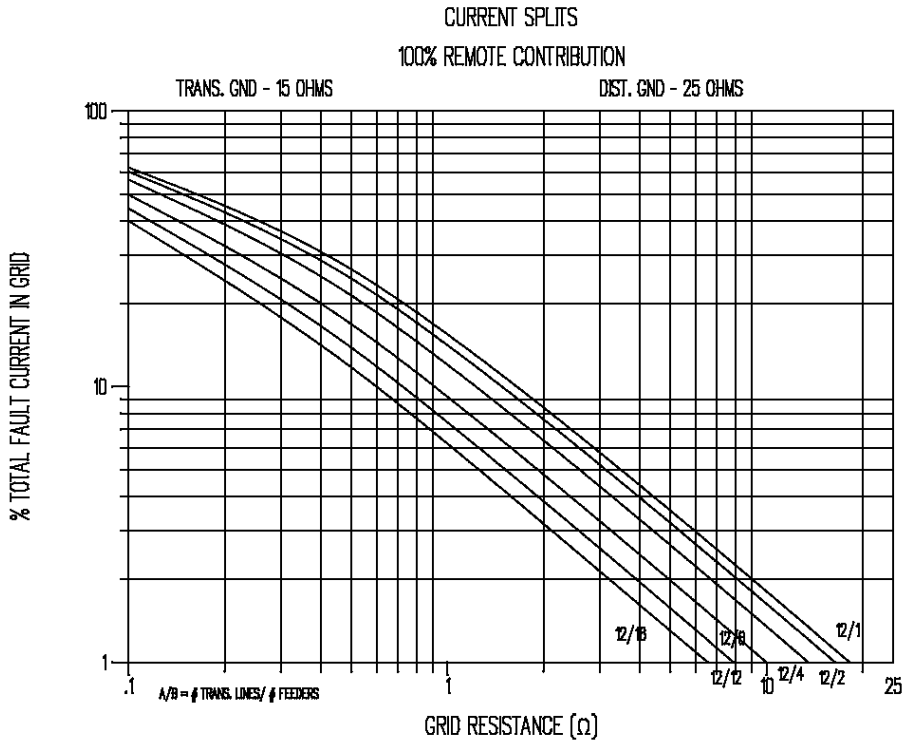

Figure C.9—Curves to approximate split factor S_f

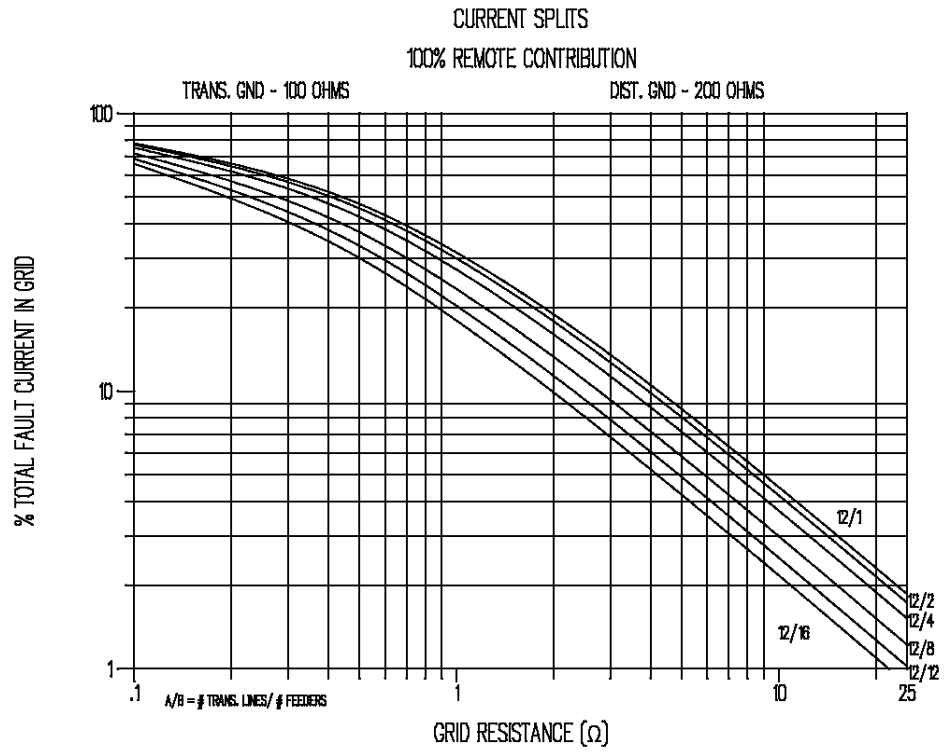

Figure C.10—Curves to approximate split factor S_f

Copyright © 2015 IEEE. All rights reserved.

Copyright The Institute of Electrical and Electronics Engineers, Inc.
Provided by IHS under license with IEEE
No reproduction or networking permitted without license from IHS

Order Number: 02120914
Sold to:EGAT [700166108393] - VARRIS.Y@EGAT.CO.TH,
Not for Resale,2016-09-15 03:57:51 UTC

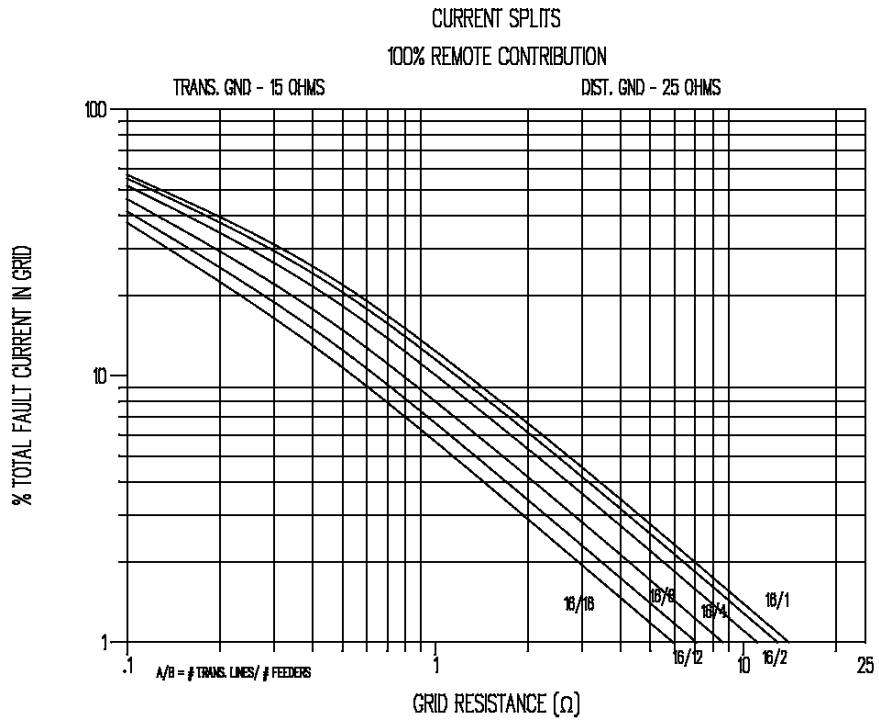

Figure C.11—Curves to approximate split factor S_f

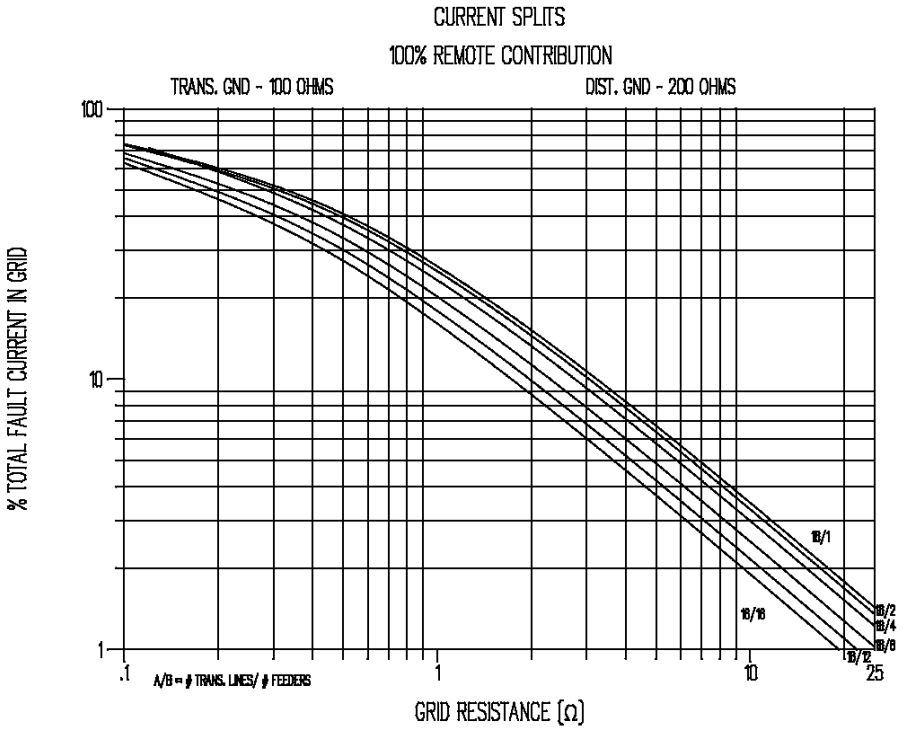

Figure C.12—Curves to approximate split factor S_f

Copyright © 2015 IEEE. All rights reserved.

Copyright The Institute of Electrical and Electronics Engineers, Inc.
Provided by IHS under license with IEEE
No reproduction or networking permitted without license from IHS

Order Number: 02120914
Sold to:EGAT [700166108393] - VARRIS.Y@EGAT.CO.TH,
Not for Resale,2016-09-15 03:57:51 UTC

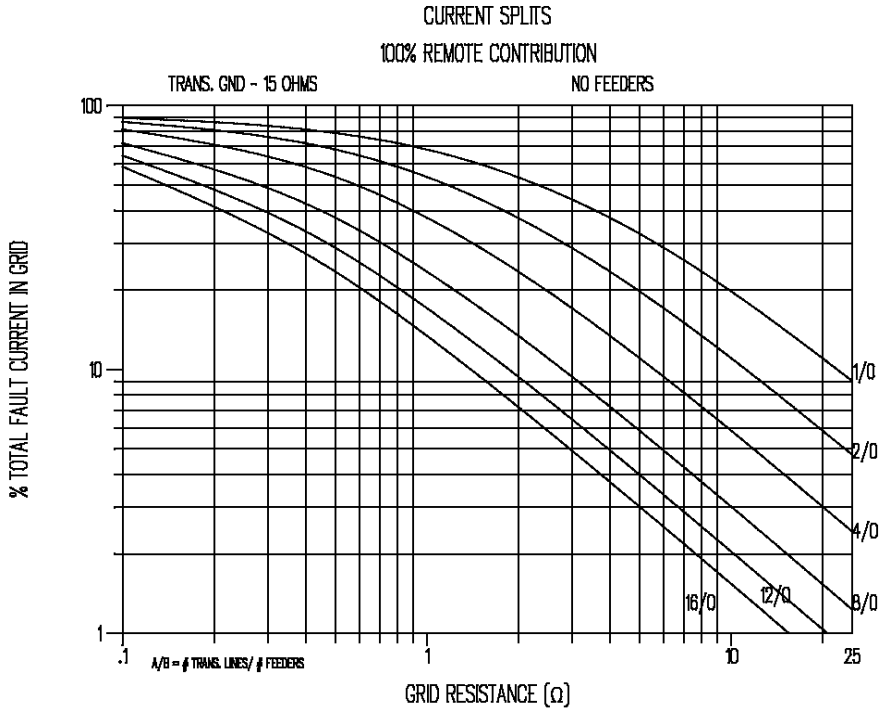

Figure C.13—Curves to approximate split factor S_f

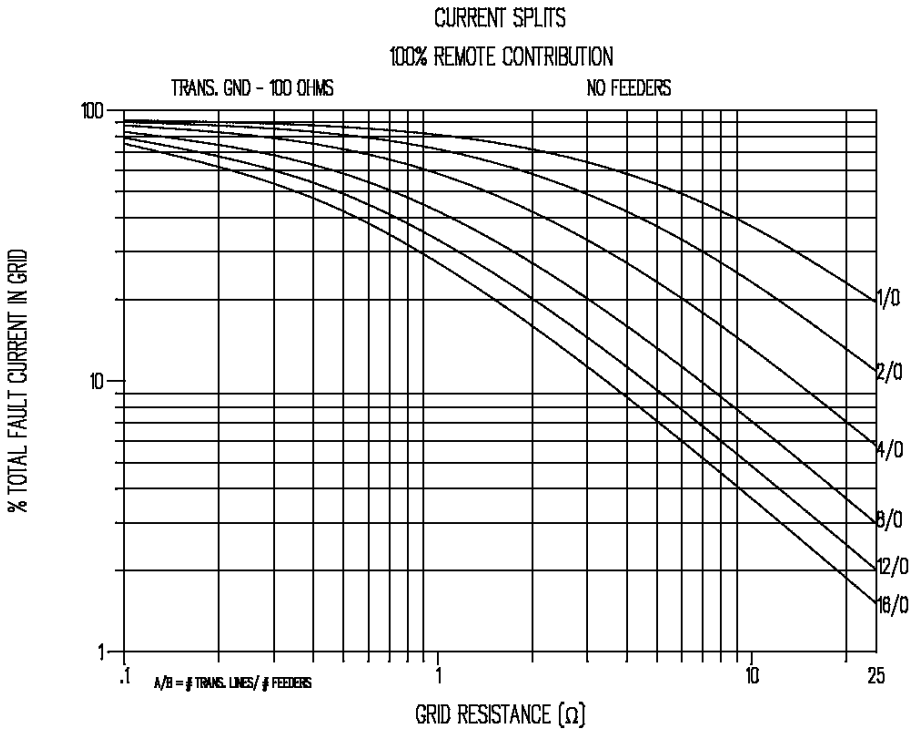

Figure C.14—Curves to approximate split factor S_f

Copyright © 2015 IEEE. All rights reserved.

Copyright The Institute of Electrical and Electronics Engineers, Inc.
Provided by IHS under license with IEEE
No reproduction or networking permitted without license from IHS

Order Number: 02120914
Sold to:EGAT [700166108393] - VARRIS.Y@EGAT.CO.TH,
Not for Resale,2016-09-15 03:57:51 UTC

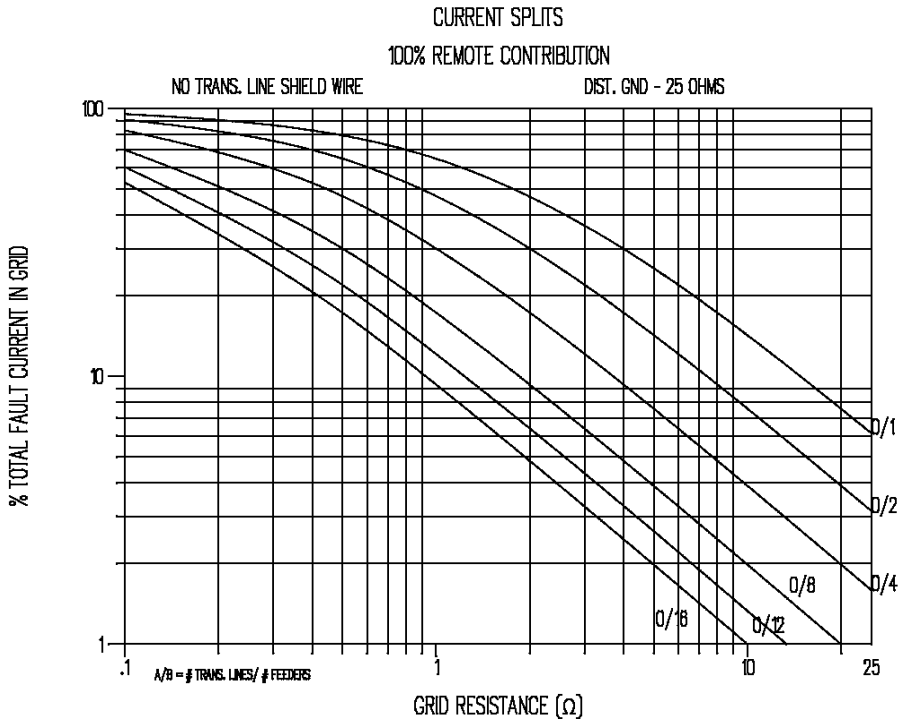

Figure C.15—Curves to approximate split factor S_f

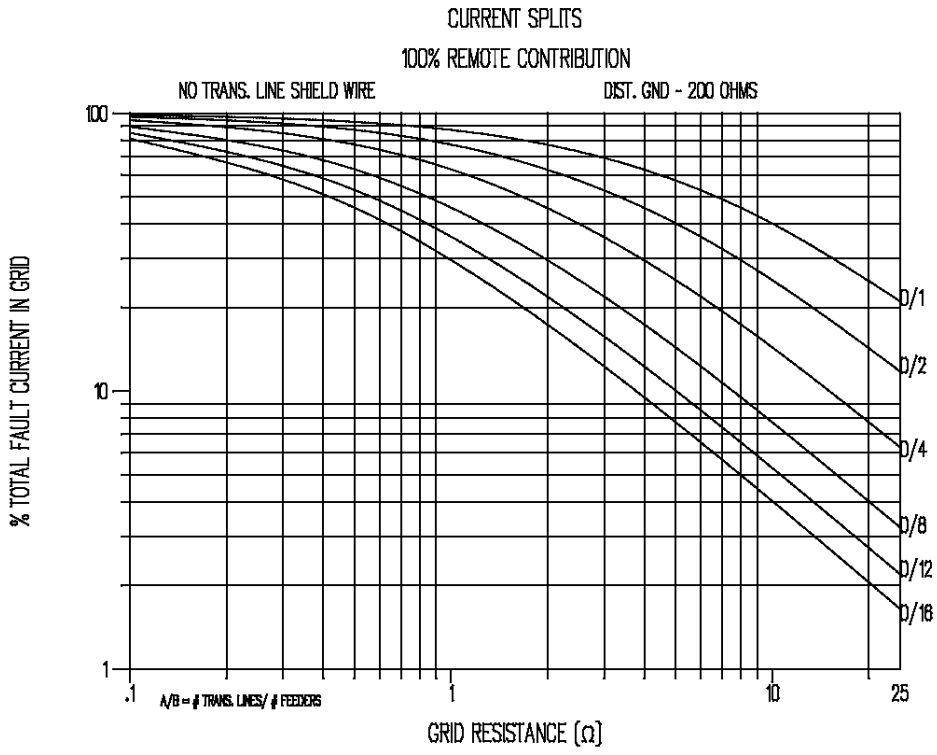

Figure C.16—Curves to approximate split factor S_f

Copyright © 2015 IEEE. All rights reserved.

Copyright The Institute of Electrical and Electronics Engineers, Inc.
Provided by IHS under license with IEEE
No reproduction or networking permitted without license from IHS

Order Number: 02120914
Sold to:EGAT [700166108393] - VARRIS.Y@EGAT.CO.TH,
Not for Resale,2016-09-15 03:57:51 UTC

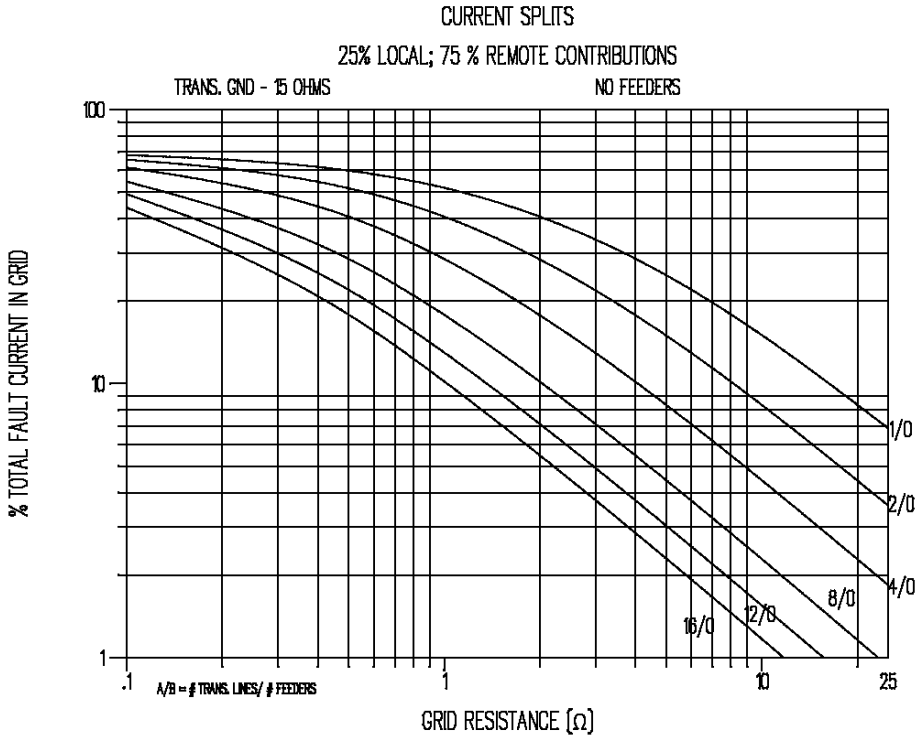

Figure C.17—Curves to approximate split factor S_f

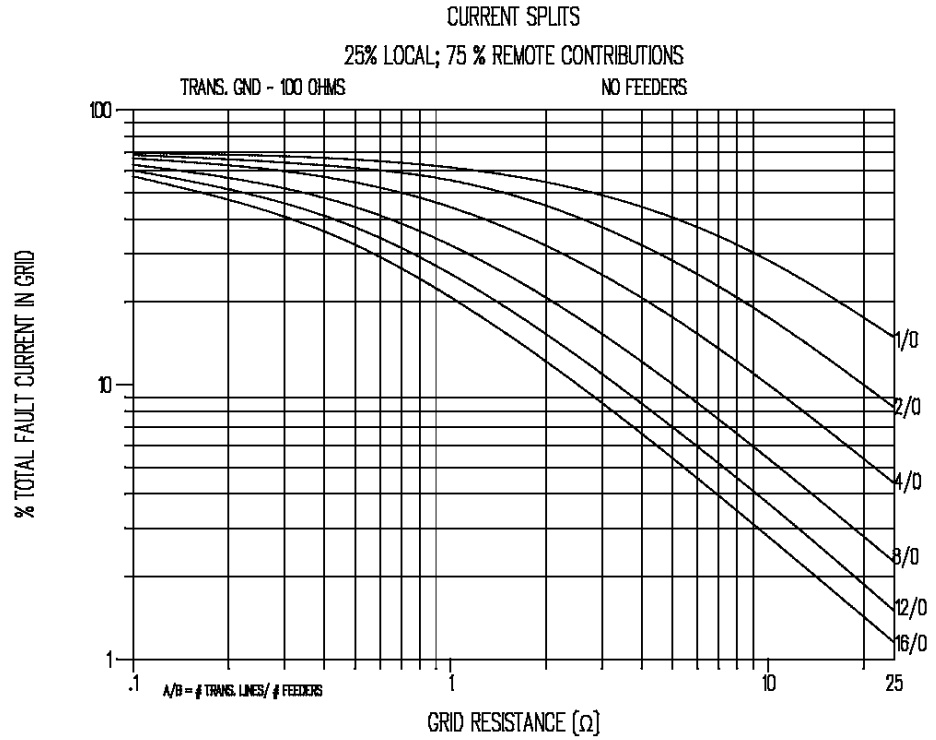

Figure C.18—Curves to approximate split factor S_f

Copyright © 2015 IEEE. All rights reserved.

Copyright The Institute of Electrical and Electronics Engineers, Inc.
Provided by IHS under license with IEEE
No reproduction or networking permitted without license from IHS

Order Number: 02120914
Sold to:EGAT [700166108393] - VARRIS.Y@EGAT.CO.TH,
Not for Resale,2016-09-15 03:57:51 UTC

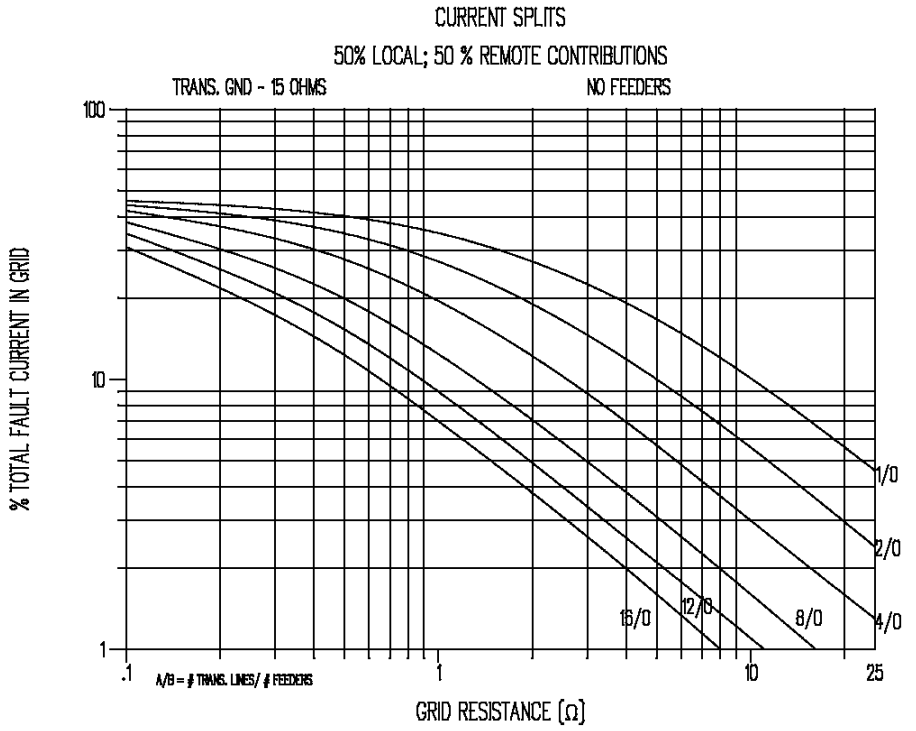

Figure C.19—Curves to approximate split factor S_f

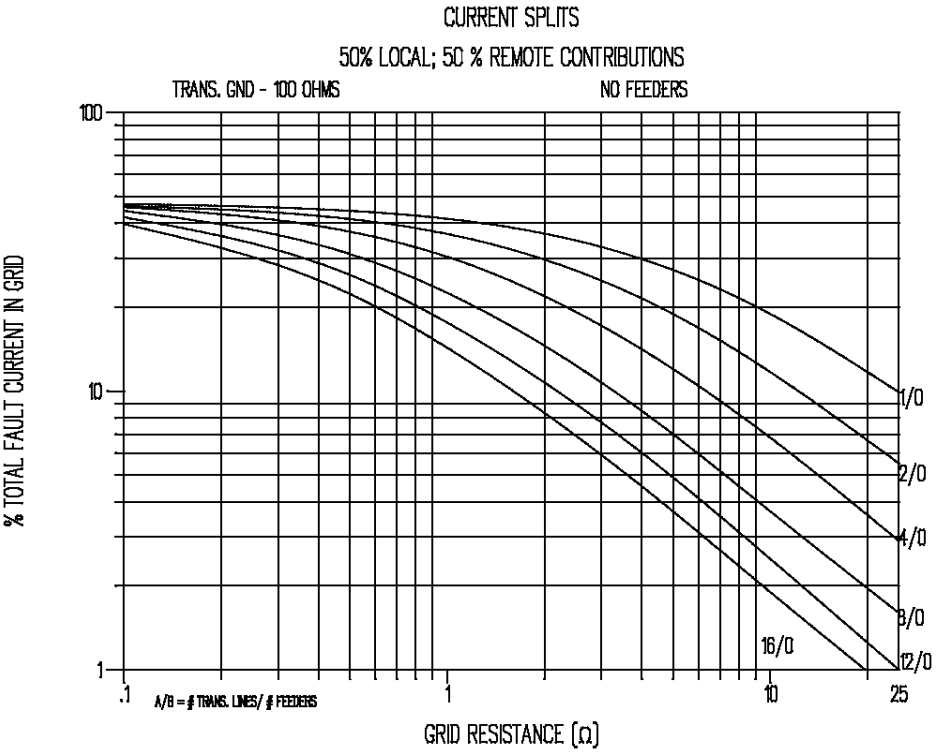

Figure C.20—Curves to approximate split factor S_f

Copyright © 2015 IEEE. All rights reserved.

Copyright The Institute of Electrical and Electronics Engineers, Inc.
Provided by IHS under license with IEEE
No reproduction or networking permitted without license from IHS

Order Number: 02120914
Sold to:EGAT [700166108393] - VARRIS.Y@EGAT.CO.TH,
Not for Resale,2016-09-15 03:57:51 UTC

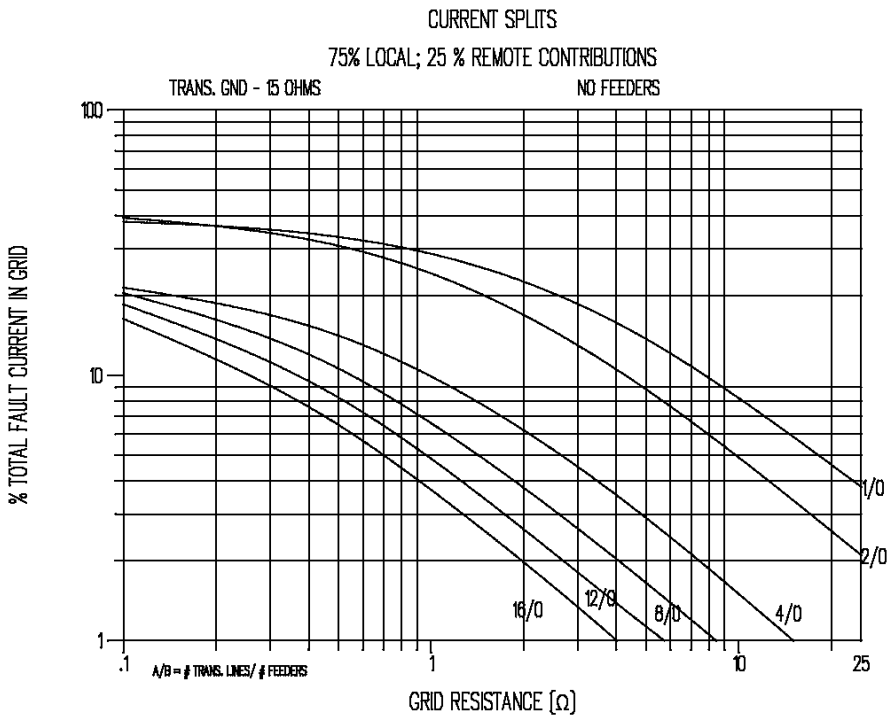

Figure C.21—Curves to approximate split factor S_f

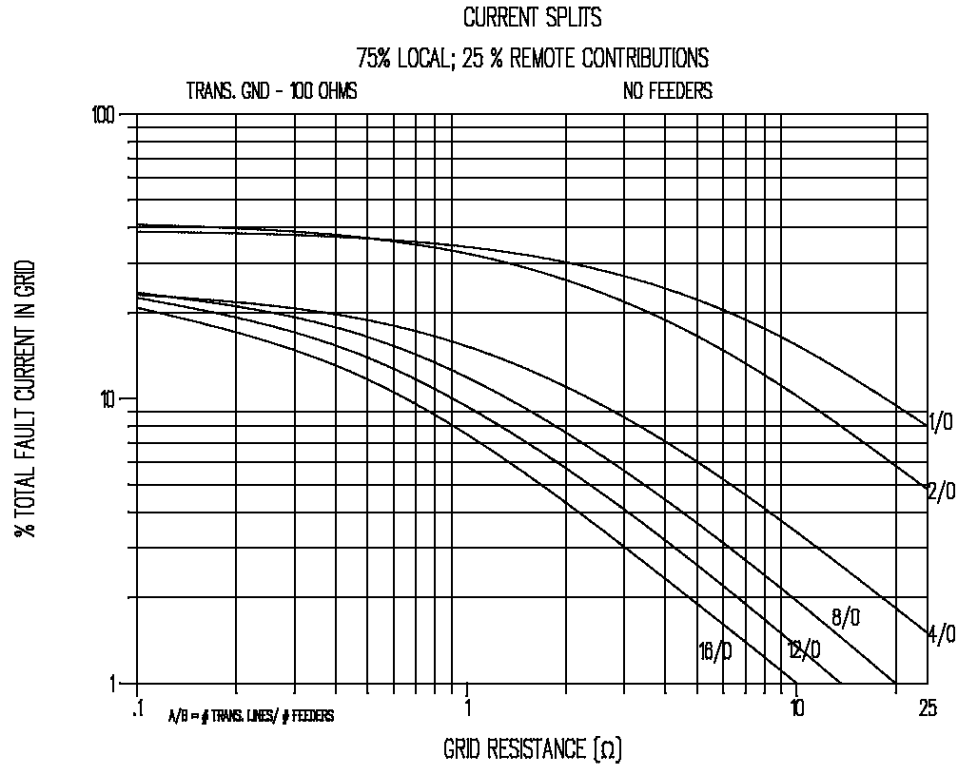

Figure C.22—Curves to approximate split factor S_f

Copyright © 2015 IEEE. All rights reserved.

Copyright The Institute of Electrical and Electronics Engineers, Inc.
Provided by IHS under license with IEEE
No reproduction or networking permitted without license from IHS

Order Number: 02120914
Sold to:EGAT [700166108393] - VARRIS.Y@EGAT.CO.TH,
Not for Resale,2016-09-15 03:57:51 UTC

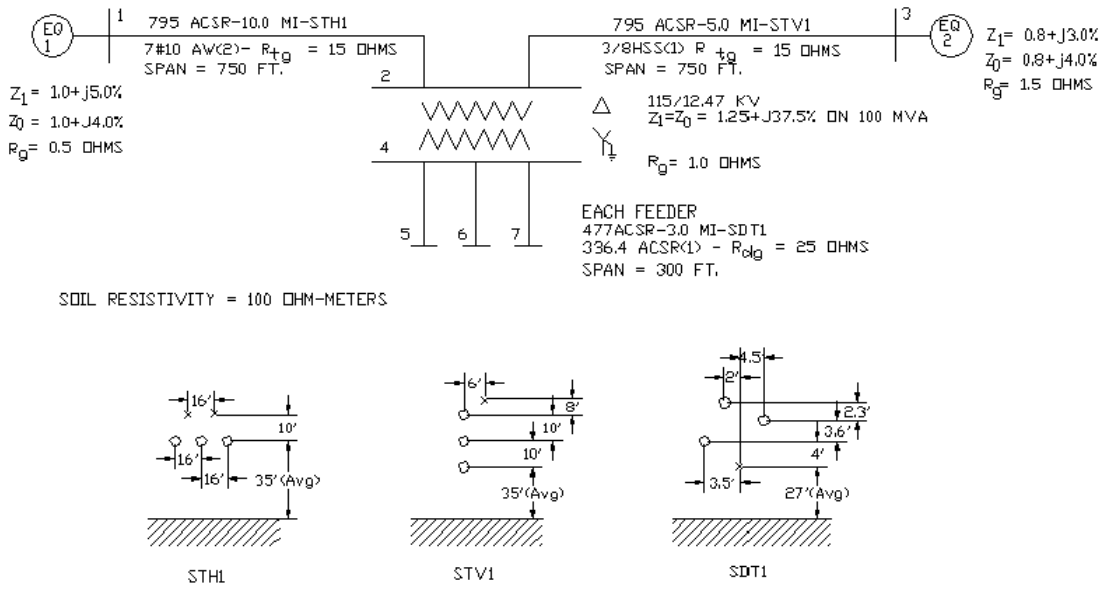

Figure C.23—System and configuration data for Example 1 of C.3

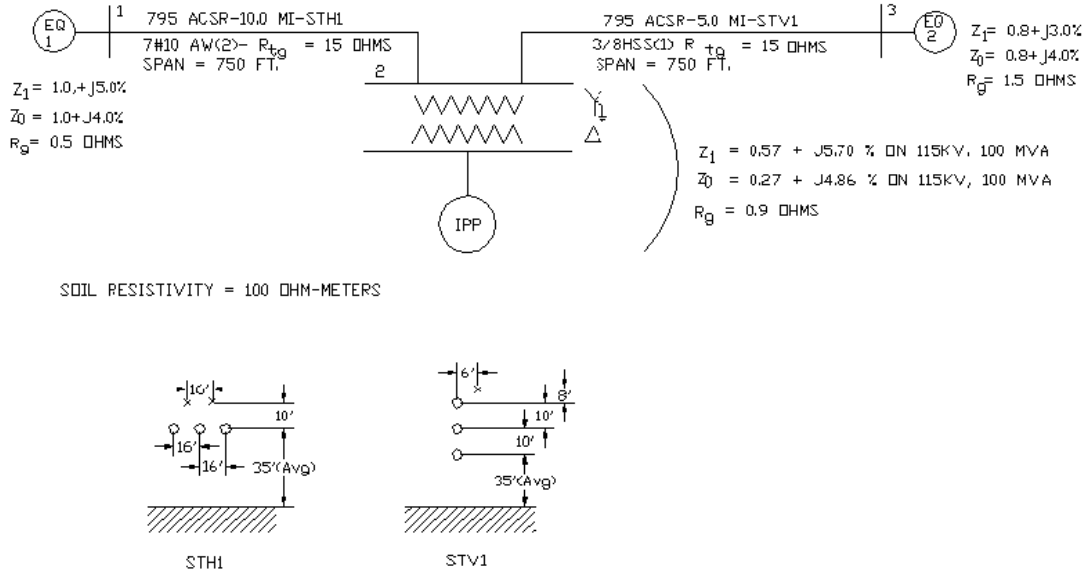

Figure C.24—System and configuration data for Example 2 of C.3

Copyright © 2015 IEEE. All rights reserved.

Copyright The Institute of Electrical and Electronics Engineers, Inc.
Provided by IHS under license with IEEE
No reproduction or networking permitted without license from IHS

Order Number: 02120914
Sold to:EGAT [700166108393] - VARRIS.Y@EGAT.CO.TH,
Not for Resale,2016-09-15 03:57:51 UTC

Annex D

(informative)

Simplified step and mesh equations

In the previous editions of this guide, the following equation was provided for determining the value of a mesh voltage (in volts) on the earth's surface above the center of a corner mesh (assuming an equally spaced rectangular grid, which is buried at depth h in a homogeneous soil of uniform resistivity). This grid may consist of n parallel conductors spaced D apart, and of an undetermined number of cross-connections. All grid wires are assumed to be of diameter d. The spacing of parallel conductors D, as well as d and h, are in meters.

$$E_m = \frac{\rho \times K_m \times K_i \times I_G}{L_M} \tag{D.1}$$

where

E_m is the mesh voltage in V

ρ is the average soil resistivity in Ω-m

I_G is the maximum rms current flowing between ground grid and earth in A

L_M is the total length of buried conductors, including cross-connections, and (optionally) the combined length of ground rods in m

K_i is the corrective factor for current irregularity

K_m is the mesh factor defined for n parallel conductors

The AIEE Working Group on Substation Grounding Practices [B4] derived the factors K_m and K_i to account for the geometry of the grounding system. The relationship between K_m and E_m depends largely on the current density in the perimeter conductors versus the current density in the inner conductors. To reflect this effect of current density and to correct some of the deficiencies in the equation for K_m, Sverak [B136] added the weighting terms, K_{ii} and K_h into the equation for K_m. The resulting equation for K_m was more accurate and versatile than previous forms of the equation

$$K_m = \frac{1}{2 \times \pi} \times \left[\ln\left[\frac{D^2}{16 \times h \times d} + \frac{(D + 2 \times h)^2}{8 \times D \times d} - \frac{h}{4 \times d} \right] + \frac{K_{ii}}{K_h} \times \ln\left[\frac{8}{\pi(2 \times n - 1)} \right] \right] \tag{D.2}$$

For grids with ground rods along the perimeter, or for grids with ground rods in the grid corners, as well as both along the perimeter and throughout the grid area

$$K_{ii} = 1$$

For grids with no ground rods or grids with only a few ground rods, none located in the corners or on the perimeter.

$$K_{ii} = \frac{1}{(2 \times n)^{\frac{2}{n}}} \tag{D.3}$$

Copyright © 2015 IEEE. All rights reserved.
Copyright The Institute of Electrical and Electronics Engineers, Inc.
Provided by IHS under license with IEEE
No reproduction or networking permitted without license from IHS
Order Number: 02120914
Sold to:EGAT [700166108393] - VARRIS.Y@EGAT.CO.TH,
Not for Resale,2016-09-15 03:57:51 UTC

$$K_h = \sqrt{1 + \frac{h}{h_0}} \tag{D.4}$$

h_o = 1 m (grid reference depth)

Because of assumptions made in the derivation of K_m, a corrective factor K_i is needed to compensate for the fact that the subject mathematical model of n parallel conductors cannot fully account for the effects of a grid geometry; that is, for two sets of parallel conductors that are perpendicular to each other and interconnected at the cross-connection points. For a large number of square and rectangular grids, the mesh voltage was obtained using a computer. From this computer-generated data, a new expression for K_i was found to better fit in the mesh voltage equation (Thapar, Gerez, Balakrishnan, and Blank [B148]). This factor is

$$K_i = 0.644 + 0.148 \times n \tag{D.5}$$

The simplified E_m equation used in the previous edition of the guide has been limited to square and rectangular grids with square meshes. In practice, a large number of ground grids have shapes other than square or rectangular. While the specific formula for K_m has remained the same as the 1986 edition of the guide, a new value of n based on the geometry of the grid and the geometry of the meshes was developed in Thapar, Gerez, Balakrishnan, and Blank [B148] to allow Equation (D.2), Equation (D.3), and Equation (D.5) to be effective for a variety of grid shapes, including symmetrical T-shaped, triangular, and L-shaped grids.

$$n = n_a \times n_b \times n_c \times n_d \tag{D.6}$$

where

$$n_a = \frac{2 \times L_C}{L_p} \tag{D.7}$$

n_b = 1 for square grids

n_c = 1 for square and rectangular grids

n_d = 1 for square, rectangular, and L-shaped grids

Otherwise

$$n_b = \sqrt{\frac{L_p}{4 \times \sqrt{A}}} \tag{D.8}$$

$$n_c = \left[\frac{L_x \times L_y}{A} \right]^{\frac{0.7 \times A}{L_x \times L_y}} \tag{D.9}$$

$$n_d = \frac{D_m}{\sqrt{L_x^2 + L_y^2}} \tag{D.10}$$

Copyright © 2015 IEEE. All rights reserved.

Copyright The Institute of Electrical and Electronics Engineers, Inc.
Provided by IHS under license with IEEE
No reproduction or networking permitted without license from IHS

Order Number: 02120914
Sold to:EGAT [700166108393] - VARRIS.Y@EGAT.CO.TH,
Not for Resale,2016-09-15 03:57:51 UTC

where

L_c is the total length of the conductor in the horizontal grid in m
L is the peripheral length of the grid in m
A is the area of the grid in m^2
L_x is the maximum length of the grid in the x direction in m
L is the maximum length of the grid in the y direction in m
D_m is the maximum distance between any two points on the grid in m

While these changes to the equations did expand their use to include a variety of practical ground grid shapes, they did not include the use of ground rods. An attempt was made to expand these equations to include the use of ground rods. If L_C represents the total grid conductor length, L_R represents the total length of all ground rods, and L_r represents the average length of each ground rod, then for grids with ground rods in the corners, as well as along the perimeter and throughout the grid.

$$E_m = \frac{\rho \times I_G \times K_m \times K_i}{L_C + \left[1.55 + 1.22 \times \left(\frac{L_r}{\sqrt{L_x^2 + L_y^2}}\right)\right] \times L_R} \tag{D.11}$$

The multiplier for L_R is an empirical function that reflects the fact that the current density is higher in the ground rods than in the horizontal grid conductors for uniform soil.

In the previous editions of this guide, the following equation was provided for determining the value of the worst case step voltage (in volts):

$$E_s = \frac{\rho \times I_G \times K_s \times K_i}{L_S} \tag{D.12}$$

where

E_s is the step voltage in V
ρ is the average soil resistivity in Ω-m
I_G is the maximum rms current flowing between ground grid and earth in A
L_S is the total length of buried conductors, including cross-connections, and (optionally) the total effective length of ground rods in m
K is the corrective factor for current irregularity
K_s is the mesh factor defined for n parallel conductors

Sverak [B136] derived a factor K_s, based on the geometry of a ground grid with no ground rods. As with the mesh voltage, this K_s is proportional to the step voltage E_s. Again, computer simulations were used to derive empirical factors to improve the accuracy of previous versions of E_S, specifically the factor n (Thapar, Gerez, Balakrishnan, and Blank [B148]).

$$K_s = \frac{1}{\pi}\left[\frac{1}{2 \times h} + \frac{1}{D + h} + \frac{1}{D}\left(1 - 0.5^{n-2}\right)\right] \tag{D.13}$$

Copyright © 2015 IEEE. All rights reserved.

Copyright The Institute of Electrical and Electronics Engineers, Inc.
Provided by IHS under license with IEEE
No reproduction or networking permitted without license from IHS

Order Number: 02120914
Sold to:EGAT [700166108393] - VARRIS.Y@EGAT.CO.TH,
Not for Resale,2016-09-15 03:57:51 UTC

where n, D, and h are defined above.

While these changes to the equations did expand their use to include a variety of practical ground grid shapes, they did not include the use of ground rods. An attempt was made to expand these equations to include the use of ground rods. If L_C represents the total grid conductor length and L_R represents the total length of all ground rods, then for grids with or without ground rods

$$E_S = \frac{\rho \times I_G \times K_S \times K_i}{0.75 \times L_C + 0.85 \times L_R} \tag{D.14}$$

These new simplified equations were compared to computer solutions for hundreds of different ground grids and the results compared favorably.

Copyright © 2015 IEEE. All rights reserved.

Copyright The Institute of Electrical and Electronics Engineers, Inc.
Provided by IHS under license with IEEE
No reproduction or networking permitted without license from IHS

Order Number: 02120914
Sold to:EGAT [700166108393] - VARRIS.Y@EGAT.CO.TH,
Not for Resale,2016-09-15 03:57:51 UTC

Annex E

(informative)

Equivalent uniform soil model for non-uniform soils

In the interest of simplicity, several assumptions have been made in developing the ground grid design equations of this guide. One such assumption is that these equations are only valid for a uniform soil resistivity model regardless of the soil under consideration. A survey indicated the need to provide a guideline for representing a soil regardless of its type by a uniform equivalent and, thus, remove this limitation in the use of the design equations.

A typical soil has several layers, each having a different resistivity. Most often lateral changes also occur, but in comparison to the vertical layers, these changes usually are more gradual. Station sites where the soil may possess uniform resistivity throughout the area and to a considerable depth are seldom found. A uniform soil interpretation of apparent resistivities obtained in the field, under these circumstances, is the most difficult task to perform even with the help of computers. Accordingly, it must be recognized that the soil model is only an approximation of the actual soil conditions and that a perfect match is unlikely. However, it has been recognized that the two-layer representation of a soil is closer to the actual soil conditions compared to its uniform equivalent.

Sometimes, in a multilayer soil, the variation in apparent soil resistivity ρ_a with respect to depth or pin spacing is not too great. Such a soil can be represented as a uniform soil with a single soil resistivity value. Although it is difficult to draw a clear line to indicate whether the soil is uniform or not, the approach taken here consists of defining the uniform soil based on the two-layer equivalents of several field-measured resistivity profiles. The computer program of EPRI TR-100622 [B64] was used to compute an equivalent two-layer soil model. The computer values indicated that a soil can be represented as a uniform soil if the difference between two extreme values of apparent resistivity is moderate. After it is determined that the soil can be approximated as uniform, the average apparent resistivity value computed from Equation (E.1) represents that soil in the design equations.

$$\rho_{a(av1)} = \frac{\rho_{a(1)} + \rho_{a(2)} + \rho_{a(3)} \cdots + \rho_{a(n)}}{n} \tag{E.1}$$

where $\rho_{a(1)}$, $\rho_{a(2)}$, $\rho_{a(3)}$... $\rho_{a(n)}$ are the apparent resistivity measurements obtained at n different spacings in four-pin method or at n different depths in driven ground rod method in Ω-m.

A majority of the soils will not meet the above criteria for the uniform soil. To determine uniform soil models to represent non-uniform soils, a similar approach was taken. The measured apparent resistivity data from several sites were used to obtain three different soil models: a two-layer soil model computed with EPRI TR-100622 [B64], and two different uniform soil models using Equation (E.1) and Equation (E.2).

$$\rho_{a(av2)} = \frac{\rho_{a(\max)} + \rho_{a(\min)}}{2} \tag{E.2}$$

where

$\rho_{a(max)}$ is the maximum apparent resistivity value (from measured data), Ω-m

$\rho_{a(min)}$ is the minimum apparent resistivity value (from measured data), Ω-m

The next step was to compute the ground grid resistance R_g, the corner mesh voltage E_{mesh}, and the corner step voltage E_{step} for a typical ground grid using EPRI TR-100622 [B64]. A 76.2 m × 76.2 m ground grid

Copyright © 2015 IEEE. All rights reserved.

Copyright The Institute of Electrical and Electronics Engineers, Inc.
Provided by IHS under license with IEEE
No reproduction or networking permitted without license from IHS

Order Number: 02120914
Sold to:EGAT [700166108393] - VARRIS.Y@EGAT.CO.TH,
Not for Resale,2016-09-15 03:57:51 UTC

with 64 meshes and uniformly distributed ground rods was selected for this investigation. The grid current was held constant at 1 kA. The length of the 5/8 in ground rods varied with the soil model. For a given soil model, this length was determined so as to reach the depth (or pin spacing) where $\rho_{a(av1)}$ or $\rho_{a(av2)}$ occurred in the measured apparent resistivity profile. For soil type 1, this occurs at approximately 12.2 m (40 ft). For soil type 2, this occurs at approximately 18.3 m (60 ft). Figure E.1 illustrates the modeled ground grid including the locations for computed step and touch voltages.

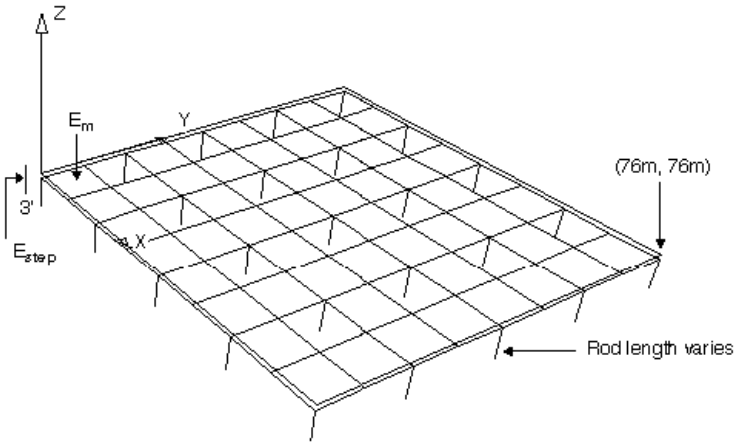

Figure E.1—The ground grid modeled for computing grounding parameters

Following the computations, the grounding parameters computed with the two-layer model were compared with those computed using the uniform soil models. This comparison indicated that the mesh and step voltages computed with the soil model represented by $\rho_{a(av2)}$ yielded values comparable to those computed with the two-layer model for the soils investigated.

Table E.1 presents the comparison of grounding parameters computed using the two-layer soil model with those computed using the uniform soil model represented by $\rho_{a(av2)}$ for two typical soils. The soil resistivity values shown in Table E.2 were modeled using computer software to determine Wenner measurements that represent assumed two-layer soil models.

Table E.1—Ground parameters computed with two-layer soil compared with those computed with equivalent uniform soil model

Soil type	Computed grounding parameters with two-layer soil model				Computed grounding parameters with uniform soil model			
	ρ_1, ρ_2, h Ω-m, Ω-m, m	R_g Ω	E_m (V)	E_s (V)	$\rho_{(av2)}$ Ω-m	R_g Ω	E_m (V)	E_s (V)
1	100, 300, 6.1	1.26	114.3	81.4	164	0.91	143	82
2	300, 100, 6.1	0.62	123.6	63	197	1.00	140.6	84.3

Copyright © 2015 IEEE. All rights reserved.
Copyright The Institute of Electrical and Electronics Engineers, Inc.
Provided by IHS under license with IEEE
No reproduction or networking permitted without license from IHS
Order Number: 02120914
Sold to:EGAT [700166108393] - VARRIS.Y@EGAT.CO.TH,
Not for Resale,2016-09-15 03:57:51 UTC

Table E.2—Calculated resistance and apparent resistivity data for soil type 1 and type 2 of Table E.1, based on the four-pin method

Probe separation		Soil type 1		Soil type 2	
(ft)	(m)	Resistance Ω	Apparent resistivity ρ_a Ω-m	Resistance Ω	Apparent resistivity ρ_a Ω-m
1	0.305	36.46	69.8	109.38	209.5
3	0.915	16.32	93.8	48.84	280.6
5	1.524	10.25	98.2	30.40	291.1
10	3.048	5.40	103.4	15.01	287.5
15	4.573	3.86	110.9	9.42	270.6
20	6.098	3.16	121.0	6.48	248.2
30	9.146	2.49	143.10	3.52	202.2
50	15.244	1.90	181.9	1.50	143.6
70	21.341	1.56	209.1	0.90	120.7
90	27.439	1.32	227.5	0.64	110.3
110	33.537	1.15	242.3	0.51	107.4
130	39.634	1.01	251.5	0.42	104.6
150	45.731	0.90	258.5	0.36	103.4

Copyright © 2015 IEEE. All rights reserved.

Copyright The Institute of Electrical and Electronics Engineers, Inc.
Provided by IHS under license with IEEE
No reproduction or networking permitted without license from IHS

Order Number: 02120914
Sold to:EGAT [700166108393] - VARRIS.Y@EGAT.CO.TH,
Not for Resale,2016-09-15 03:57:51 UTC

Annex F

(informative)

Parametric analysis of grounding systems

(Annex F is taken from Dawalibi, F., and Mukhedkar, D., "Parametric analysis of grounding systems," *IEEE Transactions on Power Apparatus and Systems,* vol. PAS-98, no. 5, pp. 1659–1668, Sept./Oct. 1979; and Dawalibi, F., and Mukhedkar, D., "Influence of ground rods on grounding systems," *IEEE Transactions on Power Apparatus and Systems,* vol. PAS-98, no. 6, pp. 2089–2098, Nov./Dec. 1979.)

To efficiently design a safe grounding system it is necessary to have knowledge of how various parameters affect the performance of the grounding system. Some of these parameters include grid conductor spacing and arrangement, number of ground rods, location and length, and soil resistivity parameters (that is, homogeneous or multilayered with various surface layer thickness and values of K, the reflection factor coefficient).

This annex gives a brief discussion of how the above parameters affect the behavior of grounding systems for uniform soil resistivity and for two-layer soil resistivity. There are many other parameters that may affect the performance of the grounding system, but it is not within the scope of this annex to discuss these parameters.

F.1 Uniform soil

F.1.1 Current density—grid only

For a grounding system consisting only of grid conductors, the current along any one of the conductors is discharged into the earth in a fairly uniform manner. However, a larger portion of the current is discharged into the soil from the outer grid conductors rather than from the conductors at or near the center of the grid (refer to Figure F.1 and Figure F.2). An effective way of making the current density more uniform between the inside and periphery conductors is to employ a non-uniform conductor spacing, with the conductor spacing larger at the center of the grid and smaller toward the perimeter. However, analysis of grids with this type of spacing cannot be accomplished using the simplified methods of this guide, but must be done using techniques similar to those described in the references.

F.1.2 Resistance—grid only

For a given area to be grounded, the effect on resistance of increasing the number of meshes in a grid-only system becomes minimal. That is, as the number of meshes increases from one, the resistance of the grid decreases. However, this decrease quickly becomes negligible for large numbers of meshes (or small parallel conductor spacing). See Figure F.3 and Figure F.4.

As shown in Figure F.5, the resistance also shows a gradual decrease with burial depth, until it approaches one half its resistance value at the surface as the depth increases to infinity. But for typical variations of burial depth found within the industry (that is, approximately 0.5 m to 1.5 m), this change in resistance with depth is negligible for uniform soil.

Copyright © 2015 IEEE. All rights reserved.

Copyright The Institute of Electrical and Electronics Engineers, Inc.
Provided by IHS under license with IEEE
No reproduction or networking permitted without license from IHS

Order Number: 02120914
Sold to:EGAT [700166108393] - VARRIS.Y@EGAT.CO.TH,
Not for Resale,2016-09-15 03:57:51 UTC

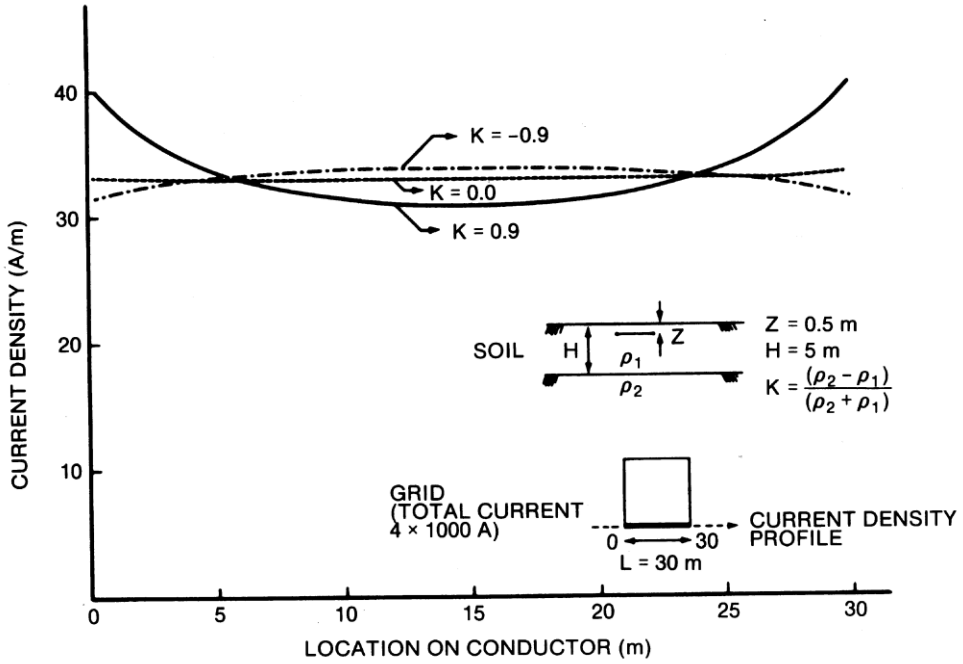

Figure F.1—One mesh grid current density

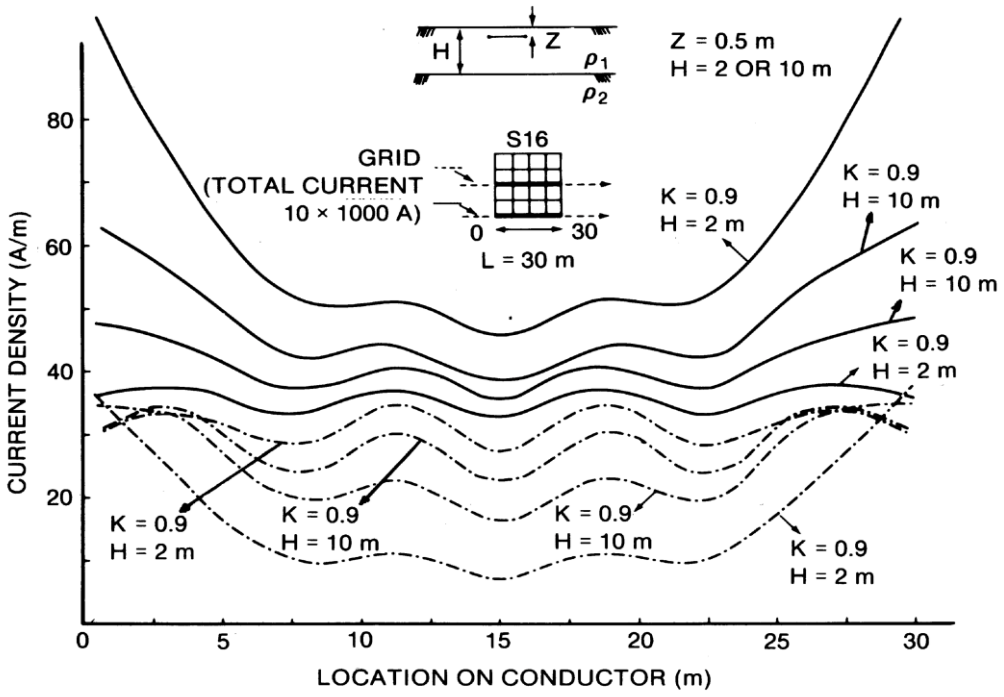

Figure F.2—Sixteen mesh grid current density

Copyright © 2015 IEEE. All rights reserved.

Copyright The Institute of Electrical and Electronics Engineers, Inc.
Provided by IHS under license with IEEE
No reproduction or networking permitted without license from IHS

Order Number: 02120914
Sold to:EGAT [700166108393] - VARRIS.Y@EGAT.CO.TH,
Not for Resale,2016-09-15 03:57:51 UTC

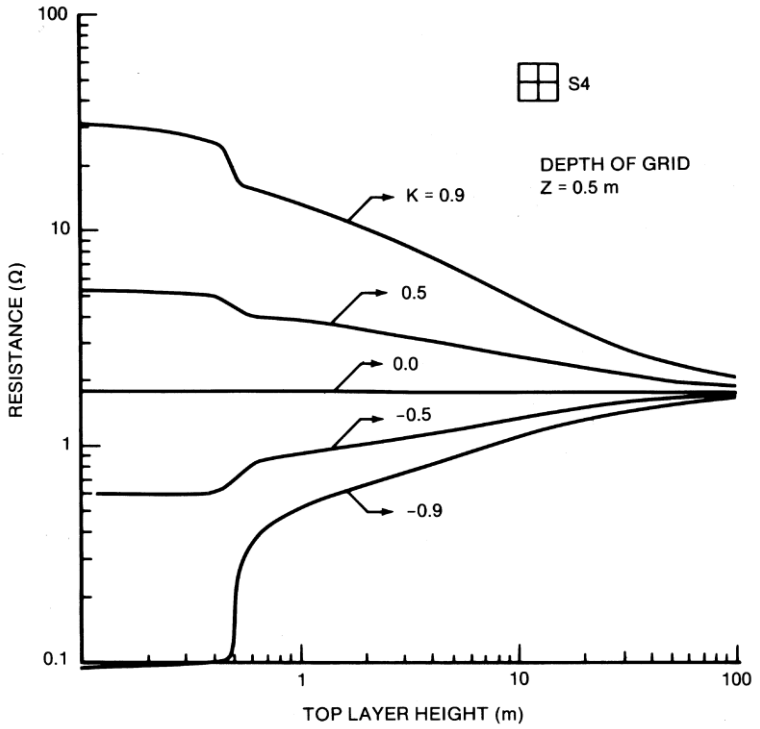

Figure F.3—Four mesh grid resistance

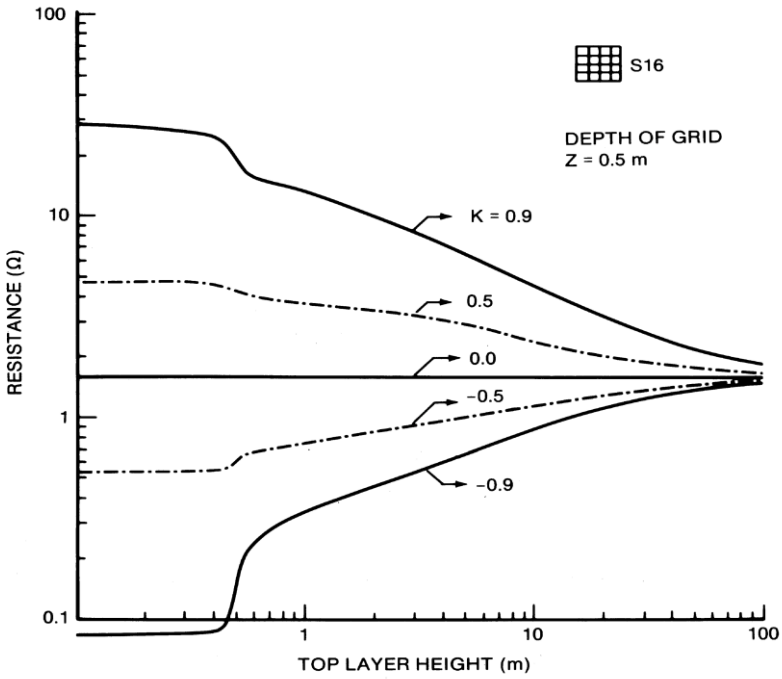

Figure F.4—Sixteen mesh grid resistance figure

Copyright © 2015 IEEE. All rights reserved.

Copyright The Institute of Electrical and Electronics Engineers, Inc.
Provided by IHS under license with IEEE
No reproduction or networking permitted without license from IHS

Order Number: 02120914
Sold to:EGAT [700166108393] - VARRIS.Y@EGAT.CO.TH,
Not for Resale,2016-09-15 03:57:51 UTC

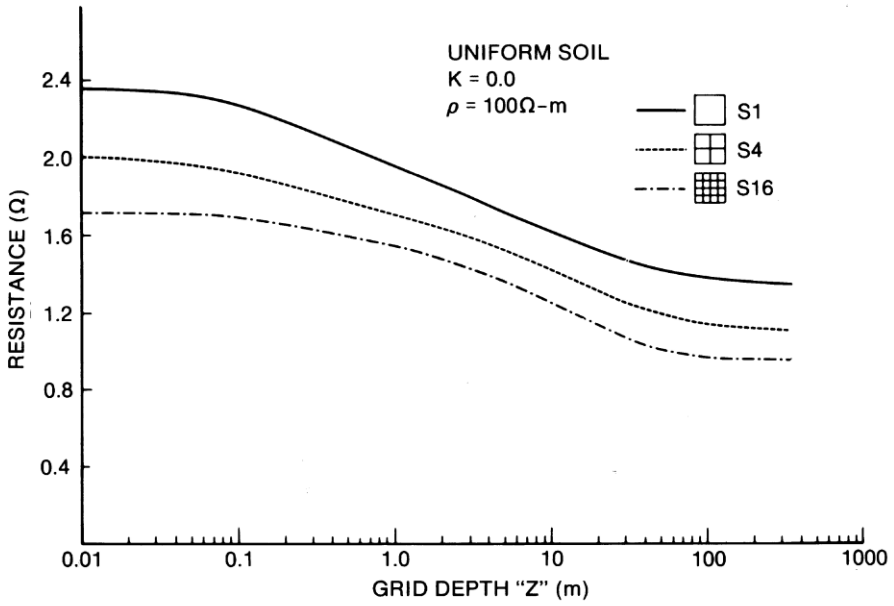

Figure F.5—Grid resistance versus grid depth

F.1.3 Step and touch voltages—grid only

Since most of the current in a uniformly spaced grid is discharged into the earth from the outer conductors, the worst touch and step voltages occur in the outer meshes, especially in the corner meshes. Increasing the number of meshes (decreasing the conductor spacing) tends to reduce the touch and step voltages until a saturation limit is reached. Beyond this number of meshes, reducing the conductor spacing has minimal effect on reducing the voltages (refer to Figure F.6, Figure F.7, Figure F.8, and Figure F.9). This saturation limit is the vertical component of voltage caused by the depth of burial of the grid, and is changed only with a change in depth of the grid.

The grid burial depth also influences the step and touch voltages significantly as shown in Figure F.10 and Figure F.11. For moderate increases in depth, the touch voltage decreases, due mainly to the reduced grid resistance and corresponding reduction in the ground potential rise. However, for very large increases in depth, the touch voltage may actually increase. The reduction in ground potential rise reduces to a limit of approximately half its value at the surface as the depth of the grid approaches infinity, while the earth surface potential approaches zero at infinite depths. Therefore, depending on the initial depth, an increase in grid burial depth may either increase or decrease the touch voltage, while the step voltage is always reduced for increased depths.

F.1.4 Ground rods only

For systems consisting only of ground rods, the current has been found to discharge into the earth at a fairly uniform rate along the length of the rod with a gradual increase with depth and with slightly higher increases in current density near the ends (refer to Figure F.12). As in the case of the grid conductors, the current density is greater in the rods near the periphery of the grounding system than for those in the center (refer to Figure F.13 and Figure F.14). Thus, the step and touch voltages are higher near the outer ground rods.

Copyright © 2015 IEEE. All rights reserved.

Copyright The Institute of Electrical and Electronics Engineers, Inc.
Provided by IHS under license with IEEE
No reproduction or networking permitted without license from IHS

Order Number: 02120914
Sold to:EGAT [700166108393] - VARRIS.Y@EGAT.CO.TH,
Not for Resale,2016-09-15 03:57:51 UTC

Increasing the length of the rods is effective in reducing the resistance of the system, and therefore, reducing the step and touch voltages. Increasing the number of rods also reduces the resistance until the grounded area is saturated, and is even more effective in reducing the step and touch voltages as shown in Table F.1. This is true because in addition to the lower resistance and lower ground potential rise, the spacing between the rods is reduced, which tends to make the earth surface potential more uniform. The comments above on the effects of grid burial depth also apply to the effects of the top-of-the-rod depths.

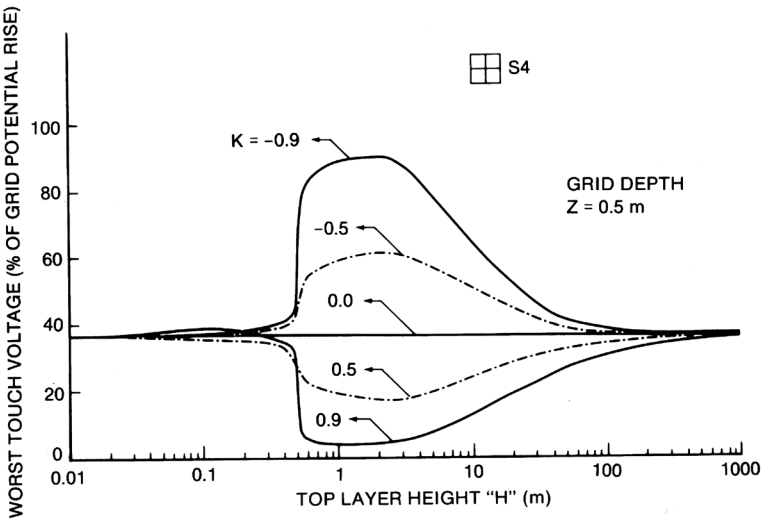

Figure F.6—Four mesh grid touch voltages

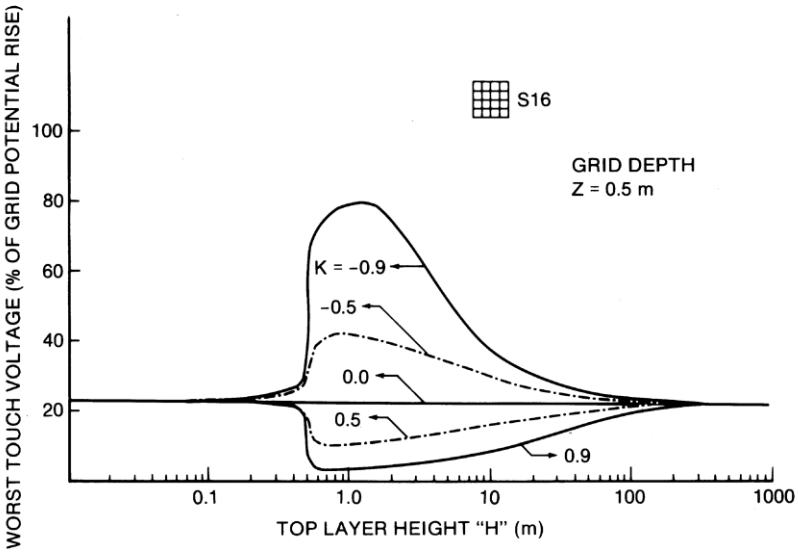

Figure F.7—Sixteen mesh grid touch voltages

Copyright © 2015 IEEE. All rights reserved.

Copyright The Institute of Electrical and Electronics Engineers, Inc.
Provided by IHS under license with IEEE
No reproduction or networking permitted without license from IHS

Order Number: 02120914
Sold to:EGAT [700166108393] - VARRIS.Y@EGAT.CO.TH,
Not for Resale,2016-09-15 03:57:51 UTC

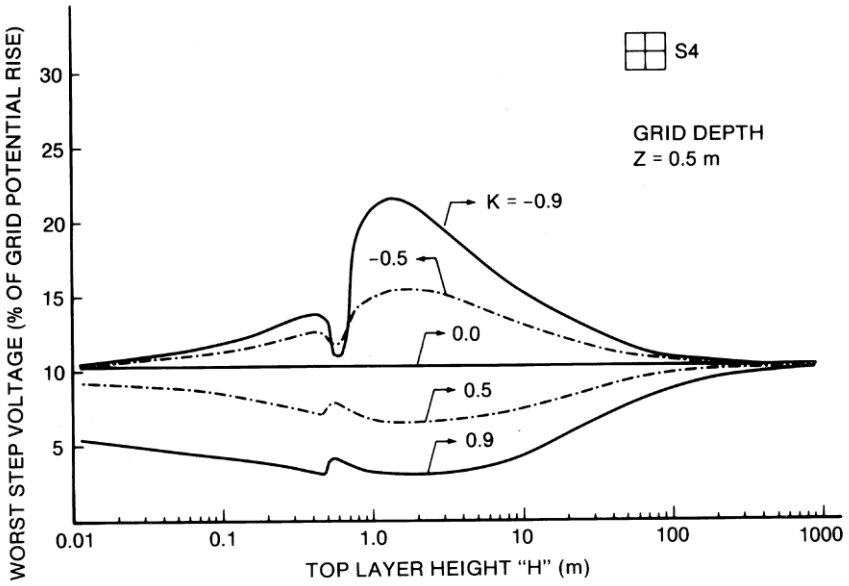

Figure F.8—Four mesh grid step voltages

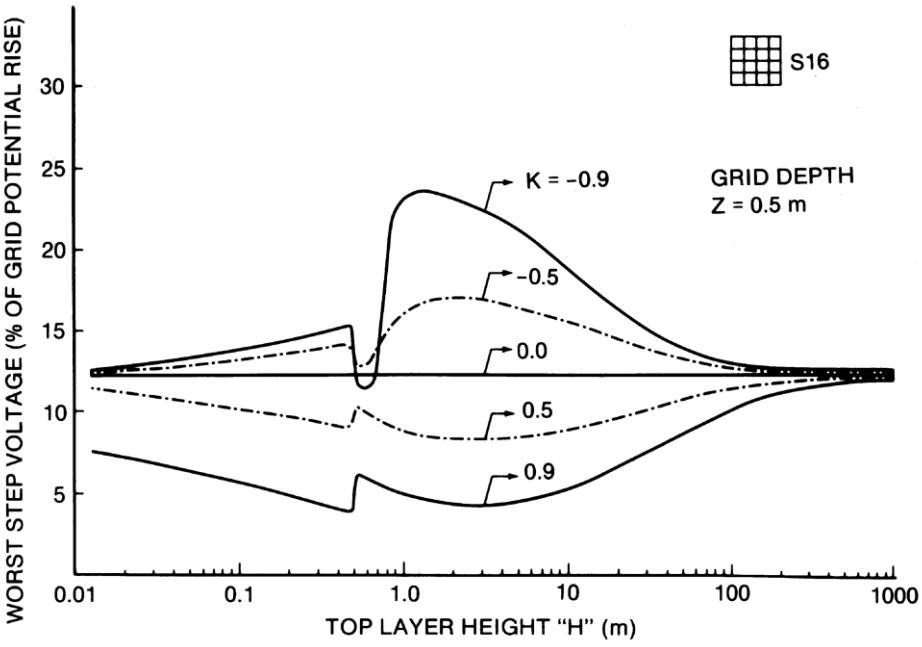

Figure F.9—Sixteen mesh grid step voltages

Copyright © 2015 IEEE. All rights reserved.

Copyright The Institute of Electrical and Electronics Engineers, Inc.
Provided by IHS under license with IEEE
No reproduction or networking permitted without license from IHS

Order Number: 02120914
Sold to:EGAT [700166108393] - VARRIS.Y@EGAT.CO.TH,
Not for Resale,2016-09-15 03:57:51 UTC

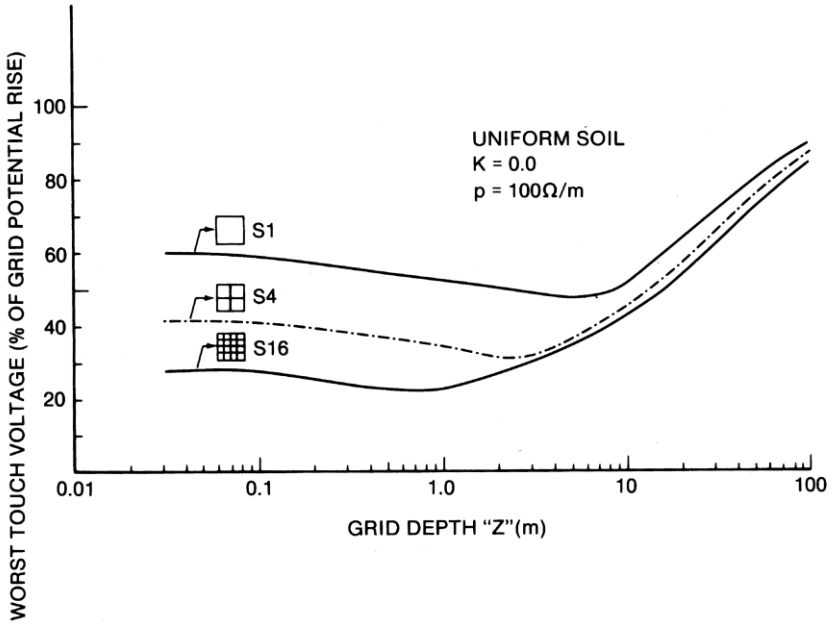

Figure F.10—Touch voltage versus grid depth

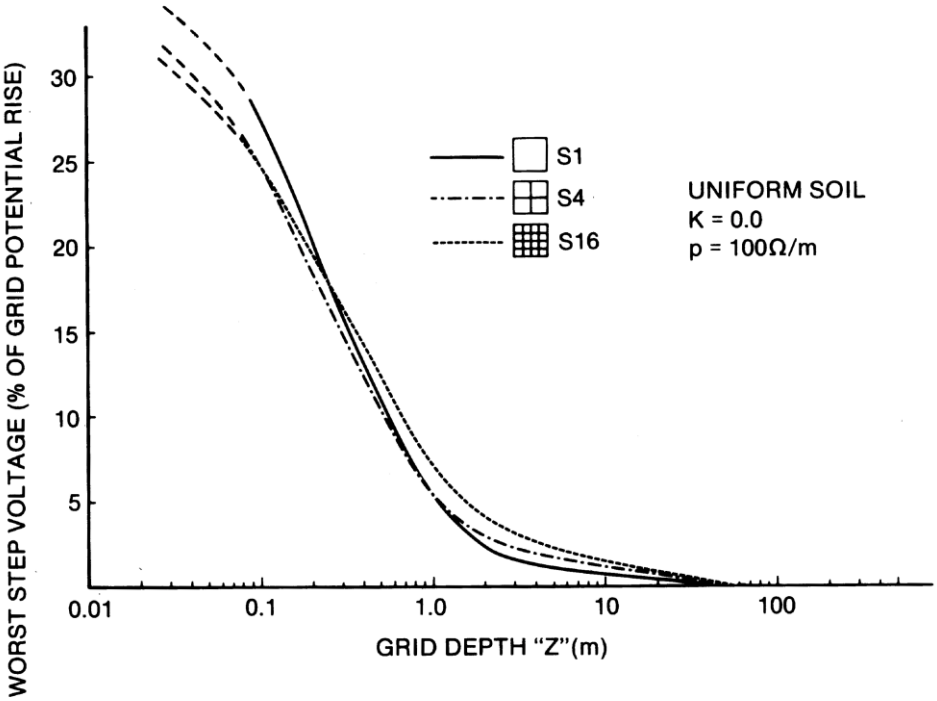

Figure F.11—Step voltage versus grid depth

Copyright © 2015 IEEE. All rights reserved.

Copyright The Institute of Electrical and Electronics Engineers, Inc.
Provided by IHS under license with IEEE
No reproduction or networking permitted without license from IHS

Order Number: 02120914
Sold to:EGAT [700166108393] - VARRIS.Y@EGAT.CO.TH,
Not for Resale,2016-09-15 03:57:51 UTC

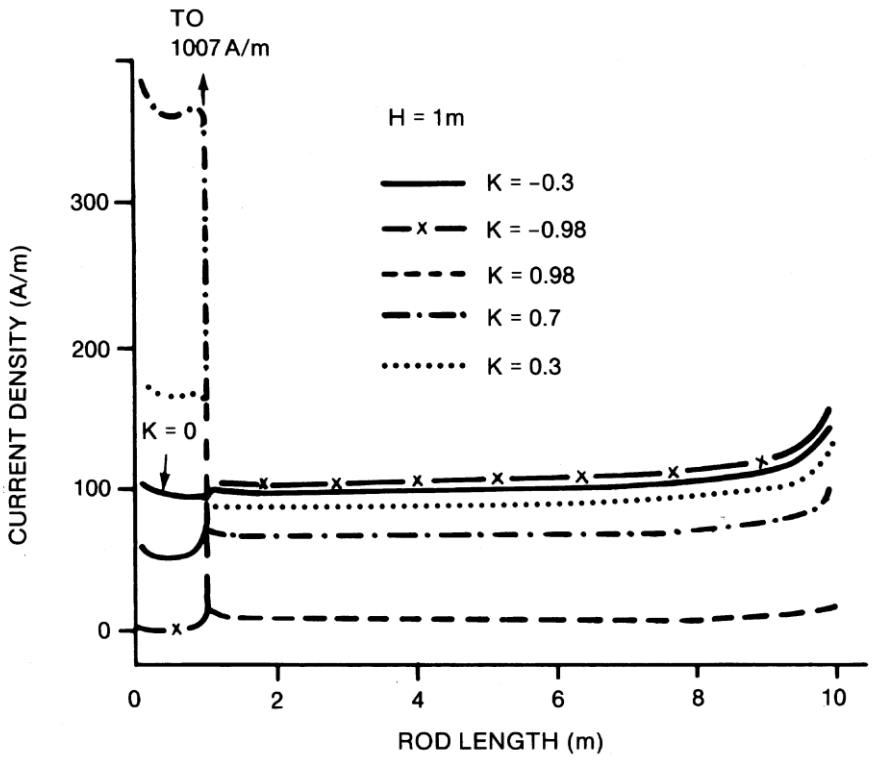

Figure F.12—Single rod current density

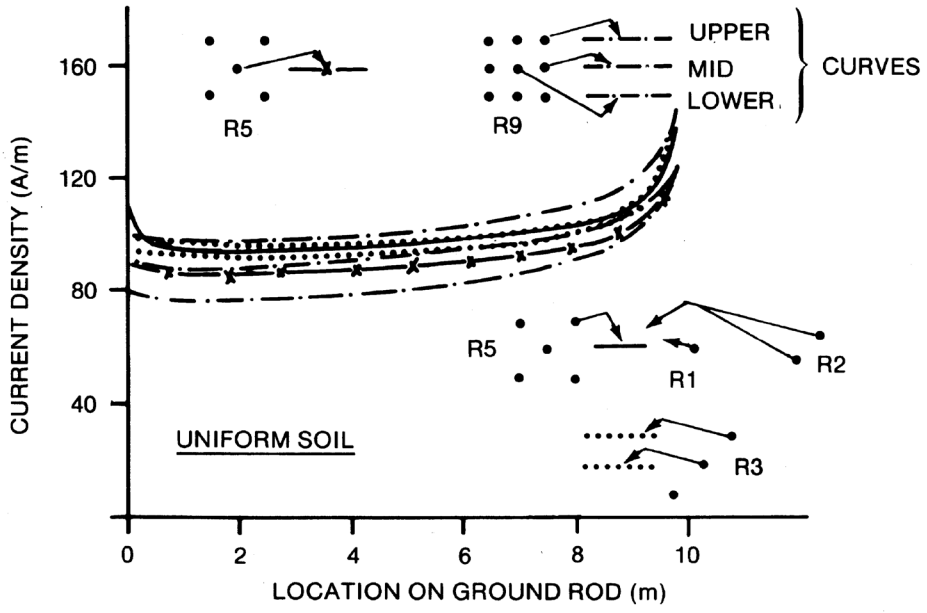

Figure F.13—Multiple driven rod current density in uniform soil

Copyright © 2015 IEEE. All rights reserved.
Copyright The Institute of Electrical and Electronics Engineers, Inc.
Provided by IHS under license with IEEE
No reproduction or networking permitted without license from IHS
Order Number: 02120914
Sold to:EGAT [700166108393] - VARRIS.Y@EGAT.CO.TH,
Not for Resale,2016-09-15 03:57:51 UTC

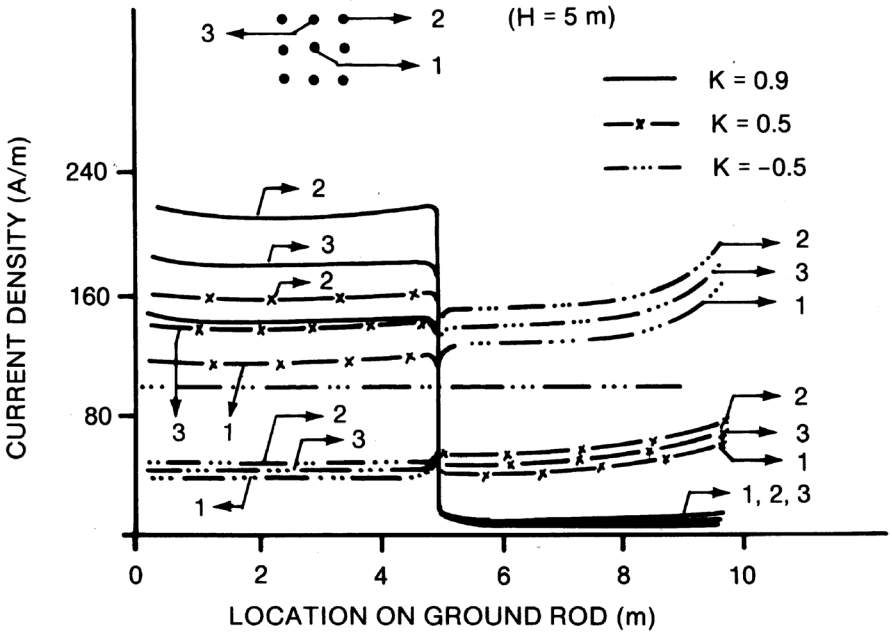

Figure F.14—Current density in multiple driven rods in two-layer soil

F.1.5 Grid and ground rod combinations

When a combination of grid conductors and ground rods are used in a grounding system, the number and length of ground rods may have a great influence on the performance of the grounding system. For a given length of grid conductor or ground rod, the ground rod discharges much more current into the earth than does the grid conductor, as shown in Figure F.15, Figure F.16, Figure F.17, and Figure F.18. This current in the ground rod is also discharged mainly in the lower portion of the rod. Therefore, the touch and step voltages are reduced significantly compared to that of grid alone.

F.1.6 Conclusions

In general, a uniformly spaced grounding system consisting of a grid and ground rods is superior to a uniformly spaced grounding system consisting only of a grid with the same total conductor length. The variable spacing technique discussed earlier might be used to design a grounding system consisting of a grid only, with lower step and touch voltages than a uniformly spaced grid and ground rod design of equal length. However, this variable spacing technique might also be used to design a better grounding system using non-uniformly spaced grid conductors and ground rods. It shall be emphasized that this type of design shall be analyzed using the detailed analysis techniques in the references.

Copyright © 2015 IEEE. All rights reserved.

Copyright The Institute of Electrical and Electronics Engineers, Inc.
Provided by IHS under license with IEEE
No reproduction or networking permitted without license from IHS

Order Number: 02120914
Sold to:EGAT [700166108393] - VARRIS.Y@EGAT.CO.TH,
Not for Resale,2016-09-15 03:57:51 UTC

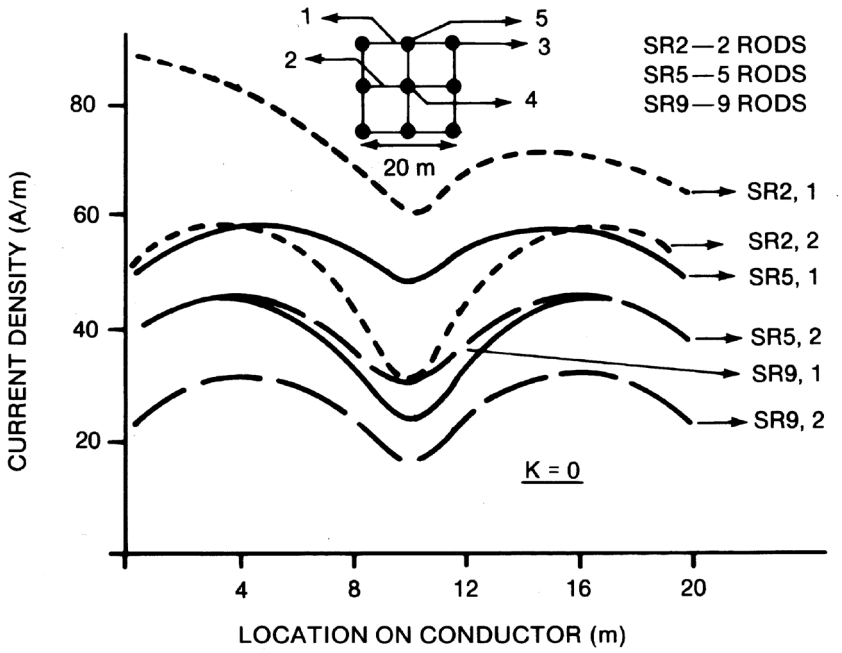

Figure F.15—Grid current density—rods and grid in uniform soil

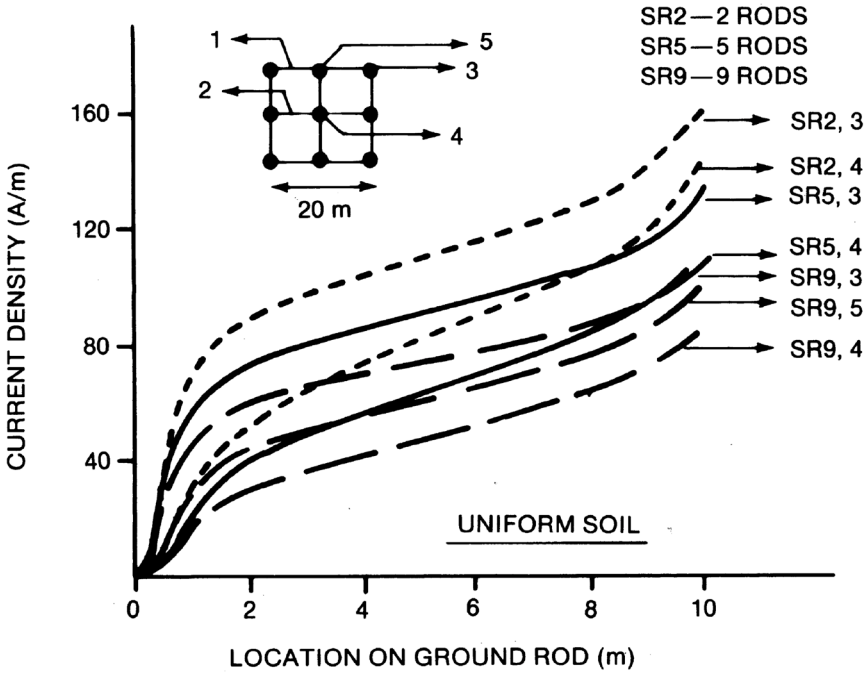

Figure F.16—Rod current density—rods and grids in uniform soil

Copyright © 2015 IEEE. All rights reserved.

Copyright The Institute of Electrical and Electronics Engineers, Inc.
Provided by IHS under license with IEEE
No reproduction or networking permitted without license from IHS

Order Number: 02120914
Sold to:EGAT [700166108393] - VARRIS.Y@EGAT.CO.TH,
Not for Resale,2016-09-15 03:57:51 UTC

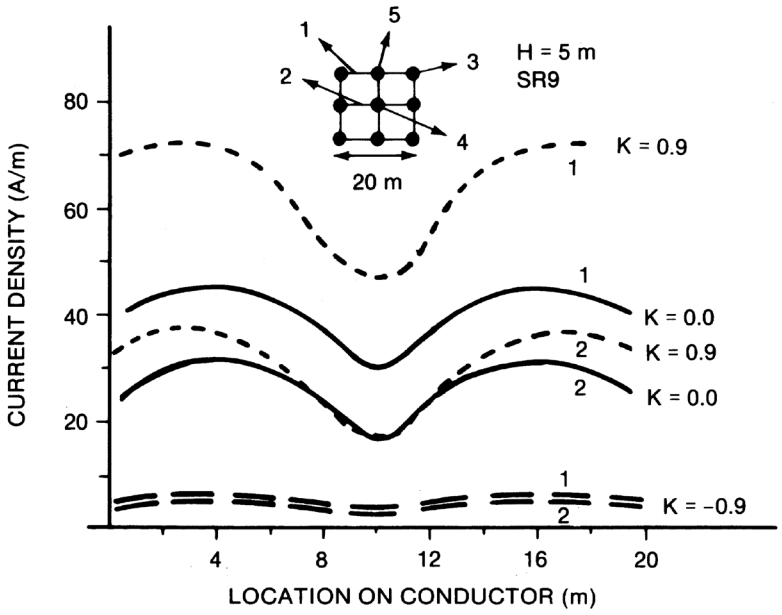

Figure F.17—Rod and grid current density—nine rods and grid in two-layer soil

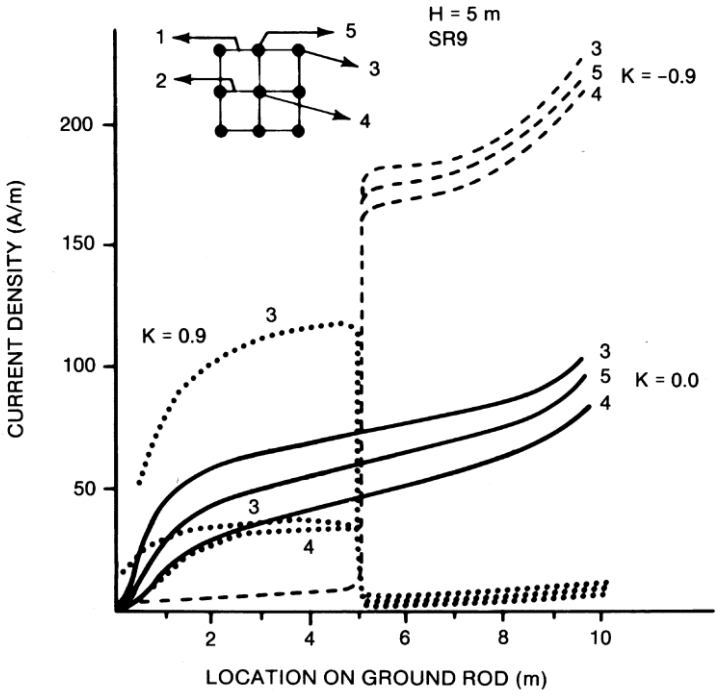

Figure F.18—Rod and grid current density—nine rods and grid in two-layer soil

Copyright © 2015 IEEE. All rights reserved.

Copyright The Institute of Electrical and Electronics Engineers, Inc.
Provided by IHS under license with IEEE
No reproduction or networking permitted without license from IHS

Order Number: 02120914
Sold to:EGAT [700166108393] - VARRIS.Y@EGAT.CO.TH,
Not for Resale,2016-09-15 03:57:51 UTC

F.2 Two-layer soil

The performance of a grounding system in multilayered earth can differ greatly from the same system in uniform soil. In addition to other parameters, the performance is affected by the resistivity and thicknesses of the soil layers and the burial depth of the grounding system. The following discussion will consider only two-layer earth models, due to the complexity and numerous combinations possible for additional layers. For an explanation of two-layer earth analysis of grounding systems, refer to 13.4.2 of this guide.

For brevity of the discussion, the following variables are defined:

ρ_1 = resistivity of upper layer of soil

ρ_2 = resistivity of lower layer of soil

K = reflection factor coefficient $\frac{\rho_2 - \rho_1}{\rho_2 + \rho_1}$

h = height of upper layer of soil

F.2.1 Current density—grid only

For grounding systems consisting only of grid conductors, the current density is highly dependent on both K and h, as shown in Figure F.1 and Figure F.2. For negative values of K ($\rho_1 > \rho_2$), the current density is fairly uniform over the entire grid with slightly higher densities in the conductor between intersection points on the grid, and is slightly higher for outer conductors than for conductors near the center of the grid. As the height of the top layer increases, this higher current density in the outer conductors becomes more dominant. This can be explained as follows. For small values of h, most of the current discharged from the grid goes downward into the low resistivity soil, while for large values of h most of the current remains in the high resistivity layer of soil, assuming that the grid is in this upper layer. As h increases, the model approaches that of uniform soil with a resistivity equal to that of the upper layer. Therefore, as in the case of the uniform soil model discussed in F.1, the outer grid conductors discharge a larger portion of the current into the earth than do the center conductors.

For positive values of K ($\rho_1 < \rho_2$), the current has a much higher tendency to remain in the low resistivity soil, even for moderately small values of h. As h increases, the current density rapidly approaches that of a uniform soil, with higher current densities in the periphery conductors.

F.2.2 Resistance—grid only

The resistance of a grid-only system may vary greatly as a function of K and h and, thus, may be higher or lower than the same grid in a uniform soil, as shown in Figure F.3 and Figure F.4. In general, the resistance of a grid is lowest if it is in the most conductive layer of soil. As h increases the resistance of the grid approaches that of a grid in uniform soil of the same resistivity as the upper layer. Assuming that the grid is located in the upper soil layer with resistivity equal to ρ_1, the following can be generalized:

a) For negative values of K ($\rho_1 > \rho_2$), the resistance of the grid will be higher than that of an identical grid in uniform soil with resistivity ρ_1.

b) For positive values of K ($\rho_1 < \rho_2$), the resistance grid will be lower than that of an identical grid in uniform soil resistivity ρ_2.

Copyright © 2015 IEEE. All rights reserved.

Copyright The Institute of Electrical and Electronics Engineers, Inc.
Provided by IHS under license with IEEE
No reproduction or networking permitted without license from IHS

Order Number: 02120914
Sold to:EGAT [700166108393] - VARRIS.Y@EGAT.CO.TH,
Not for Resale,2016-09-15 03:57:51 UTC

F.2.3 Step and touch voltages—grid only

The step, touch, and mesh voltages may also vary significantly with K, h, and grid depth. They may be very much higher or lower than a corresponding uniform soil model. See Figure F.6, Figure F.7, Figure F.8, and Figure F.9.

For grids buried near the surface of the earth, increasing the number of meshes is an effective means of reducing the mesh voltages. However, as the grid depth increases, the effectiveness of this method of reducing the mesh voltages decreases until at some characteristic grid depth, the mesh voltages begin to increase. The reasons for this phenomenon are identical to those described previously for uniform soil. For a very large number of meshes (that is, small spacing between parallel conductors), the touch voltages are relatively unaffected by h and K.

For negative values of K ($\rho_1 > \rho_2$), the highest touch voltage occurs when h is slightly greater than the grid depth. For positive values of K ($\rho_1 < \rho_2$), the highest touch voltages occur when h is less than the grid depth, or when h is much greater than the grid depth.

One way of reducing the touch voltage without increasing the total amount of conductor is to omit the cross-connecting conductors (except at the ends) and reduce the spacing between the remaining parallel conductors. It must be noted, however, that while the touch voltage is reduced, the step voltage is increased when this design is used.

F.2.4 Ground rods only

The behavior of a grounding system consisting only of ground rods may vary greatly from that in uniform soil. The major differences are because the current density in each rod can be much higher in the portion of the rod located in the lower resistivity layer, depending on the value of K. As the absolute value of K increases, so does the percentage of the current discharged from the portion of the rod located in the lower resistivity layer of soil, as shown in Figure F.12.

Assuming that the rod extends through the top layer into the bottom layer of soil, the current density in the portion of the rod in either layer is essentially uniform with a slight increase near the boundary of that layer. There is an abrupt change in current density, however, at the surface layer depth h. For rods that are mainly in the low resistivity layer, there is an appreciably higher current density in the outer rods as compared to rods near the center of the design, but for rods mainly in the high resistivity layer the difference in the current density of the outside and inside rods is much less (see Figure F.14).

As in the case of the grid, positive values of K ($\rho_1 < \rho_2$) generally give a higher resistance and negative values of K ($\rho_1 > \rho_2$) give a lower resistance for a system of ground rods as compared to the identical grounding system in uniform soil with a resistivity of ρ_1. However, as the surface layer height increases, the resistance of the rods for all values of K approaches that of the uniform model (see Table F.1).

F.2.5 Grid and ground rod combinations

Depending on the values of K and h, adding ground rods to a system of grid conductors can have a tremendous effect on the performance of the grounding system. For negative values of K ($\rho_1 > \rho_2$) and for values of h limited so that the rods extend into more conductive soil, the majority of the current is discharged through the rods into the lower layer of soil. Even for large values of h where none of the rod extends into the more conductive soil, the current density is higher in the ground rods than in the grid conductors, as shown in Figure F.17 and Figure F.18.

Copyright © 2015 IEEE. All rights reserved.
Copyright The Institute of Electrical and Electronics Engineers, Inc.
Provided by IHS under license with IEEE
No reproduction or networking permitted without license from IHS
Order Number: 02120914
Sold to:EGAT [700166108393] - VARRIS.Y@EGAT.CO.TH,
Not for Resale,2016-09-15 03:57:51 UTC

If K is positive ($\rho_1 < \rho_2$), the current density for the portion of the ground rods in the upper layer is still higher than that of the grid conductors. For positive values of K, the effects of the ground rods become largely dependent on h, or on the length of the rods in the more conductive layer. Depending on the magnitude of K and h, the lengths of the rods are effectively shortened so that they may not contribute significantly to the control of step and touch voltages. However, for moderate positive K values and large h values, the ground rods can be used to effectively improve the step and touch voltages.

Table F.1—Touch voltages for multiple driven rods

(A) Uniform soil					
	R1	R2	R3	R4	R5
Electrode type	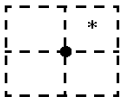	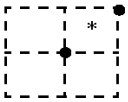	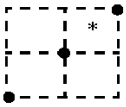	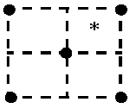	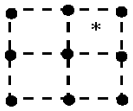
Resistance (Ω)	11.85	6.43	4.52	3.01	2.16
Touch* Voltage (%)	84.7	72.0	68.2	59.1	40.8
(B) R9 in two-layer soil (H = 5 m)					
Reflection factor K	–0.9	–0.5	Uniform soil (0.0)	0.5	0.9
Resistance (Ω)	0.169	0.926	2.16	4.21	8.69
Touch* Voltage (%)	51.1	47.4	40.8	31.8	19.3

If K is negative ($\rho_1 > \rho_2$), the step and touch voltages are reduced significantly with the addition of ground rods to a system of grid conductors. For small to medium values of h, relatively all of the current is discharged into the lower soil layer, thereby reducing the step and touch voltages. As h increases, the performance of the grounding system approaches that of an identical system in uniform soil of resistivity ρ_1.

F.3 Summary

The two-layer parameters h and K discussed above can have considerable influence on the performance of the grounding system. A system designed using the uniform soil techniques can give results for step and touch voltages and station resistance ranging from highly pessimistic to highly optimistic, depending on the specific values of various parameters. Table F.2 summarizes the effects of a two-layer soil environment on touch voltage of adding a ground rod to a grid, and on the touch voltage for a grid-rod combination.

Copyright © 2015 IEEE. All rights reserved.
--`,,,,,,`,```,,`,`,,`,-`-`,,`,,,`---
Copyright The Institute of Electrical and Electronics Engineers, Inc.
Provided by IHS under license with IEEE
No reproduction or networking permitted without license from IHS
Order Number: 02120914
Sold to:EGAT [700166108393] - VARRIS.Y@EGAT.CO.TH,
Not for Resale,2016-09-15 03:57:51 UTC

Table F.2—Touch voltages for grid and ground rod combinations in two-layer soil

(A) Uniform soil					
Electrode type	S4	SR1	SR2	SR3	SR4
	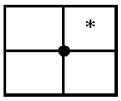	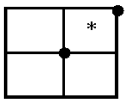	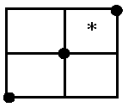	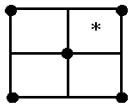	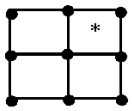
Resistance (Ω)	2.58	—	2.28	2.00	1.81
Touch* Voltage (%)	35.0	—	31.0	25.0	21.0
(B) SR9 in two-layer soil (H = 5 m)					
Reflection factor K	–0.9	–0.5	Uniform soil (0.0)	0.5	0.9
Resistance (Ω)	0.164	—	1.81	3.50	7.78
Touch* Voltage (%)	35.0	—	21.0	13.4	6.6

Copyright © 2015 IEEE. All rights reserved.

Copyright The Institute of Electrical and Electronics Engineers, Inc.
Provided by IHS under license with IEEE
No reproduction or networking permitted without license from IHS

Order Number: 02120914
Sold to:EGAT [700166108393] - VARRIS.Y@EGAT.CO.TH,
Not for Resale,2016-09-15 03:57:51 UTC

Annex G

(informative)

Grounding methods for high-voltage stations with grounded neutrals

(Annex G translated by T. W. Stringfield from Koch, W., "Erdungsmassnahmen fur Hochstspannungsanlagen mit Geerdetem Sternpunkt," *Electrotechnische Zeitschrift,* vol. 71, no. 4, pp. 8–91, Feb. 1950.)[16]

It is not economically feasible to provide grounding in high-voltage stations with grounded neutral, which will limit contact potentials to ground electrodes and the connected apparatus to less than 125 V. One has to deal with a multiplicity of potentials which may be established between the plant and the surroundings under short-circuit conditions.

Experiments with models show that by making the ground system in the form of a grid, areas within the system can be produced which will be safe. Means for safe entry into the grounding area will be given.

With a directly grounded neutral point there flows into the system at the fault point the so-called ground-fault current instead of the total single-phase short-circuit ground current (ungrounded system). This ground-fault current depends upon the generating capacity of the power plants in the area and on the impedance of the ground circuit. The grounding systems of a solidly grounded network will carry a portion of the ground-fault current which may be a minimum for faults a great distance from the station and may be a maximum, namely the total ground-fault current, for a fault in the station.

While the grounding systems may be adjusted to eliminate dangerous contact potentials by suppression of ground short-circuit currents, this is not usually demanded of solidly grounded neutral systems because it does not appear to be practicable. For ground-fault currents above 1000 A, grounding systems of vast dimensions must be installed in order to meet the usual 125 V contact potential requirement. A numerical example will show this. The surface area of an outdoor substation may be 250 m × 250 m. Here one has the possibility of placing a ground plate of 62 500 m^2 under the station. With an average ground resistivity of 100 Ω-m and the equivalent circular plate diameter of 280 m the ground resistance is

$$R = \frac{\rho}{2D}$$

or

$$R = \frac{10\ 000}{2 \times 28\ 000} = 0.18\ \Omega$$

With such a ground, a ground-fault current of 5000 A will produce a 900 V potential above the more-distant surroundings which is many times the potential allowed by VDE. In spite of this, it has the indisputable advantage that the entire station on this metal plate will have no potentials between parts within itself that are worth mentioning. For persons inside the station there will not be the slightest danger from undue contact potentials at such a high current. There would be danger only if at the moment of fault one were to enter or leave the plant or touch it from the outside. It is not practical to construct such a ground plate. However, in order not to endanger the personnel of an electrical plant, ways must be sought to fulfill this requirement.

[16] Some portions on Petersen coil systems and German (VDE) regulations omitted.

Copyright © 2015 IEEE. All rights reserved.

Copyright The Institute of Electrical and Electronics Engineers, Inc.
Provided by IHS under license with IEEE
No reproduction or networking permitted without license from IHS

Order Number: 02120914
Sold to:EGAT [700166108393] - VARRIS.Y@EGAT.CO.TH,
Not for Resale,2016-09-15 03:57:51 UTC

Besides the dangers to personnel, there will be some to the material of the control and communications equipment if it is not provided against. The sheaths of the control cables provide a connection between the controlled apparatus in the high-voltage bays and the control point. Thereby, a fault to ground in the station can cause a very large current to flow through the sheath and melt it. Communication cables which leave the plant will also conduct ground currents away since intentionally or unintentionally they come into contact with building construction parts. Thereby, the sheaths acquire the high potential of the station in their vicinity while the conductors approximate the potential of the more-distant surroundings, so that insulation failures may occur. So likewise the cables of the low-voltage plant and the windings of control motors among others may be endangered by large potential differences. Indeed, for these reasons it is not permissible to rely only on a sufficient interconnection of all apparatus such as circuit breakers, transformer cases, frame parts, etc. To this all cable sheaths within the plant must also be connected; so likewise the control mechanisms in the switching station to which the control cables are connected. Basically the entire plant should be provided with a built-up ground mat for the ground-fault current, to which all equipment parts in the plant are connected. So likewise, the existing neutral conductors of independent low-voltage systems should be tied to the ground mat. By this method there will be the least worry that significant potential differences will arise between the accessible metallic parts of the plant and the plant equipment so protected will be safe from failure.

Now, it is certain that considerable and therefore dangerous potentials can arise between the soil, the floors of buildings on one side, and the metallic parts of the plant during the time of faults. Therefore one must also consider the safety of operating personnel who in the course of their work must touch such metal parts. For this purpose the operating position may be provided either with an insulated floor capable of withstanding the high potential or with a metallic grid in the floor and tied to the ground mat or provided with both. Such metallic foot grids have been previously used for protection in Siemens-Schuckert plants with ungrounded star neutral. They consisted of small meshed wire netting cemented into the floor and tied to the grounding system, and provided absolute protection to persons standing thereon and grasping operating controls in that a highly conducting shunt path was provided between hands and feet.

As mentioned in the introduction, a large metallic plate is a suitable protection against all step potentials and contact potentials within the plant. Since such a metallic plate installation is not realizable, the question arises on how far one can go in substituting a network of ground straps and the necessary mesh spacing in order to obtain tolerable potential differences.

The investigation of the potential distribution of complicated ground electrode arrangements, which such a ground mat is, is not possible by computation, since one can derive formulae only for simple electrode shapes and even simple combinations of these electrode shapes are not amenable to calculation. For mesh-type electrode arrangements with irregular depth of burial which is the way they are used for the purpose of potential control and other complicated grounding structures, one is led to the use of models. For this purpose such model measurements using an electrolytic tank were undertaken. A metal container filled with a conducting solution served as the semi-infinite space for the current diffusion. Figure G.1 shows the circuit of the test arrangement. The potential distribution for model M can be obtained by a null method using the electrode S, the calibrated potentiometer P, and telephone receiver T. In order to reduce the electrolytic effect of the chopped direct current supply on the model, a slowly rotating switch U was placed in the direct current supply leads.

The model of the ground mat consisted of a copper wire 0.2 mm in diameter arranged in a square with 120 mm sides and set on the surface. For the usual ground straps with a cross section of 30 mm × 3 mm corresponding to an equivalent diameter of 23 mm this model represented a replica of a ground system with a length of

$$\frac{20}{0.2} \times 120 = 13\,800 \text{ mm}$$

Copyright © 2015 IEEE. All rights reserved.

Copyright The Institute of Electrical and Electronics Engineers, Inc.
Provided by IHS under license with IEEE
No reproduction or networking permitted without license from IHS

Order Number: 02120914
Sold to:EGAT [700166108393] - VARRIS.Y@EGAT.CO.TH,
Not for Resale,2016-09-15 03:57:51 UTC

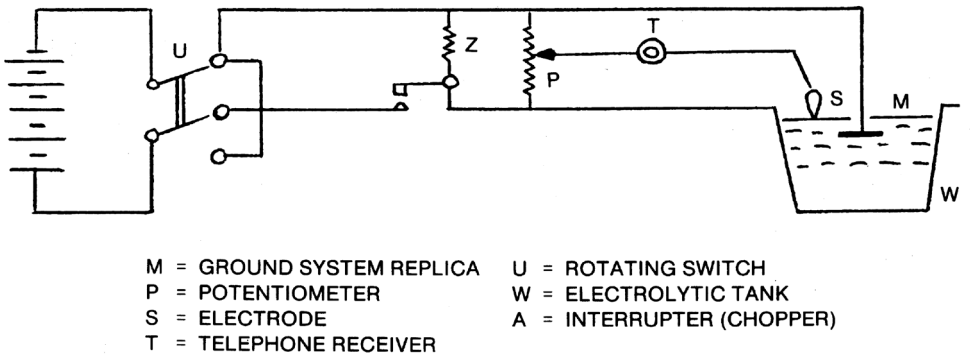

Figure G.1—Circuit for obtaining potential distribution

or 13.8 m on a side. After obtaining the potential distribution, the square was subdivided to contain four squares by the addition of a wire cross, the four sub-squares were similarly subdivided until 64 sub-squares were attained and in each case the potential inside the square was measured. As the mesh becomes finer the effect approaches a plate electrode. In Figure G.2, Figure G.3, Figure G.4, and Figure G.5, the potential at the center point of each square is given in percent of the potential of the ground mat. The potential differences which characterize the step potentials and thereby the hazard are according to these figures for fine-mesh electrodes 11% to 20% of the total potential. The mesh spacing of the mat with 64 meshes is, according to the above-mentioned model scale, 13.8/8 = 1.7 m. The potential distributions in cross sections through the mats at A–B, C–D, E–F and G–H of Figure G.2, Figure G.3, Figure G.4, and Figure G.5 are shown in Figure G.6. To determine the effect of only a partial fine mesh inside the outer edge, the arrangement shown in Figure G.7 was investigated and as shown in Figure G.8 with further subdivision of a single mesh. From this it follows that in the area of a fine mesh the same relations (proportions) hold as in the complete meshing of the total grounding area. The still finer subdivision of a single mesh results in a further raising of the potential inside the mesh, that is, a corresponding decrease of the potential differences and thereby the step potential.

The measurements show, as might be expected, that by using a fine mesh a considerable reduction in potential differences within the mat area can be obtained. Further, it is apparent that small protected areas can be produced by partial matting without completely matting the entire grounding area. Practical application of such finer meshing can be found principally in outdoor stations in the neighborhood of accessible equipment where the hazard is greatest.

A reduction of the effect, which will not completely eliminate potential differences, can be arrived at by a fill of coarse grit (gravel) to a depth of about 1 cm over such a ground grid. With this, everything practical has been done in order to minimize the hazard, if not to eliminate it entirely.

To be sure, there remain the locations of the passageways to the protected areas which remain a hazard when traveling over them during the time of a fault. Figure G.6 shows the high potential drops at the edges of the wide meshed areas, where step potentials of about 45% of the total potential to the ground electrode can be encountered. If one must obtain absolute safety, then on the passageways one must resort to the so-called potential ramps in order to obtain a small, and as far as possible, uniform potential drop. Wooden passageways have likewise already been used in the Siemens-Schuckert works in 200 kV stations.

The means of potential control through grounding straps buried at progressively deeper depths is shown in principle in Figure G.9, the effectiveness of which was proved by the leveling off of the potential surface in a model. Figure G.10 shows the application of potential control around the footing of a tower when one does not desire to, or is not able to, employ a fence.

The magnitude of the expected step potential for a ground mat depends upon the ground resistance, the short-circuit current and the mesh density. If one takes the area of an outdoor substation 250 m square, then

Copyright © 2015 IEEE. All rights reserved.

Copyright The Institute of Electrical and Electronics Engineers, Inc.
Provided by IHS under license with IEEE
No reproduction or networking permitted without license from IHS

Order Number: 02120914
Sold to:EGAT [700166108393] - VARRIS.Y@EGAT.CO.TH,
Not for Resale,2016-09-15 03:57:51 UTC

a ground strap around the periphery will be 1000 m long. Without regard to the cross-connections and matted grounds, the ground resistance of this strap is $R = \rho/\pi L\ [ln\ (2L/d)]$; where ρ is the ground resistivity (generally 100 Ω-m), L is the length of the strap in centimeters, and d is the equivalent diameter of the strap as a conductor with a semicircular cross section (for the usual ground-strap d = 2.3 cm). With these figures R = 0.36 Ω. The resistance is thus only twice as great as for a solid plate 250 × 250 m. The resistance will be reduced by the cross-connections which are required for tying in the apparatus to be grounded.

With a short-circuit current of, for example, 5000 A, the voltage to the ground system will be about 1800 V. With a ground rating as shown in Figure G.5, the greatest step potential to be expected will be about 11% to 12% of this value, or 200 V, the effect of which on persons can be reduced effectively by using gravel fill. According to Figure G.8, with a mesh spacing of 0.85 m the potential inside the mesh is 7% of the ground mat potential and for a ground mat potential of 1800 V the step potential can thereby be reduced below 125 V if necessary.

The systematic application of the protective measures described makes the separation of the operating ground from the protective ground superfluous. The separation of operating and protective grounds gives no protection for faults inside the station and from experience these must be considered. The installation of a separated star neutral ground system requires a tremendous amount of land outside the station. There is no advantage worth mentioning for this since a protective ground is still required inside the station. It therefore can only be recommended that the star-neutral point be connected to a suitable ground system as described in the foregoing or otherwise for a separate grounding system to employ the requisite materials for an ample development of the protective ground system.

Tying together both systems (protective and operating) has the noteworthy advantage that for a ground fault within the station the ground-fault current component of the faulted station need not be carried by the ground mat but is conducted directly over the grounding conductors which are tied to the star neutral point. Also, one has only to reckon with the difference between the total ground-fault current and the station component, whereby there is a considerable reduction in ground mat potential and step potential.

The overhead ground wire of the outgoing station transmission lines may be advantageously connected to the station ground, and effectively reduce the total ground resistance; this is especially so where the ground wire which appears to be necessary for star neutral grounded systems with high ground-fault currents is of ample design.

G.1 Summary

Large contact and step potentials under fault conditions must be considered in high-voltage stations using grounded star neutral point. Potential differences which may endanger cable insulation and low-voltage apparatus and facilities (for example, windings of control motors) may be eliminated by metallic interconnection of equipment housing, sheaths of control and service cables and their neutral conductors, and the construction parts in the control house. For protection of personnel at the danger points, narrow meshed ground mats with mesh spacing of about 1 m will serve. The potential distribution of such ground mats may be investigated by means of electrolytic tanks. A separate operating ground for the star neutral point is not recommended, since connection of the latter to a general ground system designed according to the viewpoint outlined herein, has advantages over separation. Approaches to parts of the ground system which have potential control can be made safe by the so-called potential ramps.

Copyright © 2015 IEEE. All rights reserved.

Copyright The Institute of Electrical and Electronics Engineers, Inc.
Provided by IHS under license with IEEE
No reproduction or networking permitted without license from IHS

Order Number: 02120914
Sold to:EGAT [700166108393] - VARRIS.Y@EGAT.CO.TH,
Not for Resale,2016-09-15 03:57:51 UTC

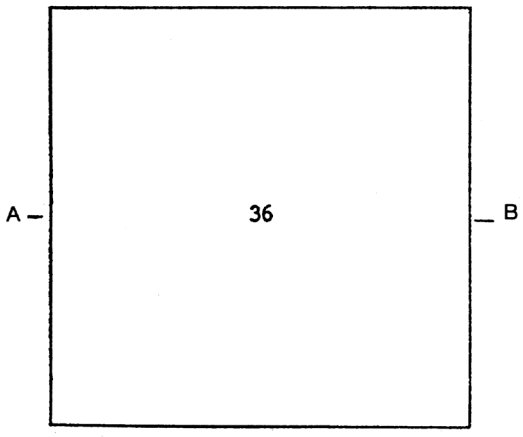

Figure G.2—Measured potential distribution for various ground mats

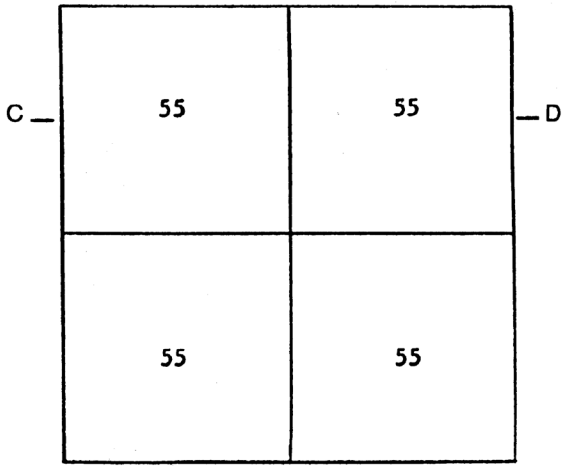

Figure G.3—Measured potential distribution for various ground mats

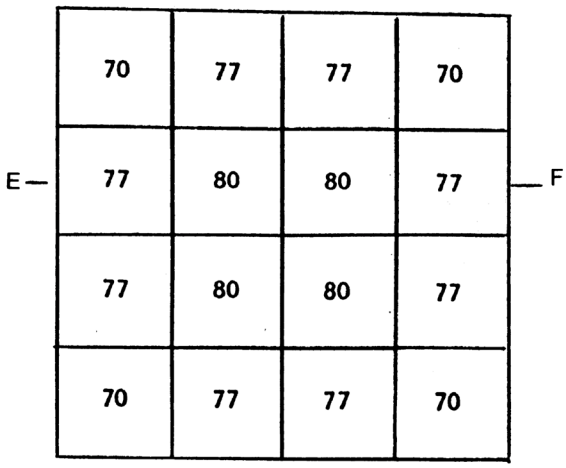

Figure G.4—Measured potential distribution for various ground mats

Copyright © 2015 IEEE. All rights reserved.

Copyright The Institute of Electrical and Electronics Engineers, Inc.
Provided by IHS under license with IEEE
No reproduction or networking permitted without license from IHS

Order Number: 02120914
Sold to:EGAT [700166108393] - VARRIS.Y@EGAT.CO.TH,
Not for Resale,2016-09-15 03:57:51 UTC

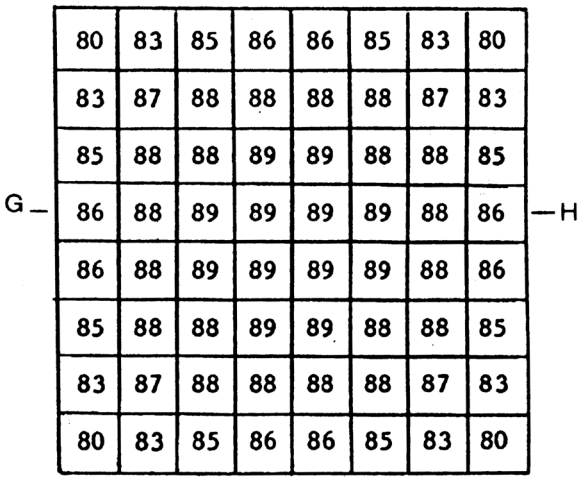

Figure G.5—Measured potential distribution for various ground mats

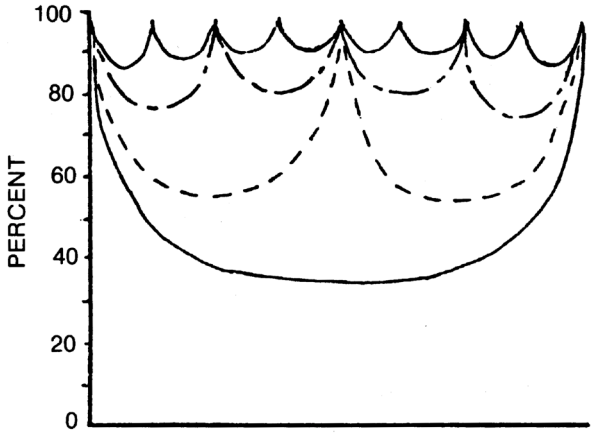

Figure G.6—Distribution for a ground mat with various mesh densities; ground mat potential = 100%

Copyright © 2015 IEEE. All rights reserved.

Copyright The Institute of Electrical and Electronics Engineers, Inc.
Provided by IHS under license with IEEE
No reproduction or networking permitted without license from IHS

Order Number: 02120914
Sold to:EGAT [700166108393] - VARRIS.Y@EGAT.CO.TH,
Not for Resale,2016-09-15 03:57:51 UTC

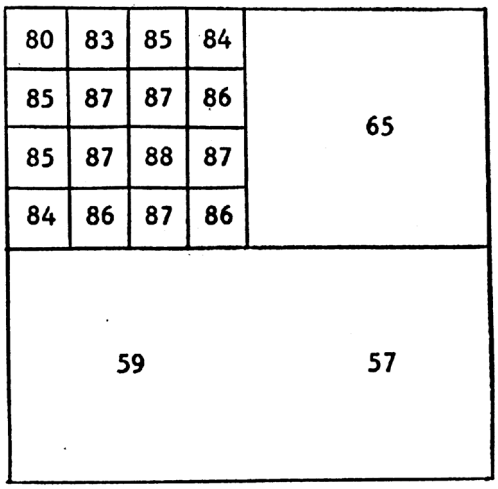

Figure G.7—Potential distribution for ground mats with fine meshes in portions

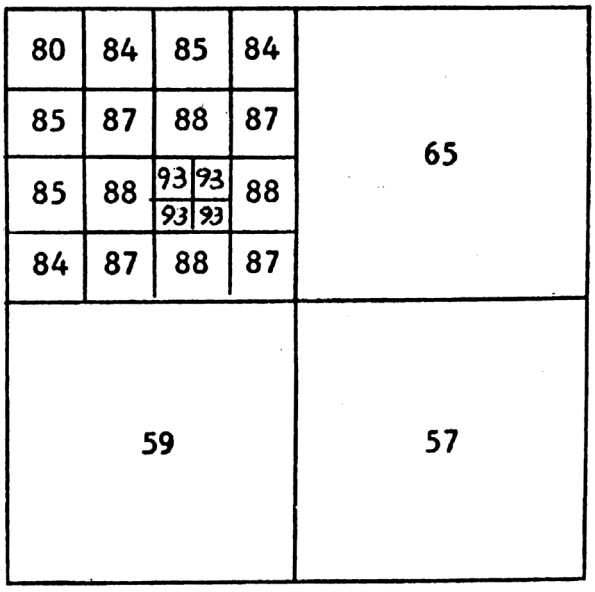

Figure G.8—Potential distribution for ground mats with fine meshes in portions

Copyright © 2015 IEEE. All rights reserved.

Copyright The Institute of Electrical and Electronics Engineers, Inc.
Provided by IHS under license with IEEE
No reproduction or networking permitted without license from IHS

Order Number: 02120914
Sold to:EGAT [700166108393] - VARRIS.Y@EGAT.CO.TH,
Not for Resale,2016-09-15 03:57:51 UTC

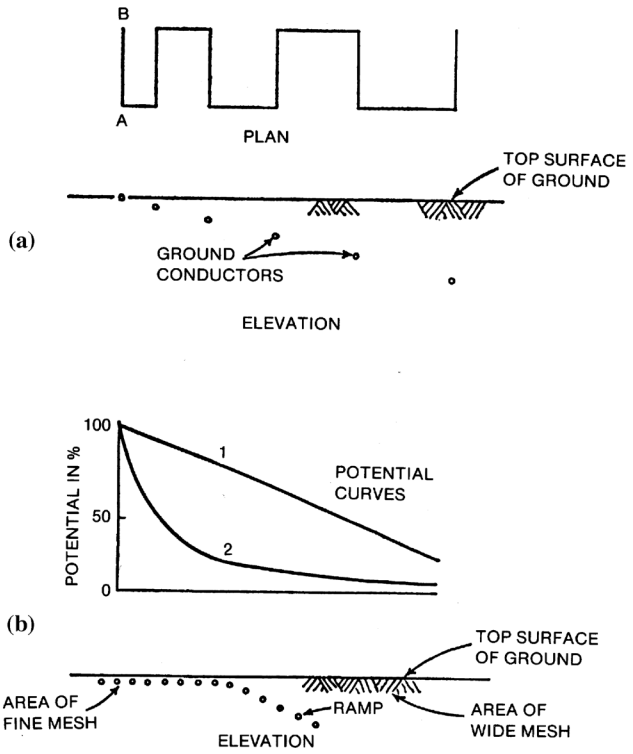

Figure G.9—Potential distribution in a ground mat with ramp (Curve 1) and without ramp (Curve 2)

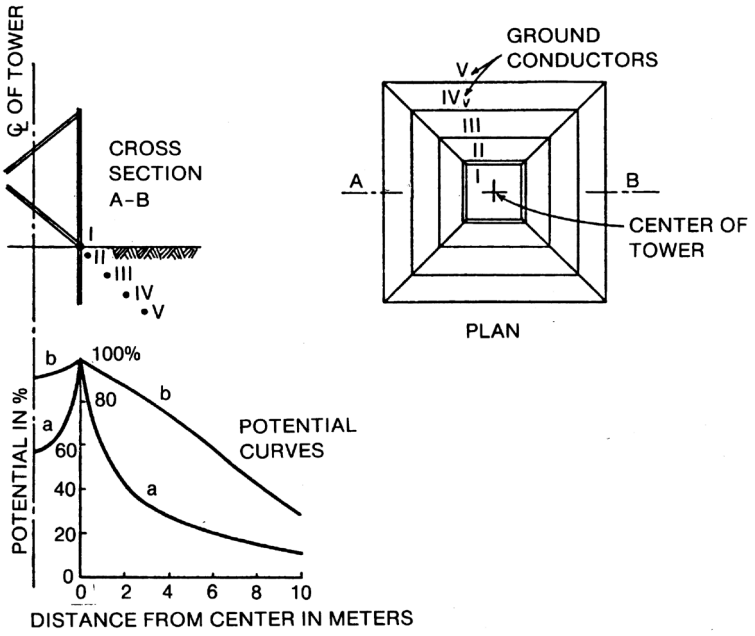

Figure G.10 Potential distribution around a mast in the direction A–B for a mast with ramp (Curve b) and without ramp (Curve a)

Copyright © 2015 IEEE. All rights reserved.

Copyright The Institute of Electrical and Electronics Engineers, Inc.
Provided by IHS under license with IEEE
No reproduction or networking permitted without license from IHS

Order Number: 02120914
Sold to:EGAT [700166108393] - VARRIS.Y@EGAT.CO.TH,
Not for Resale,2016-09-15 03:57:51 UTC

Annex H

(informative)

Benchmark

H.1 Overview

This annex provides the users with benchmark case results to use in comparing and evaluating software tools and methodologies that provide analysis of substation grounding. The specific objectives are as follows:

a) Compare equations and methods found in this guide with some of the available commercial software.

b) Illustrate the variations in complexity of simple grids versus more complex and interconnected grounding systems, and demonstrate some of the limitations of the methods or software.

c) Provide a basis for checking the accuracy of other or future software or methodologies.

All methods, whether simple formulas or complex computer modeling, involve some approximations or assumptions for grounding analysis; thus, no representation is made that these benchmark results are exact. For each category of analysis, several methods were compared and the results tabulated. These results were also reviewed by the developers of the computer programs.

The computer software used in these benchmark cases include: CDEGS, ETAP, SGW, SDWorkstation, and WinIGS. This is not a complete list of all available software, but is representative of commercially-available software. Not all software has the same modeling capabilities—each type of analysis lists the software used for that specific analysis. The following provides contact information for obtaining these softwares.

— CDEGS: Safe Engineering Services (SES), 1544 Viel, Montreal, Quebec, Canada, H3M-1G4, www.sestech.com

— ETAP: Operations Technology, Inc. (OTI), 17 Goodyear, Suite 100, Irvine, CA, 92618-1812, www.etap.com

— SGW: Electric Power Research Institute (EPRI), 3412 Hillview Avenue, Palo Alto, CA, 94304, www.epri.com

— SDWorkstation: Electric Power Research Institute (EPRI), 3412 Hillview Avenue, Palo Alto, CA, 94304, www.epri.com

— WinIGS: Advanced Grounding Concepts (AGC), P. O. Box 29547, Atlanta, GA 30359, www.ap-concepts.com

The benchmarks are divided into three categories—soil analysis, grid analysis (resistance, touch and step voltages, transfer voltages), and ground fault current division.

H.2 Soil analysis

Although there are several methods and software available that can evaluate soil resistivity field measurements into multilayer soil models, the equations of this guide are limited to uniform soil models

Copyright © 2015 IEEE. All rights reserved.

Copyright The Institute of Electrical and Electronics Engineers, Inc.
Provided by IHS under license with IEEE
No reproduction or networking permitted without license from IHS

Order Number: 02120914
Sold to:EGAT [700166108393] - VARRIS.Y@EGAT.CO.TH,
Not for Resale,2016-09-15 03:57:51 UTC

and the grounding analysis software used in this annex, except CDEGS, is limited to a two-layer soil model. There are also many methods, as described in IEEE Std 81, for measuring soil resistivity. By far, the most common method of measurement is the four-pin (Wenner) method. A less-often used method is the three-pin (driven-rod) method. The benchmark cases of soil resistivity interpretation are restricted to analysis of measurements made using the four-pin and three-pin methods. In order to make it possible to compare at least two computation methods for all examples, the soil structure has been limited to uniform and two-layer soils, although there are frequently situations in which it is desirable to model more complex soil structures. Because of the difficulties and errors introduced into the actual field measurements, it is difficult, if not impossible, to determine the "correct" two-layer soil model for a set of field measurements. In fact, the soil resistivity usually varies both laterally and with depth over the substation area, so there is no exact two-layer or multilayer soil model. Because of this, "exact" sets of field measurements were mathematically derived that correctly represent a perfect two-layer soil.

The mathematically-derived field measurements are shown in Table H.1 and Table H.3 for soil models with ρ_1 = 300 Ω-m, ρ_2 = 100 Ω-m, and h = 6.096 m (20 ft), and for ρ_1 = 300 Ω-m, ρ_2 = 100 Ω-m, and h = 6.096 m (20 ft). The plots of apparent resistivity versus pin spacing for these two soil models are shown in Figure H.1 and Figure H.2. For these computer simulations, the pins were modeled as nominal 5/8 in CCS ground rods inserted 0.15 m (0.5 ft) into the soil to represent typical pin depths used in actual field measurements.

Table H.1—Four-pin field measurements for two-layer soil models*

Spacing m (ft)	ρ_1 = 300 Ω-m, ρ_2 = 100 Ω-m, h = 6.096 m (20 ft)		ρ_1 = 100 Ω-m, ρ_2 = 300 Ω-m, h = 6.096 m (20 ft)	
	Resistance (Ω)	Apparent resistivity (Ω-m)	Resistance (Ω)	Apparent resistivity (Ω-m)
0.3048 (1.0)	109.38	209.5	36.46	69.8
0.9144 (3.0)	48.84	280.6	16.32	93.8
1.524 (5.0)	30.40	291.1	10.25	98.2
3.048 (10.0)	15.01	287.5	5.40	103.4
4.572 (15.0)	9.42	270.6	3.86	110.9
6.096 (20.0)	6.48	248.2	3.16	121.0
9.144 (30.0)	3.52	202.2	2.49	143.1
15.24 (50.0)	1.50	143.6	1.90	181.9
21.336 (70.0)	0.90	120.7	1.56	209.1
27.432 (90.0)	0.64	110.3	1.32	227.5
33.528 (110.0)	0.51	107.4	1.15	242.3
39.624 (130.0)	0.42	104.6	1.01	251.5
45.72(150.0)	0.36	103.4	0.90	258.5

* These data were analyzed using the guidance in 13.4.2.2 and the computer programs RESAP (component of CDEGS), SOMIP (component of SGW), SDWorkstation, and WinIGS. The comparisons for each soil model are presented in Table H.2.

Copyright © 2015 IEEE. All rights reserved.
Copyright The Institute of Electrical and Electronics Engineers, Inc.
Provided by IHS under license with IEEE
No reproduction or networking permitted without license from IHS
Order Number: 02120914
Sold to:EGAT [700166108393] - VARRIS.Y@EGAT.CO.TH,
Not for Resale,2016-09-15 03:57:51 UTC

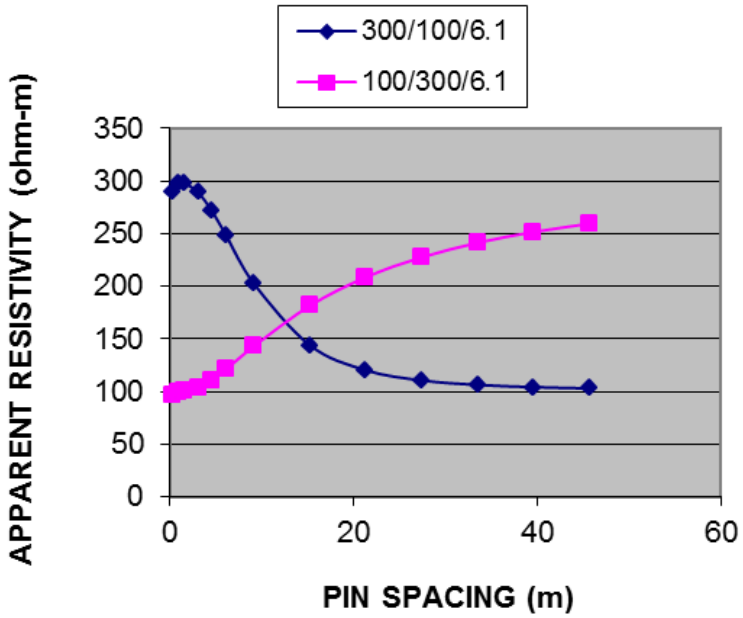

Figure H.1—Soil resistivity versus pin spacing for four-pin test

Table H.2—Two-layer soil models derived from four-pin field measurements of Table H.1

Method	ρ_1 = 300 Ω-m, ρ_2 = 100 Ω-m, h = 6.096 m (20 ft)			ρ_1 = 100 Ω-m, ρ_2 = 300 Ω-m, h = 6.096 m (20 ft)		
	ρ_1 (Ω-m)	ρ_2 (Ω-m)	h	ρ_1 (Ω-m)	ρ_2 (Ω-m)	h
STD 80-2000 (SUNDE CURVE)	290.0	100.0	5.6 m (18.37 ft)	100.0	270.0	7.0 m (22.97 ft)
RESAP	297.6	100.2	6.13 m (20.1 ft)	99.0	297.9	5.94 m (19.5 ft)
SOMIP	300.1	100.4	6.07 m (19.9 ft)	99.8	298.8	6.04 m (19.8 ft)
SDWorkstation*	294.5	100.1	6.22 m (20.4 ft)	84.4	237.8	2.54 m (8.33 ft)
WinIGS	300.7	100.4	6.035 m (19.8 ft)	100.1	299.5	6.096 m (20.0 ft)

*Does not allow measurements below 1.77 ft spacing.

Copyright © 2015 IEEE. All rights reserved.

Copyright The Institute of Electrical and Electronics Engineers, Inc.
Provided by IHS under license with IEEE
No reproduction or networking permitted without license from IHS

Order Number: 02120914
Sold to:EGAT [700166108393] - VARRIS.Y@EGAT.CO.TH,
Not for Resale,2016-09-15 03:57:51 UTC

Table H.3—Three-pin field measurements for two-layer soil models

Rod depth m (ft)	ρ_1 = 300 Ω-m, ρ_2 = 100 Ω-m, h = 6.096 m (20 ft)		ρ_1 = 100 Ω-m, ρ_2 = 300 Ω-m, h = 6.096 m (20 ft)	
	Resistance (Ω)	Apparent resistivity (Ω-m)	Resistance (Ω)	Apparent resistivity (Ω-m)
0.3048 (1.0)	647.6	299.27	218.3	100.88
0.9144 (3.0)	270.6	296.54	92.68	101.56
1.524 (5.0)	177.1	294.74	61.52	102.39
3.048 (10.0)	97.63	290.03	35.13	104.36
4.572 (15.0)	67.85	284.45	25.43	106.61
6.096 (20.0)	50.82	272.63	20.63	110.67
9.144 (30.0)	21.77	165.77	18.22	138.73
15.24 (50.0)	10.91	129.68	14.58	173.30
21.336 (70.0)	7.41	118.36	12.16	194.23
27.432 (90.0)	5.64	112.46	10.42	207.77
33.528 (110.0)	4.57	108.85	9.13	217.46
39.624 (130.0)	3.84	106.09	8.12	224.33
45.72 (150.0)	3.32	104.18	7.31	229.38

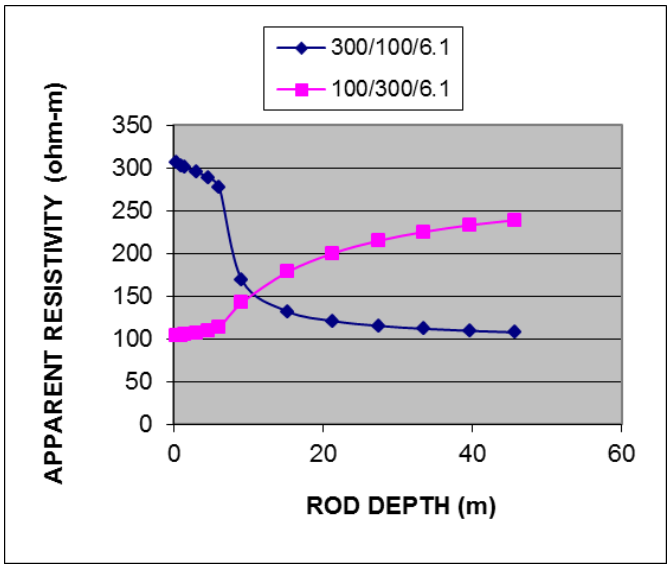

Figure H.2—Soil resistivity versus pin spacing for three-pin test

Copyright © 2015 IEEE. All rights reserved.
Copyright The Institute of Electrical and Electronics Engineers, Inc.
Provided by IHS under license with IEEE
No reproduction or networking permitted without license from IHS
Order Number: 02120914
Sold to:EGAT [700166108393] - VARRIS.Y@EGAT.CO.TH,
Not for Resale,2016-09-15 03:57:51 UTC

Table H.4—Two-layer soil models derived from three-pin field measurements of Table H.3

Method	ρ_1 = 300 Ω-m, ρ_2 = 100 Ω-m, h = 6.096 m (20 ft)			ρ_1 = 100 Ω-m, ρ_2 = 300 Ω-m, h = 6.096 m (20 ft)		
	ρ_1 (Ω-m)	ρ_2 (Ω-m)	h	ρ_1 (Ω-m)	ρ_2 (Ω-m)	h
STD 80-2000 (SUNDE CURVE)	NA	NA	NA	NA	NA	NA
CDEGS	NA	NA	NA	NA	NA	NA
SDWorkstation	289.6	97.0	6.096 m (20 ft)	96.7	291.5	6.04 m (19.8 ft)
WinIGS	301.5	100.6	6.096 m (20 ft)	104.1	268.8	6.096 m (20 ft)

H.3 Grounding system analysis

In the 1961 edition of IEEE Std 80, the equations for touch and step voltages were limited to analysis at very specific points and were limited to analysis of uniformly-spaced conductors in symmetrical grids. IEEE Std 80-2000 included improvements on those equations to account for odd-shaped grids and ground rods, but still analyzed only specific points for touch and step voltages. Other methods, and especially computer programs based on a fine-element analysis of the grounding system, might allow more flexibility in modeling the conductors and ground rods making up the grounding system, and might analyze touch and step voltages and transferred voltages at any point desired. This clause analyzes the grid resistance, touch and step voltages, and transferred voltages (if applicable) for grids ranging from simple evenly-spaced symmetrical grids with no ground rods to non-symmetrically shaped and spaced grids with random ground rod locations and with separately-grounded fences. The grid current for all cases is 744.8A. The grid analysis is performed using the equations in IEEE Std 80, and computer programs CDEGS, ETAP and WinIGS. In order to make it possible to compare at least two computation methods for all examples, the soil structure has been limited to uniform and two-layer soils, although there are situations in which it is desirable to model more complex soil structures.

Each program has several features for displaying the touch and step voltages, as well as determining the absolute worst case voltages. For consistency in comparing results between the programs, the touch and step voltages were evaluated at very specific points and with specific guidelines on the points evaluated to determine the worst case voltages. For example, to determine the step voltage at the corner of the grid, the earth surface potentials were determined at points over the corner of the grid and 1m outside the grid along the diagonal. The step voltage was computed as the difference between the potentials at these two points. For cases where several points (i.e. a grid of points) were used to determine the worst case touch voltage, the evaluated points were spaced 0.5m apart.

Again, in order to make it possible to compare at least two computation methods for all examples, the soil structure has been limited to uniform and two-layer soils.

Copyright © 2015 IEEE. All rights reserved.
Copyright The Institute of Electrical and Electronics Engineers, Inc.
Provided by IHS under license with IEEE
No reproduction or networking permitted without license from IHS
Order Number: 02120914
Sold to:EGAT [700166108393] - VARRIS.Y@EGAT.CO.TH,
Not for Resale,2016-09-15 03:57:51 UTC

H.3.1 Grid 1—symmetrically spaced and shaped grid, uniform soil, no ground rods

The ground grid for this comparison is shown in Figure H.3. The equations in IEEE Std 80 compute the touch voltage at the center of the corner mesh (T1), so this point was chosen for comparison. The actual maximum touch voltage for this grid shape might be on the diagonal near the center of the corner mesh, but located slightly nearer the perimeter of the grid (T3). For some cases, it might also be directly over the extreme corner (perimeter) of the grid (T2). Thus, these two points were also analyzed for comparison. The equations in IEEE Std 80 compute the step voltage as the difference between the earth surface potential 1 m apart, with one point directly over the corner of the grid and the other on a diagonal and 1 m beyond the first point. Though the actual worst case step voltage might be at a different location, comparisons were limited to this one location (S1) for this case. The comparisons are shown in Table H.5.

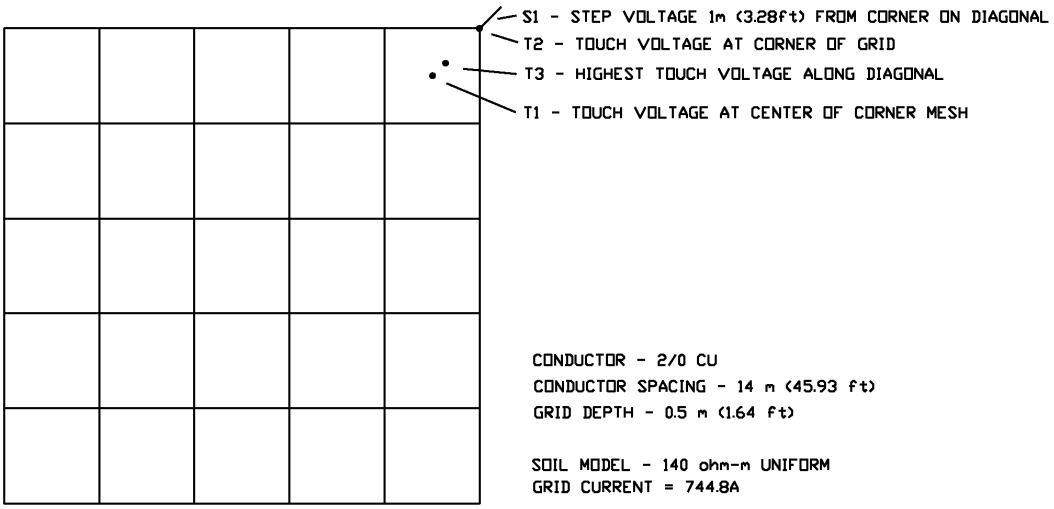

Figure H.3—Grounding system parameters for Grid 1

Table H.5—Comparison of results for grid analysis

Case	R_{GRID} (Ω)	R_{FENCE} (Ω)	GPR grid (V)	Touch voltages (V)				Step voltages (V)		Transfer voltage grid-to-fence (V)
				T_1	T_2	T_3	T_4	S_1	S_2	
Grid 1 STD 80	1.05	NA	780.0	232.0	NA	NA	NA	96.0	NA	NA
Grid 1 CDEGS	1.0	NA	743.9	194.9	147.4	202.7	NA	89.3	NA	NA
Grid 1 ETAP	1.01	NA	751.7	200.9	164.2	209.0	NA	87.2	NA	NA
Grid 1 WinIGS	1.0	NA	744.9	196.3	151.2	203.4	NA	88.7	NA	NA

NOTE—IEEE 80 resistance calculated using Equation (57), mesh voltage using Equation (85) through Equation (96) and step voltage using Equation (97) through Equation (99).

Copyright © 2015 IEEE. All rights reserved.
Copyright The Institute of Electrical and Electronics Engineers, Inc.
Provided by IHS under license with IEEE
No reproduction or networking permitted without license from IHS
Order Number: 02120914
Sold to:EGAT [700166108393] - VARRIS.Y@EGAT.CO.TH,
Not for Resale,2016-09-15 03:57:51 UTC

H.3.2 Grid 2—symmetrically spaced and shaped grid uniform soil, with ground rods

The ground grid for this comparison is shown in Figure H.4. This case is the same as Grid 1, with the addition of twenty 7.5 m (24.6 ft) rods located at each intersection around the perimeter of the grid. The touch and step voltages were computed at the same locations as for Grid 1. The comparisons are shown in Table H.6.

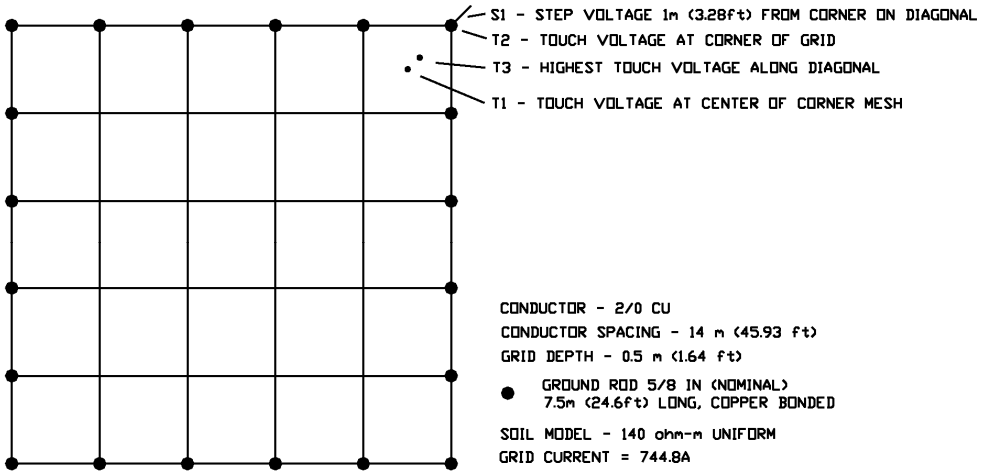

Figure H.4—Grounding system parameters for Grid 2

Table H.6—Comparison of results for grid analysis

Case	R_{GRID} (Ω)	R_{FENCE} (Ω)	GPR grid (V)	Touch voltages (V)				Step voltages (V)		Transfer voltage grid-to-fence (V)
				T_1	T_2	T_3	T_4	S_1	S_2	
Grid 2 STD 80	1.022	NA	761.0	163.0	NA	NA	NA	80.0	NA	NA
Grid 2 CDEGS	0.917	NA	682.8	145.4	85.8	149.6	NA	70.7	NA	NA
Grid 2 ETAP	0.92	NA	687.9	150.2	77.2	154	NA	79.3	NA	NA
Grid 2 WinIGS	0.919	NA	684.8	146.9	91.0	151.3	NA	71.5	NA	NA

NOTE—IEEE 80 resistance calculated using Equation (57), mesh voltage using Equation (85) through Equation (96) and step voltage using Equation (97) through Equation (99).

--`,,,,,,`,```,,`,`,,`,-`-`,,`,,,`---
Copyright © 2015 IEEE. All rights reserved.
Copyright The Institute of Electrical and Electronics Engineers, Inc.
Provided by IHS under license with IEEE
No reproduction or networking permitted without license from IHS
Order Number: 02120914
Sold to:EGAT [700166108393] - VARRIS.Y@EGAT.CO.TH,
Not for Resale,2016-09-15 03:57:51 UTC

H.3.3 Grid 3—symmetrically spaced and shaped grid, two-layer soil, with ground rods

The ground grid for this comparison is the same as for Grid 2, except the soil model is changed to a two-layer soil with ρ_1 = 300 Ω-m, ρ_2 = 100 Ω-m, and h = 6.096 m (20 ft). See Figure H.5. The touch and step voltages were computed at the same locations as for Grid 1. The comparisons are shown in Table H.7.

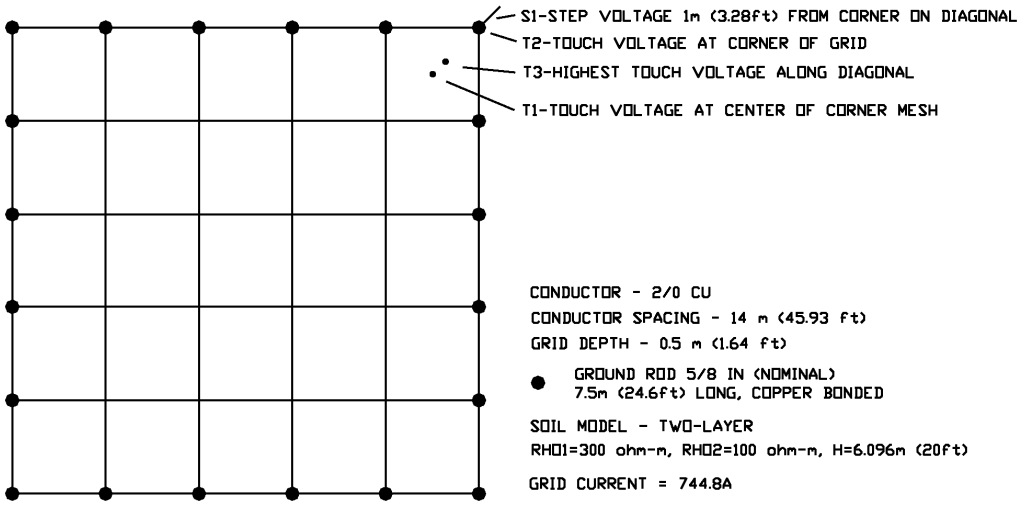

Figure H.5—Grounding system parameters for Grid 3

Table H.7—Comparison of results for grid analysis

Case	R_{GRID} (Ω)	R_{FENCE} (Ω)	GPR grid (V)	Touch voltages (V)				Step voltages (V)		Transfer voltage grid-to-fence (V)
				T_1	T_2	T_3	T_4	S_1	S_2	
Grid 3 STD 80	1.395	NA	1039.0	222.0	NA	NA	NA	109.0	NA	NA
Grid 3 CDEGS	0.97	NA	719.5	261.0	128.1	262.5	NA	101.9	NA	NA
Grid 3 ETAP	0.97	NA	726.4	268.5	111.6	269.7	NA	117	NA	NA
Grid 3 WinIGS	0.972	NA	723.8	264.5	136.3	266.2	NA	103.5	NA	NA

NOTE—IEEE 80 resistance calculated using Equation (57), mesh voltage using Equation (85) through Equation (96), step voltage using Equation (97) through Equation (99) and soil resistivity using Equation (52).

Copyright © 2015 IEEE. All rights reserved.
Copyright The Institute of Electrical and Electronics Engineers, Inc.
Provided by IHS under license with IEEE
No reproduction or networking permitted without license from IHS
Order Number: 02120914
Sold to:EGAT [700166108393] - VARRIS.Y@EGAT.CO.TH,
Not for Resale,2016-09-15 03:57:51 UTC

H.3.4 Symmetrically spaced and shaped grid, separately-grounded fence, two-layer soil, with ground rods

The ground grid for this comparison is the same as for Grid 3, except a separately-grounded fence is added, located 3 m outside the grid perimeter conductor, and with a fence perimeter ground conductor located 1 m outside the fence. The touch and step voltages were computed at similar locations as for Grid 1. In this case, however, additional touch and step points were computed. For this case, touch voltages T1, T2, and T3 were computed as differences between the surface potentials at these points and the GPR of the main ground grid. T4 was computed as the difference between surface potential at the corner of the fence perimeter conductor and the GPR of the fence perimeter conductor (connected only to the separately-grounded fence). Step voltages S1 and S2 were computed as differences between earth surface potentials 1 m apart along the diagonal. S1 had the first point located over the corner of the perimeter conductor of the main grid, while S2 had the first point located over the outer (fence) perimeter conductor. The comparisons are shown in Table H.8.

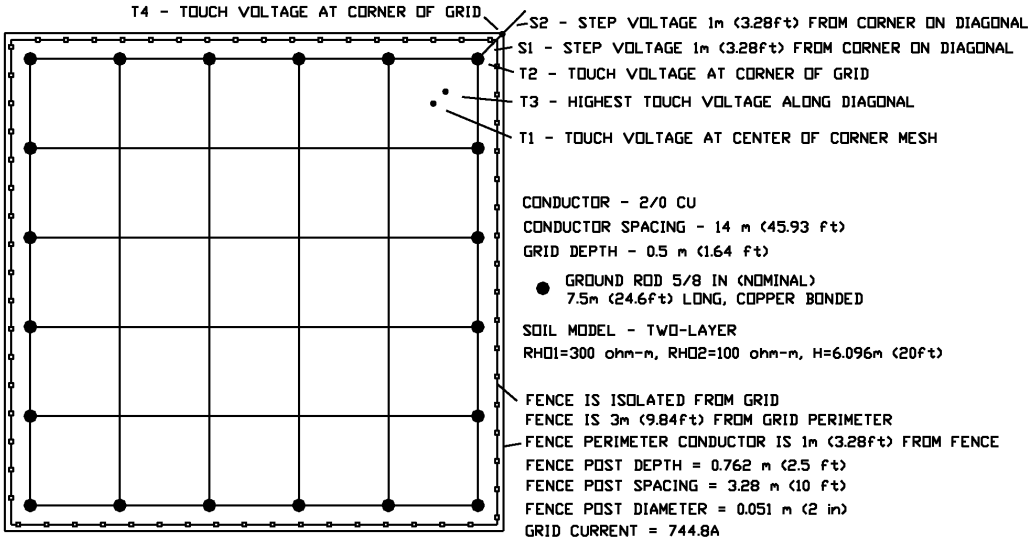

Figure H.6—Grounding system parameters for Grid 4

Table H.8—Comparison of results for grid analysis

Case	R_{GRID} (Ω)	R_{FENCE} (Ω)	GPR grid (V)	Touch voltages (V)				Step voltages (V)		Transfer voltage grid-to-fence (V)
				T_1	T_2	T_3	T_4	S_1	S_2	
Grid 4 STD 80	NA	NA	NA	NA	NA	NA	NA	NA	NA	NA
Grid 4 CDEGS	0.96	1.6	717.9	259.7	127.1	261.1	51.1	97.4	38.1	309.2
Grid 4 ETAP	NA	NA	NA	NA	NA	NA	NA	NA	NA	NA
Grid 4 WinIGS	0.97	1.62	722.6	263.6	130.1	264.9	49.9	97.0	37.4	312.4

NOTE—Used average soil resistivity based on Equation (51) in Clause 13.

Copyright © 2015 IEEE. All rights reserved.
Copyright The Institute of Electrical and Electronics Engineers, Inc.
Provided by IHS under license with IEEE
No reproduction or networking permitted without license from IHS
Order Number: 02120914
Sold to:EGAT [700166108393] - VARRIS.Y@EGAT.CO.TH,
Not for Resale,2016-09-15 03:57:51 UTC

H.3.5 Grid 5—symmetrically spaced non-symmetrically shaped grid, fence grounded to main grid, two-layer, with ground rods

The ground grid for this comparison is shown in Figure H.7. This grid is non-symmetrical in shape (L-shaped), though it still has symmetrically spaced grid conductors. It also has ground rods of uniform length at every other intersection around the perimeter, and has a grounded fence within the confines of the main grid and bonded to the grid. The touch and step voltage equations in Clause 16 can be used for this type of grid, but it is not known exactly where the touch and step voltages are being computed. For the computer programs, the touch and step voltages were computed at numerous points to determine the worst case for each. The worst case touch voltage was computed at all points 0.5 m apart within the fence, plus all points within reach (1 m) outside the fence. The worst case step voltage (S1) was computed at all points 0.5 m apart within an area defined inward from 1 m outside the perimeter of the grid. For direct comparison, the step voltage (S2) was also compared by determining the difference between earth surface potentials 1 m apart along the diagonal at the upper left corner of the grid. The comparisons are shown in Table H.9.

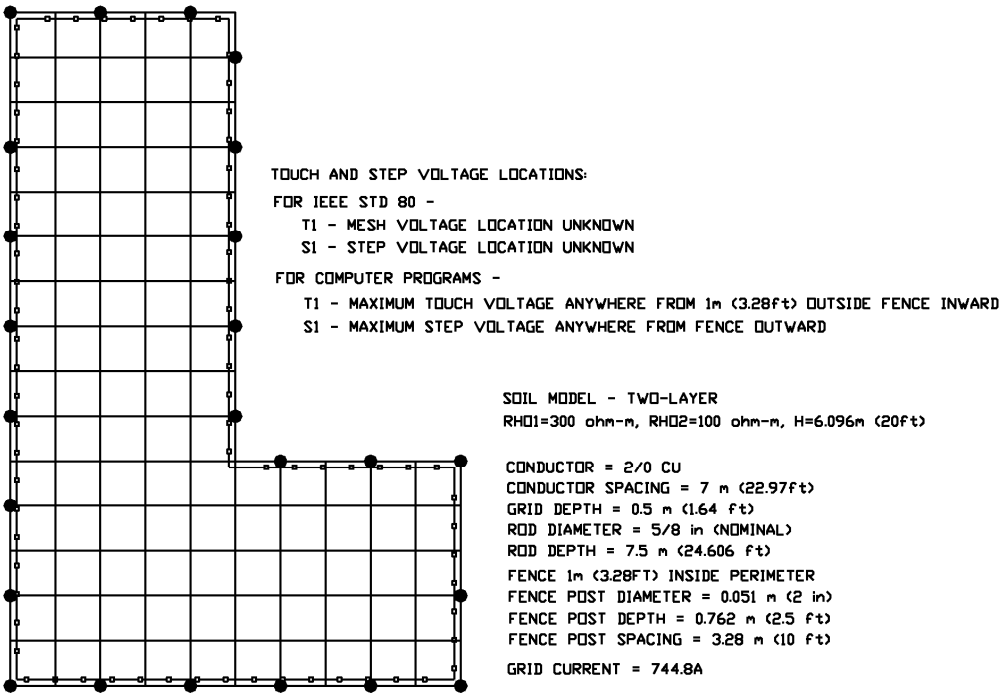

Figure H.7—Grounding system parameters for Grid 5

Table H.9—Comparison of results for grid analysis

Case	R_{GRID} (Ω)	R_{FENCE} (Ω)	GPR grid (V)	Touch voltages (V)				Step voltages (V)		Transfer voltage grid-to-fence (V)
				T_1	T_2	T_3	T_4	S_1	S_2	
Grid 5 STD 80 (1)	1.35	NA	1005.8	146.5	NA	NA	NA	110.6	NA	NA
Grid 5 CDEGS	0.81	NA	602.7	131.6	NA	NA	NA	83.0	NA	NA
Grid 5 ETAP	0.81	NA	606.4	138.1	NA	NA	NA	90.7	NA	NA
Grid 5 WinIGS	0.81	NA	606.4	138.1	NA	NA	NA	90.7	NA	NA

NOTE—IEEE 80 resistance calculated using Equation (57), mesh voltage using Equation (85) through Equation (96), step voltage using Equation (97) through Equation (99) and soil resistivity using Equation (52).

Copyright © 2015 IEEE. All rights reserved.

Copyright The Institute of Electrical and Electronics Engineers, Inc.
Provided by IHS under license with IEEE
No reproduction or networking permitted without license from IHS

Order Number: 02120914
Sold to:EGAT [700166108393] - VARRIS.Y@EGAT.CO.TH,
Not for Resale,2016-09-15 03:57:51 UTC

H.3.6 Grid 6—non-symmetrically spaced and shaped grid, non-orthogonal conductors, two-layer soil, with ground rods at random locations and unequal lengths

The final ground grid for comparison is similar to Grid 3, but with conductors on the diagonal and with corner grounds 7.5 m long and all other ground rods 2.5 m long. The soil model is changed to a two-layer soil with ρ_1 = 100 Ω-m, ρ_2 = 300 Ω-m, and h = 6.091 m (20 ft). See Figure H.8. The touch and step voltage equations in Clause 16 are not intended for this type of grid, so IEEE Std 80 results are not included in this case. For the computer programs, the touch and step voltages were computed at numerous points to determine the worst case for each. The worst case touch voltage was computed at all points 0.5 m apart within the perimeter conductor. The worst case step voltage (S1) was computed at all points 0.5 m apart within an area defined inward from 1 m outside the perimeter of the grid. For direct comparison, the step voltage (S2) was also compared by determining the difference between earth surface potentials 1 m apart along the diagonal at the upper left corner of the grid. The comparisons are shown in Table H.10.

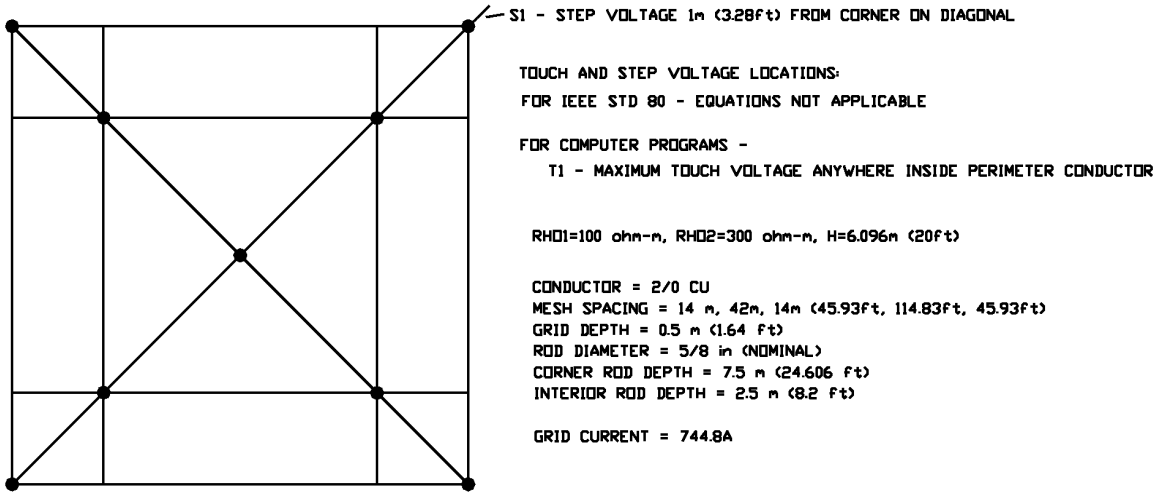

Figure H.8—Grounding system parameters for Grid 6

Table H.10—Comparison of results for grid analysis

Case	R_{GRID} (Ω)	R_{FENCE} (Ω)	GPR grid (V)	Touch voltages (V)				Step voltages (V)		Transfer voltage grid-to-fence (V)
				T_1	T_2	T_3	T_4	S_1	S_2	
Grid 6 STD 80	NA	NA	NA	NA	NA	NA	NA	NA	NA	NA
Grid 6 CDEGS	1.42	NA	1054.4	134.4	NA	NA	NA	96.4	NA	NA
Grid 6 ETAP	1.43	NA	1068.2	140.2	NA	NA	NA	99.2	NA	NA
Grid 6 WinIGS	1.43	NA	1063.1	136.6	NA	NA	NA	77.4	84.9	NA

NOTE—Used average soil resistivity based on Equation (51) in Clause 13.

Copyright © 2015 IEEE. All rights reserved.
Copyright The Institute of Electrical and Electronics Engineers, Inc.
Provided by IHS under license with IEEE
No reproduction or networking permitted without license from IHS
Order Number: 02120914
Sold to:EGAT [700166108393] - VARRIS.Y@EGAT.CO.TH,
Not for Resale,2016-09-15 03:57:51 UTC

H.4 Grid current analysis (current division)

Two example systems were modeled to compare the grid current versus the total available fault current. The first case was for a typical distribution substation, with one transmission line (remote source only) and one distribution feeder. The second case was for a typical transmission substation, with four transmission lines (remote sources) and one autotransformer (local source). The grid current was determined using the current split curves of Annex C, and computer programs CDEGS, and WinIGS.

H.4.1 Grid current for distribution substation—remote source only

Figure H.9 shows the system data for this example. The transmission line has a shield wire that is grounded at each pole, with pole ground resistance equal to 15 Ω. The distribution feeder neutral is grounded at every pole, with pole ground resistance equal to 25 Ω. The substation grounding system (grid plus ground rods, only) is 1.0 Ω. All line configuration dimensions, line sequence impedances, and equivalent source impedances are included in Figure H.9. The results are shown in Table H.11.

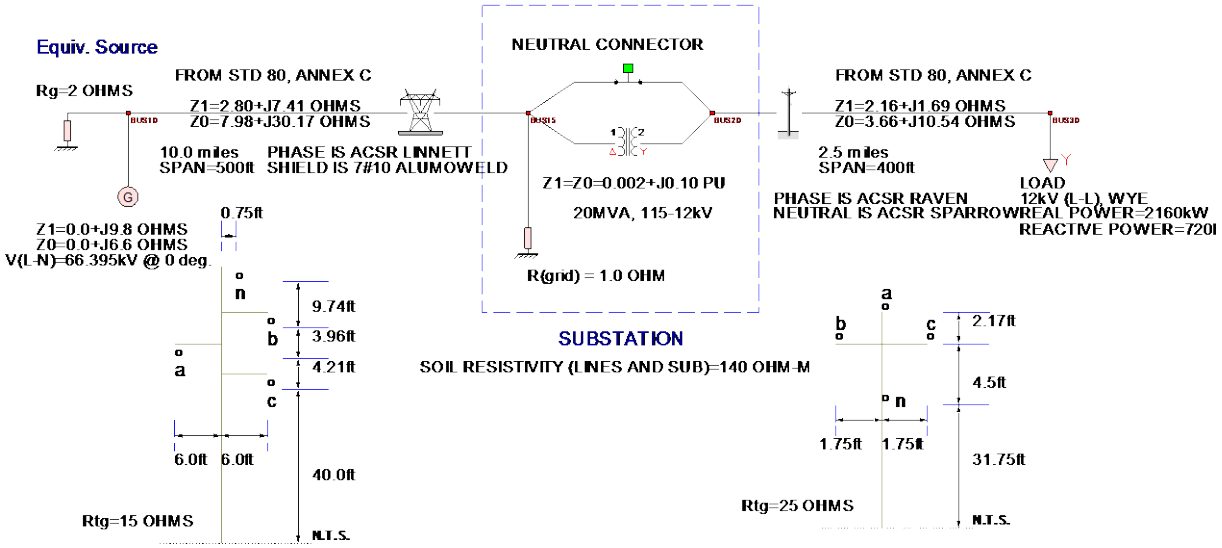

Figure H.9—System data for distribution substation current division

Table H.11—Grid current for distribution substation current division example

Method	Ground fault at 115 kV bus		
	I_f (A)	S_f	I_g (A)
STD 80-2000 (curves)	2748.4	0.5	1374.2
CDEGS	2877.3	0.50	1431.3
WinIGS	2891.4	0.49	1426.0

Copyright © 2015 IEEE. All rights reserved.
Copyright The Institute of Electrical and Electronics Engineers, Inc.
Provided by IHS under license with IEEE
No reproduction or networking permitted without license from IHS
Order Number: 02120914
Sold to:EGAT [700166108393] - VARRIS.Y@EGAT.CO.TH,
Not for Resale,2016-09-15 03:57:51 UTC

H.4.2 Grid current for transmission substation—remote and local sources

Figure H.10 shows the system data for this example. The transmission lines have shield wires that are grounded at each pole, with pole ground resistance equal to 15 Ω. The autotransformer has a common grounded winding, and includes a delta-connected tertiary winding. The substation grounding system (grid plus ground rods, only) is 1.0 Ω. All line configuration dimensions, line sequence impedances, and equivalent source impedances are included in Figure H.10. Results are shown in Table H.12 using the 25/75 local/remote split curve, as suggested in Annex C.2 (e). This calculation is done for both 230 kV and 115 kV bus faults to determine the worst case grid current, as suggested in Annex C.2 (g). The 100% remote contribution split factor is also shown to illustrate the effect of having a portion of the total fault current from local contributions.

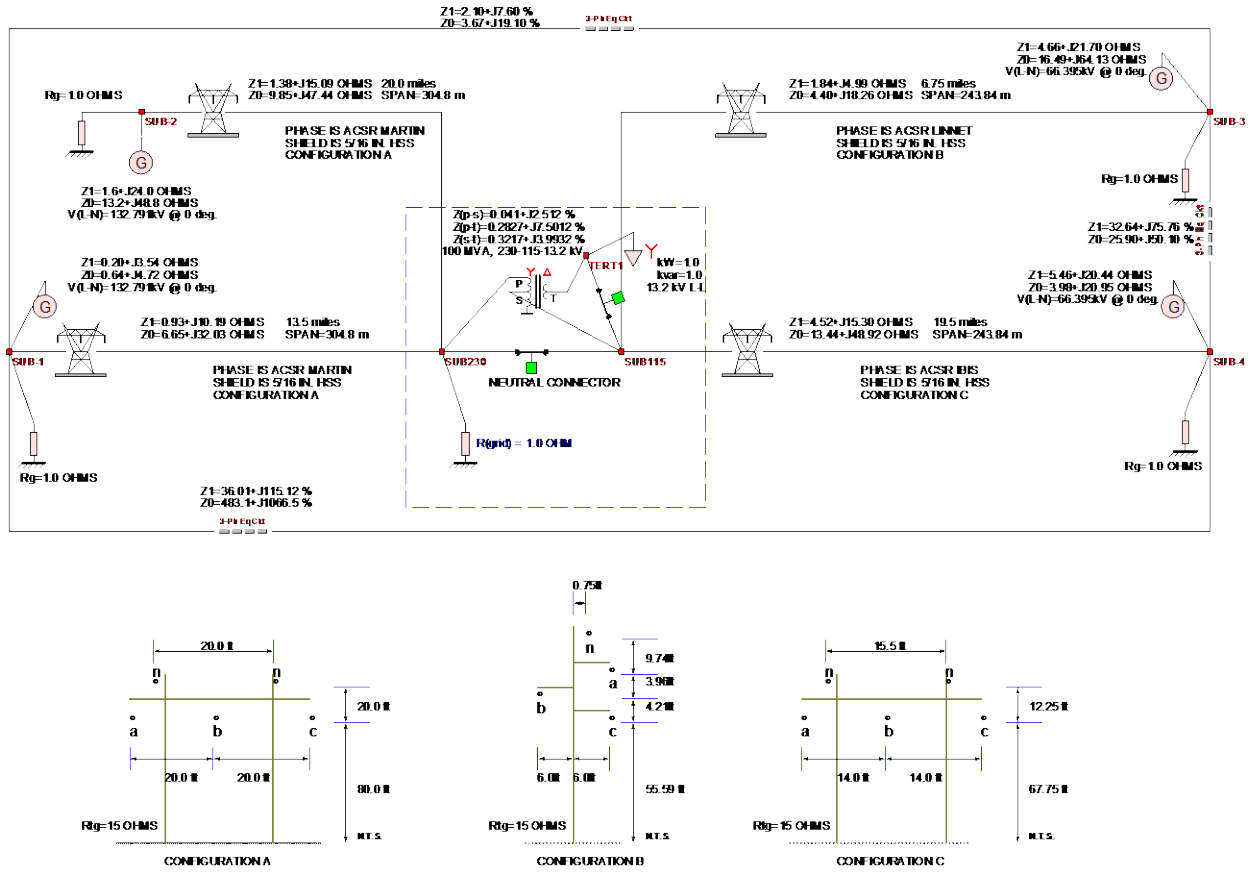

Figure H.10—System data for transmission substation current division

Copyright © 2015 IEEE. All rights reserved.

Copyright The Institute of Electrical and Electronics Engineers, Inc.
Provided by IHS under license with IEEE
No reproduction or networking permitted without license from IHS

Order Number: 02120914
Sold to:EGAT [70016610839 3] - VARRIS.Y@EGAT.CO.TH,
Not for Resale,2016-09-15 03:57:51 UTC

Table H.12—Grid current for transmission substation current division example

Method	Ground fault at specified bus				
	I_f total (A)	I_f remote (A) (%)	I_f local (A) (%)	S_f	I_g (A)
STD 80-2000 (curves)	AT 230 kV 12051	12 162 (100.9%)	343 (1.8%)	0.38	4579 (100% remote)
	AT 115 kV 19140	10 510 (54.9%)	8652 (45.2%)	0.29	5551 (25% local and 75% remote)
CDEGS	11 895.4	12 083.0 (101.6%)	3561.4 (29.9%)	0.33	3956.5
WinIGS	12 055.5	8655.9 (71.8%)	3701.0 (30.7%)	0.34	4102.0

Copyright © 2015 IEEE. All rights reserved.
Copyright The Institute of Electrical and Electronics Engineers, Inc.
Provided by IHS under license with IEEE
No reproduction or networking permitted without license from IHS
Order Number: 02120914
Sold to:EGAT [700166108393] - VARRIS.Y@EGAT.CO.TH,
Not for Resale,2016-09-15 03:57:51 UTC

--`,,,,,,`,```,,``,`,,`,-`-`,,`,,`,,`---
Copyright The Institute of Electrical and Electronics Engineers, Inc.
Provided by IHS under license with IEEE
No reproduction or networking permitted without license from IHS
Order Number: 02120914
Sold to:EGAT [700166108393] - VARRIS.Y@EGAT.CO.TH,
Not for Resale,2016-09-15 03:57:51 UTC

Consensus

WE BUILD IT.

Connect with us on:

Facebook: https://www.facebook.com/ieeesa

Twitter: @ieeesa

LinkedIn: http://www.linkedin.com/groups/IEEESA-Official-IEEE-Standards-Association-1791118

IEEE-SA Standards Insight blog: http://standardsinsight.com

YouTube: IEEE-SA Channel

445 Hoes Lane, Piscataway, NJ 08854 USA | standards.ieee.org

Tel. +1 732-981-0061 Fax +1 732-562-1571

Copyright The Institute of Electrical and Electronics Engineers, Inc.
Provided by IHS under license with IEEE
No reproduction or networking permitted without license from IHS

Order Number: 02120914
Sold to:EGAT [700166108393] - VARRIS.Y@EGAT.CO.TH,
Not for Resale,2016-09-15 03:57:51 UTC